FOURTH ANNUAL HEDS-UP FORUM

194 pgs
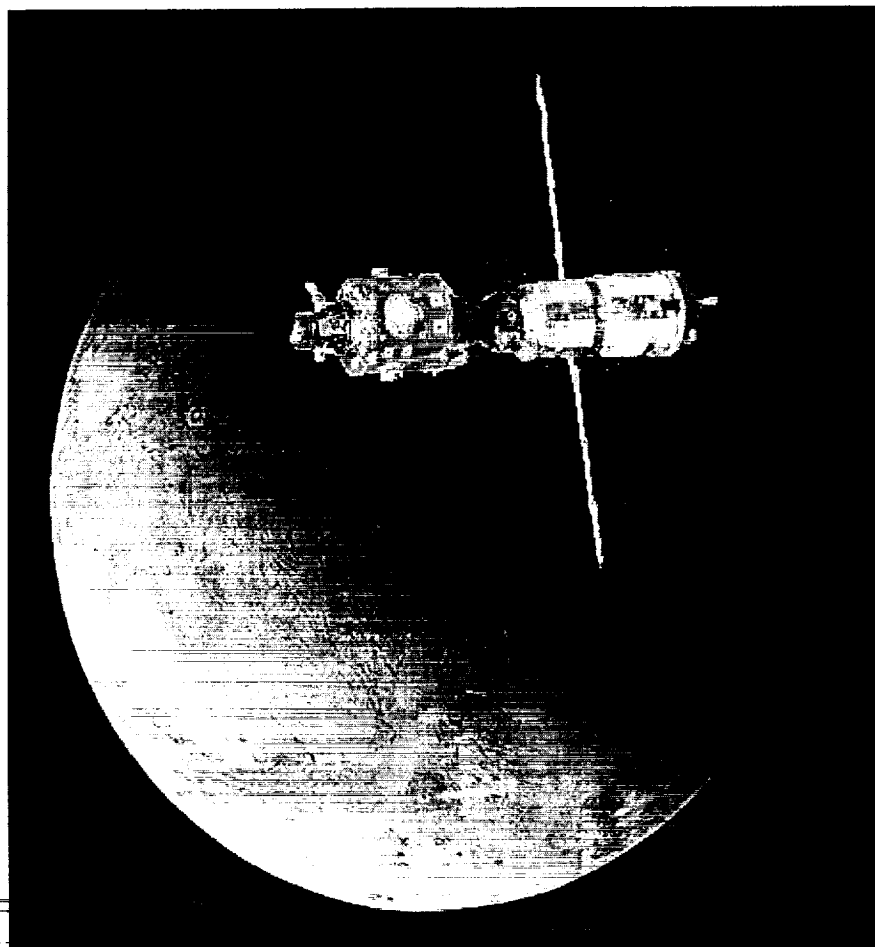
May 3–5, 2001
Lunar and Planetary Institute, Houston, Texas

LPI Contribution No. 1106

FOURTH ANNUAL HEDS-UP FORUM

May 3–5, 2001
Lunar and Planetary Institute, Houston, Texas

Edited by
Kathleen M. Johnson

Sponsored by .
Lunar and Planetary Institute
National Aeronautics and Space Administration
Office of Space Flight, Advanced Projects Office

Compiled in 2001 by
LUNAR AND PLANETARY INSTITUTE

This volume may be cited as

Johnson K. M., ed. (2001) *Fourth Annual HEDS-UP Forum.* LPI Contribution No. 1106, Lunar and Planetary Institute, Houston. 185 pp.

This volume is distributed by

ORDER DEPARTMENT
Lunar and Planetary Institute
3600 Bay Area Boulevard
Houston TX 77058-1113
Phone: 281-486-2172
Fax: 281-486-2186
E-mail: order@lpi.usra.edu

Mail order requestors will be invoiced for the cost of shipping and handling.

Cover design by team from the University of Colorado at Boulder.

PREFACE

The HEDS-UP (Human Exploration and Development of Space–University Partners) program was instituted to build new relationships between university, faculty, students, and NASA in support of the Human Exploration and Development of Space. The program has provided a mechanism for university students to explore problems of interest to NASA through student engineering-design projects, led by a university professor or mentor, and aided by the HEDS-UP staff. HEDS-UP program management advised teams on the selection of projects that were aligned with the goals of the HEDS strategic enterprise, and provided contacts with NASA and industry professionals who served as mentors. Students became acquainted with objectives, strategies, development issues, and technologic characteristics of space exploration programs. In doing so, they prepared themselves for future engineering challenges, often discovering that the program was on their critical path to professional advancement. Many of the ideas were innovative and of interest to NASA. Industry benefitted from HEDS-UP as a mechanism to converge with talented students about to enter the work force. In addition, universities became more involved in the teaching of space exploration, and students were encouraged and mentored as they included education outreach as an element in their work. This in turn highlighted their performance to others and universities in their communities.

The culmination of the HEDS-UP program each year has been the HEDS-UP Forum, held at the Lunar and Planetary Institute (LPI) in Houston, Texas. During the Forum, teams presented their design projects to the university and industry participants and NASA personnel via written reports, oral presentations, models, prototypes, and experiment demonstrations. NASA, industry, and academic professionals presented discussion of current issues and topics of interest in space exploration. Included at the Forum was an informal poster session, where all attendees further discussed the teams' research findings.

The Fourth Annual HEDS-UP Forum was held May 3–5, 2001. This year's Forum included representation of 13 university teams, three of which were graduate student teams. Each team contributed a 15–20-page written report; these reports are reproduced in this volume. The agenda for the Forum shows the order of presentation talks by the university teams, NASA presenters, and LPI presenters. Invited speakers included Mr. John Connolly of the NASA Johnson Space Center, Dr. Alex Ignatiev of the University of Houston, Dr. Michael Duke and Dr. Paul Spudis of the LPI, and Dr. Larry Kuznetz of the University of California, Berkeley.

The Forum was organized by Dr. Kathleen Johnson, Education Manager at the LPI. Other staff members at the LPI provided logistical, photography, and publications support. A special thanks and acknowledgment goes to Dr. Michael Duke for pioneering this stellar event.

Funding for the HEDS-UP Program was provided by the Office of Space Flight's Advanced Project Office at NASA Headquarters.

Kathleen Johnson
Education Manager
Lunar and Planetary Institute

CONTENTS

Omit To
P.11

AGENDA

May 3, 2001

7:30 a.m.	Continental Breakfast
8:30 a.m.	Welcome to LPI — Kathleen Johnson
8:45 a.m.	Michael Duke, Lunar and Planetary Institute — *"Future Goals and Initiatives for the HEDS Strategic Enterprise"*
9:15 a.m.	Paul Spudis, Lunar and Planetary Institute — *"Exploration of the Moon"*
9:45 a.m.	Alex Ignatiev, University of Houston — *"Construction of Solar Cells on the Moon"*
10:15 a.m.	Break
10:30 a.m.	University of Colorado, Boulder — *"Hyperbaric Chamber Pass-through Module"*
11:15 a.m.	Embry-Riddle Aeronautical University — *"Mars Communication Outpost"*
12:00 noon	Lunch
1:30 p.m.	Colorado School of Mines — *"Extraction of Water from Martian Regolith"*
2:15 p.m.	University of Maryland — *"Deep Space Human Space Station"*
3:00 p.m.	Break
3:15 p.m.	University of Washington — *"Mini-Magnetospheric Plasma Propulsion System for a Manned Mission to Mars"*
4:00 p.m.	Massachusetts Institute of Technology —*"Experimental Package for Paleontological Research on Mars"*
4:45 p.m.	Pennsylvania State University — *"Adaptive Robotics for Martian Exploration"*
6:00 p.m.	Poster Session and Reception

May 4, 2001

7:30 a.m.	Continental Breakfast
8:15 a.m.	Sharon Steahle, LPI —*"Logistics Dos and Don'ts (Or, How to Get Reimbursed for your Travel)"*
8:30 a.m.	University of Maryland — *"Crewed Rover for Lunar and Mars EVA"*
9:15 a.m.	University of California, Berkeley — *"Human Exploration of Mars"*
10:00 a.m.	Break
10:15 a.m.	Rowan University — *"Mars Mission Rocket Propulsion System"*
11:00 a.m.	Georgia Institute of Technology — *"Human Exploration of a Near-Earth Asteroid"*
11:45 a.m.	University of Washington — *"Closed Ecological System"*
12:30 p.m.	Lunch
2:00 p.m.	Embry Riddle Aeronautical University — *"Orbital Debris Collection System"*
2:45 p.m.	University of Colorado, Boulder — *"Project LaMar: Laser-powered Mars Rover"*
3:30 p.m.	Break
3:45 p.m.	John Connolley, NASA Johnson Space Center — *"Human Exploration of Mars"*
4:15 p.m.	Larry Kuznetz, University of California, Berkeley — *"More Than Mars, Much More"*
5:00 p.m.	Adjourn

May 5, 2001

9:00 a.m.	Continental Breakfast, Forum Evaluations
10:00 a.m.	Award Ceremony
10:30 a.m.	Adjourn
	Lunch and relaxation at Space Center Houston

The Forum

The Forum was a stimulating two-way exchange of ideas, with university teams presenting the results of their studies and NASA, industry, and others presenting recent advances in space exploration and plans for the future.

Dr. Kathleen Johnson, Education Manager at the Lunar and Planetary Institute, gave the welcoming address to the participants at the Fourth Annual HEDS-UP Forum.

Dr. Paul Spudis, Deputy Director and Staff Scientist at the Lunar and Planetary Institute, discussed the advantages to exploring the Moon in the near future.

Dr. Alex Ignatiev, professor at the University of Houston–Clear Lake, addressed the Forum on the construction of solar cells on the Moon.

Kathleen Johnson and Mike Duke officially welcoming students and faculty advisors to the Fourth Annual HEDS-UP Forum. Dr. Duke later spoke to the audience on future goals and initiatives for the HEDS strategic enterprise.

The Teams

The research team of the University of Washington, under the direction of Dr. Frieda Taub, studied a closed ecological system to support animal grazer populations.

Graduate students from the Georgia Institute of Technology, under the direction of Dr. John Olds, studied a possible human rescue mission to the asteroid 16 Psyche based on a failed Mars mission scenario.

The team members of Rowan University developed an insect-like rover named the MILLIPEDE, under the management of Dr. Eric Constans and Dr. Anthony Marchese.

The student team of Penn State, under the advisement of Dr. Mike Jacobs, proposed an asteroid mining mission.

Team members of the University of Colorado at Boulder designed a hyperbaric chamber pass-through mechanism, under the advisement of Dr. Kurt Maute.

The University of California students studied an advanced two-system space suit with direction from Professor Tom Budinger (department chair) and Dr. Larry Kuznetz (former NASA scientist).

The team members of the University of Washington presented missions to Mars incorporating the Mini-Magnetospheric Plasa Propulsion (M2P2) system under the direction of Dr. Adam Bruckner and Dr. Robert Winglee.

The JFEET Team from the Colorado School of Mines designed a system for water extraction from the martian soil, under the direction of Dr. Barbara McKinney and Dr. Bob Knecht.

NO IMAGE AVAILABLE

The University of Maryland graduate students contributed a design of a utility rover for research operations on Mars, advised by Dr. David Akin.

The team members of the University of Maryland developed the Clarke Station, an artificial gravity space station, under the advisement of Dr. David Akin and Dr. Mary Bowden.

The students of the Massachusetts Institute of Technology designed a Deployable Instrument Package for Paleontological Research (DIPPR), under the guidance of Dr. K. V. Hodges.

The students of the University of Colorado at Boulder presented Project LaMaR, a laser-powered Mars rover, directed by Dr. Lisa Hardaway of UC Boulder and Mark Henley and Dr. Seth Potter of The Boeing Company.
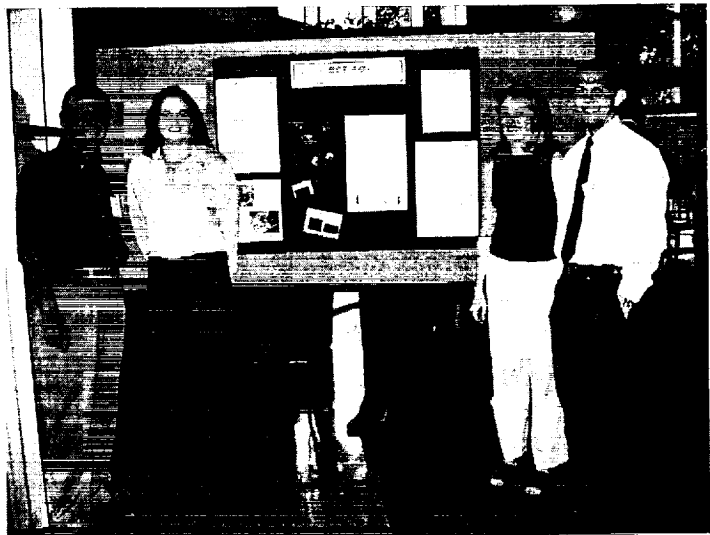
The team of Embry-Riddle Aeronautical University, directed by Dr. Mahmut Reyhanoglu, contributed a design of a martian communications outpost.

The Poster Session

Advisor Larry Kuznetz of the University of California, Berkeley, discusses one of the student research projects with judges Lewis Peach (USRA Headquarters) and David Gan (University of California, Berkeley).

The team from Pennsylvania State University shows off their asteroid mining proposal.

Rowan University and the MILLIPEDE.

A student and advisor use a few moments to revisit data and finalize their strategic plans.

The Winners

A panel of judges based their awards on both a written report and the oral presentation made to the Forum. And the winners are . . .

First place went to the University of Colorado's Project LaMaR team for their laser-powered Mars rover.

The University of Maryland team was awarded second place for the Clarke Station, an artificial gravity space station.

Team members from the Georgia Institute of Technology received the Outstanding Award for their asteroid rescue mission.

Water Extraction from Martian Soil

Colorado School of Mines
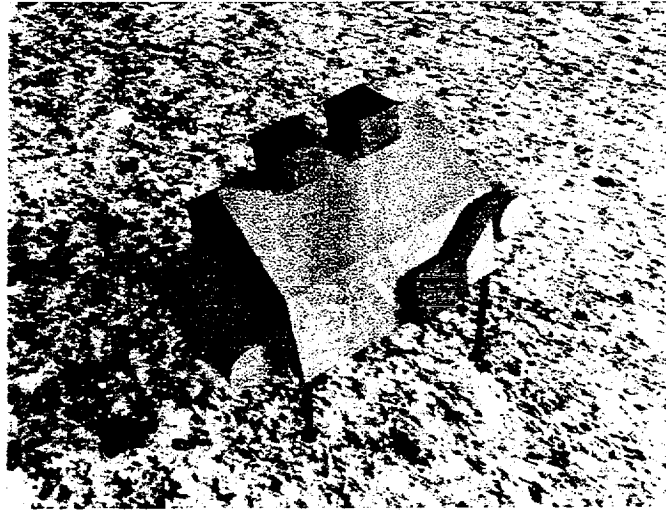
TEAM JFEET

Jordan Wiens
Forest Bommarito
Eric Blumenstein
Ellsworth, Matt
Toni Cisar

Advisors:
Barbara McKinney
Bob Knecht

1. ABSTRACT

With the projected growth in space exploration, several milestones have been set for future space programs. One milestone in particular is the landing of a human on the planet Mars. However, one major barrier to the successful placement of persons on Mars is a lack of water on the Martian surface. Because of the massive quantity of water that would be necessary for a mission to Mars, it is not possible to transport the amount necessary from Earth to Mars. Water would be necessary for human consumption as well as a base for jet propulsion fuel. Past unmanned missions to Mars, such as the Viking missions of the 1970's, have revealed the presence of small quantities of water in Martian soil. Research has determined that the water in the soil can be recovered when the soil is heated to a temperature between 200°C and 500°C. Team JFEET has designed a system with the capability to extract water from the soil of Mars, and then meter and deliver the water to a storage tank for later use.

The system uses simple concepts with few moving parts, creating a design that is reliable, efficient, and semi-autonomous. C.R.A.T.E.R., another design team from Colorado School of Mines, has designed a system that will provide the Martian soil necessary for process. This soil is placed on a conveyor belt that runs into a pressurized casing. A small motor attached to a sprocket on the belt's bearing, and placed at a downward angle in order to maximize gravitational assistance will automate the belt. The sand is transported into the casing where it is exposed to microwaves. These microwaves are emitted from two magnetrons attached to the roof of the casing. Microwaves are used to most efficiently free bound water molecules from the soil. From there, the vaporized water molecules will collect and condense on the roof of the casing. Once the water condenses, it runs down the roof into a gutter system that transports the water into a metering device. After the water is metered, it is siphoned into a storage unit. Power necessary for this process is provided by a silicon solar cell. The designed system meets NASA's and our physical and operational constraints, such as maximum mass and minimum water production rate (Table 1).

Team JFEET began in the spring of 2000 by evaluating several possible furnace systems to recover water from the Martian soil. The array of furnace systems devised had various energy sources, such as: the use of focused light, the thermal heating of soil in an oven apparatus, and the use of microwave energy. Each evaluated system had its own benefits, but most were outweighed by factors such as complexity or project specifications. After inspecting the various systems, it has been determined that a microwave energy based system presents the best possibility for success.

For the spring of 2001, team JFEET has continued to explore the potential of the original design. The microwave system provides the greatest efficiency, applies energy directly to the water, and has few moving parts. In addition to this, microwave energy based systems have a history of reliability. The efficiency of the system lies in the utilization of microwaves and internal power sources. The internal motor will be isolated from the harsh Martian environment thereby increasing its reliability. The appeal of microwaves is that they transfer energy almost entirely to the water molecules wasting little energy on the soil.

To achieve the goal of usable water on Mars, NASA requires a system capable of removing water from the soil. This system must be capable of operating reliably and maintenance free for at least 500 hours, storing the water, and must be powered by solar energy. The microwave system designed by Team JFEET presents the best chance for achieving this goal.

2. INTRODUCTION

The exploration of deep space is the final frontier for humankind. A plan to settle Mars is being researched at great lengths, but any human missions to Mars will require a water source for both process and human consumption. Due to the absence of free water on the Martian surface, NASA has expressed the desire to develop a unit capable of extracting water from Martian soil (Duke). This proposed design is capable of extracting water from Martian soil, metering the quantity of extracted water, and then delivering the water to a storage system for later use. The extraction system must operate autonomously with no on-site maintenance and be able to withstand acceleration forces of up to 5G. This system will operate in

conjunction with a previously designed soil collection system, which will provide soil to the extraction system. A design that presented the best possibility for success under the constraints given in Table 1 was chosen after considering and evaluating several potential solutions. Team JFEET has developed a system that incorporates microwave energy in conjunction with a conveyor belt mechanism to process soil and extract bound water. The system is referred to by code name: Microwave Pizza Oven (MPO).

Table 1: Specifications

SPECIFICATION	CLIENT REQUIREMENT
Maximum Mass	20 kg
Temperature Range	200°C to 500°C
Water Extraction	200g/hr
Operating Period	500hrs
Power Source	Solar Energy

Previous exploration missions to Mars, such as the Viking missions, have determined that water can be extracted from the soil if the soil temperature is increased to between 200°C and 500°C. These same missions also determined that water is present in the soil at approximately 2% by mass. Therefore, a system such as the MPO which is capable of heating the soil, collecting the water, and finally providing the water for storage is necessary if any future missions, especially manned missions, to the Red Planet are to be successful.

In continuation of our work in EPICS 151, Team JFEET has explored the potential of our previous reactor design. We previously researched various possibilities for accomplishing the required mission. Some possibilities included systems that utilized solar heating and/or conventional thermal heating. While these two methods of heating are simple and effective, they are also extremely inefficient when compared to a microwave unit. During the development of the various systems, the anticipated surface conditions in Table 2 were used in all calculations.

Table 2: Anticipated Surface Conditions (Hamilton, Williams)

SURFACE CONDITION	Range	
	Low	High
Temperature (C)	-123	37
Wind Speed (m/s)	0	30
Atm. Pressure (kPa)	0.60	0.81

The initial design, as seen on the cover page, contains five major subsystems: power source, conveyer belt, casing, magnetrons, and water metering. When continuing this research, we have focused on three subsystems (conveyor belt, casing, and magnetrons) in order gain a greater understanding of the overall design.

3. TECHNICAL PLAN

3.1 Description of Potential Designs

Several different designs were considered as possible solutions for the extraction of water when originally launching the project in the spring, 2000. All designs were analyzed and evaluated on the grounds of overall advantages, disadvantages, feasibility of design, durability of product, and ability to meet given design restrictions. During the evaluation of the designs, a numeric value was assigned to each category for each design on a scale of one to ten (with one indicating worst possibility for success and ten indicating best possibility for success). Tabulated results can be found in Appendix. Further details for

each potential design are outlined below.

Inclined Pipe:

Electrical heating elements would heat the soil as it passes through a rotating inclined pipe. Similar to a commercial kiln, soil is heated to release water. The released vapor would rise from the soil, travel along the inside surface of the inclined pipe then exit out the top of the pipe. The dehydrated soil would pass out the bottom of the pipe for disposal.

Kettle/Pot:

An enclosed vessel to heat the soil via conventional electric heating. Soil is placed into the kettle/pot where electric heating would increase the temperature of the soil to release water vapor. The released vapor is then collected and condensed into liquid water. The liquid water would then be measured and stored for later use.

Sifter:

Combination sieve and heating element that is used to heat soil. A bin above a sifting screen collects holds the soil. As the soil passes through the sifting screen, which is electrically heated, the soil temperature is increased to the point where water vapor is released.

Funnel:

Similar concept to that of the sifter method. A funnel design meters the flow of soil onto a conveyor belt. Conventional heating elements within the belt then heat the soil to release the water.

Conveyor Belt (Pizza Oven):

Used in conjunction with a soil metering system, such as the funnel, would carry the soil near heating elements that would heat the soil to release water vapor.

Focused Light:

Incorporates focused sunlight to concentrate the application of energy. The focused light would heat a portion of the soil to release water vapor.

Microwaves:

This design, unlike the other designs, does not rely upon the use of conventional thermal heating or the concentration of sunlight to heat the soil. High power radio waves (microwave energy) are used to apply sufficient energy to the soil to increase the temperature of the water, and thus generate water vapor. This method heats the water contained within a uniformly distributed flow of soil. The microwaves apply energy to the water directly, and don't require the direct heating of the soil unlike conventional heating methods.

3.2 Limitations of Designs

The pipe and pot options were eliminated based on the projected number of moving parts and total mass. The greater number of moving parts lead to a greater chance of mechanical failure, in addition to

increased time for engineering and development. Also, both design options used a conventional heating method (electrical). Conventional heating presents a much higher energy requirement than would be necessary with a non-conventional method, such as microwaves.

The team eliminated the sifter and funnel options because of the high potential for blockage, making the required one-year of maintenance free operation very unlikely. An additional subsystem to remove blockages would only create further complexity of the system. Again, both systems were dependent upon the use of conventional heating, which as stated above, has a lower efficiency than that of microwave heating.

Based on the complexity of the system to perform reliably for the required amount of time without on-site maintenance and adjustment, we eliminated the focused energy option as a possible solution. Team JFEET felt that the research and development necessary to design a system that could reliably deploy a solar collector and continuously adjust the position of the collector was prohibitive at this time.

Ultimately, Team JFEET chose the design that incorporated microwave energy for the energy source in combination with a conveyor belt mechanism to move the soil. Microwave energy has higher efficiency, and unlike the other systems, has the ability to heat the water independently of the soil (Bloomfield). Some energy applied to the water will be lost to the soil through conduction, however this loss is minimal when compared to the energy that would be required to heat the soil then heat the water. The MPO will compensate for the energy losses by increasing the energy output of the microwaves. The conveyor belt method allows for a continuous flow of soil, and is not as susceptible to blockage, like the sifter or funnel methods. The primary energy source for the generation of microwave energy and part-time driving force of the conveyor belt will be solar energy. Though Martian days are a few minutes longer than Earth days, day light times are approximately equal therefore calculations can be based on Earth days. Because of the requirement that the system use solar power all calculations for MPO operation were performed assuming 12 hours per day of operation, along with 12 hours per day of idle time when the MPO will be in darkness.

Past research has shown microwave energy as a possible solution for the generation of water on Mars. Microwaves, unlike conventional thermal heating methods, have the advantage of being tunable, so that most of the energy is used to heat the water and not the soil. Microwave ovens have been determined to be quite reliable, having the potential of operating for ten years or more without requiring maintenance (Zurbin).

The major drawback encountered in project continuation is the hazard of microwaves. The primary health effect of microwaves is thermal effects. Microwave frequencies produce skin effects; however the radiation may penetrate the body and be absorbed in deep body organs without skin effect, which is the warning sign. Without a warning sign prolonged exposure to microwaves could prove dangerous, if not fatal (OSHA). Because of the potential safety hazards that come from working with microwaves, it has been decided that a working magnetron is not a priority of team JFEET, at this stage in our design. After inspection of the initial design it was determined that focus should be placed on the design of the microwave energy unit, the belting apparatus and the water collection subsystems. Table 3 below is a decision matrix outlining the different methods of evaluation for each subsystem.

Table 3: Decision Matrix

	PROS	**CONS**
Microwave: Theory	Low cost, less work, build off of proven knowledge	Less understanding, no working model
Microwave: Experimentation	More work, better knowledge for presentation	Dangerous, high cost
Belt: Theory	Free, less work, proven equations	Less understanding, no fabricated belt for presentation
Pre-made Belt: Experimentation	Easy, verifiable performance, possible manipulation	High cost, may not fit prototype, limit control over design
Home-made Belt: Experimentation	Understanding of working model, control over all construction aspects	Large amount of work, moderate cost
Water Collector: Theory	Free, less work, proven equations	Less understanding, no fabricated collector for presentation
Water Collector: Experimentation	Understanding of working model, control over all construction aspects	Large amount of work, moderate cost

Based on this matrix, the microwave will be inspected by theory, due to extreme health hazards associated with working with microwave radiation. Theory will be integrated into the belt construction in order to develop an operational subsystem, while the water collector design will be expanded from the theoretical equations. Varying each one of the belt variables while leaving the others constant will be conducive to determining the most efficient belt design.

4. CONVEYOR BELT

Though an overall basic component, the conveyor belt subsystem has many details that must be considered when looked at more closely. In order to most efficiently expose the soil to the microwaves, and thus extract the water contained, a conveyor belt was the best option. The belt, originally designed to be entirely gravity driven, has now been equipped with a small internal motor, allowing the speed of the belt to be automated and regulated. This modification also allows the amount of time the soil is exposed to the microwaves to be precisely set. The belt is still placed at an angle in order to provide gravitational assistance.

When initially designing the belt several variables were discovered, each needing to be optimized in order to maximize both belt and overall system efficiency. Variables include belt length, belt width, soil support, and the angle the belt will be held at. After examining each separately, it became apparent that all variables seemed interdependent. Separating one variable from the rest required looking outside the scope of the belt subsystem. The solution came from microwave experimentation, which determined that maximum heating efficiency would occur with a minimum soil thickness. Relating this information back to the belt subsystem, the soil support was selected. Rather than the original plan calling for ledges, a roughly textured belt now suits the operation better. Knowing soil thickness, along with total necessary soil throughput, the width and total length of the belt could be calculated. A width of .229m and a total length of .457m were chosen to keep the system compact while at the same time allowing the subsystem to be integrated easily with the casing. Soil thickness also determined belt angle based upon the angle of repose, which is the angle at which the sand would begin sliding down the belt. Therefore, a downward

angle of 30° was chosen because anything beyond that would prove to be too steep.

In order to process 10.0kg of soil per hour, the belt needs to run at a speed of 13.8m/min. Using equations obtained from the literature, a portion of the power necessary to drive the belt will be provided by the gravity, even though the gravity on Mars is 3.69m/s², only about 1/3 that of gravity on Earth (Mulhern Belting). A 9-volt motor equipped with a small gear has been included in order to better regulate the belt speed. The gear on the motor will be linked with a chain to a larger gear on the belt bearing. The difference in gear sizes provides a favorable gear ratio for high torque, limiting strain on the motor.

Another feature of the belt is that it must be able to withstand both extremely high and low temperatures that will be present during operation. While the belt will be exposed to extremely high temperatures inside the system through heat conduction from the soil, it will also be exposed to the volatile conditions of the Martian environment. Working with this constraint, the belt chosen must be microwave save, that is, the microwaves must not heat it. That would most likely alter the belt's chemical properties.

The conveyor belt will be attached to the frame of the furnace by two metal rods running through each of the rollers, and two support rods extending from one roller to the other. That is the only way that the belt is connected, but it is an integral part of the system. It runs the soil through the system and provides a fresh flow of dirt, which allows the operation to take place. In essence, the belt controls the flow and amount of soil that runs through the microwaves, so it actually determines that the specifications for the system are met.

5. MICROWAVE

The JFEET team decided to use microwave energy to extract the water in the Martian soil and the water that is chemically bound to the soil. Advantages over other methods include the specific items listed below.

- Greater efficiency than a thermal energy source
- Directly heat the bound and unbound water while not wasting energy by heating the soil
- Moving parts are minimal in number
- High reliability
- No warm-up period, instant on—instant off
- Energy is not attenuated by atmosphere

5.1 Calculations

The following are assumptions made when performing calculations for the magnetron section of the water extraction unit.

Table 5: Design Assumptions

Duty Cycle	12hrs on/12hrs off
Mass flow rate:	0.400 kg/hr 20.0 kg/hr
Specific Heat (Cp):	4.20 kJ/kg•C
Temperature Change	500°C
Mass of Magnetron	5 kg to 8 kg

*For the purpose of calculations, mass values for "sand" were used (Cengel).

Using the above assumption and the First Law of Thermodynamics, the power requirement from the magnetron section was calculated to be 2.4kW from Equation 3 below.

Equation 1 (Eq. 1), The First Law of Thermodynamics:

$$\sum \dot{m}_i (h_i + \frac{1}{2}v_i^2 + gz_i) - \sum \dot{m}_e (h_e + \frac{1}{2}v_e^2 + gz_e) + Q + W = \frac{dU}{dt}$$

By assuming steady state and negligible elevation change, the Equation 2 (Eq. 2) is derived from Eq. 1:

$$Q = \dot{m}(h_e - h_i)$$

To determine the amount of energy required to fulfill the parameter constraints, Equation 3 (Eq. 3) was used:

$$Q = \dot{m} C_p (T_e - T_i)$$

If the initial soil temperature was greater than 0°C, less power would be required (See Reference Table 2). With a lower power requirement, either less electrical power would be required, or more mass could be processed. Thus heating the water in the soil requires approximately one half the amount of energy necessary than if using electrical thermal heating. The use of electrical thermal heating would require the heating of the soil, which would then heat the water, while microwaves are capable of heating the water directly. Some energy will be lost to the soil due to conduction; however even with the energy loss the energy requirement is still less then that from the electrical heating method.

Due to the low atmospheric pressure on Mars (0.7 kiloPascals on average) and the low temperatures at night, the possibility of the system being at the triple point during operation had to be considered. By setting the time of operation during the daylight hours, this possibility had an extremely low probability of occurrence due to the high temperature during the daylight hours (averaging 40°C). In addition to working in the daylight, the system will be in a pressurized casing and that will reduce the chances of triple point occurring even further.

5.2 Experimentation

To research the potential of release bound water using microwaves, experiments were conducted with nickel sulfate (VI), a compound containing six bonded water molecules. Nickel sulfate is bright green in color and when the water is released, the substance turns pale green. For the first experiments, nickel sulfate (VI) was tested to determine if microwaves released the energy level required to free both the bonded and unbound water. In the subsequent experiments, tests were performed using varying depths to determine the required time for full penetration (explain). All of the experiments were conducted in a household microwave, and the results of all tests can be found on Graph: Nickel Sulfate (VI). Time Experiments were grossly over simplified in that focused magnetrons were not used. Use of scattered microwaves as opposed to focused microwaves means the graph would not be valid under actual model conditions. The main goal of the experiments is to show that microwaves will release bound water.

Penetration time vs. thickness
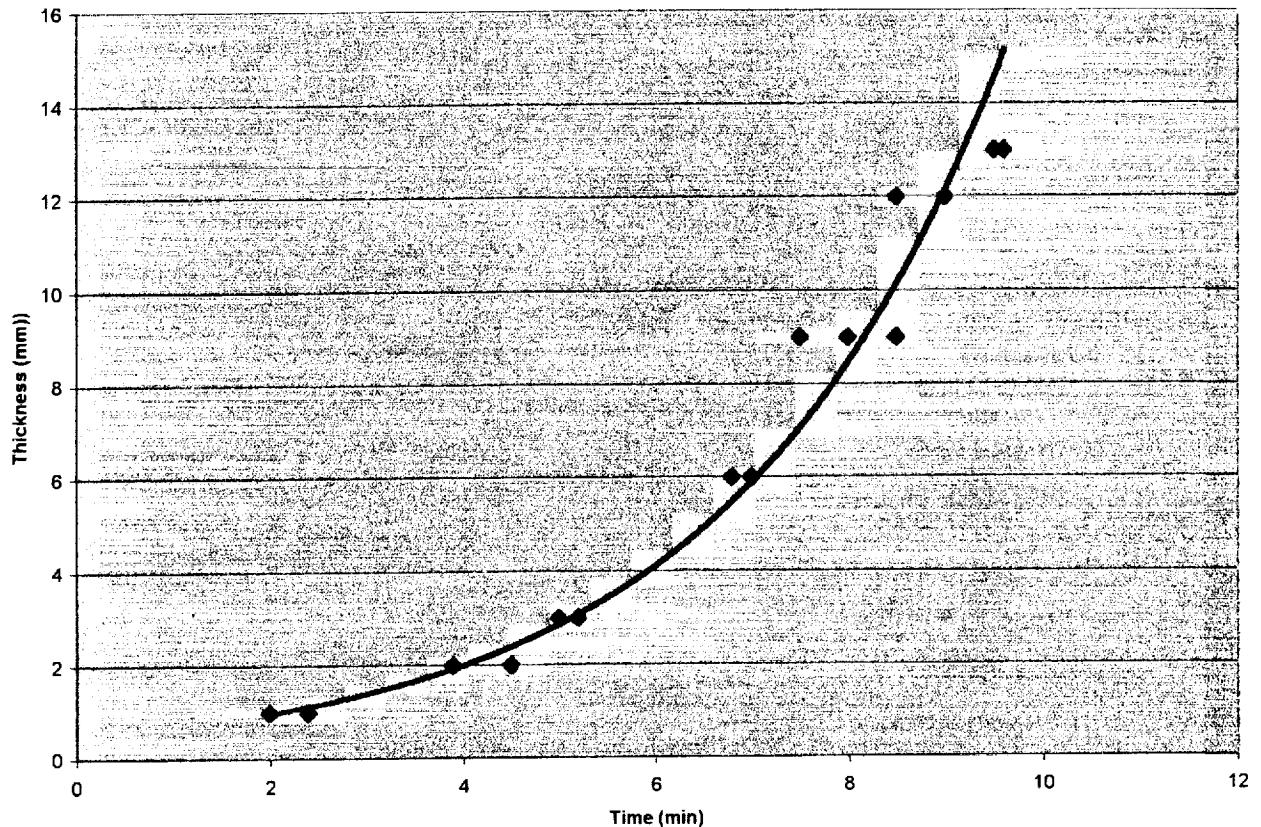
Graph: **Nickel Sulfate (VI) time Experiments**

From the graph it is possible to see the relationship between the full penetration time and the thickness of the nickel sulfate (VI).

5.3 Results

Experiments prove that water can be released from a bound state by using microwave energy. This fact is important because with no water release this design is not feasible. As stated before, there are huge differences in conditions of the experiment and conditions that the model would see. Use of actual focused magnetrons on samples is too dangerous at this point but in later research the actual magnetrons will be necessary. In the future Team JFEET would like to begin working with the magnetrons and finding the differences in absorption with respect to different materials. Finding the amount of efficiency gain versus conventional heating would also prove to be an interesting idea to explore. Not only would the results of those future experiments prove useful in this application but aid many other industrial applications outside of the space program. The microwaves are what make this design efficient and it is very important to quantify that efficiency in the future.

5.4 Interface

The microwave subsystem will provide the energy source necessary to increase the temperature of

the water to at least 500°C, and thus release it from the soil. The two magnetrons will be mounted in series above the conveyor belt near the end of the heating compartment closest to the entrance, which will allow for a condensation section in the compartment opposite to the magnetron section.

The microwave unit will operate at kilowatts at 2.45 GHz. This frequency was chosen because it does not interfere with the electromagnetic spectrum and also contains convenience in implementation. The condensation section will provide and area for the water vapor to cool and condense for collection. To prevent water vapor from entering the magnetron assembly, the magnetron output will be covered with a protective panel transparent to Rf energy in the range of 2.45GH, which will prevent the possibility of corrosion or shorting of the magnetrons caused by the water or water vapor. The magnetron will receive electrical power via an electrical distribution system from the solar panel subsystem. Use of microwaves within the metal casing should not present a problem. The metal casing would simply reflect the microwave energy before it is absorbed by the water within the soil.

6. CASING

Water collection is one of the most important parts of the entire system. The basic functions of this subsystem is to trap and condense free water vapor, and then collect the water in liquid state and carry it off to storage. The first step in this process involves heating of the water stored inside the soil, causing evaporation. The evaporated water will condense on the ceiling while the soil is moved through the casing and dumped off the system by the conveyer belt. The casing will allow evaporated water to condense on the ceiling and run down the sides. The walls of the system will be strategically positioned such that the water will pool and be collected on the sides by a gutter system and run to the back right side of the casing. Once collected, the water will run through a measuring device and into the storage tanks. Though the theory of this water collection process is sound, experiments need to be done in order to fully understand the process.

The casing is to be constructed with lightweight sheet metal coated with white enamel. The sheet metal will best withstand large temperature fluctuations and supply a durable covering for our water extraction system. Likewise, the white enamel is applied to the metal in order to best work with the metal to reflect the microwaves inside, therefore increasing the intensity of waves on the soil. Initially, the casing will be seven flat pieces of sheet metal. The enamel coating will also help prevent corrosion of the casing due to the presence of water vapor. Each piece is to be welded together for strength. The assembled casing will then be welded to the second and fourth axles of the conveyer belt. This assembly will allow approximately 15cm of overhang between the conveyer belt and casing, which is ample room for the input and output of soil. The magnetrons will also be welded in the slots on top of the casing. Finally, metal gutters will be welded inside the casing. The gutters will collect the condensed water and carry it to one corner of the case. For this to happen, one gutter must be sloped 6°, and the short gutter above the belt exit is sloped 8° so gravity will move the water to the water metering sub-system. The external dimensions of the entire water extraction system are 23cm wide, 30cm long, and 25cm high. The dimensions exclude a layer of insulation around the casing system. Further research is recommended for insulation appropriate for the surface conditions of Mars.
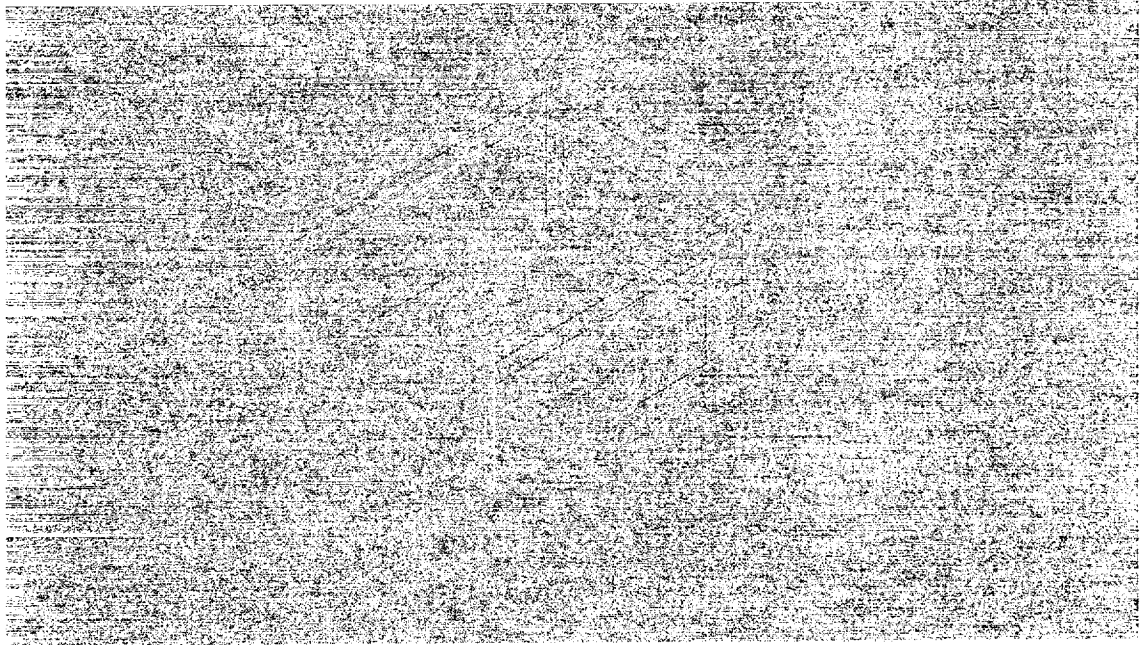
6.1 Experimentation

Experiments were performed to test whether or not the water would actually collect on the ceiling and run down the sides.

- Using plexi-glass, a simple case design was constructed that resembled the actual project casing.
- Construction of the casing was such that the angles at which the roof panels were aligned could be adjusted
- Water was boiled under the plexi-glass to simulated the evaporated water which would be released from the soil
- Roof angles were maximized so that water could run down the sides of the casing without "raining" on the cooking dirt below

6.2 Results

After multiple trials using multiple angles, the ideal angle for the plexi-glass to have is a 90-degree angle between the separate pieces, which yields a 45° angle for each piece in relation to the vertical.

The ends of the casing need to be securely enclosed as to not let any evaporated air to escape and hinder the entire purpose of the project. The condensing water will not "rain" at the 45°angle. It will take time for the evaporated water to condense enough on the ceiling for it to run down the sides to the storage tanks.

After completion of experimentation, results show that this subsystem will indeed be capable of integration into the final system. The theory is complete, and the experimentation procedures uphold the theory. The extensive experimentation now provides the data necessary needed to properly construct the entire system. Conclusions have also been made stating that the material that the collection system is constructed out of will play a vital role in the actual ability to have the water condense. The whole casing system as well as the rest of the oven will be in a pressurized environment. This allows the water to condense under the set conditions of the regulated environment. The 20g of water per hour will be measured and stored in tanks provided, while the 10kg of soil per hour are cycled through casing by a conveyer belt run off gravity and a small motor powered by solar energy.

6.3 Potential Obstacles

As engineers, JFEET is obligated to explore some of the potential obstacles that might be encountered with the water collection system. The main foreseen obstacle is creating the idealized

pressurized environment. The amount of power needed to create such an area could provide problems. So alternatives, such as allowing the water vapor transform to ice, have been considered. This idea would be implemented if pressurization of the entire system proves infeasible.

7. WATER METERING AND TRANSPORTING SYSTEM

Initial specifications require the ability to collect, measure, and provide for storage the water that is extracted from the soil. The collection process will be accomplished with a set of gutter that will mount inside the system case. The collected water in the gutters will be passed via a flexible plastic tube that will run along the outside of the casing to a small compartment that is attached to the outside of the main case. This small-attached case will be of the same material as the main casing. A slightly smaller container is enclosed that will hold the water and then eventually release it for metering. The holding tank will be in the shape of a trapezoidal prism. The trapezoid will have a long height of 7cm, a short height of 5cm, a width of 5cm, and a depth of 2cm. The top edge of this prism is horizontal, therefore perpendicular to the vertical sides. That leaves the bottom of the prism to slope downward for a vertical drop of 2cm. The tank will hold 50g of water before emptying each time. To comply with project specifications, which call for 200g of water per hour, the holding tank will empty approximately four times per hour while the system is operating.

The water will exit the holding tank using the principles of siphoning. "A siphon is an instrument, usually in the form of a tube to form two legs of unequal length, for conveying liquid over the edge of a vessel and delivering it at a lower level. The action depends upon the influence of gravity (not on the difference in atmospheric pressure) and upon the cohesive force that prevent the columns of liquid in the legs of the siphon from breaking under their own weight" (Britanica). A small tube will be attached to the low point of the holding tank and run vertically up the outside of the front surface. At a distance of 1.5cm from the top of the holding tank the tube will pass through a ring protruding from the front surface. After passing through the ring, the tube drops vertically passed the bottom of the holding tank and continues down to the storage tanks.

As the holding tank fills with water, the water level in the tube rises equally. When the water level in the holding tank rises to the apex of the inverted U in the tube, the water will begin to flow down the long end of the tube. This will create a siphon effect and drain the entire tank of water into the storage tanks. To calculate the quantity of water stored, the number of times the tank empties needs to be counted.

A switch device, which consists of a 5mm diameter, hollow, plastic, spherical float, a 3.5cm bent plastic rod, a pivot point, and two gold electrical contacts, will count each time the tank empties. The float is connected to one end of the bent plastic rod and floats along the top of the water level inside the holding tank. The bent rod is positioned over the center point on the top edge of the back surface at the rod's bending point. The rod is attached by, and pivots around, a pin running through the rod's bending. The rod, bent at a point 2.7cm from the end, is attached to the float, extending the rod 0.8cm outside the holding tank. The rod is bent to an angle of 70° from the horizontal at the pivot point. At this time the actual metering portion of the system will be introduced, working with an electrical circuit.

A gold wire, which comes from a circuit board, is coiled around the short end of the plastic rod. A gold contact surface will be attached to the center of the back surface of the holding tank 7mm below the pivot point. Another gold wire is attached to this contact surface runs to the aforementioned circuit board. Gold was chosen because of its high electrical conductivity and resistance to corrosion. Every time the water tank approaches its full point, the float will rise with the water level and, in turn, move the outer arm of the bent plastic rod towards the gold surface on the back surface of the holding tank. When the water level reaches its maximum height, the gold wiring on the plastic rod and the gold surface on the back of the holding tank will be in contact. Each time the two gold materials separate, the electrical circuit is broken and that will break the signal that is being received at the circuit board. The circuit board will be able to count the electrical impulses and multiply it by the capacity of the holding tank, thus finding the amount of water collected.

8. OUTREACH

In the spring of 2000, Team JFEET presented the MPO design in a school-wide competition. Among those in attendance were EPICS students as well as other Colorado School of Mines students, CSM faculty and staff, and field specialists. In winning that competition the team was given the opportunity to continue with the development of the water extraction unit. Utilizing information learned from that experience, the team modified the design and increased the understanding behind certain key concepts. The team also met with engineer Darren Clark from Lockheed Martin. This visit gave better ideas of what an engineer in the aerospace industry thought of the feasibility of the project. Team JFEET has been working in conjunction with last year's representatives from the Colorado School of Mines, C.R.A.T.E.R., to integrate the EPICS program at CSM. Just recently a public presentation was held at CSM where Team JFEET, C.R.A.T.E.R., and other similar projects were presented. In attendance were CSM faculty, Mike Duke and his colleague, and the other EPICS groups. It is important to embrace community involvement in and around the Colorado School of Mines area, all of these endeavors have allowed Team JFEET to do that.

9. CONCLUSION

Team JFEET has designed a system, referred to as the MPO, capable of extracting water from the soil of Mars. The MPO meets design constraints for mass, water production, durability, while microwave energy to extract water from the Martian soil in the most efficient manner. The MPO design minimizes the number of moving parts, has high reliability, and most importantly does not waste power by heating the water and soil indiscriminately, as would be the case with electrical thermal heating of the soil.

Heating of the soil with microwaves is accomplished with electrical energy provided by silicon solar cells. The silicon cells greatly increases the quality the overall system by providing a reliable source of high-output energy. High-energy output is important due to the length of daylight at the equator of Mars, where the MPO is expected to operate.

The soil will be processed with the use of a conveyor belt mounted on an angle to take advantage of gravity assistance. The recovered water vapor will be condensed and delivered to the water metering and transport subsystem. The water metering and transport subsystem utilizes the basic principles of siphoning to measure the water collected. There is only one moving point in the subsystem, the float and plastic rod, which helps decrease the chance for error. A siphon depends on the natural force of gravity, and although the gravity on Mars is less than that of Earth's, it does not have a significant enough effect to change the siphon system.

A microwave-based system is capable of heating the water directly, and does not heat the soil. Therefore, the microwave energy is applied to the water, which is then heated to the required temperature. Due to conduction of heat, some of the energy in the water will be lost to the surrounding soil, but this loss is believed to be less with the microwave system than with other forms of conventional heating. Ultimately, the best choice for a water extraction system is one that uses the least amount of moving parts, has a high history of reliability, directly applies energy to the material, and has a high efficiency. Taking these requirements into consideration it becomes apparent that Team JFEET's MPO is the best selection.

Overall, our system will have a mass of less than 20kg and produce 200g of water per hour.

10. FUTURE STUDIES

The experimentation up until now has been limited to crude models at best. Pending results of this competition the next step would be to seek outside funding that would enable project continuation. Ultimately Team JFEET would like to create a prototype and model it in Martian like conditions. This is the only way to prove the true effectiveness of the design. To this point research, theory, and basic experiments have been driving the current design. The contrast of theory and reality is huge and can only be realized by building a prototype. Once a working prototype is completed, advanced experimentation can commence, revealing the strengths and weaknesses of the design.

REFERENCES

Cengel, Yanus, Boles, Michael. Thermodynamics: An Engineering Approach, 3ed McGraw-Hill: Boston, 1998.

Litton Systems, Inc. "Litton Magnetron Specification." http://www.littoned.com/magweb_table.html. (March 27, 2000).

Bloomfield, Louis A. "How Things Work: Microwave Ovens." University of Virginia. http://rabi.phys.virginia.edu/HTW//microwave_ovens.html.

Robert Zubrin. The Case for Mars. Touchtone: New York, 1996.

Calvin J. Hamilton. "Views of the solar System." http://plantscapes.com/solar/eng/mars.htm (January 20, 2000).

G.A. Lundis and J. Appelbaum, "Photovoltaic Power Options for Mars," http://powerweb.grc.nasa.gov/pvsee/publications/mars/marspower.html, (March 27,2000).

B.I. McKissock, A Solar Power System For an Early Mars Expedition. National Aeronautics and Space Administration: Washington D.C., 1990.

G.A. Lundis, "Mars Dust Removal Technology," http://powerweb.lerc.nasa.gov/pv/SolarMars.html, (March 27,2000).

Mulhern Belting, "Belting Construction & Styles," Professional Belters: New Jersey. http://www.mulhernbelting.com/styled.htm. (April 5, 2000).

KVP Falcon, "Conveyor Belting," Plastic Belting Specialists: Oklahoma City. http://www.kvpfalcon.com/engineering/pdf_kvpf/is61000_1.pdf. (April 5, 2000).

David R Williams. "Mars Fact Sheet," NASA Goddard Space Flight Center: Greenbelt. http://nssdc.gsfc.nasa.gov/planetary/factsheet/marsfact.html. (April 5, 2000).

http://www.britanica.com/bcom/eb/article/3/0,5716,69733+1,00.html. (March 28, 2000).

Mike Duke, NASA Consultant, School of Mines Lecture. (January 19, 2000).

Daniel Winterhalter. NASA Jet Propulsion Laboratory, Pasadena, CA. http://quest.arc.nasa.gov/qchat_survey. (February 23, 2000).

APPENDIX

Decision Matrix

	Advantages	Disadvantages	Feasibility	Durability	Restrictions	Total
Inclined Pipe	Few moving parts, continuous operation, easy to collect vapor	mass	8	7	bulky, 7	22
Kettle/Pot	Simple, few moving parts, easy to get rid of, amount vs. time	insulation, high energy	8	8	mass, 6	22
Sifter	No moving parts, simple	soil clog, high temp, work fast	5	8	soil flow, 4	17
Funnel	No moving parts, simple, small amt. of soil to heat	clogging, collecting H20	8	7	rock size, 6	21
Conveyor Belt (pizza oven)	Continuous operation, soil output	energy intensive, moving parts	6	4	energy, 5	15
Focused Light	Solar energy, high temp for small area	night operation, setup & alignment	3	6	sunlight, 6	15
Microwave	Compact	energy needed to operate	8	9	energy/mass, 7	24

S2/CP/IN/90

Asteroid Rescue Mission

Georgia Institute of Tech nology

Team Members:
Stephen Izon
Tim Kokan
Steven Lee
Jeff Miller
Randy Morrell (Team Lead)
Dave Richie
Reuben Rohrschneider
Sebastien Rostan
Eric Staton
Dr. John Olds (Faculty Advisor)

Abstract

This paper is in response to a request for papers from the Lunar and Planetary Institute in Houston, Texas as part of a National University Competition. A human rescue mission to the asteroid 16 Psyche was designed based around a failed Mars mission scenario. The scenario assumed the second human Mars mission, based on the Mars Design Reference Mission 3.0, failed to propulsively capture into Mars orbit, resulting in a higher energy trajectory headed towards the asteroid belt on an intercept trajectory with 16 Psyche. The task was to design a mission that could rescue the astronauts using existing Mars mission hardware prior to the failure of their life support system.

Analysis tools were created in the following six disciplines for the design of the mission: trajectory, propulsion, habitat and life support, space rescue vehicle and earth reentry vehicle, space transfer vehicle, and operations. The disciplinary analysis tools were integrated into a computational framework in order to aid the design process. The problem was solved using a traditional fixed-point iteration method with user controlled design variables. Additionally, two other methods of optimization were implemented: design of experiments and collaborative optimization. These were looked at in order to evaluate their ease of implementation and use at solving a complex, multidisciplinary problem. The design of experiments methodology was used to create a central composite design array and a non-linear response surface equation. The response surface equation allows rapid system level optimization. Collaborative optimization is a true multidisciplinary optimization technique which benefits from disciplinary level optimization in conjunction with system level optimization. By reformatting the objective functions of the disciplinary optimizers, collaborative optimization guides the discipline optimizers toward the system optimum.

The size and complexity of this design led to severe problems for the advanced optimization methods. The design space was non-smooth, multi-modal, and highly non-linear. Gradient based optimizers could not dependably gather gradient information or find their way out of local minima. Response surface methods produced poor results due to the non-quadratic nature of the design space. Therefore, the traditional fixed-point iteration method proved to be the most easily implemented and produced the best results.

1 Introduction

1.1 *Purpose*

This paper, in conjunction with the presentation given at the Lunar and Planetary Institute (LPI) in Houston, Texas in addition to several out-reach programs, is part of a National University Competition sponsored by LPI. The competition is an open-ended competition in which the competing universities are allowed to choose their project to design. The only constraint placed on the project is that it must be applicable to the Human Exploration and Development of Space.

The design proposed by the Spacecraft and Launch Vehicle Design class at the Georgia Institute of Technology is a human mission to a near Earth asteroid.

This paper out-lines the process that was used by the Georgia Institution of Technology design team in the design of a manned vehicle to travel to an asteroid in the main asteroid belt. This paper has two main focuses. The first major focus is on the individual tools that were developed specifically for this project in the following areas: trajectory, propulsion, habitat, space rescue vehicle /Earth return vehicle (SRV/ERV), space transfer vehicle (STV), and operations. The second focus is on the method of optimization that was employed by the design team in order to develop a converged design that would meet the mission success and time constraints while maximizing safety and minimizing cost.

1.2 *Disaster Scenario*

It is the year 2020 and the second manned space vehicle has been sent to Mars, carrying an international crew of six. A malfunction occurs during the vehicle's voyage, causing the vehicle to swing by Mars, hurtling through space towards the asteroid belt. They have no way of returning home using available hardware, and the length of time their food supply and life support system will last is limited. The design presented herein is in response to these events, aimed at a mission intended to rescue the crew from the asteroid belt and return them safely to earth. The ill-fated mission is part of the Mars Design Reference Mission so a brief description of the this is given in the next section, followed by a detailed description of the actual disaster.

1.2.1 Design Reference Mission

The Mars Design Reference Mission (DRM) is a product of the NASA Exploration Study Team. The DRM was last amended in June of 1998. The DRM has two primary roles. First, it serves as a template to which alternative approaches to the human exploration of Mars can be compared and contrasted. Second, it is intended to stimulate additional ideas and further progress in exploration. For this design, it is assumed that the DRM has been implemented into NASA's space program and that actual manned missions to Mars are taking place.

The DRM can be broken down into a single mission architecture, which is comprised of the following sequences of events:

1. In the first launch opportunity, two cargo missions are launched to Mars; one cargo vehicle carries a lander with a propellant production plant and ascent vehicle, the other carries an earth return vehicle. Each cargo mission requires the use of two Magnum launch vehicles.
2. The cargo lander lands on the surface of Mars where the propellant production plant produces and stores methane and liquid oxygen from the Martian environment. The Earth return vehicle enters into Mars orbit.
3. In the second launch opportunity, which is generally about twenty-six months after the first launch opportunity, the crew transit vehicle is launched. This vehicle carries along with it the crew lander. This also requires two Magnum launch vehicles. The crew reaches Mars in 130-180 days on a fast transit trajectory.
4. The crew performs various scientific activities on the surface of Mars for approximately 520-580 days.
5. The crew then uses the ascent vehicle from the previous launch opportunity (which now has stored enough locally produced methane and LOx for ascent) to rendezvous with the earth return vehicle that is waiting in Mars orbit.
6. The crew returns to earth on a 130-180 day fast transit trajectory

According to the DRM, two cargo missions would also be launched in the same year as the second launch opportunity of the previous mission, and another crew transit vehicle would launch in the following launch

opportunity. One complete mission architecture is comprised of two cargo vehicles launched in one opportunity and one crew transit habitat launched in the following opportunity. Each mission architecture requires a total of 6 Magnum launch vehicles spread over two launch opportunities.

1.2.2   Disaster Events Timeline

December, 2020

Two cargo vehicles were launched on May 11, 2018 as support for the second manned mission to Mars. A crew transit vehicle departed for Mars on July 29, 2020. The crew vehicle is scheduled to perform a propulsive capture into Mars orbit and descend to the surface in the crew lander on December 6, 2020. However, as the crew vehicle approached Mars, one of the reaction control thrusters on the transfer vehicle failed and the crew was unable to achieve the correct orientation for a propulsive capture into Mars orbit.

Since the main engine could not perform the deceleration ΔV at Mars, the spacecraft completed a Mars swing-by and hurtled towards the asteroid belt. The swing-by at Mars provided an increase in velocity of 2200 m/s, creating a higher energy heliocentric trajectory that does not encounter the Earth at any time. As a result, NASA mission control decided to have the spacecraft prepare for a safe landing on an asteroid. This is done in order to minimize the difficulty of rendezvous and rescue.

The best candidate asteroid in terms of location and relative velocity to the spacecraft is asteroid 16 Psyche. Psyche was chosen since it will lie near the spacecraft's current trajectory while also having a velocity vector close enough to that of the spacecraft. The spacecraft will then use the Mars lander's propulsion system to perform a soft landing on Psyche. The spacecraft will travel for 372 days until encountering Psyche and performing a propulsive ΔV to land.

Table 1-1: Disaster Trajectory Characteristics

Variable	Value	Units
$\Delta V_{Gravity-Assist}$	2242	m/s
Eccentricity - ε	0.419	
Aphelion Radius - r_a	3.190	AU
Perihelion Radius - r_p	1.307	AU
Semi-Major Axis - a	2.249	AU
Period - P	1232	Days
$TOF_{Mars->Psyche}$	532	Days
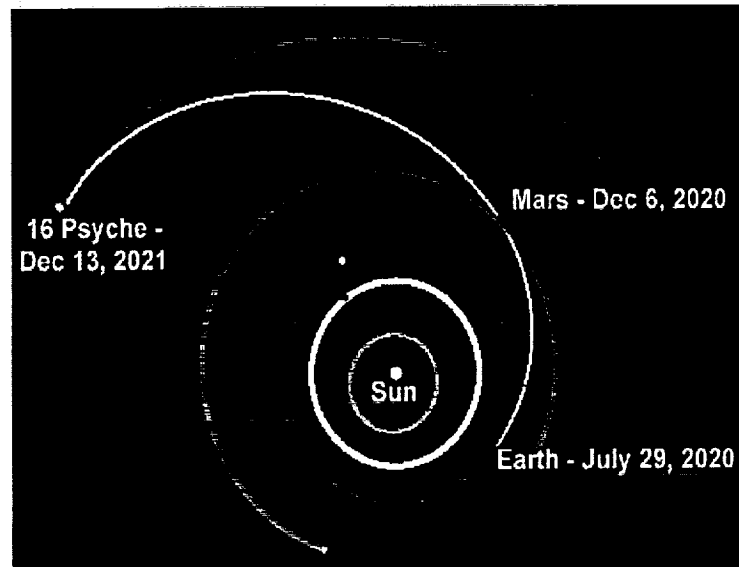
Figure 1-1: Disaster Trajectory Picture

1.2.3   Disaster Trajectory

After the swing-by of Mars, the crew gains velocity and begins an eccentric orbit through the asteroid belt. Table 1-1 provides the characteristics of the new disaster trajectory after the gravity-assist around Mars. Figure 1-1, is a picture of the disaster trajectory from launch at Earth, through the gravity-assist around Mars, to intercept of the asteroid Psyche.

1.2.4   Asteroid Physical and Orbital Characteristics

Psyche is an M-class asteroid composed primarily of a nickel-iron compound. The semi-major axis of Psyche is nearly twice that of Mars, and the orbital period is 5.0 years. Psyche is chosen as a good asteroid to intercept because it has a relatively small eccentricity and inclination as compared to other candidate asteroids. This means that a rescue mission to Psyche will require a smaller total ΔV than one in which a large motion outside of the ecliptic plane is required. Table 1-2, below, provides the physical and orbital parameters of Psyche.

Table 1-2 Physical and Orbital Parameters of Psyche

Physical Parameters of Psyche			Orbital Parameters of Psyche		
Parameter	Value	Units	Parameter	Value	Units
Diameter	253.2	km	Semi-Major Axis - a	2.923	AU
Rotational Period	4.2	hr	Period - P	5.00	Years
Density - ρ	8000	kg/m^3	Eccentricity - ε	0.139	
Mass - m	$6.8*10^{19}$	kg	Inclination - i	3.09	Degrees

1.3 Constraints

The goal of the mission is to safely rescue the six astronauts stranded on Psyche. At first glance this appears to be simple, but under close scrutiny there are many constraints the problem imposes. First, the crew's survival time on the asteroid is limited. The resulting time constraint is a result of life support system durability and food supply.

The Mars DRM gives a trip time of 120-180 days to reach Mars with a planet stay time of 520-580 days. This yields a nominal LSS operation span of 760 days. It was assumed that the nominal operating time would be designed to a 3σ (approximately 99.97%) probability that the LSS will fail within 760 days. A conservative estimate is that there is a 50% probability that the LSS not fail with 1.5 times the nominal 760 days, or 1170 days.

From these two estimates a crew survival probability plot (see Figure 1-2) was generated based on the assumption that once the LSS fails, the crew will die. It is assumed for this design that an 80% or greater probability of crew survival means mission success..

Given that the Mars mission was considered to last a maximum of 760 days, food supplies would have to be stored for this duration. Once the Mars vehicle passes Mars, the crew would have 620 days of food remaining. They will be stranded in space for an unknown amount of time prior to rescue, so the logical course of action would be to put the crew on half-rations. This would allow remaining food to last 1240 days. The 80% crew survival probability based on LSS longevity is the dominating factor in the mission's success, rather than potential food shortage.
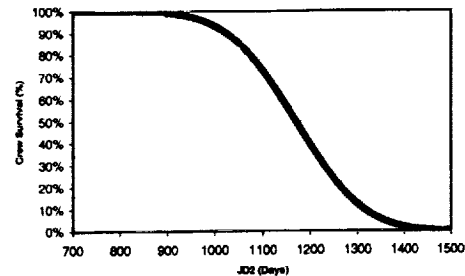
Figure 1-2: Crew survival probability.

Given this time constraint, it is important that the required hardware be produced rapidly. Assuming the subsequent Mars mission has been forfeited, existing hardware is available for modification and use, as described in section 1.2.1. Therefore, the rescue mission design will primarily be a modification of existing DRM hardware in order to create a solution to the design problem.

2 Solution Process

A mission architecture was chosen based on preliminary work showing that a direct route to and from Psyche requires the lowest ΔV transfer within the time constraint. A ballistic reentry was also chosen due to lower overall mass. In order to get a better handle on the problem it is divided into sub-disciplines. This allows a more detailed approach be taken as each group member can become an expert in a specific field related to the problem. However, breaking up the design process has the disadvantage that the team knowledge becomes spread out, and thus a communication system must now be used to pass the necessary information between disciplines. More importantly, it is desirable to derive an optimal solution not only at the discipline level, but also at the system level. Two organized methods of doing this, namely Fixed Point Iteration (FPI) and Collaborative Optimization (CO), are described below along with the individual sub-disciplines.

2.1 Optimization

Numerical optimization methods were used to assist in the determination of a design solution that maximizes the chance of survival of the Mars astronauts while meeting all mission constraints. Several different system level optimization methods were used: fixed-point iteration (FPI), design of experiments (DOE), and collaborative

optimization (CO). Additionally, several discipline level optimizers were used, to include, sequential quadratic programming and genetic algorithms.

All three system level design methods were implemented using a commercial framework integration code, ModelCenter. ModelCenter is capable of integrating multiple computer codes in several different formats, on different types of computers, running on separate workstations. ModelCenter automates the passing of information between the different disciplinary analysis codes, includes built in system optimizers, and can automatically iterate a design until it is converged. ModelCenter is run through an intuitive, graphic interface that allows the problem to be set up in a reasonable short amount of time. The chief drawback found with ModelCenter is its inability to parallel process even when the design is structured to allow it.

2.1.1 Fixed-Point Iteration

At the system level, the design of a space vehicle contains a feedback loop of several variables. A consistent design requires a method in which input variable values used by one discipline are the same as those output by previous disciplines. The most straightforward way of converging a design of this type is to use fixed-point iteration (FPI). This method starts with intelligent guesses of the variable values that have feedback loops. Each discipline then runs its own analysis, passing the results to the next discipline in line. When the last discipline is finished, the output is compared to the initial input and a new guess is made. This process is repeated until the output variables are the same as the input variables within a desired tolerance. Using a design structure matrix

Figure 2-1: Design structure matrix configured for fixed-point iteration.

(DSM) as depicted in Figure 2-1 illustrates this process. In a DSM, lines above the disciplines represent feed-forward loops, while lines below the disciplines represent feedback loops. Solid dots represent a link between disciplines. Often the order of the disciplines can be changed to reduce, or even eliminate, feedback loops. The FPI solution has three feedback paths that require convergence.

This method has the advantages of being simple to implement and leaving each discipline expert in control of his own area of expertise. Interestingly, the process can converge quickly if an intelligent scheme is used for guessing the next input in the loop. This scheme can even be made to rely on the knowledge of an experienced designer. Since a system level optimum requires a compromise between the desires of each discipline with a system level goal in mind, FPI can result in discipline level optima at the expense of system level optimum. FPI does not have the capability of reaching a compromise between disciplines, but merely ensures these disciplines are using consistent input and output values.

2.1.2 Design Of Experiments

Design of experiments (DOE) is a system level optimizer that finds an optimum value using a curve fit of the design space. A different optimization scheme is then used on the resulting response surface. To create the response surface an experimental array is used to define specific combinations of design variable values for each run. This design problem was pared down to seven design variables leaving the remainder fixed. Using a full factorial array all interactions between variables can be captured, but would require 2187 runs. The computation time required for this many runs is prohibitive. To reduce the number of runs a central composite design (CCD) was chosen. CCD uses fewer points while still capturing some variable interactions, and only requires 143 runs. If the interaction terms in the response surface are chosen well, the model will still accurately represent a quadratic design space. Knowledge of several outputs is desired which requires a separate surface for each output. With multiple outputs, optimization must be run using an overall evaluation criterion with weighting factors on each output. DOE is used in conjunction with FPI to find a converged solution for each run in the experimental array.
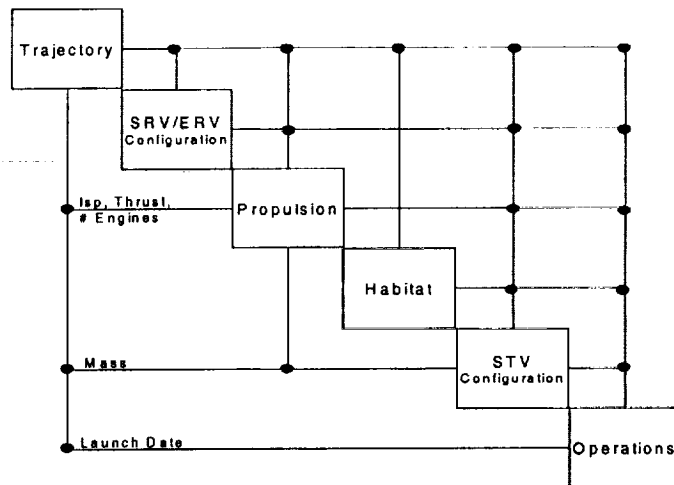
2.1.3 Collaborative Optimization

Collaborative optimization (CO) is a true system level optimization scheme that is capable of forcing the disciplines to work toward a common goal while finding a consistent solution. The principle behind CO is that each discipline maintains control over any variables that do not affect other disciplines. The scheme leaves optimization of discipline level metrics with the discipline experts. Conflict between discipline and system level optimizers is resolved by changing the discipline level objective function. For example, instead of trying to minimize the I_{sp} in the propulsion module, the discipline optimizer will minimize the error, or J-value, between a system provided target I_{sp} and the local I_{sp}. For every variable that links disciplines, there must be a system level variable and an associated J-value. In order to achieve a consistent solution, all J-values must be identically zero. This allows the system level optimizer to control the design within feasibility limits. The discipline is still able to freely control any variables that do not couple with other disciplines; therefore control of details is left to the disciplinary expert. This also reduces the size of the problem for the system level optimizer and hence minimizes computation time.

Figure 2-3: Design structure matrix configured for collaborative optimization.

CO has the distinct advantage of keeping the discipline expert in control of his or her own discipline and hence confidence in the final design is maintained. Furthermore, a true system level optimum is achievable since the system optimizer can find a balance between conflicting disciplinary interests. Since each discipline now only depends on the system level optimizer for input as shown in Figure 2-2, analyses can be run in parallel, reducing the overall computation time. Despite fixing many of the problems of FPI, this system is not without its disadvantages. Setup is significantly more difficult as legacy codes often require extensive modification in order to accept a new objective function. In addition, the use of a gradient-based system level optimizer necessitates high quality output from the disciplines. This means that the discipline level optimizer must consistently find the best solution such that the system level optimizer receives accurate gradients.

2.1.4 Discipline Level Optimization

In order for the system level optimizer in the collaborative optimization scheme to accurately find gradients of all the coupling variables, it is necessary that each disciplinary code return the true optimum solution every time. For example, if the system level optimizer perturbs one coupling variable a small amount in a 'good' direction, but the disciplinary level optimizer fails to find the better solution (or finds a worse solution) the system level optimizer will conclude that this coupling variable has no effect (or a 'bad' effect) on the overall objective function. The proper selection of discipline level optimizers is therefore critical to the performance of the overall optimization.

Discipline level optimization was initially attempted using a sequential quadratic programming (SQP) method. Although SQP is an extremely effective optimization method, it requires that the design space be unimodal and smooth. Most of the disciplinary codes have design spaces that are non-smooth and have several local minima. This is caused not only by the complex interactions of the variables, but by the fact that several design variables in the codes are either integer valued or behave as step functions. When testing the SQP optimizer on the remaining disciplines, occasional instances were found in which a global optimum was not reached. Thus even in these disciplines the design space was not well enough behaved to instill confidence that SQP returns the best solution.

Optimization methods suitable for use in non-smooth, multi-modal problems fall into the category of heuristic methods. Both a genetic algorithm (GA) and a tabu search optimizer were tested on each discipline. The GA method proved to converge to better solutions and did so in less time, although it still took much longer than SQP. For example, most of the codes would take less than 10 seconds to converge using SQP but take several minutes with GA. It was observed, however, that after the first minute only minor improvements were found, and so the optimization time was capped at 2 minutes. The GA optimizer also employed a local SQP search on the best designs in its population to improve its performance. A separate GA optimizer was linked to each disciplinary code, with the population size, mutation rate, and convergence criteria set for best performance on that particular code.

The GA optimizer used for the spreadsheet-based discipline codes is a commercial optimizer made by Frontline. Frontline's GA optimizer, Evolutionary Solver, integrates well into Microsoft Excel and can be automated using a Visual Basic (VB) routine. The VB code attached to every spreadsheet loaded the constraints and design variables into the Evolutionary Solver, which then returned the solution. The STV Configuration code had difficulties due to its iterative solution technique for finding vehicle mass - an occasional individual design selected by the GA optimizer would fail to iteratively converge, crashing the spreadsheet and optimizer. Thus, additional VB coding was needed for this discipline in order to reset the inputs and outputs whenever this happened.

For Matlab based codes, both SQP and GA were used. The SQP optimizer is Matlab's built in optimization function, fmincon, available in the optimization toolbox. The GA is taken from North Carolina State University's Meta-Heuristic Research and Applications Group. Specifically, the Genetic Algorithm Optimization Toolbox written in Matlab was used. These two methods were used together to reduce the time required to find the minimum. Each time a Matlab code is called it first runs SQP to see if it can find a minimum within the desired tolerance close to the starting position. If it cannot, then the GA is called with a fixed number of iterations. This ensures that the entire design space is searched and the global minimum is found. After the GA terminates, SQP is run to refine the best solution. This method permits the code to run fast when it is close to the global minimum (which is typically the case when finite difference derivatives are taken), but not get trapped in local minima.

2.2   Tools

Disciplinary design codes were developed for each box on the DSM in Figure 2.1. Cost and safety calculations have been moved into each discipline to lower the number of coupling variables necessary for CO. The space rescue vehicle and earth reentry vehicle have also been combined since preliminary work showed that the vehicles had many similar requirements and could share a platform. Because of the tight coupling between launch vehicle scheduling and ground manufacturing and operations, the launch vehicle and operations modules were combined. This reduced the number of disciplines from ten to six, significantly reducing the number of coupling variables, and hence the load on the optimizer. The application of both FPI and CO was done using ModelCenter as a framework to automate the process. Microsoft Excel and Matlab were chosen as the programming languages for their ease of integration with ModelCenter. Following are descriptions of each disciplinary module.

2.2.1   Cost

Since system cost is of prime importance to the design, cost models were carefully chosen from historical data when possible and modified when necessary. To determine the cost of the rescue mission, the following key assumptions were made:

- All hardware for the next Mars launch (one complete mission architecture) is available for the rescue mission, including six Magnum launch vehicles along with all hardware associated with the crew lander, cargo lander, and earth return vehicle.
- Additional costs arise from modifications to existing hardware and required manufacturing time.
- The design does not include any calculations for profit (the goal is simply to rescue the astronauts).

Cost was integrated into each discipline's design worksheet. This eliminated the need for a separate cost worksheet, thereby reducing the number of design variables required for the CO process. So, cost was calculated within each discipline and then sent as an output to the optimizer where the total cost is calculated.

Cost estimating relationships (CERs) were used to determine the costs incurred by each discipline. These cost estimating relationships are basically mathematical equations relating the cost of a specific piece of hardware to some characteristic performance parameter, usually based on mass. The CERs had the following form, where c is a complexity factor, and a and b are constants:

$$Cost = c\left\{a(mass)^b\right\}$$

CERs are generally based upon historical data, where costs of previous missions are analyzed and curve fits are applied to the data. However, since the rescue mission is a manned space mission, there is limited historical data upon which to base the CERs. Therefore, the CERs were based upon the data provided by NAFCOM96, a CER database for launch vehicles. Since the CERs in the NAFCOM96 database were based upon launch vehicle data, the CERs had to be slightly modified to account for both differences between launch vehicles and manned space missions and the accelerated schedule of hardware design, development, testing, and integration. These modifications were usually made to the complexity factors.

2.2.2   Safety

Successful completion of the mission requires two things – the stranded astronauts must be recovered alive, and the mission must not incur any further loss of life. To this end it is important to design a vehicle that does not simply meet the functional requirement of the mission, but attains the mission objective while minimizing the risk to the, rescue personnel and the recovered crew. Since the Mars DRM hardware is to be used in a modified form, it makes sense to compare the safety of the rescue mission with that of the original DRM. A scale was defined where a value of 1.0 represents a safety factor equal to that of the discipline's DRM counterpart. Values less than 1.0 represent a decrease in safety, whereas values greater than 1.0 reflect improved safety. A lower bound exists at zero since this represents certain mission failure.

Specific key factors are used to calculate the safety of each discipline. These factors are further described in each discipline's sub-section. Once these key factors have been identified based on the advice of the individual disciplinary designer, a normal distribution of reliability is placed on each factor. Weighting the relative importance of the contributing factors within each discipline is accomplished by means of exponents. All the weighted contributing factors are then multiplied together and output as the safety of that discipline. Figure 2-3 shows a sample calculation for the propulsion module. All six discipline safety values are multiplied together yielding the overall mission safety factor.
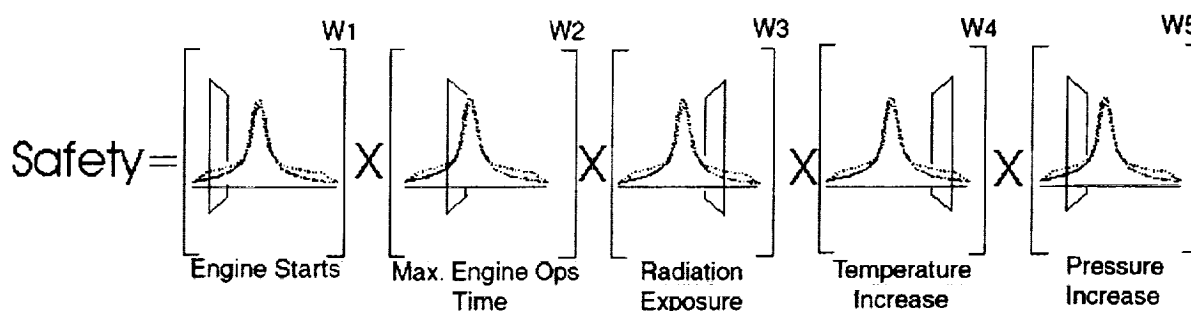
Figure 2-3: Sample safety calculation for the propulsion module.

2.2.3   Trajectory

A new trajectory must be found for the rescue mission that intercepts the stranded astronauts in a reasonable time and with a reasonable ΔV requirement. The ΔV required at each burn and the earth entry velocity are calculated using a patched conic method. Due to the computation time required to execute the analysis, and the large number of function calls typical of system level optimization, a program was written to create tabular data of the patched conic method output parameters. Data was obtained for all four ΔVs, the departure inclination angle, and the minimum distance to the sun on each transfer. Only direct transfers from the Earth to Psyche were considered since early sweeps indicated that inner planet swing-bys are not advantageous. Gravity losses at each burn are approximated and added to the ΔV found using the table data. Additional ΔV is also added if the desired heliocentric inclination angle is outside the range achievable from a 28.5° earth inclination through departure timing. The following are parameters that can be changed in the trajectory module.

- Julian dates: the absolute departure date and trip time determine the alignment of the planets and the energy required to move between them. These are the primary influences on the magnitudes of the required ΔVs.
- Wait time: this is the time that the rescue vehicle spends on Psyche before departing. This allows the return trip time and departure date to be varied.

There are eight system level inputs to the trajectory module: the mass of the STV at each of four thrust maneuvers, the thrust of an engine, the number of engines at the initial burn, the number of engines for the three remaining burns, and the specific impulse of the engines. The trajectory code outputs the Julian dates for Earth departure, asteroid arrival, and earth arrival, the ΔV required at each of four maneuver points, the Earth arrival entry velocity, the Earth departure inclination, the minimum distance to the Sun, and the safety relative to the original Mars mission based on number of thrust maneuvers.

2.2.4 Propulsion

The baseline engine for this mission is the Mars DRM 3.0 tri-carbide bi-modal NTR using liquid hydrogen as a propellant. The propulsion code uses the analysis approach in Space Propulsion Analysis and Design by Humble. An efficiency coefficient was applied to the generic equations in Humble in order to reproduce the design specification for the NTR as listed in the Mars DRM 3.0. Changes could be made to optimize the engine performance for this mission. Since time is the major constraint for this mission, only minor changes to the engine were considered. The following are parameters that could be reasonably changed within the mission time requirements.

Table 2-1: Baseline NTR Specifications.

Thrust	kN
Isp	960 s
Expansion Ratio	300
Percent bell nozzle	110%
Mass	1830 kg
Length	3.2 m
Diameter	1 m
Power	25 kWe

- Propellant Temperature and Reactor Pressure: it was assumed that the baseline engine would be designed to operate below the true maximum temperature and pressure to increase the safety of the engine; thus, increased performance can be traded for decreased safety in the manner that the SSME is operated at 109%.

- Nozzle Geometry: Increasing the nozzle's expansion ratio and length increase the engine's performance, but at the cost of added mass and size. Additionally, designing, manufacturing, and integrating a new nozzle requires a large amount of time.

- Number of Engines: Since the thrust level of the engines can only be varied over a small range, large increases in total thrust must be accomplished by adding more engines. If too few engines are used, gravity losses become significant.

There are ten system level inputs to the propulsion code: the mass of the STV at each of the four trajectory thrust maneuvers and the change in velocity associated with each of these maneuvers, the required total thrust, and the required I_{sp}. The propulsion code provides the following parameters as output to the system level: engine I_{sp}, thrust per engine, size (length and diameter) of an engine, the mass of an engine, the total time to prepare the propulsion system for the rescue mission, the cost of the modifications to the propulsion system, and a safety factor of the propulsion system relative to the Mars mission.

2.2.5 Habitat

One of the important components of the rescue vehicle is the habitat. Due to the time constraint and higher required crew capacity, the only suitable habitat is a modified version of the one designed and used for the Mars mission. The life support system (LSS) needs to be modified in order to make it adequate for the rescue mission, which necessitates a longer operational time and higher load than for which originally designed.

The habitat used is the Transhab, the same habitat as in the Mars DRM. The Transhab is an inflatable structure that weighs approximately 13,200 kg, has a length of 11 m, an inflated diameter of 8.2 m and an inflated volume of 339.8 cubic meters. Figure 2-4 shows a cut-away view of the Transhab.

The first decision to be made is the number of crew assigned to the rescue mission. The Transhab was designed to support a crew of six. It was assumed in the initial problem that all six astronauts going on the Mars mission would be alive and rescued. That means that if a large crew were sent out to the asteroid there would be a problem accommodating everyone on the return trip. Therefore it was decided that the rescue crew would include three people, the minimum number of people required to operate the rescue vehicle. This would mean that a total of nine people would be on the return trip. This is a larger number than what the Transhab was designed for but it was determined to be acceptable due to cost and time constraints.

The second area that must be examined is the Life Support System. The LSS system designed for the Mars mission would require modifications to support a crew of 9 instead of 6 for an operating time greater than the 760
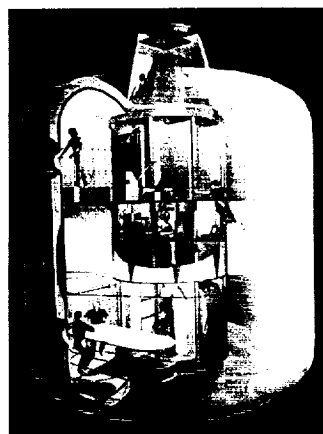

Figure 2-4: Cutaway view of the Transhab.

days it was designed for. The Advanced Life Support Research and Technology Development Metric developed by NASA was used as the basis for a detailed breakdown of the LSS. The Advanced Life Support System (ALSS) was designed specifically for use with the Transhab and is a derivative of the LSS used aboard the International Space Station (ISS). A summary of the ALSS is as follows: Mass=3,900 Kg, Power=14.5 kWe, and a single person's food intake is 1.7 kg/day. The ALSS was designed for an operating time of 400 days and a crew of six. When modifying the ALSS the dry mass was scaled by multiplying it by a ratio of the operation time of the rescue mission (Earth to the Asteroid and back to Earth) divided by the number of days the ALSS was originally designed for. Everything else about the ALSS remains the same.

Another component of the LSS that required some attention is radiation shielding for the crew. While the Transhab is designed to protect the crew from in-space radiation and solar radiation, it is not designed to travel closer to the sun then the Earth's orbit. The possibility existed that a transfer orbit to or from 16 Psyche would cross inside the Earth's orbit. In this case additional shielding would have to be added to the Transhab to provide protections against radiation.

The above assumptions and decisions made about the Transhab were incorporated into an Excel spreadsheet. The required inputs are the departure date from Earth, the arrival date at the asteroid, the date of arrival back at Earth, and the closest distance the vehicle will get to the Sun. The dates are used to scale the LSS mass and power to the mission, along with the amount of food that would have to be taken. The closest distance the vehicle gets to the sun is used to determine the amount of additional radiation shielding needed. The only internal variable is the safety margin on the LSS. This is included in order to give the module's optimizer a way to change the safety and hence match system level goals. Increasing the safety margin increases mass, cost, and safety of the habitat.

The outputs calculated by the habitat spreadsheet are the overall mass of the modified Transhab, the time required to make any needed modifications, the cost of those modifications and the safety of the modified Transhab compared to the one used on the Mars mission.

2.2.6   Space Rescue Vehicle/Earth Reentry Vehicle

The selection of a baseline vehicle comprises the majority of the work completed for this module. Presented is a brief description of the baseline vehicle followed by an explanation of the resulting module.

After exploring several high cost/high risk rescue options, the following method, which combines the forecasted benefits of hardware availability (i.e. low cost and minimal preparation time), common hardware design, fabrication, and installation procedures, mature technology, and reduced operator training, was adopted. This yields the best low-cost, reliability alternative for the mission. The resulting SRV/ERV design uses the latest DRM Mars Ascent Vehicle (MAV) capsule with the following modifications.

- Replace the LOX/CH$_4$ tanks and RL-10 engines in favor of a more easily stored, commercially available MMH/N$_2$O$_4$ system coupled with an R-40B engine and matching nozzle based on the Space Shuttle design.
- Add a bolstered heat shield almost identical to the DRM but with more mass. Bolstering the heat shield is necessary due to the planned high ballistic reentry velocity at Earth.
- Add a touchdown system for asteroid landing / lift-off support via Apollo lunar module style collapsible landing legs (i.e. collapsed for launch vehicle packaging).

Once on the surface, the 2-man rescue crew performs a surface EVA in order to extract the downed space crew using extra tooling brought along to aid the ground rescue operations and add mission redundancy. Next, the 8-man crew departs the asteroid surface in the SRV capsule and mates with the remaining portion of the STV. After the earth return portion is completed, the landing legs and ascent/descent propellant tanks are jettisoned, a propulsive braking ΔV is performed, and the capsule is used for ballistic reentry.

Several key assumptions about the mission were made in developing the SRV/ERV design spreadsheet. Only significant assumptions are listed. First, the circular parking orbit at the asteroid was assumed to be 10 km. This is important for determining the asteroid ascent and descent ΔV along with the associated propellant required for mission completion. The gravitational constant μ was estimated for the asteroid. Next, it is assumed that the downed crew is stranded on the asteroid surface and thus requires rescue vehicle touchdown on the surface. Note that several constant design parameters are taken directly from the Mars DRM. Other parameters not explicitly stated in the DRM were estimated. Finally, the packaged SRV diameter is assumed to be 7.5m. Earth reentry calculations for maximum heat flux rate use the Allen-Eggers approximation, which linearizes the initial high acceleration portion of the trajectory. The resulting heat flux rate places an upper limit on the reentry angle at the fusion point of carbon. The entry corridor is also limited on the low end by the angle at which the vehicle skips out of the atmosphere.

This baseline vehicle was modeled parametrically. Only the following variables were changed in the model.

- Rescuer tooling mass: this provides a redundant operation benefit, yielding a safer rescue process. Increased safety is based on a utility per unit mass calculation.
- Propellant tank radius: this variable is primarily affected by both the required descent and required ascent ΔV, which drives the required propellant mass. This variable primarily affects overall vehicle dimensions and mass.
- Propulsive brake: part of the Earth approach velocity can be reduced by performing a combination of two propulsive ΔVs on Earth approach, one done by the STV at the Earth sphere of influence and one by the SRV/ERV near atmospheric reentry. The latter of these increases the mass of the SRV/ERV as the heat shield design mass increases but this improves safety, which in turn helps keep g loading within limits.
- Landing leg diameter: the diameter of the landing legs when unfolded can be modified for increased stability on landing. This increases the vehicle weight, and cost, and safety.
- Earth reentry angle: the reentry velocity has the largest impact on the value of this variable. Changing it can modify the heat shield mass and crew g load, and hence the cost and safety.

The SRV/ERV design uses the velocity at reentry and desired Earth return ΔV (in the case where a slightly propulsive ΔV is required when entering the Earth's sphere of influence in order to ensure that a safe g loading will be applied to the crew upon reentry). The process outputs are vehicle mass, length, preparation time, cost, and safety relative to the Mars DRM.

2.2.7 Space Transfer Vehicle

The baseline configuration for this mission is outlined in the Addendum to the Mars DRM 3.0 as the "all propulsive bimodal NTR carrying Transhab" vehicle. The baseline vehicle is the earth return version outlined in the DRM. It was assumed that the option to use a Transhab as an in-space habitat was chosen. Minor modifications could be made to one of these vehicles, and parts of identical vehicles built for other missions could be added on quickly and with little cost penalty.

The Space Transfer Vehicle (STV) spreadsheet uses the ideal rocket equation to calculate total mass at four distinct points throughout the mission. The spreadsheet uses the ΔVs from the system level optimizer, along with the I_{sp}, to calculate the amount of propellant required for each burn. When propellant mass is added to dry mass, total mass increases. More propellant is then required for the same ΔV. Additional propellant mass increases total mass and again more propellant is needed. Numerical iteration is used to find the points at which there is enough propellant at each of the four mission stages to provide for the required ΔVs. Several factors contribute significantly to the additional mass of the STV. These factors and the input and output values they affect are summarized as follows:

- Specific Impulse: the specific impulse of the engines has a large affect on the amount of propellant required, and thus the overall mass of the vehicle. Even small increases in I_{sp} reduce total mass at each mission point significantly.
- Engine Mass, Habitat Mass, SRV Mass: each of these components is present for most of the mission. The amount of propellant required to move them all decreases rapidly as their masses decrease.
- Number of engines: the number of engines at trans asteroid injection (TAI) is important because it dictates the number of baseline 'core' modules that are added to the baseline vehicle. The baseline vehicle has three engines. By adding additional, pre-existing 'core' modules taken from other baseline vehicles, the number of engines at TAI can be increased by factors of 3 with little cost penalty. Additional engines require the modification of the baseline vehicle and incur cost and time penalties. Since the subsequent burns require only three engines, additional core modules are jettisoned after the TAI burn to reduce mass.
- Time in LEO, trip time: propellant boil-off is calculated based on these times. As time increases, the amount of propellant lost increases, so more must be taken.
- Reinforcing structure, connecting hardware, fuel pumps & lines, structural redundancy factor: propellant that cannot be contained in onboard tanks is stored in external tanks attached to the STV. Reinforcing structure mass, connecting hardware mass, and fuel pumps & lines mass all depend on the amount of propellant carried externally. Propellant stored in external tanks is burned first, empty tanks are jettisoned immediately to decrease mass.
- Safety: several factors are used to calculate the safety of the STV relative to the DRM vehicle. Safety increases as the structural redundancy percentage and propellant safety margin increases. However, increases in both these factors add mass and therefore cost.

The STV sheet has sixteen system level input variables: the length, mass, and diameter of an engine, the number of engines at TAI and asteroid orbital insertion, the first four ΔVs, specific impulse, earth departure date, asteroid arrival date, and Earth arrival date, assembly orbit inclination, habitat (Transhab) mass, SRV mass, and SRV length. These inputs are all used to determine the size of the vehicle to be launched, and the mass of the vehicle at each mission point. The STV sheet provides the following output parameters: STV cost, STV safety, mass of propellant not launched with STV, number of Magnum launch vehicles required to launch the vehicle, STV integration and preparation times, and the STV mass at each of the four mission points.

2.2.8   Operations

The Operations discipline encompasses three primary areas: ground manufacturing and integration of the rescue vehicle, launch of the rescue vehicle components into Low Earth Orbit (LEO), and assembly of the vehicle in LEO. The goal of operations is to place an assembled rescue vehicle in LEO as quickly as possible at a minimum cost while not compromising safety.

In order to analyze the three areas, several assumptions are made. First, each worker assigned to ground manufacturing and integration of the rescue vehicle is assumed to cost $110,000 per year/worker. Second, the modification of rescue vehicle components is done in parallel, but the integration must wait for all components to be modified. The orbital assembly is assumed to take place at an altitude of 407 km and at an inclination of 28.5° in a circular orbit. Lastly, seven crewmembers are assumed to be working on the in-space assembly. The crew is delivered to the rescue vehicle's assembly orbit via the Space Shuttle. The following variables have a large effect on the output.

- Modification and integration time rush factors: rush factors increase the man hours put into work on a specific component of the rescue vehicle and hence lower the time required to complete the task. However, lowering a rush factor increases cost and hurts the safety of the operation.
- Launch vehicle selection and rush factors: two launch vehicles are available to the rescue mission, the Magnum heavy lift expendable, and a high flight rate reusable launch vehicle (RLV). The Magnum has a capacity of 80 metric tons, and costs $2,200 per kg. Only six Magnum vehicles are available. The RLV can lift 18 metric tons into the assembly orbit and only costs $1,600 per kg. Rush factors can be placed on the launch preparation time in much the same way as described above. Launch vehicles are chosen based on cost per kg to the assembly orbit with available volume as a constraint.
- In-space assembly time: in-space assembly time is modified much the same way as the modification and ground integration rush factors. Again, safety is compromised and cost increased for a faster than normal assembly.

The operations module takes, as input, the estimated modification and integration times for each of the rescue vehicle sub-systems, the mass of propellant not launched with the STV hardware, the launch inclination, the number of Magnum launch vehicles that are to be used for STV hardware launch, and the target launch date. The target launch date is treated as a limit on the time available for departure preparation.

3   Results

3.1   FPI Solution

The first design convergence was done using fixed-point iteration by manually picking suitable values for all system level variables. This intelligent selection of design variables is the traditional method of converging a design. It was selected as the starting point of this design process due to its simplicity for comparison to designs converged using other methods. It became apparent during this process that the feasible design space of the project was smaller than initially believed due to the exponential growth of mass with I_{sp} at the ΔVs required for this mission.

Table 3-1. FPI Design Results

Design Variables		Objectives		Design Specifications	
Isp	1010 s	Cost	$3.21 Billion	Initial mass	939,221 kg
Thrust	700 kN	Safety	0.795	Dry mass	79,977 kg
Launch Date	14-Sep-21	Survival	0.989	ΔV total	20.8 km/s
Asteroid Arrival Date	14-Jan-23			Re-entry g-load	8.85 g
Earth Return Date	12-Dec-24				

3.2 DOE Solution

The seven design variables with the most influence on the design are specific impulse (Isp), total thrust at trans-asteroid injection (thrust), launch date (LD), asteroid arrival date (AAD), earth return date (ERD), velocity change by the NTR prior to re-entry (ΔV_4), and velocity change by the ERV prior to re-entry (ΔV_5). A baseline value and ranges were set for each of the variables.

Table 3-2. DOE Design Variable Ranges

Variables	Units	$-\sqrt{2}$	-1	0	$+1$	$+\sqrt{2}$
Isp	[s]	960 s	975 s	1010 s	1045 s	1060 s
Thrust	[kN]	441 kN	508 kN	669 kN	830 kN	897 kN
LD		8-Nov-21	31-Oct-21	11-Oct-21	21-Sep-21	12-Sep-21
AAD		31-May-23	13-Sep-23	3-May-23	22-Dec-22	5-Apr-23
ERD		22-Oct-24	13-Oct-24	24-Sep-24	5-Sep-24	26-Aug-24
$\Delta V4$	[m/s]	0 m/s	439 m/s	1500 m/s	2561 m/s	3000 m/s
$\Delta V5$	[m/s]	0 m/s	439 m/s	1500 m/s	2561 m/s	3000 m/s

The CCD array for these seven variables results in 143 design runs, enough data to facilitate quadratic curve fits to the objective functions and constraints. Cost, rescue mission safety (safety), and original crew survival (survival) are the three objective functions considered for the design. Two constraint Response Surface Equations (RSEs) were also created: 1) the number of days after JD1 that operations was ready to launch (late) which must be less then zero, and 2) the deceleration during re-entry (gload) must be less than 10 g.

The RSE generated by the CCD array was found to be highly inaccurate. Although several variables were accurately modeled by the RSE, others (such as cost) showed large discrepancies, indicating that the quadratic assumption was poor. By limiting the range of the variables to a small region of the RSE design space, a few solutions were obtained. The three solutions below were optimized for cost, safety, and survival, respectively.

Table 3-3. DOE Results

Isp	Thrust	JD1	JD2	JD3	Cost	Safety	Survival	Late	gload
[s]	[kN]				$BIL			[day]	[g]
960	454	10-Oct-21	2-Feb-23	16-Oct-24	6.73	0.594	0.999	0	12.1
971	516	18-Oct-21	25-Mar-23	22-Oct-24	12.2	0.796	1.000	0	9.61
982	675	1-Oct-21	10-Mar-23	22-Oct-24	0.516	0.769	1.000	-96	9.99

3.3 CO Solution

In order to solve the CO version of this design, two different system level optimization methods were attempted: sequential quadratic programming (SQP) and the Method of Feasible Directions (MoFD). Both methods are gradient based which allows them to converge to a solution much more efficiently than non-gradient or heuristic optimization methods. However, in order for gradient-based methods to work, accurate gradient information must

be gathered. Since many of the discipline level modules had non-smooth, multi-modal design surfaces requiring heuristic optimizers, the gradient information returned to the system level optimizer was often poor. In order to improve the gradient information, large gradient steps were programmed into the system level optimizer and more time was given to the discipline level optimizers. Despite these improvements, the system level optimizer still had difficulty reaching the feasible region of the design space, which necessitated relaxation in the convergence criteria of the target values. An example of the convergence history using the SQP optimizer is shown below, along with the optimum solution it found.
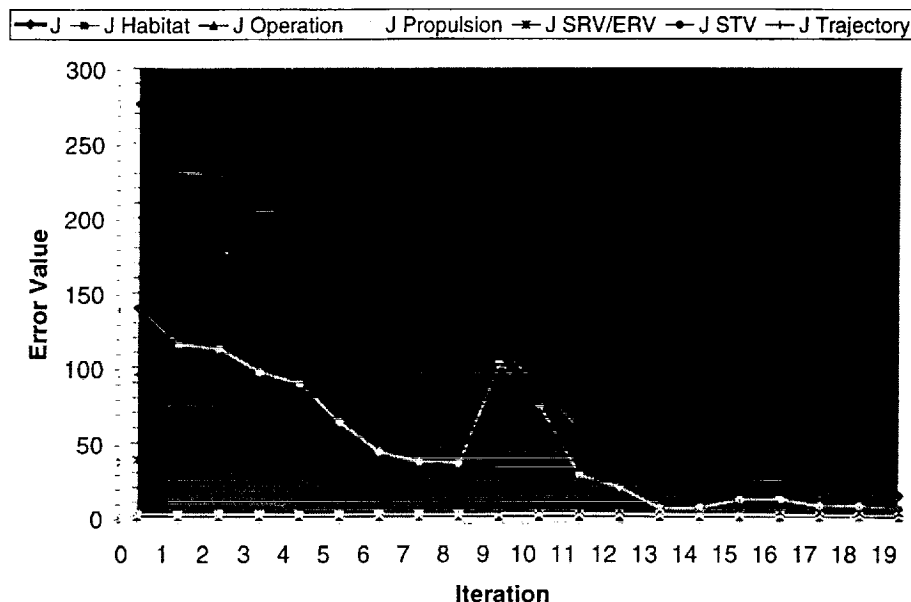
Figure 3-3. Plot of error values (J's) for each discipline and total showing the gradual convergence of target and calculated values
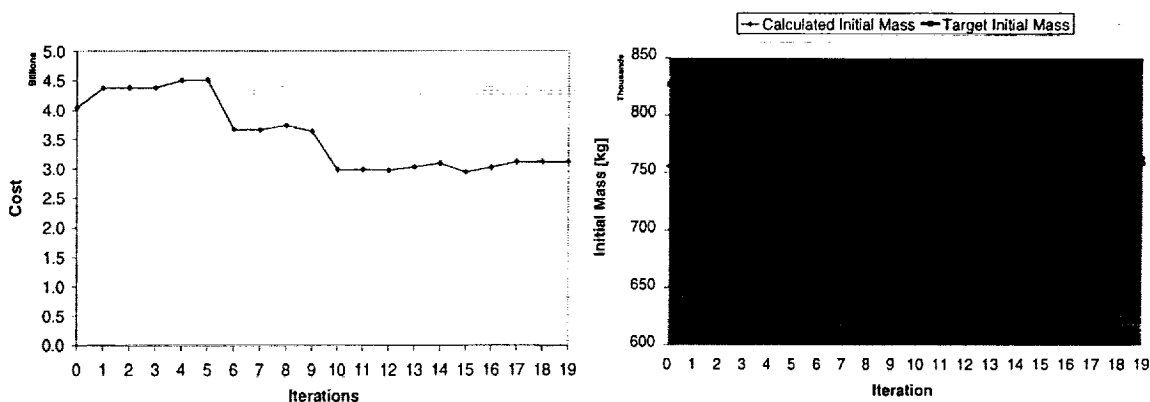
Figure 3-2. Plot of gradual improvement (decrease) in objective function cost

Figure 3-1. Plot of target and calculated initial mass showing gradual convergence of the two values

Table 3-4. CO Design Results

Design Variables		Objectives		Design Specifications	
Isp	1077 s	Cost	$ 3.11 Billion	Initial mass	763,107 kg
Thrust	634 kN	Safety	0.413	Dry mass	88,827 kg
Launch Date	12-Sep-21	Survival	0.993	ΔV total	19.9 km/s
Asteroid Arrival Date	12-Dec-22			Re-entry g-load	< 10 g
Earth Return Date	27-Dec-24				

4 Conclusion

This design has attempted several optimization schemes to solve this design problem. FPI produced the best results with a human controlling the design variables. Theoretically CO should produce a better solution, implying that work needs to be done on the implementation of CO for this problem. A penalty function at the discipline level as suggested in [Braun] may help consistency of gradients for the system level optimizer. The DOE method may benefit from a higher order curve fit, requiring more runs since the design space does not appear to be quadratic. For this problem, the traditional method of a human controlling the design variables and using FPI to converge a solution proved to be the fastest solution and the best results.

5 Outreach

Throughout the course of the Spring 2001 Semester, the Georgia Tech team led several projects aimed at educating the public and building community interest in the space program. For example, two team members presented typical aerospace engineering projects, tasks, and applications to an all-day, Society of Women Engineers-sponsored, program aimed at local high school girls. These two students gave an accurate picture of what aerospace engineering is about. In another project, two more team members discussed the world of aerospace engineering with a local cub scout troop. The GT students answered countless questions about space related issues, even questions about the team's involvement in the upcoming LPI design competition at Johnson Space Center. Finally, in perhaps its largest outreach project , the entire Georgia Tech design team organized the AIAA-sponsored model rocket contest open to all undergraduates – tomorrow's technical future. For more information, these outreach activities are further described on the website:

http://atlas.cad.gatech.edu/~ae6322a/outreach.html

6 References

Bate, Roger R., Donald D. Mueller, and Jerry E. White. 1970. Fundamentals of Astrodynamics. New York, Dover Publications, Inc.

Bishop, Robert H., Dennis V. Byrnes, Dara J. Newman, and Christopher E. Carr, and Buzz Aldrin. "Earth-Mars Transportation Opportunities: Promising Options for Interplanetary Transportation," AAS Richard H. Battin Astrodynamics Conference, 20-21 March, 2000, College Station, TX.

Braun, Robert, Peter Gage, Ilan Kroo, and Ian Sobieski. "Implementation and Performance Issues in Collaborative Optimization," AIAA Symposium on Multidisciplinary Analysis and Optimization, September 4-6, 1996, Bellevue, WA.

Hale, Francis J. 1994. Introduction to Space Flight. Englewood Cliffs, New Jersey: Prentice-Hall, Inc.

"Human Exploration of Mars: The Reference Mission of the NASA Mars Exploration Study Team," Hoffman, S.J. and Kaplan, D.I., eds., NASA Special Publication 6107, July 1997.

Humble, Ronald W., Gary N. Henry, and Wiley J. Larson, eds. 1995. Space Propulsion Analysis and Design, 1st ed. New York: The McGraw-Hill Companies, Inc. Primis Custom Publishing.

Kos, L. "Human Mars Mission: Transportation Assessment," AIAA Defense and Civil Space Programs Conference and Exhibit, October 28-30, 1998, Huntsville, AL.

Larson, Wiley J. and James R. Wertz, eds. 1999. Space Mission Analysis and Design, 3rd ed. El Segundo, CA: Microcosm Press and Kluwer Academic Publishers.

Mankins, J.C., N. Marzwell, and H. Feingold. "Lunar Exploration and Development: New Approaches to the Moon," IAF 50th Astronautical Congress, 4-8 Oct 1999, Amsterdam, The Netherlands.

"Reference Mission Version 3.0 Addendum to the Human Exploration of Mars: The Reference Mission of the NASA Mars Exploration Study Team," Drake, B.G., ed., Exploration Office Document Ex 13-98-036, June 1998.

S3/c-P/IN/91

A Deployable Instrument Package for Paleontological Research

Arnold, J., Broniatowski, D., Da Silva, L., Davis, V., Gleyser, A., Kam, L., Macias, M., Neubert, J., Ponda, S., Richards, M., Rodriguez, C., Ruddy, B., Smith, L., Solish, B., Wesley, C.T., and Yang, J. (Hodges, K.V., faculty advisor)

2001 HEDS-UP Team, Massachusetts Institute of Technology, Cambridge, MA 02139

Abstract

The search for evidence of past life is likely to be an important part of Martian exploration. Unfortunately, the number of potentially fossiliferous outcrops at any landing site may be quite large, and it would be advantageous to have some automated way of ranking those outcrops with respect to their paleontological potential. The Deployable Instrument Package for Paleontological Research (DIPPR) is designed to perform such a function. DIPPR consists of a family of one large and four small rovers carrying arrays of cameras and spectrometers for outcrop characterization. The large rover would be responsible for long-range observations, heavy computational tasks, and transport of the smaller rovers. The smaller rovers would have the capability to approach outcrops closely and perform more detailed scans. Outcrop characterization protocols would involve a progressively updated calculation of "paleontological probability index", a semi-quantitative measure of the likelihood that a particular outcrop may contain fossils. Ultimately, DIPPR would produce a paleontological probability map of the landing site, which could be used by astronauts to determine how best to plan extravehicular excursions for fossil hunting. While designed to be used by astronaut teams working on Mars, DIPPR also could be operated remotely from Earth with relatively minor design modifications.

Introduction

Observations made during the Mars Global Surveyor mission indicate that liquid water has existed on the Martian surface in the past and may exist today in the shallow subsurface (Head et al., 1999; Malin and Edgett, 2000a,b; Zuber et al., 2000). Combined with the documentation of chemical and morphological signatures in Martian meteorite ALH84001 that are suggestive of the operation of organic processes on early Mars (e.g., McKay et al., 1996; Thomas-Keprta et al., 2001), such findings constitute a compelling argument that the search for evidence of fossil life should be one of the principal goals of the first stages of manned exploration of Mars. Unfortunately, the fossil record on Earth is far from completely preserved, and – although we do not have to contend with the ravages of plate tectonics on Mars as we do on Earth – we should not expect that fossils will be easily found on the Martian surface. As the authors of a recent NASA strategy report put it, searching for well-preserved fossils on Mars will be like searching for the "proverbial needle in a hay stack" (Carr et al., 1995).

How do we improve the odds of a successful search for fossils on Mars? Paleontological experience here on Earth suggests that the key is looking in the right places. The first step must be to choose a landing site which exhibits characteristics of an area that might have harbored and preserved life in the past using appropriate space borne remote sensing techniques. While such methods will improve the likelihood of success, a productive search for Martian fossils will require additional tools to help astronaut teams "high-grade" potential study sites at length scales ranging from kilometers to microns. In this report, we describe a concept and design for a mobile, semi-autonomous instrument package. This package could be deployed by Martian astronauts to provide the data necessary to make informed decisions about which potential study areas have the highest probability for containing fossils and thus should be earmarked for more detailed study by astrogeologists. In this manner, the package would promote a streamlined mission plan, minimizing the number of extravehicular excursions necessary for effective fossil exploration and maximizing the efficient use of surface time by astronauts.

Concept

We envision the Deployable Instrument Package for Paleontology Research (DIPPR) as a family of versatile, sensor-bearing rovers. These rovers will carry a variety of instruments designed to collect

imagery and compositional data that will permit on-board and remote computers to establish the probability that any potential study site might contain fossils. Based on such information, paleontological probability gradients can be mapped over accessible regions of the Martian surface. This information can then guide astronauts in making decisions about which sites to study in greater detail.

The rovers in the package can be thought of as a family of semi-autonomous vehicles that have specific functions but also work as a team to optimize their versatility, efficiency, and mobility. In a typical deployment, a large rover capable of long-range scanning would collect low-precision data to develop a coarse paleontological probability map. The results would be analyzed using on-board decision-making software, which would help to determine where smaller rovers would be deployed for more detailed work. Although the rover family could proceed with these detailed studies autonomously, the data obtained in long-range scans, including the assigned paleontological probability map, would be transmitted in real-time to astronauts at the Martian base station. Furthermore, the astronauts would have the option of manually overriding the automatic short-range deployment operation, if desired.

At short range, the small rovers would carefully scan outcrops for chemical, mineralogical, and morphological signatures of rocks that have high probabilities of containing fossils. Based on its analysis of the results, DIPPR would then transmit a high-resolution paleontological probability map to the base station. This map would serve as a fundamental resource to guide astronaut investigations of potentially fossiliferous outcrops. Although DIPPR is designed as an aid for *in situ* human exopaleontological research, minor modifications of the design and appropriately deployed communications satellites could permit the remote operation of such an instrument package from Earth.

Most of the sensors on DIPPR are based on established technologies that were used on the Pathfinder Mission (NASA Mars Exploration, 1997a) or are intended for use on the Athena Payload (Athena Project, 2000). What is novel about DIPPR is not the design of the instruments in the package, but rather the way in which data obtained by those instruments are utilized. The ability of the LMR array to respond to its own observations promotes the highly efficient use of astronaut time and energy. Moreover, DIPPR's capacity for routine data interpretation could greatly improve the ability of astronauts who have not had extensive training in paleontology to conduct effective research.

The Science of Mapping Probability Gradients for Fossil Discoveries

The first step toward a successful search for evidence of ancient Martian life will be to identify rock outcrops that are most likely to contain preserved fossils. In general, this excludes exhaustive studies of igneous and most metamorphic rock outcrops. It is tempting to limit the search for fossils to sedimentary outcrops, but this step alone is not sufficient to significantly expedite the process of Martian fossil exploration. The Martian surface displays vast regions with a sedimentary substrate, and our experience on Earth is that relatively few outcrops of sedimentary rocks contain well-preserved fossils. Therefore, we need protocols for identifying appropriate rock types and establishing a ranking scheme for their probability of containing fossils. In addition, these protocols must be based on data that can be obtained using instruments appropriate for deployment on a rover-sized vehicle.

Evaluating the Potential of Outcrops to Contain Appropriate Rock Types

Some DIPPR rovers would be equipped with cameras capable of taking panoramic images of relatively large regions of the Martian surface, or with relatively low-spatial resolution spectrometers capable of crude determinations of outcrop composition. Such long-range information would be evaluated by on-board computer systems to develop a preliminary probability map by comparing the observed outcrop characteristics with a digital catalog of geomorphic and geochemical features that are indicative of sedimentary rock outcrops on Earth. For example, landforms that look like mesas or outcrops that exhibit horizontal features suggestive of stratification would be considered indicative of the presence of sedimentary rocks, whereas narrow conical landforms and outcrops with no apparent bedding would be rejected – or at least given low priority – for further consideration. Crude estimates of outcrop chemistry would aid the site selection process further. While this approach might eliminate some potentially fossiliferous outcrops, the goal is to direct the astronauts toward outcrops that have the greatest likelihood of containing fossils.

Rock Types and their Paleontological Potential

Once the long-range image scans have determined that certain outcrops may have a high potential for containing sedimentary rocks, short-range scans must be used to determine the paleontological potential of rock types actually encountered. Although some igneous materials, such as air fall tuffs, and some low-grade metamorphic rocks display fossils here on Earth, sedimentary deposits are likely to be the most fruitful targets for paleontological research on Mars. Of these, sedimentary conglomerates and breccias have the lowest potential, whereas other siliciclastic rocks and chemical-biochemical sedimentary rocks are more favorable. Fossils are most abundant on Earth in the carbonate rocks limestone and (less frequently) dolomite. Limestone forms most often as a consequence of the direct underwater biochemical deposition of calcite and aragonite at rates ideal for the preservation of organisms. Other carbonate rocks, such as travertine deposited around hot springs, may preserve algae and biofilms. Dolostone typically forms by the diagenetic replacement of limestone and may preserve structures of biological origin that existed in the limestone precursor. It is important to note, however, that there are currently no known carbonate rock deposits on Mars; however, we do not exclude the possibility of finding such deposits due to the low spatial resolution of recent and previous studies.

Chert and evaporite, both chemical/biochemical sedimentary rocks, are also important fossil resources on Earth. Chemically-deposited chert forms from silica gels that may entrap microorganisms during deposition. (The oldest known fossils on Earth were preserved in chemically deposited chert; Schopf, 1999.) Biochemically-deposited chert typically represents the accumulated shells of diatoms and other silica-producing organisms. On Earth, highly consolidated biochemical chert does not typically preserve the structures of these organisms very well. Poorly consolidated biochemical chert preserves fossils well on Earth, but would be eroded away rapidly in an environment similar to Mars. Diagenetic chert usually forms when silica-rich fluids percolate through siliciclastic and carbonate rocks; in some instances, this process does not disturb pre-existing fossils. Evaporite rocks form during protracted periods of evaporation in closed lakes and ocean basins. As with limestone, no evaporites are known on Mars at present, but we do not exclude the possibility of unknown deposits. Although they are generally good at preserving organic material, the highly saline conditions under which evaporites form are not very conducive to life (Dietrich and Skinner, 1979).

Fine-grained siliciclastic rocks such as shales and mudstones are also prime targets for fossil hunting. Making up nearly half of all sedimentary rocks in the stratigraphic record on Earth, fine-grained siliciclastic rocks are, for the most part, representative of sediments deposited in quiet water. Such conditions are particularly well suited for the preservation of soft-bodied organisms, and terrestrial shales typically contain between one and ten weight-percent organic carbon (Boggs, 1992). Sandstones are less likely to contain fossils because sand deposits typically have high porosity, which can encourage the decay of organic material after burial. If the sand was rapidly lithified in a wet environment, however, some fossils might be preserved.

Preservation Considerations

Certain conditions that either enhance or reduce the ability of a rock to preserve fossils are shared among all fossil-bearing rocks. Oxidizing conditions, which are commonly related to dry environments, hinder fossil preservation by oxidizing organic remains to CO_2 and by providing an ideal environment for aerobic microorganisms to participate in decomposition. Reducing conditions, associated with stagnant bodies of water and swamps, tend to improve fossil preservation because such conditions are inhospitable to many organisms that promote decomposition of organic materials (Dietrich and Skinner, 1979). These redox conditions are preserved in sedimentary rocks, and can be used to determine the likelihood of fossil preservation in those rocks.

Identifying and Ranking Potentially Fossiliferous Rock Types

The identification and characterization of Martian rocks is a difficult task, especially without human assistance. Traditional techniques of field geology include visual examination, textural analysis, and the testing of physical and chemical characteristics. While such methods are easily taught to humans, many are surprisingly difficult to automate. Visual examination, for example, involves complex image processing that is effortless for humans, but still imperfectly implemented with electronic apparatus. To a field geologist, the "feel" and "taste" of a rock are important components of rock identification, yet humans are

far better at sensory perception than the most sophisticated robot. Even such "low-tech" methods as measuring hardness or testing for the presence of calcium carbonate with hydrochloric acid are difficult for machines, particularly in the Martian environment. On the other hand, automated probes can be built with some capabilities that human's do not have. In particular, various forms of spectrometry may be used for mineral identification. Once a rock's mineralogy is known, it is a relatively simple matter to determine its , type with only limited textural analysis that is well within the capabilities of existing optical sensors.

DIPPR's algorithms for classifying the paleontological potential of a given outcrop would be based on a series of mineralogical and textural evaluations as follows. Initial spectral scans would be evaluated for indications of the presence of certain sets of minerals:

♦   Mafic Minerals – pyroxene, olivine, amphibole, chromite, etc.

♦   Moderate- to High-Pressure Metamorphic Minerals – garnet, kyanite, coesite, etc.

♦   High-Temperature Metamorphic Minerals – sillimanite, cordierite, etc.

These mineral groups are only found in quantity in igneous and metamorphic rocks, which do not typically preserve fossils. Therefore, any rocks containing more than ten modal percent of minerals from these groups would be removed from paleontological consideration.

After this preliminary consideration, identification of the remaining candidate rocks would be based on their most common mineral constituents, which are referred to in this report as "primary minerals". DIPPR's working definition of various candidate rocks is based on an abundance of more than forty-five modal percent of primary minerals as follows (Carmichael, 1982):

♦   Siliciclastic Rock – clay minerals (e.g., kaolinite, illite) or quartz

♦   Carbonate Rock—calcite, dolomite, aragonite

♦   Evaporite—halide minerals (halite, sylvite, etc.), or sulfates (gypsum, anhydrite, etc.)

♦   Chert—cryptocrystalline quartz

In some cases, mineral content alone will not constitute sufficient information for the determination of rock type and short-range imagery must be analyzed for distinguishing features. For example, sandstone and chert both have quartz as a primary mineral but chert is microcrystalline and sandstone is made up of easily discernable grains. Grain size also helps to distinguish fine-grained and coarse-grained siliciclastic rocks that have very different paleontological potentials. Grain shape studies based on close-up imagery will provide a means of evaluating the level of deformation or metamorphism of candidate rocks and further evaluating their potentials; sutured grain boundaries and the presence of contorted microlamination would lead to the assignment of lower paleontological potentials.

The actual ranking of observed rocks for paleontological potential would follow rules based on terrestrial experience. Limestones and fine-grained siliciclastic rocks are most likely to retain fossils, so they would receive high and sub-equal preliminary rankings. Chert is relatively less likely to be fossiliferous and would be ranked lower. Evaporites and sandstones would be ranked lower still. Preliminary scores would be modified based on accessory mineral compositions and other factors that increase or decrease the probability of fossil preservation. For example, the presence of accessory minerals containing oxidized iron and manganese, such as hematite and limonite, would suggest oxidizing conditions and would lower the rock's ranking slightly. In contrast, the presence of minerals like pyrite would suggest reducing conditions and would raise the rock's ranking. Sensor indications of the presence of organic material in any sample would result in the highest ranking. A chert's rank would be increased if it either displayed sedimentary layering or formed nodules in a carbonate or siliciclastic matrix, since such chert on Earth seem more likely to preserve fossils.

The Modification of Rankings Based on Pattern Recognition

Relatively highly ranked materials would be examined for the presence of shapes that might constitute further evidence of fossil content. Protocols for classifying patterns of both possible macroscopic and microscopic fossils would be based on systems used on Earth to classify fossil types. Rock surfaces would be examined for the basic shapes and structures that typically characterize terrestrial fossils:

1) Straight or coiled single cones, tubes, or cylinders

2) Colonial tubes

3) Valves

4) Multielemental or multiplated structures

5) Reticulate and cystose networks.

Rocks with surfaces displaying such features will receive higher rankings. If these features were developed in materials with chemical compositions that frequently characterize fossil replacement minerals, such as silica and apatite, the ranking would be even higher. Progressively higher resolution images could be used to search interesting macroscopic shapes for microstructures indicative of an organic origin and could be used to examine the sample for unicellular and multicellular microorganisms and the dissociated skeletal fragments of macro organisms . Highly suggestive shapes could be compared to digital reference catalogs of terrestrial species to further hone the ranking procedure.

Development of Final Paleontological Potential Maps

Based on these rankings, each studied section of each outcrop would receive a numerical score representing its calculated potential for containing fossils. The score would be entered automatically into a standard geographical information system (GIS) database and thus registered with high-resolution digital elevation data to develop a map of paleontological potential for astronaut use. We anticipate that such maps would be the fundamental resources used by astronauts and Mission Control to plan extravehicular excursions for the collection of appropriate samples and final evaluation of candidate outcrops for their fossil contents.

DIPPR Design

A family of rovers carrying various sets of analytical tools and cameras will collect the data necessary for building paleontological potential maps. In this section, we describe the philosophy behind the family rover design and the general technical specifications of the instruments employed.

The Martian Rover Family Unit

Our Martian rover (MR) family concept grew out of a design developed in the Fall of 2000 as part of an MIT freshman-level subject called "Solving Complex Problems". (The problem was to develop a mission to Mars to search for signs of past or present Martian life. Our complete mission design may be accessed via http://web.mit.edu/12.000/www/finalpresentation/). The MR family, which consists of four little Martian Rovers (LMRs) and a single big Martian rover (BMR), was conceived to minimize potential problems that might be encountered by lone rovers, to improve the quality of data communication across great distances on the Martian surface, and to generally increase the efficiency of rover-based research. The BMR would be capable of long-range satellite communications and could accomplish power-intensive computations. It also would accommodate a larger sensor payload. Most importantly, the BMR would have the capacity to carry the LMRs and act as a charging station. Control of LMR activities typically would be delegated to the BMR, but human control would be possible through relays of commands through the BMR communications system. . This structure improves the likelihood of a successful deployment in a variety of ways. LMRs would be assigned to particularly dangerous tasks (such as close encounters with outcrops or navigation over rough ground) and the loss of a single LMR would not jeopardize the overall success of the mission. Moreover, functional LMRs could inspect a damaged LMR and potentially make field repairs. Communication would be made more reliable by relaying data from the LMRs to the BMR, and redundant data storage on LMRs and the BMR would improve data security.
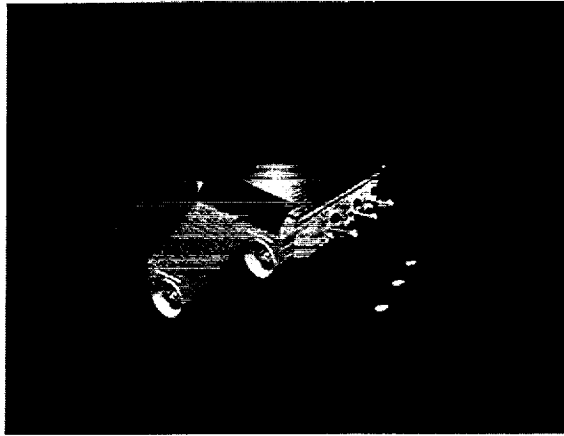
Figure 1: A Little Martian Rover

Little Martian Rovers

Each LMR would consist of a Sojourner-like rover body with some special modifications. For example, the wheels used on Sojourner would be replaced with six evenly spaced legs. Although a legged rover is heavier than a comparable wheel-based design, negative ramifications of the extra weight are mitigated by the relative ease with which a legged rover can negotiate rocky terrain. The legs would consist of two aluminum bars with a foot attached to the longer bar. The hip joints on the legs would be used for rotational motion, and the knee joints would provide lateral motion. A second modification would be the mounting of a fully articulated sensor arm at the front of the rover. This adaptable device would accommodate long-focal length cameras (used primarily for navigation), short-focal length cameras (for mesoscopic and microscopic imaging of outcrops), and narrow field-of-view spectrometers. A third new feature would be a tool mounted on the back of the rover to prepare fresh rock surfaces. Power would be drawn from battery packs that would be recharged by high-efficiency solar cells mounted on the LMR. In the event that these cells are incapable of maintaining sufficient charge for effective operation of the rover, each LMR would have the capability of traveling back to the BMR to recharge The communications system on an LMR would be very similar to the system used for Sojourner, allowing the LMR to communicate with the BMR via basic UHF. The LMRs may move up to 500 meters from the BMR before their signal starts to degrade (NASA Mars Exploration, 1997a,b).

Big Martian Rover

With a total height, width, and length of about 0.75 m, 1 m, and 1.5 m, respectively, the BMR would be responsible for the long-distance transportation of the rover family, as well as long-distance communications and high energy-usage operations of the mission. The BMR would be substantially larger than Sojourner with an enclosed deck. It would have six wheels, each with a diameter of 0.5 m, which would be mounted on a suspension system similar to the JPL-developed Rocker-Bogie system. The LMRs would enter the BMR via a ramp to a rear hatch that would be closed during transport. Power would be supplied by a solar array that would be similar in design and efficiency to the LMR array but which would be much larger. A communications/navigations mast would be mounted on the front of the BMR; it would accommodate a 360-degree camera as well as a satellite uplink and rover-to-base communications systems. The BMR also will be equipped with a navigational camera, a long-range spectrometer, and a device to expose fresh rock surfaces.

DIPPR Payload

Cameras

Panoramic cameras would be employed on the rovers for navigation and long-range outcrop analysis. On the BMR, a camera capable of 360° imaging at high resolution would be required for effective visual analysis of outcrops at multi-kilometer distances from the rover, as well as long-distance navigation and landmark identification. Since the LMRs would not require such an extensive imaging system, a fixed wide-angle camera mounted on the front of the rover would suffice for navigation, obstacle avoidance, and

Conclusion and Recommendations for Future Studies

DIPPR is a family of Martian rovers designed specifically to assign paleontological probability indices to specific outcrops based on real-time analysis of sensor observations and to use such information to create paleontological probability maps of the Martian surface to guide human exploration. Deployment of the DIPPR system would be semi-autonomous, guided in real-time by ongoing revisions of paleontological probability index estimates as rovers in the family make progressively more detailed observations.

We believe our approach to the analysis of the data obtained using this technology is novel. DIPPR would be capable of the computational assessment of a broad spectrum of outcrop characteristics — including pattern, texture, and mineralogical variability – in order to make reasonable conclusions about the past geological processes acting on the site and the probability of finding fossils preserved there. On Earth, such conclusions are made exclusively by trained human geologists. The expense and risk associated with Martian surface geology studies is such that tools such as DIPPR might greatly increase their efficiency and effectiveness.

The greatest challenge associated with advancing DIPPR from the concept stage to reality lies in the development and testing of appropriate "smart" software systems. Some aspects of this problem are straightforward; for example, existing edge detection algorithms may be modified easily to develop software to identify and evaluate simple geometric patterns that might be indicative of stratification. However, the DIPPR system would be called upon to detect and evaluate complicated morphological patterns that might be indicative of actual fossils or indirect evidence of prebiotic chemistry. Most algorithms suitable for such analysis are still in the developmental stage in artificial intelligence laboratories. While the appropriate software may take some time and effort to engineer, there are no obvious impediments to the task and we recommend that NASA encourage such avenues of research as a next step toward the development of successful and versatile "robotic field geologists".

References

Analytical Spectral Devices, Inc. 1998. ASD: FieldSpec® UV/VNIR Portable Spectrometer. http://www. asdi.com/prod/fs_vnir.html (2001, April 29).

Athena Project, 2000, Mars Exploration Rovers – Instruments. <http://www.athena.cornell.edu/ instruments/ > (April 25, 2001).

Boggs, S., 1992, *Petrology of Sedimentary Rocks*: New York, Macmillan, 707 p.

Canny, John. *A computational approach to edge detection*, IEEE PAMI 8(6) 679-698, November, 1986.

Carmichael, R. S. (Ed.), 1982. *CRC Handbook of Physical Properties of Rocks, Volume I.* Boca Raton, FL: CRC Press.

Carr, M. H., Clark, B., DesMarais, D. J., DeVincenzi, D. L., Farmer, J. D., Hayes, J. M., Holland, H., Jakosky, B., Joyce, G. F., Kerridge, J. F., Klein, H. P., Knoll, A. H., McDonald, G. D., McKay, C. P., Meyer, M. A., Nealson, K. H., Shock, E. L., and Ward, D. M., 1995, An exobiological strategy for Mars exploration, NASA Exobiology Program Office: <http://exobiology.nasa.gov/ Exobiology_Program/Mars_Exo_Strategy_Doc.html> (April 29, 2001)..

Clark, R.N., A.J. Gallagher, and G.A. Swayze, 1990. Material Absorption Band Depth Mapping of Imaging Spectrometer Data Using a Complete Band Shape Least-Squares Fit with Library Reference Spectra. *Proceedings of the Second Airborne Visible/Infrared Imaging Spectrometer(AVIRIS) Workshop.* JPL Publication 90-54, 176-186.

Clark, R.N., Sam Vance, and Rob Green, 1998. Mineral Mapping with Imaging Spectroscopy: the Ray Mine, AZ. <http://speclab.cr.usgs.gov/PAPERS/ray.mine.1.1998/ray.mine.avproc.html> (April 30, 2001).

Dietrich, R. V., & Skinner, B. J., 1979. *Rocks and Rock Minerals.* New York: Wiley.

Head, J. W., Hiesinger, H., Ivanov, M. A., Kreslavsky, M. A., Pratt, S., and Thomson, B. J., 1999, Possible ancient oceans on Mars: Evidence from Mars Orbiter Laser Altimeter Data: Science, v. 286, p. 2134-2137.

thermal emission spectrometer. Combining the rover's positional and outcrop distance information, it should be possible to identify the position of the target outcrop on any available digital elevation model and thus "project" the panoramic image of the outcrop onto a topographic model. The rover positional and outcrop distance information also can be used to project the spectrometer data onto the same model. The original and projected panoramic images would be analyzed in an effort to detect evidence for stratification using contrast and color variation as the primary determinants. We would rely heavily on the effective and well-known Canny edge detection algorithm (Canny, 1986) to develop edge displays that would be used to quantify the degree of stratification for various faces of the outcrop. By the same token, the coarse spectrometric data would be used to establish rock types, which would then be assigned an area-averaged numerical score based on the normalized propensity of each identified rock type to preserve fossils. These two sources of quantitative data would be combined to determine a preliminary paleontological probability index for the outcrop.
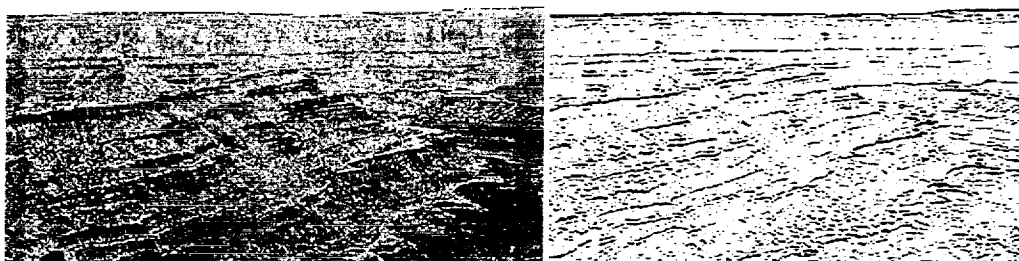

Figure 2: Example of use of Canny edge detection algorithm

Short-Range Data Analysis

Outcrops having sufficiently high paleontological probability indices would be targeted for further study. The LMRs would be deployed for that purpose. Short-range data obtained by the smaller rovers would include close-up panoramic images, higher-resolution images of rock surfaces obtained with other cameras, a detailed topological characterization of the outcrop obtained using range-finding devices and both types of cameras, and mineralogical abundance data with high spatial resolution. A first-pass study of each outcrop would be accomplished using all LMR's in the family, which would be observing at distances of several tens of meters. In a manner similar to that used to evaluate the long-range data, more reliable paleontological probability indices would be determined for various parts of the outcrop. If no high-index areas were identified, the outcrop would be assigned a modified area-averaged index and would not be studied further by DIPPR. If such areas were identified, the LMRs would move in for more detailed study at the scale of meters. In this fashion, progressively higher modified indices would be used to focus study at progressively higher spatial resolutions until promising outcrops had been mapped in great detail. Ultimately, this information would be combined to determine the paleontological probability for the studied region and, after a sufficient number of deployments, such data would form the basis for regional paleontological probability maps.

Rationale

This approach to long- and short-range data interpretation is regarded as a substantially more efficient way to develop paleontological probability maps than is its most logical alternative: a systematic, painstaking study of all accessible outcrops using short-range instrument packages. Continual updating of paleontological probability indices based on positive and negative feedback from sensor and camera data would permit study to be concentrated on the portions of outcrops deemed most likely to contain fossils. Eventually we would expect the best outcrops to contain small (centimeter-scale) surfaces with very high indices. These would be of sufficiently limited dimension to make coring and sample recovery practical, and such samples would be transported first to the BMR and eventually to the base station for preliminary study.

infrared bands. Imaging spectrometers in these bands have been built for space applications with very high spectral and spatial resolutions, making them ideal for use on the BMR. Point spectrometers in these bands are extremely small and light, and have sharp spatial resolution and extremely high spectral resolution (Analytical Spectral Devices, Inc., 1998). While DIPPR would require the design of new versions of these instruments, the basic design and engineering work needed to implement them on a Mars rover has already
, been done.

A model thermal-infrared imaging spectrometer for the BMR is the mini-TES, part of the Athena payload (Athena Project, 2000). It is small and light, with sufficient spectral resolution to identify primary rock-forming minerals that are expected on Mars. Additional resolution and/or spectral coverage might be necessary to characterize the abundances of accessory minerals, but it would be relatively straightforward to upgrade mini-TES's capabilities. Although mini-TES could also work as a point spectrometer, its optics are designed to look at distant outcrops, not nearby mineral grains. Thus, a better model for the LMR spectrometers would be the Analytical Spectral Devices VNIR point spectrometer, which is extremely lightweight and uses little power. It acquires data through a fiber-optic cable, the terminus of which could be mounted on the LMR sensor arm (Analytical Spectral Devices, Inc., 1998). While it is not designed for space use, it could be modified to be space-certified.

Rock Resurfacing Tool

While the LMRs would have the capability to conduct most tests necessary for rock identification and shape analysis without assistance, it may prove necessary from time to time to obtain a fresh surface on an outcrop for detailed work. In such cases, a rock resurfacing tool might be used. Such tools have been designed for the Athena Mission, in the form of the Rock Abrasion Tool (RAT), and we envision mounting a similar design on the LMRs (Athena Project, 2000). The RAT is a small grinding wheel, with a diamond-based abrasive and a stiff wire brush for cleaning. Since any rock resurfacing tool would likely draw a large amount of power for a short time, the LMR batteries would be used to provide power for the tool.

Navigational Aids and Safety Devices

A sophisticated software system would be employed to permit the MRs to navigate potentially hazardous terrain. Receiving input from the navigational cameras, an accelerometer, and three inclinometers, the navigation software would quickly calculate position, orientation, movement direction, and acceleration and adjust the motion of the MR to correct for "stumbles" and choose as clear a path as possible. In general, these systems would be similar for all rovers, but there would be some algorithmic differences. For example, the BMR navigation software would include clauses permitting both long- and short-range navigation, whereas the LMR navigation software would have lower tolerances for obstacle size and use different algorithms for the coordination of leg movements.

In order to produce accurate paleontological potential maps, it would be important for all MRs in the family to be equipped for exact location determination. This would be accomplished by registering all rover movements relative to the Martian base station. (Presumably the position of the base station is known well.) In addition to simply counting wheel revolutions and leg movements using on-board computers, we envision having the ability to triangulate the position of all rovers relative to one another and known geomorphic features using laser rangefinders mounted on each rover. Both locational methods would be augmented by the use of stereoscopic images to evaluate the apparent height and width of distant landforms that have precisely determined true height and width characteristics as determined from digital elevation models.

Data Analysis Procedures

A primary concern in the design of DIPPR has been to maximize overall mission efficiency by progressively minimizing the number of outcrops that astronauts must study in detail. To accomplish this, we have focused much of our effort on determining optimal procedures to assess sites for their potential to be fossiliferous and, on that basis, to assign them relative priorities for detailed study.

Long-Range Data Analysis

Long-range data would consist of panoramic images, a computed position and orientation for the observing rover, an estimation of the distance to a target outcrop from stereographic image analysis and laser range-finding, and generalized mineral abundance information for the outcrop obtained with the

visual analysis of outcrops at distances of several hundred meters or less. An example of a camera system that would meet our needs is the Pancam system, being implemented as part of the Athena payload on the two Mars Exploration Rovers [MERs] slated for launch in 2003 (Athena Project, 2000). The Pancam is a mast-mounted stereo camera system with very high resolution, which includes several filter wheels to provide rudimentary spectroscopic data and color imagery. These characteristics make it ideal for use as the panoramic camera on the BMR, but leave Pancam a bit overqualified for the LMRs. For the LMR camera, a wider field-of-view than the Pancam's 18.4°×9.2° would be preferred, whereas the extensive set of filters would be unnecessary, as would the mast and servomotor control. Nonetheless, Pancam serves as an excellent model for the DIPPR cameras, and further technical details can be found on Cornell's Athena Payload website (Athena Project, 2000).

Microscopic imaging cameras would be employed on the LMRs for use in close-up analysis of the surfaces of rock outcrops. Mounted on the LMR's articulated sensor arm, the microscopic imaging camera [MIC] needs to have a resolving power on the order of $10\mu m$, in order to accurately image mineral grains as small as 100 μm. Its magnification needs to be adjustable up to a resolution of about $100\mu m$, with a field of view that covers several square centimeters. These specifications are based on the need for the ability to determine whether a silica-rich siliciclastic rock is a sandstone, chert, or conglomerate. Identifying mineral grains in these rocks requires both high and low magnification, since grains in conglomerates can exceed several centimeters in size, while sand grains can be as small as $100\mu m$.

A camera with some microscopic imaging capability was part of the ill-fated Mars Polar Lander, and a fully functional MIC is slated for the MERs in 2003 (Athena Project, 2000). While the actual specifications of the Athena payload MIC are unclear, DIPPR's MICs will most likely require a shorter focal length and greater magnification range, given the location where the MER MIC is mounted, looking down from the rover's undercarriage.

Spectrometers

There is a wide array of spectrometers available today which are capable of identifying the mineralogy of a rock sample, including UV/VIS, VNIR, Thermal IR, Raman, and Mössbauer spectrometers. Each has its own particular advantages and disadvantages, which must be taken into account when choosing spectrometers for DIPPR. DIPPR will require two distinct classes of spectrometer: an imaging spectrometer for the BMR and point spectrometers for the LMRs. The imaging spectrometer will need to be able to accommodate a 360° field of view, and to characterize mineral abundances in outcrops up to several kilometers away at 1 meter per pixel or better spatial resolution. The point spectrometer must be able to determine the mineralogy of an outcrop's surface to the level of individual mineral grains, or on the order of 100 μm. Both spectrometers must be able to identify all of the minerals specified previously in this paper. This constraint immediately removes the Mössbauer spectrometer from consideration, since it only identifies minerals containing iron (Athena Project, 2000).

All of the remaining spectrometers, however, have the ability to identify the necessary minerals, thus the field must be narrowed by considering the engineering constraints of the mission and the present technology. UV/VIS spectrometers are very accurate and useful for determining mineralogy on Earth, but have not been fully adapted to use in space yet. As such, they are an unproven technology. Raman spectrometers, however, have been adapted for planetary exploration (Athena Project, 2000). Since Raman spectrometers have no long-range capability, one could not be used for the BMR imaging spectrometer (Lane, 2001). A Raman spectrometer could, however, be used for the LMR spectrometer. However, Raman spectroscopy is still a relatively new technology, and no missions have used it yet. Furthermore, Raman spectroscopy requires precise control of the separation between the instrument and sample, and so only works at distances on the order of 1cm. Therefore, given current engineering constraints and technology, we choose not to use Raman spectroscopy in DIPPR.

VNIR (visible-near-infrared) and thermal IR spectrometers are proven technology in space. Numerous Earth-observing satellites use imaging VNIR spectrometers, and very small, light, and field-portable terrestrial VNIR instruments are in use by geologists around the world (NASA Jet Propulsion Laboratory, 2001; Analytical Spectral Devices, Inc., 1998). Thermal IR spectrometers are also used on Earth-observing satellites, as well as two Mars-observing satellites and the 2003 MERs. In most cases, these spectrometers are combined to some degree, so that a single instrument includes visible, near-infrared, and thermal-

Lane, L., 2001, Personal Communication, Operational Systems Division, NASA Jet Propulsion Laboratory.

Malin, M. C., and Edgett, K. S., 2000a, Evidence for recent groundwater seepage and surface runoff on Mars: Science, v. 288, p. 2330-2335.

Malin, M. C., and Edgett, K. S., 2000b, Sedimentary rocks of early Mars: Science, v. 290, p. 1927.

McKay, C.P. and C.R. Stoker, 1989. The early environment and its early evolution on Mars: Implications for life. *Rev. Geophys.* 27, 189-214.

McKay, D. S., Gibson, E. K., Thomas-Keprta, K. L., Vali, H., Romanek, C. S., Clemett, S. J., Chillier, X. D. F., Maechling, C. R., and Zare, R. N., 1996, Search for past life on Mars: Possible relic biogenic activity in Martian Meteorite ALH84001: Science, v. 273, p. 924-930.

NASA Mars Exploration, 1997a, Mars Pathfinder frequently asked questions. <http://mars.jpl.nasa.gov/MPF/rover/faqs_sojourner.html#stray> (April 25, 2001).

NASA Mars Exploration, 1997b, Introduction to the microrover. <http://mars.jpl.nasa.gov/MPF/rovercom/rovintro.html > (April 25, 2001).

USGS Spectrometry Laboratory, 2000, Tetracorder: What is it, how to get it. <http://speclab.cr.usgs.gov/tricorder.html>. (April 30, 2001).

NASA Jet Propulsion Laboratory, 2001, ASTER Home Page. <http://asterweb.jpl.nasa.gov/> (April 29, 2001).

Schopf, J. William. *Cradle of Life: the Discovery of Earth's Earliest Fossils.* Princeton, NJ, Princeton University Press, 1999.

Thomas-Keprta, K. L., Clemett, S. J., Bazylinski, D. A., Kirschvink, J. L., McKay, D. S., Wentworth, S. J., Vali, H., Gibson, E. K., McKay, M. F., and Romanek, C. S., 2001, Truncated hexa-octahedral magnetite crystals in ALH84001: Presumptive biosignatures: Proceedings of the National Academy of Sciences, v. 98, p. 2164-2169.

Zuber, M. T., Solomon, S. C., Phillips, R. J., Smith, D. E., Tyler, G. L., Aharonson, O., Balmino, G., Banerdt, W. B., Head, J. W., Johnson, C. L., Lemoine, F. G., McGovern, P. J., Neumann, G. A., Rowlands, D. D., and Zhong, S., 2000, Internal structure and early thermal evolution of Mars from Mars Global Surveyor Topography and Gravity: Science, v. 287, p. 1788-1793.

54 /ᶜᴾ/ /ᴺ╳⁹ᵘ

PENNSTATE
1855

Mining the Foundation of the Future

Submitted by the 2001 Penn State HEDS-UP Team pursuant to the NASA 2001 HEDS-UP Student Design Competition

Student Team Co-Leaders

Joe Fledderman (jpf137@psu.edu) & Kevin Sloan (kfs113@psu.edu)

Student Team

Levent Cakcak, Vicki Christini, Dexter Cooke, Josh Geiple, Alex Hamling,
Joe Masiero, Bryan Mayrides, Mike Pritts, Joel Richter, Jeanette Schreiber,
Jamie Szmodis, Jon Trump, Laura Yingling

Student Team Faculty Advisor

Mike Jacobs

1. Abstract

"In fact, a two-kilometer-wide asteroid holds more metal than all the ore mined on Earth since the beginning of civilization." - Mark Alpert, issue editor at Scientific American.

An asteroid mining mission presents the opportunity to obtain large quantities of raw material already outside of Earth's gravitational pull. Such materials would be best put to use for construction of infrastructure in outposts set up on either the Moon, Mars, or future space stations. Mining on an asteroid presents several challenges that prevent conventional mining techniques from being implemented. These challenges force a creative thought process with respect to the design approach. Given the difficulty of this situation, one mining method sticks out as the most practical.

We will be utilizing a three-component mission involving a ferry transportation unit, a canister unit, and a mining unit. This mission is designed to operate almost entirely autonomously. In the first stage of the mission, the ferry, which will be equipped with the VASIMR propulsion system, will bring the miner and canister out to the asteroid. The miner and canister will land on the asteroid and begin the mining stage of the mission. The miner will initiate the excavation of ore using the Laser Cutting System (LCS). With a series of intricate cuts using a drilling laser, the miner will slice a section of the asteroid into smaller pieces. The ore retrieval arm will transport this cut-up metal to the canister. Once the canister has been filled, the ore will be ready to be shipped. The ferry will return, bringing with it an empty canister, and then will carry the full canister back to its destination, most likely either Earth, Mars of the Moon. This process will continue as long as this is the most economical method of collecting metals. The process can also be expanded by adding a second miner and canister set.

2. Introduction

The date is July 20, 1969. Every American is on the edge of their seat as they watch Neil Armstrong make footprints in the Sea of Tranquility. They gaze into their brand-new color televisions in awe of the grandeur and brilliance of the men and women who fulfilled the dream of landing on the moon.

The date is now February 12, 2001: Just another mid-February Monday, or so we think. Not many Americans knew of the next "giant leap for mankind", as NEAR-Shoemaker successfully completed the first-ever asteroid landing. Though

Americans may not have been as interested in NEAR-Shoemaker as they were in Apollo 11, it holds great importance for the future of the space program.

Since John F. Kennedy's mandate to go to the moon, Americans have been continuing to satisfy their curiosity and furthering their knowledge of space. In order to utilize all it has to offer, we must expand our explorations to greater magnitudes. By harvesting the raw materials of space, we can enhance and encourage further exploration.

Because of the need for vast amounts of raw materials to further our exploration and colonization of space, the Penn State HEDS-UP 2001 team decided on a mission to mine an asteroid. The main asteroid belt, located between Mars and Jupiter, is the prime location to send a miner capable of harvesting enormous quantities of ore. The main belt has many useful asteroids, making the job of finding a desirable candidate a little easier. There are also advantages to mining a near Earth asteroid, so we do not want to rule out that possibility. Our system will involve a miner, which will be remain on the chosen asteroid indefinitely, a canister, a versatile storage device, capable of handling liquid fuel, and solid ore, and a ferry ship, which will transport the canister, and initially the miner.

3. Approach

Students from a wide variety of majors at Penn State University met twice weekly throughout the course of the Spring 2001 Semester. The students participating in this extracurricular project did not receive any academic credit for their involvement. Many of the students had little knowledge of asteroids, or even space missions in general. The group began with a discussion of current space missions, as well as future planned missions.

Mission Criteria

Because there are so many potential mission ideas which we could have developed, we felt it necessary to establish base criteria that would serve as the guidelines for any mission ideas which we considered. Our main criterion was that the mission fit into the plans of NASA for the future of space exploration. By examining the current missions and future goals, we crafted a proposal to complement NASA's aims. In addition, we wanted our mission to be expandable based on its success. In essence, we wanted our mission to fit into a modular sequence of missions that would work together to establish a more prominent presence in space. These two main design criteria allowed us to narrow down our mission significantly.

Mission Selection Process

With the ever increasing potentials of the space program, one question keeps arising; "what next?" Since the initial voyages to the Moon, humankind has yet to venture outside of low earth orbit. Eventually humankind will desire to venture out to the further reaches of space. The Moon does not offer much of a quenching for our adventurous thirst, and we have already begun to look past that. The most logical next step will be to send human missions to our neighbor, Mars. Several different groups, such as the Mars Society, are looking into the feasibility of such a mission. Because Mars is the only hospitable planet within humankind's current reach, plans are to send several missions to Mars, and eventually establish colonization efforts there. Depending on the success of these initial colonization efforts, such efforts could expand to support a large population there. As with any society, a certain amount of raw material is required for the construction of shelters and other infrastructure. The early structures will be constructed of pre-fabricated modular components that will be easy to set up on site. The materials will have to be shipped from Earth. While this is the most practical solution for the short-term missions, this will not suffice for any long-term efforts. In order to establish a society of any decent size, a rather exorbitant amount of raw materials will be needed. Because it currently costs about $22,000 to launch a single kilogram of material from Earth's surface, it is not economically feasible to launch thousands of tons of materials from Earth. This leaves the dilemma of how to transport the needed materials to Mars. One possible solution would be to travel to an asteroid and mine this material. The costs to transport material from an asteroid would be only a tiny fraction of the costs of launching it from Earth. It is with colonization efforts such as this in mind that the Penn State HEDS-UP Team has decided to design an asteroid mining mission.

Before we settled on mining asteroids in the asteroid belt, we discussed other possible missions. We talked about expanding on our rover mission from last year's competition, or possibly building outposts on our moon or the Martian moons. However, to do any of these missions we need materials. Transporting all of the raw materials needed build bases on other planets from Earth is very inefficient due to launch costs. Carrying building supplies to distant planets, such as Mars, or other moons, is not the best option as it is highly economically inefficient. The success of the NEAR-Shoemaker mission this past February brought with it inspiration. No longer is the space program limited
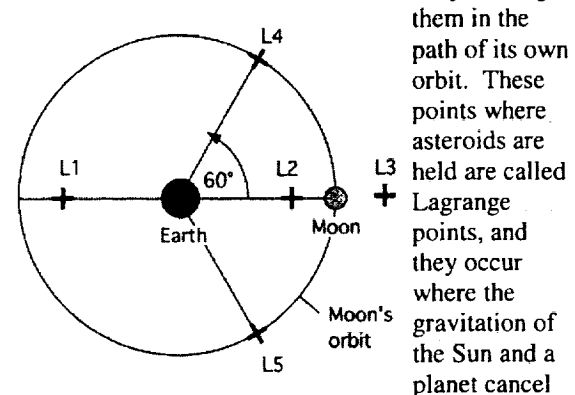
to conventional mission approaches. This is where the idea to mine an asteroid arose. We began to realize that in order to establish humankind's presence in outer space, the ability to use local and available resources is imperative.

Mission Destination

Once we decided on asteroid mining, we had to decide on where to go. With this in mind, we began to research the presence of asteroids in our solar system.

Many asteroids orbit the Sun in a 1 ½ AU wide area between Mars and Jupiter, known as the asteroid belt. It is believed that there are millions of asteroids in the belt, though the average separation between them is 10 million kilometers.

While Jupiter's gravity affects the belt asteroids, it also controls some asteroids by holding them in the path of its own orbit. These points where asteroids are held are called Lagrange points, and they occur where the gravitation of the Sun and a planet cancel each other out. Lagrange points exist in many parallel situations, including the moon orbiting around the Earth, as shown in the figure above. There are two Lagrange points in Jupiter's orbit, one 60 degrees ahead of Jupiter, and one 60 degrees behind it. The asteroids here are called Trojan asteroids, and almost 1,000 asteroids are contained between the two, though more are found at L4, the leading Lagrange point, than at the trailing point, L5. Asteroids are also found in elliptical orbits that bring them into the inner regions of the solar system.

These asteroids that pass through our area of the solar system are broken down into groups. The first, Amors, are asteroids which cross Mars' orbit but do not quite reach Earth's orbit. Another group are the Apollos, which cross Earth's orbit with a period of greater than one year. The last group are the Atens, which also cross Earth's obit, but with a period of less than a year. Currently there are approximately 250 identified near-Earth asteroids (NEAs) known of, and it is estimated that 100,000 others are yet to be discovered.

Besides identification due to their location, asteroids are also classified based on their composition. The most common type is C,

compromising more than 75% of known asteroids. These are characterized by very low albedos, about 0.03, making them extremely dark, and giving them a virtually featureless spectra in the ultraviolet, visible and near infrared. These carbonaceous asteroids have a chemical composition similar to that of the Sun, without the hydrogen, helium and other volatiles. They are found mostly in the outer asteroid belt, along with D and P types, which are other classes closely related to C-type.

The next most common type is S, accounting for 17% of known asteroids. The S-types are relatively bright, with albedos between 0.10 – 0.22 and their spectra show absorption bands mixed with a reddish color. These asteroids are composed of metallic nickel-iron mixed with iron and magnesium silicates. S-types are located mainly in the inner portion of the asteroid belt.

Another type, M, makes up about 5% of the known asteroids. These asteroids are about the same brightness as the S-type, with albedos ranging from 0.10 to 0.18, and their spectra are somewhat reddish-slopping and straight. M-type asteroids are almost of pure nickel-iron. The inner-most edge of the asteroid belt is home to these types of asteroids.

There are other, less prominent classes of asteroids, many akin to C-types. After reviewing the composition and location of the major types, we decided that M-class are the only type that would yield the large amounts of metals we are looking for. We had been concerned with the possible presence of a silicate crust, but M-types appear to have an entirely metallic surface, which has been seen in examining 16 Psyche, 216 Kleopatra and others.

The best option which we have now would be to either travel to the asteroid belt or to a near Earth asteroid and mine a large M-class asteroid. We chose to narrow this down further to the asteroid belt due to the abundance of suitable asteroids, and its close proximity to Mars, which would be the most likely destination for the ore.

4. Study Results
4.1 Mission Overview

The mission will begin on Earth with the construction of the miner, canisters, and ferry, also know as Canister Linkage and Movement Project (CLAMP). These components will be transported to space aboard the space shuttle and assembled at an orbiting facility, such as the International Space Station (ISS). During the initial transit to the asteroid, the spacecraft will be composed of a stack containing the ferry, the miner, and the canister respectively. The spectrometer and computers on

the miner will choose an asteroid before it arrives. Once a suitable asteroid is selected, the entire craft will descend into orbit using the engines on the ferry. At this time, the canister and miner will separate from the ferry and land on to the asteroid. Once in position, the miner will begin its operation. The canister will land and follow the miner around, transferring fuel and collecting ore. While the mining occurs, CLAMP will leave orbit and return to Earth for maintenance, refueling, and obtaining a new canister. When CLAMP returns to the asteroid, it will send the new canister to the surface. Meanwhile, the ore-filled canister will liftoff from the asteroid and rendezvous with the ferry in the asteroids' orbit, using onboard thrusters and guidance. These two will dock and take the ore to wherever it is needed.

4.2 The Ferry
Ferry Overview

The ferry was designed to have three main components: 1) the engine block, which will consist of a VASIMR engine, 2) the 'brain' block, which will contain standard interplanetary navigation computers, as well as all the other hardware necessary to make it completely autonomous, and 3) the clamping system used to attach and detach from the canisters. The main purpose of CLAMP will be to bring the miner and the first canister out to the asteroid, and then shuttle fuel-filled canisters out to the asteroid, while bringing back ore-filled ones. (While multiple CLAMPs may be needed to shuttle the canisters to and from the asteroid, if production by the miner is higher than expected, the current proposal only calls for one.)

SWISH
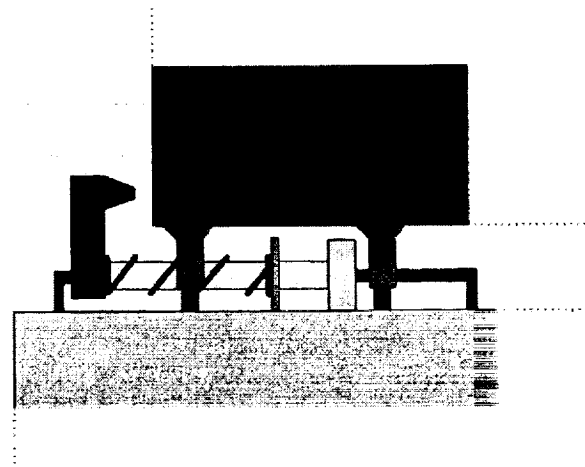
The SWISH system (Securing With Interacting Springs and Hydraulics)

Canister securing clamps (a.k.a. the SWISH system: Securing With Interacting Springs and Hydraulics)

Due to the nature of the trip the canister-CLAMP system would undertake, and the shapes of the components of this system, a securing mechanism had to be designed. It would have to be reliable enough to work completely automated in interplanetary space and be able to perform its function many times without repair, while still being able to secure and control the canister for the long trip ahead of it. To this end, our group decided on using the following system.

The above picture is a side view of the SWISH system, with the canister at the top and CLAMP at the bottom. Shown in the picture is one of the several locking mechanisms, which will be placed in radial symmetry around the top of CLAMP. The SWISH system is centered around a rail, which will run from the center of CLAMP to its edge. Moving from the inside out, the first component encountered is a hydraulic press coming out from the top of CLAMP. This runs all the way to the locking claw, where it is attached. The rail runs unhindered through the center of the hydraulic press and tube. The next component is the spring base, which connects the spring to CLAMP, and provides support for the spring. The rail and hydraulic tube run unhindered through the spring base. The next component is the spring. It is important to note that when the SWISH system is in the closed position around a canister, the spring will still be extended beyond its relaxed length. This will provide a constant inward force on the locking claws, which will act as a fail-safe and prevent the canister from separating from CLAMP, should the hydraulics fail. The spring surrounds the hydraulic tube, but does not hinder its motion. The next components are the shocks, which are not drawn at their correct position, but only shown to aid the visual model. There will be multiple shocks on CLAMP, spread evenly over CLAMP's top surface, which will aid the docking procedure. The final component is the locking claw. The bottom half of the claw is where the spring and hydraulic press terminate. The rail runs unhindered through the claw. The top half of the claw has a locking pin, shaped like a truncated cone, which will fit inside of the holes on the canister and miner, and secure them for transport.

It should be noted that the miner will have a SWISH system on top of it, too, in order to secure the first canister brought out to the asteroid, as well as any canister it is currently filling, if and when it decides to move to a different asteroid. This mission

option will be discussed further in the **Mission Adaptability** section.

The SWISH system functions in the following manner: The CLAMP system contains an arm very similar in nature to the Canada Arm being built for the International Space Station. Initially, the Canada Arm on CLAMP will orient the canister and CLAMP, so that they are aligned in the necessary direction to facilitate easy docking. The hydraulics will push the claws outward, until the canister can clear them, and then hold them there. Then the Canada Arm will bring the canister and CLAMP together, until the canister strikes CLAMP's shocks. The hydraulics will release pressure, and the claws will move in from the force exerted by the springs, securing the canister. Undocking is a simple reversal of this procedure.

Propulsion

VASIMR Concept
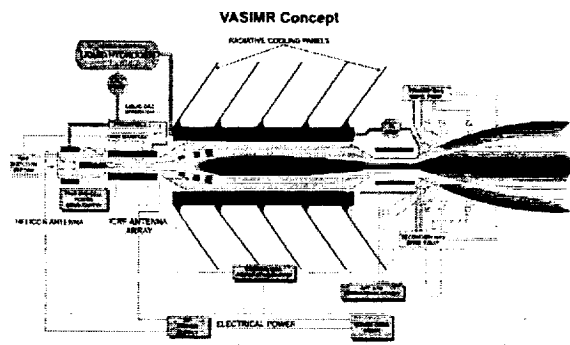
For the propulsion system of the CLAMP, we choose to use the VASIMR (Variable Specific Impulse Magnetoplasma Rocket). It consists of three linked magnetic cells, one fore, one central, and one aft, each with a specific function. The forward cell handles the injection of the propellant gas and its ionization. The central cell acts as an amplifier and further heats the plasma. The aft cell is a magnetic nozzle, and converts the fluid energy into a directed flow. Plasma ions are injected from the forward cell, and then accelerated through an ion cyclotron. After the ions have gained enough energy, they are shot out the aft cell to produce thrust. A major reason for choosing the VASIMR system is its ability to use constant power throttling. This enables the fastest possible round trip time for a given amount of propellant. Since the miner will ore enough metal to fill a canister in approximately one year. This means that a canister has to be delivered to the asteroid at least once every year. Using the VASIMR, CLAMP will be able to make the round trip from the asteroid to low Earth orbit and back to the asteroid, again, in about one year. This makes VASIMR the ideal choice of a propulsion system for this mission.

4.3 The Miner
Initial Design Considerations

The most difficult aspect of our mission to design was the miner unit. Mining on an asteroid presents so many complications and unknowns that a radical design approach must be implemented. Not knowing very much about mining in general, we first did research into some of the mining techniques currently used on Earth. The more popular methods included drilling and blasting. However, if we wish to mine an asteroid, we must first look at the basic facts regarding asteroids.

First, an asteroid has a negligible local gravity. Only do the largest of asteroids have a gravity that is even remotely measurable. Secondly, asteroids do not contain any sort of atmosphere; they are simply part of the large vacuum of space. These two facts alone present obstacles as far as mining is concerned. If we are to drill, we are exerting a large amount of force into the ground. From basic Newtonian Mechanics we know that the ground will be exerting an equivalent reactionary force back at the miner. Such a force would easily throw the miner back off of the asteroid. If we decided to go about any sort of blasting process, we would run into several difficulties.

First of all, there is no atmosphere, and thus no oxygen to fuel an explosion. Assuming that oxygen cartridges could be provided to fuel the explosion, there are too many erratic factors. Aside from the unpredictability of using explosives in space, there is entirely too much of a danger presented to the miner. Having to consider these design constraints, we designed a miner unit that worked in a completely different manner.

Miner Overview
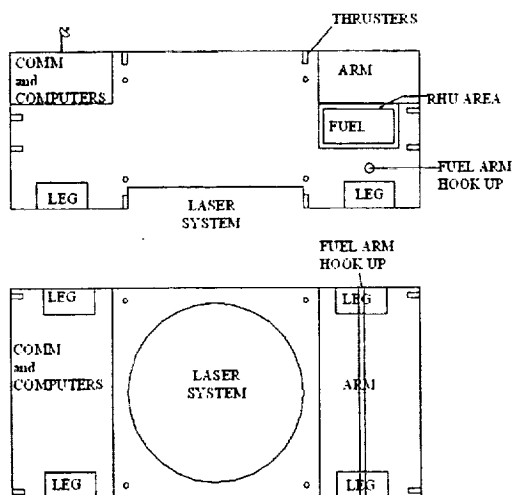
Side and top views, respectively

The asteroids present a natural reserve of minerals for future development. Yet for this resource to be useful, it must first be extracted from its current resting spot so that it may be brought to humans, so they can manipulate it into a more usable form. To this end, the miner will be able to break up the ore deposit into pieces between the size of gravel and soccer balls. The physical breaking apart of the rock will be done by a laser. The laser will vaporize a thin line through the rock, effectively slicing the rock into pieces. The gravel mix can then be loaded onto the ferry and returned to either the moon, Mars, or the ISS so that it can then be first processed into ingots of metal and then shaped into usable devices.

Laser Cutting System (LCS)
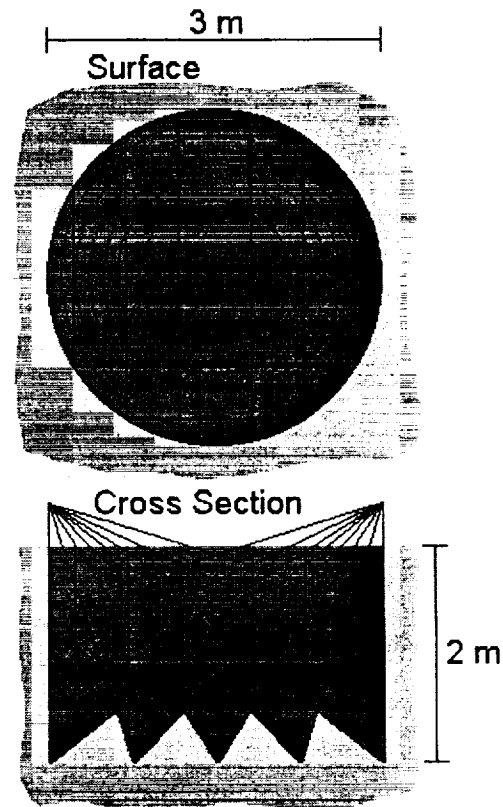
The laser drilling process will be the longest phase of the mining operation so much thought went into finding the most efficient pattern to use. There is inherently a trade off between the size of pieces cut and the time required to cut them. To maximize efficiency, the pieces must be as large as possible while still being easy to move around and store compactly. We concluded that the most efficient pattern would be to cut cones with progressively smaller angles until the entire cylindrical shape is cut into small pieces that are free from the surrounding metal. To prevent all the pieces from being shaped

like a torus, the laser also cuts a grid through the area being mined. With the pictured cutting pattern, the entire shape to be broken up into pieces no larger than ~ 0.5 meters, with the majority being much smaller. The entire surface area cut is 140 m^2. The mix of small and large pieces allows for maximum space efficiency within the canister because the small pieces will fit in the cracks around the larger ones.

In order to cut the ore in this pattern, we have designed a circular track with a three-meter diameter that will hang just below the center of the miner. The track will be suspended by four hydraulic presses that allow it to be lowered out of its storage bay in the miner. If the miner is not sitting on level ground, these presses will be able to adjust to different heights in order to partially level the track and make drill the hole at the desired angle. A small motor and the emission point of the laser will hang from the track, moving on a circular gear fitting in a C-shaped joint. The entire apparatus will hang from a wheel above in order to support its weight (minimal on the asteroid). The laser will be mounted on a joint in order to allow it to make the necessary angled cuts. In order to cut a section of ore, the laser must drill until it reaches the desired depth, then advance on the track by the diameter of the laser and drill again. Once it completes the circle, it adjusts the angle and repeats the process. After all the cone-shaped cuts are finished, the laser drills a grid over the entire area by positioning itself along the track at a point perpendicular to the desired cut and adjusts the cutting angle every time the desired depth is reached.
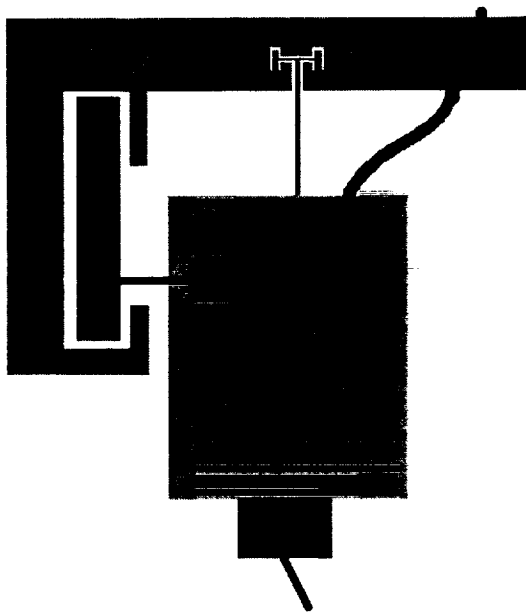
Cutaway of laser and track

Because the canister holds 96 m^3 it will be necessary to collect material from seven holes to fill it up. With the round trip time of the ferry estimated to be one year, this would require one hole to be drilled and the ore collected approximately every 50 days. Collecting will only take a couple days at most, so that leaves a very conservative estimate of 45 days to drill the hole. With the above configuration it will require 140 m^2 to make the desired cuts. The speed required from the laser would then depend on the diameter of the laser. Assuming a diameter of 10^{-3} m, the total distance cut would be 140,000 meters, and the speed required would be ~ 2.2m per minute. The cutting pattern could be modified to reduce the number of cones and grid cuts. This would make the pieces more unwieldy and allow less ore to be transported back to earth, but if a sufficiently powerful laser is not developed by the time of this mission, the cutting could be scaled back to allow for enough time to mine a canister load of ore within the round trip time of the ferry.

Scooping Arm
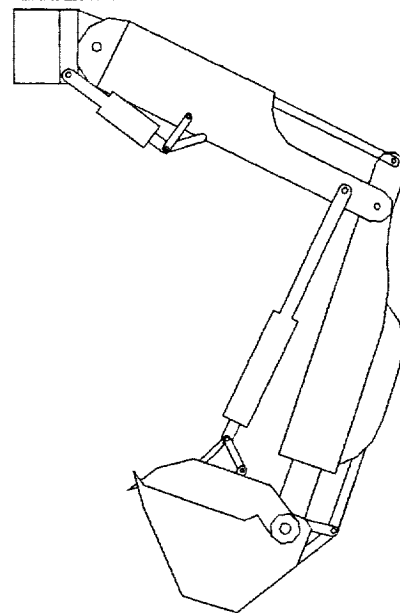
In order to collect loose material and to transport it to the canister, we designed an arm similar to a backhoe. The arm connects to a top corner of the miner and rotates in all directions. The first section of the arm is about 3.3m and is hinged to the second part of the arm that is about 3.5m in length and its angle is controlled by hydraulics. The bucket is about 1m long and .5m deep and the width of all components is near half a meter. The flat bottom of the bucket contains electromagnets that can magnetically charge the bucket, further assisting the

collection process. Excess silicates and other non-magnetic rocks will not be attracted to the bucket, minimizing unwanted debris. If the magnets would happen to fail, or if for an unforeseen reason we would need to resort to scooping with the bucket, a lid closed during transport ensures no debris is propelled towards the miner during the process. The two arm sections fold into one another with the bucket in between, so that the entire apparatus can be stored in 1mx2mx4m section on the topside of the miner, to be extended only when necessary. Both the lid and the bucket are controlled through hydraulics. The power requirements for the hydraulic pump and motors should not exceed 25kW, based on power requirements of backhoes. Technological advances and the fact that there is no gravity should lower this number.

As mentioned above, we were attempting to design a mining system that would cause no negative forces back against the miner. Unfortunately the arm will cause a small amount of these forces to be present. However measure have been taken to correct this problem, and will be described in future sections.

Thrusters/Legs

The miner is equipped with a total of 24 thrusters, 4 on each side of the miner. The dimensions of the thruster are 0.1 m in diameter and 0.25 m in length. The thruster will use a liquid fuel such as hydrazine, stored within the miner.

The thrusters are located equal distances from the center of mass, and spaced a close to the edges of the miner as possible. This balance is aimed to reduce moments being created from unequal thruster firing or from unequal shifts in mass within the miner.

This mobility is important for the positioning and movement of the miner for all aspects of the mining operation. Initially the thrusters will be used to land and move the miner to an acceptable mining position. After landing the thrusters become important as a backup system for holding the miner in place whenever forces, such as the ore scooping arm, lift it off the surface of the asteroid. When the thrusters are used in combination with each other three-dimensional rotation and translation becomes possible. This is necessary for moving from one mining site to another.

The legs are designed to be adjustable in height, holding the miner unit above the asteroid surface anywhere from about 5 cm to 60 cm. This allows the miner to rest flat on the surface despite small changes in the elevation of the asteroid under each individual corner of the miner. The legs extend and retract by a screw and thread system, as shown in

the diagram. When the screw turns, the parallel threads in contact move up or down, thus pivoting each segment of the leg and changing the vertical height from the asteroid surface.
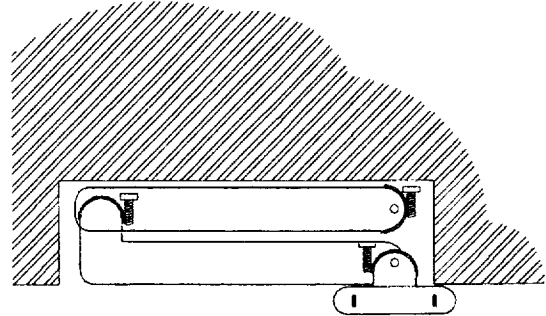
The miner unit is anchored to the asteroid by electromagnets placed in the feet of the legs. These electromagnets produce the necessary force to counteract any forces that might push the miner off the asteroid surface (mainly any digging by the arm). Using a design given in *Electromagnetic Devices* by Herbert C. Roters, such an electromagnet producing 500 N of attractive force on the asteroid would require only about 10 watts to run. This force, when exerted by each leg, should be more than enough to hold the miner on the surface and counteract all upward forces. The minimal temperature increase caused by resistance in the coils in the electromagnet is dissipated by driving a heat sink in to the surface of the asteroid. Of course, this heat sink must be made of a strong, highly heat conductive metal alloy, and is designed to have maximum surface area in contact with the "ground" of the asteroid, thereby dissipating the heat built up by the magnet into the heat conductive iron-nickel material of the asteroid.

Power

In order to power the miner, a new technology is needed. We expect that the arm will use about 25 kW of power and the laser could use as much as 30 kW. While these will not be operated at the same time, the continuous power consumption would be about 30 kW. To have a wide safety margin and to ensure that sufficient power is available, we believe the power source should provide 35 kW. With power consumption at this level, no traditional power generation technologies will work. The asteroid belt is too far from the sun to allow the use of solar power, which would be a bulky, unpractical alternative. Battery power would be nearly useless because we expect the miner to operate for about 10 years before returning to earth for maintenance and it would be drained quickly. The current solution to power generation for missions to

the outer planets of the solar system is the use of
RTGs (Radioisotope Thermoelectric Generators), but
due to the large power requirement, this will not be
feasible either. With current RTG technology, each
unit produces about 280 W, so in order to produce
sufficient power, 125 RTGs would be needed. This
would be extremely expensive and would take up an
unacceptable amount of space. The solution is to use
a nuclear reactor, such as the SP-100, which is
designed for use in space. It would be able to provide
between 10 and 100 kW of power, which is exactly
for what we are looking. This program was canceled
a few years ago due to lack of a clear mission, but
much progress was made. Extensive development
and commercialization of space would require such a
power source, so developing the technology would
bring great benefits that extend beyond this mission.

Fuel Arm Connection

The thrusters located on the Miner will
require fuel. The fuel, probably hydrazine, will be
brought out with each canister. In order to transfer
the fuel from the canister to the miner, a fuel transfer
arm had to be designed.
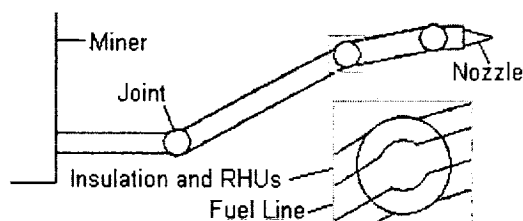
The fuel arm is housed completely within
the main body of the miner with an opening on the
long side of the miner. It is assumed that the canister
can be positioned on the side of the miner within 2 to
3 meters, thereby exposing the entry plug on the side
of the canister for the fuel arm to attach to. The
nozzle will find the entry plug by means of an
automated docking procedure.

The entire length of the fuel arm is covered
in insulation and a number of Radioisotope Heater
Units (RHUs). These are imbedded in the insulating
layer to prevent the liquid fuel from freezing. The
fuel arm is equipped with three ball-in-socket joints
that allow the fuel arm to be positioned into the entry
plug. The joints have limited freedom of movement
because they must accommodate the fuel line housed
within the arm.

The fuel storage tank on the canister is
equipped with a divider capable of applying pressure
on to the fuel, which forces the fuel to flow through
the fuel arm into the miner. Four hydraulic jacks
evenly spaced around the edges would create the
necessary pressure.

Asteroid Recognition and Science Components

The Miner will be equipped with various
pieces of equipment to gather in-depth knowledge of
the asteroid. The Miner will include a spectrometer
to determine the chemical composition of the surface
rocks along with the rocks that are mined. While
most previous analyses of the solar system have
relied on surface readings, the Miner will create a
unique opportunity to study the internal body of a
non-terrestrial object. Additionally, the ore returned
to Earth will be studied in great detail to allow us to
learn much more about the composition of asteroids.

A high-resolution, wide-angle camera would
be installed on the side of the Miner to take detailed
photos of the surface of the asteroid. A camera will
also be placed on the underside of the Miner so that
pictures can be taken of the internal walls of each
hole being dug. This could reveal any layering of the
metal or the depth of any minor surface reactions
such as desert varnish or oxidation.

A strain gauge will be available to determine
the strength of gravity on the asteroid. From the
gravity readings, the overall density of the asteroid
can be determined. This information should make it
possible to speculate whether the internal
composition of the asteroid consists of heavier
elements. If the center does consist of heavier
metals, it may become preferable to attempt to
modify the mining operation such that deeper holes
are dug, or holes are dug on top of previous holes, so
that the heavier, rarer metals may be reached.

Such analytical devices will help scientists
more fully understand the chemical composition and
thus the geological and formational history of the
asteroids and perhaps the solar system as well.

4.4 The Canister
Canister Overview

Mined ore can not be put to any good use if
it can not be transported back to Earth's orbit to be
processed. Therefore, it was necessary to design a
system that would be able to transport the ore from
the asteroid back to Earth orbit. Also, a system had
to be design which could bring needed fuel and parts
out to the miner, so it would not have to return to
Earth for maintenance, but could rather stay and mine
the asteroid for as long as possible. It was decided
that a vessel that could accomplish both of these tasks
at the same time would suit the mission's needs the
best. With this in mind, the canister design was
chosen.

ORE

← MOVING
AIRTIGHT
SEAL

FUEL

FUEL PIPE →

← COMPUTERS,
RTG..

Internal View

Side

Thrusters

Support Leg

Thrusters

Top
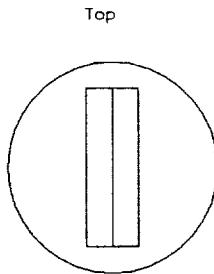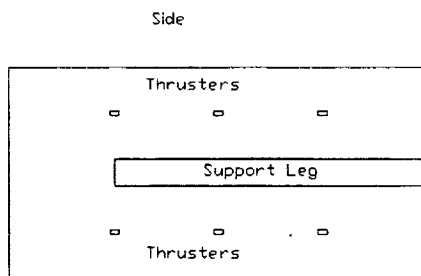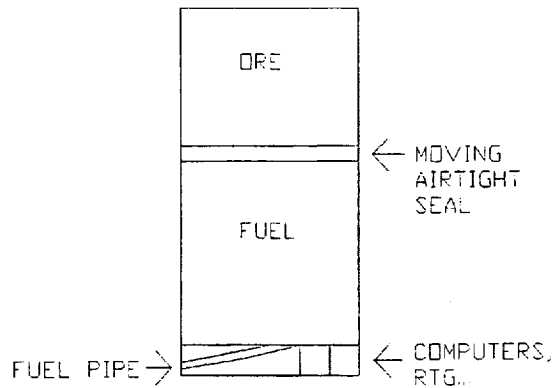
Side and top views, respectively

The canister will have the following features: first, it will be encircled by three rings of four positionable thrusters, which will allow the canister to hover along the surface of the asteroid when it needs to follow the miner around, as well as allowing it to position itself correctly for fuel hookup with the miner. Second, the canister will have three legs every 120 degrees around the outside of it, which will be placed down to stabilize the canister as it is being filled. Third, it will have a set of two sliding doors on the top, each 3m by .5m, which will provide an opening of 3 square meters for the mined ore to enter. Fourth, the canister will have SWISH docking points every 60 degrees around the bottom of it. Fifth, the canister will have a fuel hookup near its base, that the miner's fuel arm will be able to attach to. Sixth, the canister will have all the necessary power supplies and computers in the

bottom .5m of its height. It is from this point that all the thrusters, fuel discharge, and the orientation will be autonomously controlled. Finally, the canister will have within it a moveable pressure seal. This system will be discussed in more detail below. It should be noted that there will have to be more than one canister active at all times: one at the asteroid, being filled, and one in transit with ore or fuel.

Fuel/Ore divider

In order for the canister to be able to hold both liquid fuel, and replacement parts and ore, a unique type of storage system needed to be designed. The storage area of the canister will act like a syringe. In the lower portion of the canister, liquid fuel will be kept pressurized by a movable, airtight seal against the inside perimeter of the canister. On top of this seal solid objects, such as spare parts, or the mined ore, will be able to be kept in a non-vacuum sealed chamber. As the liquid fuel is pumped out, the airtight seal will follow the level of the fuel down. This will make the chamber for the ore larger, enabling us to carry more materials to their destination. This will also keep the pressure in the fuel chamber at a high enough rate to push the fuel into the miner, as necessary.

Canister Power Source

The canister will require electricity for the computer and navigation system, the ore storage compartment doors, the stabilizing legs and the moving canister divider. No more than one system will be in operation at the same time, except for the computer, which will run constantly, so we estimate that peak power usage will be less than 1 kW. Heat energy will also be needed to keep the fuel from freezing. We examined possible power sources to find out what would be the most effective way to power the canister. Solar energy density decreases by the inverse square of distance, so available solar power in the asteroid belt will be about 10% of what it is at earth. Additionally, asteroids rotate, which keeps any given spot on them pointed away from the sun half the time. The canister needs to be maneuverable and able to land and take off frequently and having solar panels that are many of meters long would compromise this ability. Because of these considerations, we felt that solar power would not be an effective method of powering the canister.

The power source that most closely meets the mission needs is an RTG. An RTG (Radioisotope Thermoelectric Generator) generates about 250 W of electricity by using the heat generated by the natural decay of plutonium to heat a piece of metal. This is

connected to another piece of metal kept at a lower temperature, which induces current through the metal. Current induction in this manner is called the Seebeck effect. The most recent RTGs used in space exploration are those that power Cassini. Three RTG units were used, producing a total of 888 W of electricity at launch. The amount of electricity generated is gradually reduced over time due to the fact that radioactive decay is a consuming process that eventually extinguishes itself. By the end of Cassini's mission, which will be 11 years after launch, the RTGs will produce 628 W, still a very usable amount. The RTGs on the canister can be replaced as necessary when it returns to earth to be unloaded, but the lifespan of the generators should allow for many years of operation. A useful byproduct of the electricity generation process is the significant amount of waste heat, which would be used to keep the fuel temperature above freezing levels.

4.5 Mission Window

There are certain times, or windows of opportunity, when we should send the ferry to the asteroid belt to ensure the shortest trip. The closest M-class asteroids in the asteroid belt are located at about 2 AU. Therefore, the shortest trip from the Earth to the asteroid is 1 AU, or 1.496e11 m. Using the VASIMR propulsion system, we are estimate that we can travel this distance in about 8 months, or 240 days. So we want to launch our ferry when the asteroid is lagging behind Earth 240 days, or 200 degrees. Eight months later, the ferry and the asteroid will both arrive at the same spot in the asteroid's orbit. One of these transfer opportunities will occur every 19 months. The best of these opportunities will be when Earth is at the opposition of its and the asteroid's orbit during the launch. If and when this happens will depend on the specific asteroid chosen and its relative position to the Earth, but it should be about every 13 years.

4.6 Future Adaptability

Due to the modular nature of this mission, it offers a wide range of adaptability to fit varying needs in the future as they arise. Should future technologies allow for higher mining rates, multiple canisters can be loaded during each stage of the mission. Also, multiple miner units can be employed. While the additional miners can be set up on the initial asteroid, they can also be used on different asteroids to obtain a wider variety of metal. With any of the situations described above, additional ferries would be needed to handle the extra workload. As can be seen, any combination of ferries, canisters

and miners can be combined to obtain an optimum amount of ore.

5. Assumptions, Recommendations, Conclusion

Assumptions

For the design of this mission, several assumptions had to be made. Many of these assumptions stemmed from the period of when such a mission would occur. As discussed earlier, this mission would not be implemented until Mars colonization efforts or a similar large-scale mission sequence are underway. Such efforts we speak of would not take place for probably at least another thirty years. In that time, there will be numerous advancements in technology. Among those technologies include drilling laser capabilities, the VASIMR drive, and the SP-100 power generator. The VASIMR and SP-100 are both programs that NASA has cut recently due to budget cutbacks. We feel that these are two programs that are very important to the future of space exploration that will resume well before this mission would take place.

Future Studies

The results which we have presented are only the preliminary stages of a full investigation into the topic of asteroid mining. This was a one-semester long study that looked into only the more basic aspects of the mission approach. Any future studies will need to analyze the different components in much more detail.

Mining Process

The mining process, more than any other aspect of this mission, needs to be scrutinized on many levels. While the basic concepts are sound, much more extensive research and testing must be done with the details of the process. It would be very helpful to do testing of laser capabilities in such a situation. The specific laser cutting method must be tested and perfected. The laser design used on the miner involved the laser being on for extremely long amount of time. For such a high-intensity laser, it must be tested for long-term usage abilities. Also, the design of the arm must be perfected. The use of electromagnets on the bucket or the miner arm to retrieve the ore is an area that has not been thoroughly tested. Similar arm designs have been heavily tested in construction applications on Earth, however they do not involve the use of

electromagnets of the buckets. This technology would obviously have relevant applications in terrestrial construction.

Mission location

The tests of determining the miner's exact strengths and weaknesses will also help with the asteroid selection process. Through the use of spectral analysis, and other methods, an asteroid can be selected that has an ideal composition on its surface. Current studies have only analyzed a small portion of the asteroids in the solar system so that we can not yet effectively select an asteroid to mine. However, a full analysis of both near-Earth asteroids as well as those located in the main asteroid belt will yield a better idea of where this mission is headed. This information will also offer much insight as to the time frame between launch windows.

6. Outreach

Throughout the semester we hosted or participated in the scholastic and public events and activities listed below in order to create appreciation for and spread information about the importance of space development and asteroid mining.

Friday, April 20, 2001
HEDS-UP Presentation to Dr. Chris Churchill's STS 497I Space Exploration Class.

Saturday, April 21, 2001
Exhibit with Mars Society at Space Day event at Penn Sate. This event, organized by the PA Space Grant Consortium (PSGC), allowed students and members of the community to view exhibits of various Penn State groups and programs whose purpose is space-related research and education. It was held from 10am until 3pm in Heritage Hall of the HUB-Robeson Center. For more information on Space Day at Penn State please visit http://www.psu.edu/spacegrant/spaceday/index.html.

Wednesday, April 25, 2001
Presentations open to public. Beginning at 7:30pm, the first presentation will commence, with a second following at 8:30pm, both held in 108 Wartik Lab.

World Wide Web
The group's web page http://www.personal.psu.edu/kfs113/hedsup/ was frequently updated throughout the project. The page not only provided team members with access to current information on the progress of the project, but it also was an educational tool for students and the

community, having many links to sites on asteroids, Mars, and other space-related issues. Links to pages such as the NASA HEDS-UP page http://cass.jsc.nasa.gov/lpi/HEDS-UP/, the PSU Chapter of the Mars Society http://chapters.marssociety.org/pa/PSU/, and many others, enhanced the site by giving team members easy access to vital space-related information.

7. References

[1] Alpert, Mark. "Making Money in Space." Scientific American. <http://www.sciam.com/specialissues/0399space/0399alpert.html>.
[2] Arnett, Bill. "Asteroids." <http://www.seds.org/billa/tnp/asteroids.html>.
[3] "Asteroids." National Geographic.com. <http://www.nationalgeographic.com/features/97/asteroids/>.
[4] "Backhoe Attachments." Hobby Horse Ranch. <http://www.hobbyhorseranch.com/options4.htm#king9>.
[5] Bell, Edwin V., II. NSSDC Photo Gallery Asteroids. National Space Science Data Center. <http://nssdc.gsfc.nasa.gov/photo_gallery/photogallery-asteroids.html>.
[6] Binzel, Richard P., Tom Gehrels, Mildred Shapely Matthews, eds. *Asteroids II*. The University of Arizona Press: Tucson, 1989.
[7] "Cassini Mission to Saturn: The Spacecraft's Power System." The Planetary Society. <http://www.planetary.org/html/news/Cassini/hot-top-cassini3.html>.
[8] Chang Diaz, Franklin R., et. al. "The Development of the VASMIR Engine." <http://spaceflight.nasa.gov/mars/reference/aspl/develop.pdf>.
[9] Chang Diaz, Franklin R., et. al. "The Physics and Engineering of the VASMIR Engine." American Institute of Aeronautics and Astronautics. <http://spaceflight.nasa.gov/mars/reference/aspl/2000_3756.pdf>.
[10] Comins, Neil F. and William J. Kaufmann III. *Discovering the Universe*. 5th ed. W. H. Freeman and Company: New York, 2000.
[11] Fermi, Enrico. *The Evolution of the Small Bodies of the Solar System*. Elsevier Science Publishing Company Inc.: New York, 1987.
[12] Hirose, A., A.I. Smolyakov, C. Xiao, G. Conway. "Plasma Physics." Physics and Engineering Physics, University of Saskatchewan. <http://physics.usask.ca/research/plasma.htm>.
[13] Ilin, Andrew V., et. al. "Particle Simulations of Plasma Heating in VASMIR."

American Institute of Aeronautics and
Astronautics. <http://spaceflight.nasa.gov
/mars/reference/aspl/2000_3753.pdf>.
[14] "Inside the Ion Drive." MSNBC.com.
<http://www.msnbc.com/news/206711.asp?cp1=
1>.
[15] "Iridium." Webelements. <http://www.
webelements.com/webelements/elements/text/Ir/.
[16] Kuper, Charles G. *An Introduction to the
Theory of Superconductivity.* Clarendon Press:
Oxford, 1968.
[17] "Laser Drilling." Laserage Technology
Coperation. <http://www.laserage
.com/drilling.htm>.
[18] Lewis, John S. *Mining the Sky.* Addison-
Wesley Publishing Company Inc.: New York,
1996.
[19] The Mars Society.
<http://www.marssociety.org>.
[20] NASA Human Space Flight.
<http://spaceflight.nasa.gov/>.
[21] "NEAR Shoemaker." National Space
Science Data Center. <http://nssdc.gsfc.
nasa.gov/planetary/near.html>.
[22] "Nuclear Design Analysis Of A SLHC
Space Nuclear Rocket Engine." Innovative
Nuclear Space Power and Propulsion Institute,
University of Florida. <http://www.inspi.ufl.edu
/research/nuclear_thermal_prop/nuclear_design_
analysis_of_a_slh.html>.
[23] Petro, Andrew, et. al. "A Flight
Demonstration of Plasma Rocket Propulsion."
American Institute of Aeronautics and
Astronautics. <http://spaceflight.nasa.gov
/mars/reference/aspl/2000_3751.pdf>.
[24] Prado, Mark. "Asteroids: What, where and
how many?" Permanent.com. <http://www.
permanent.com/a_geolog.htm>.
[25] "Propulsion: Advanced Space Propulsion
Laboratory." NASA Human Space Flight.
<http://spaceflight.nasa.gov/mars/technology/pro
pulsion/aspl/>.
[26] Roters, Herbert C. *Electromagnetic
Devices.* Jon Wiley & Sons: New York, 1941.
[27] "Solar System Orbit Diagrams and
Distribution Graphs." JPL/SSD.
<http://ssd.jpl.nasa.gov/orbit_diagrams.html>.
[28] "SP-100 Power Source." NASA Spacelink.
<http://spacelink.nasa.gov/NASA.Projects/Human.Ex
ploration.and.Development.of.Space/Human.Space.F
light/Shuttle/Shuttle.Missions/Flight.031.STS-
34/Galileos.Power.Supply/SP-100.Power.Source>.
[29]. Vanderah, Terrell A. *Chemistry of
Superconductor Materials.* Noyes Publications: Park
Ridge, NJ, 1992.
[30] Williams, David R. "Asteroids and Comets."
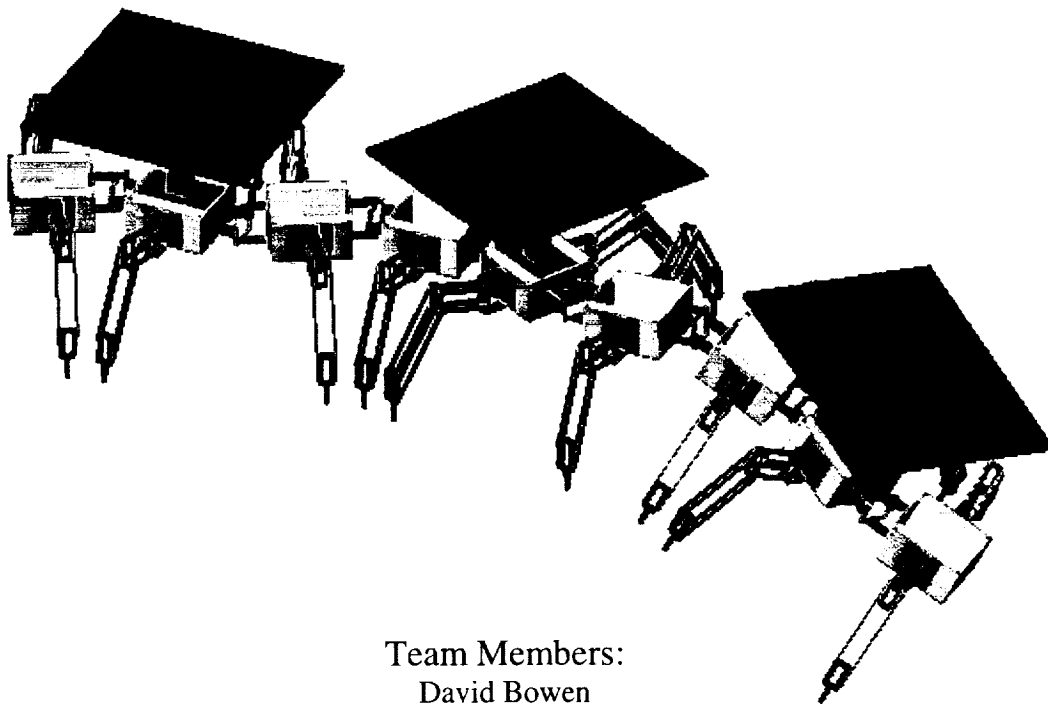
National Space Science Data Center.
<http://nssdc.gsfc.nasa.gov/planetary/planets/asteroid
page.html>.

$S_5/cP/IN/63$

The Modular Martian MILLIPEDE

Rowan University
College of Engineering

Team Members:
David Bowen
Mark Cotler
Vernon Schwanger
Scott Watson

Project Managers:
Dr. Eric Constans
Co-PM: Dr. Anthony Marchese

May 1, 2001
HEDS-UP Forum

ABSTRACT

The exploration of Mars is scientifically appealing and can benefit the human race by providing solutions to land and mineral deficiencies. While previous missions have been difficult and costly, some like the Mars Global Surveyor have led to exciting discoveries. As the next logical step, studying the surface of Mars provides many technological challenges, including how to navigate the hazardous desert-like terrain.

Through the use of an insect-like walker, appropriately named the MILLIPEDE, a land-based mission to Mars can become a reality. This vehicle can be used in conjunction with cutting edge scientific experiments to provide almost any function necessary for such a mission. The following document provides the background, design approach and results of each system on the MILLIPEDE. It also explores possible uses of the device and technology used in conjunction with the walker to make it a beneficial tool for surveying Mars.

INTRODUCTION

With every passing day, new advancements in space travel and technology take us closer to reaching the stars. The exploration of other planets offers a wealth of knowledge - not only about the galaxy and its history, but also about life in general. For these reasons, exploring Mars, the closest planet to Earth in likeness and distance, would be the next logical step. One might ask, "Why explore Mars?" Numerous reasons support the decision to explore and study Mars.

For example, Mars could be another location to colonize and to gather raw materials for use here on Earth. More specifically, Mars could contain water. This is a valuable resource and an essential ingredient in the creation and maintenance of life. Therefore, the possibility that Mars could support life is conceivable. That alone is an extremely important reason for conducting research and planning missions to better understand Mars.

Scientists at NASA are in the process of creating a living document describing a future manned mission to Mars. NASA is currently able to study and explore Mars only from afar by using satellites and landing semi-autonomous vehicles. These tools collect data and send the information back to be interpreted by scientists and engineers. This data is then used to refine the mission's objectives detailed in the living document. Hence, if the means through which the data is collected were to be improved then the mission objectives would also be improved.
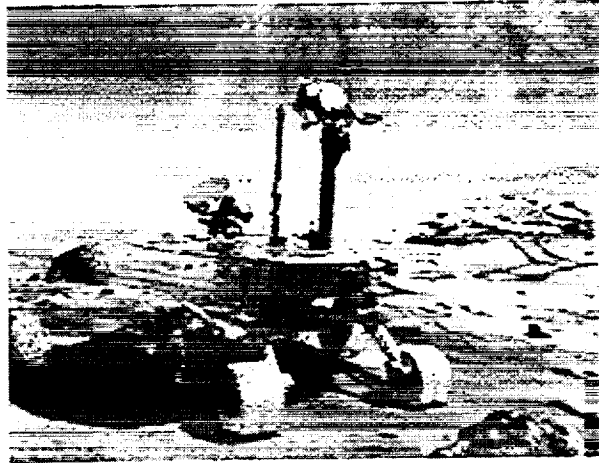
APPROACH

One current area of research is to collect data and take pictures from the surface of Mars using semi-autonomous vehicles. The vehicles, both satellites and surface rovers, play a major role in the exploration of Mars. Although satellites are a good way of collecting data they will not be discussed in great detail. Instead, this paper will deal mainly with surface vehicles and associated technology in the exploration of Mars.

Mobility on Mars: Wheels vs. Legs

The Martian rovers that are currently in use are small and have wheels. They are not very difficult to power or control. The problem with wheeled vehicles is that they are inherently suited to flat ground and have limited degrees of freedom, thus limiting the amount of terrain that they can traverse and their usefulness to explore and collect data.

On Earth roads are relatively level, cleared and paved to accommodate vehicles with wheels. However, on Mars there are no paved or cleared roadways. The Martian surface is cluttered with rocks of various sizes that cause navigation problems for small, wheeled rovers. In order to navigate the Martian surface a rover must take a circuitous route to avoid large obstacles and prevent it from getting stuck. These maneuvers are both energy consuming and counter productive because of the downtime needed for frequent recharging of the energy source. Clearly, a vehicle more suited to the chaotic terrain on Mars is needed.

An ideal solution would be to design a vehicle that was autonomous, versatile and agile. The first step in developing such a vehicle is to examine real-life models, both natural and artificial. Terrestrial man-made vehicles are typically limited to smooth terrain; even tanks cannot negotiate large boulders. In contrast, insects use many small legs to navigate all types of terrain. The surface of Mars can be seen as very similar to the rocky soil on Earth from the perspective of a tiny millipede. Something as simple as this tiny
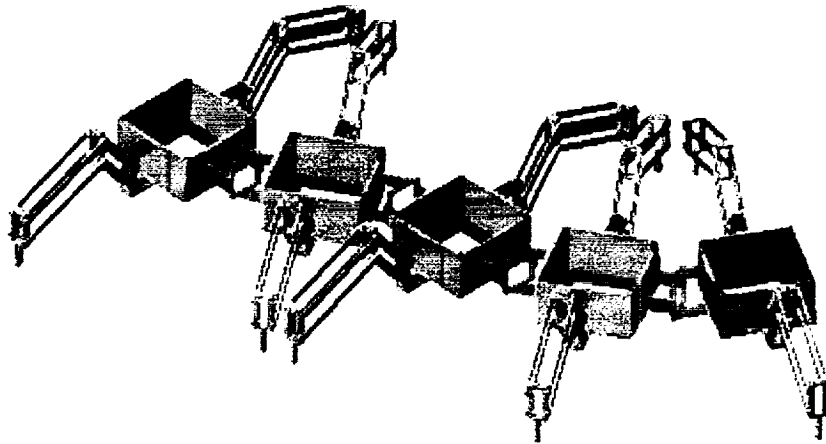
insect could be used on a larger scale as a model for a highly sophisticated walking mechanism.

There are several benefits to using a walking vehicle. As discussed earlier, the use of legs would allow the vehicle to traverse more difficult types of terrain. The walker would be able to step over obstacles that a normal wheeled vehicle would have to circumvent, thus making the line of travel more direct. This would save time and power for use in collecting data and samples.

Specialization vs. Modularity

Another important design consideration is the question of specialization versus modularity. Conventional surface exploration vehicles are limited to performing a few specific tasks such as mapping and specimen collection. Designing a *single* vehicle to accomplish all conceivable mission duties is clearly impractical; therefore, a module-based transportation system is needed to tackle the wide variety of possible tasks.

Currently, vehicles are constructed on a mission specific basis to perform certain experiments or tasks. The construction and design of these vehicles is very expensive and time-consuming. More ideally, a group of vehicles, or a single vehicle made up of many parts or modules, could perform a variety of tasks, thereby saving money and time.

Modular, walking vehicles, linked together like a millipede with each segment having a different operation to sustain the whole, could be made into any configuration necessary for a mission to Mars. This concept of a modular walker, or the MILLIPEDE, will be discussed in the next several sections.

RESULTS

Reason for Modularity

A modular walker design was chosen for several reasons. First, design and construction is much easier with a uniform module system. In other words, each module is the same, and can be fabricated easily and cost-effectively in mass production. This quick construction saves time and money in preparation for a mission.

Another reason modularity was chosen is that it allows for universal applications of the walker design. Modules can be used to fulfill power requirements, for collection and storage of materials, and for all types of scientific experiments. The modular unit was designed specifically for surveying and analysis of the Martian terrain. Therefore, the power and size constraints can accommodate various equipment and systems.

Built-in control and communication transceivers help make the walker an intelligent and powerful device. While in formation as a train of modular units, the walker can function as a multi-disciplinary device with one source of control, or "brain". It can easily segment itself and still function as well as the original device, because each module is equipped with its own control system that is linked to other modules via communication ports and transceivers. This passive control system keeps one unit in control of the rest of the train until a segment detaches. The original control unit retains control of the other units that are still attached, while the detached segment enacts its own control system on one of its own units. This function has many potential advantages as shown in the following example: While in a train formation, one of the legs of the MILLIPEDE becomes lodged in between two rocks. The leg cannot be dislodged by the current configuration, so the train separates into several smaller trains of modular walkers. These walkers can continue on their original destination or assist the trapped walker from a more advantageous position.

Another feature of the control and communication system is that the units can relay information to each other. This not only helps the units work together, but also preserves any information that is obtained by a module that becomes non-functional during the mission. Combined with communication satellites, each unit can not only communicate

---

Modules

The solution to meeting changing needs in planetary exploration.

- Power Modules
  - Gather and provide power to the rest of the system
  - Allow for flexible power requirements and centralized generation systems

- Scientific Modules
  - University and industry sponsored projects and experiments can be easily implemented in one system.

with the others but also with Earth, sending data during missions and receiving new instructions.

Module Implementation

Power Modules

As discussed earlier, various types of modules are used in the walker. One that is absolutely necessary is a power module that not only stores and provides power, but is also rechargeable. Solar cells, or more specifically, photovoltaic cells, are used to transform energy from the sun into electrical power that is distributed throughout the system or stored in deep-cycling batteries for later use. This way, the walker can recharge during the day and still have power to run during the night. However, solar power alone has some drawbacks that will be discussed later. Alternative power sources can also be included in these power modules to provide more effective or efficient power.

Although the power modules act as the primary source of power for the walker, each module can be fitted with its own battery. This would allow each module to be independent of the others and of the power module, and would thus provide greater universality and redundancy. Another option available, which may be specific to certain module implementations, is the addition of a shallow-cycling battery for short bursts of high power. While most modules may not need this additional supply, it can be fitted in the module that needs it and be charged by the power module. Parallel arrangements of the power lines create redundancy in case of failure. Circuit breakers in each module also help protect other modules if one develops a short circuit.

Scientific Modules

A major reason for the modularity of the walker is in the wide range of functions that it must be able to serve. As mentioned earlier, creating one unit to do several tasks often becomes complicated and sacrifices the effectiveness of the unit. Also, once the unit serves its purpose it cannot be easily reused for other purposes. Therefore, a simple unit that could serve any number of functions is ideal. It is with this idea that the MILLIPEDE is geared towards its main purpose of scientific exploration and engineering measurements.

One such example is surveying the surface of Mars. Modules with robotic arms are used for soil and rock collection. An opening in the bottom of the compartment allows for easy access to the surface. Mineral excavation is another useful implementation of a module. While a human could easily do

these jobs, the walker allows for many more involved applications, such as sub-surface mapping. Microwaves transmitted into the surface of the planet reflect an "image" in a concept called Ground Penetrating Radar (GPR). Small machines about the size of a lawn mower and safe enough for a human to operate have been in use for some time on Earth. However, this procedure has never been attempted off-planet, and could provide a great deal of useful information for both scientists and engineers. Scientists could, in effect, peel away the surface layers of Mars, revealing the planet's history and life cycles. The same information could be interpreted to find safe landing and building areas, as well as mineral and water deposits below the surface. The advantage of the walker is quite evident in this application, as the walker would be able to cover vast areas and traverse all types of terrain. Through the use of several GPR units, given enough time, the walker could obtain a sub-surface map for the majority of the planet. This feature, combined with the Martian communication satellites (discussed later) would allow scientists on Earth to view the walker's mapping progress.

TECHNICAL ANALYSIS

Structural Design

The most fundamental component of the modular walker is the modular compartment, or cell. The cell is a box-shaped object designed to power, support and protect the drop-in mission module. The top of the cell is completely open, while the bottom has a smaller opening for easy access to the ground. All four walls are identical except for one feature: the two sidewalls that support the legs also protect the power channels in the cell.

As mentioned earlier, the power operates on two main busses; each is redundant and protected at each cell in case of failure or catastrophe. The power housing in each side of the module is supported with insulation and thicker walls to protect the module from interference and protect the cables from developing a short circuit. The mission modules themselves have protective housing on either the top or the bottom or both, so as not to restrain the design and function of the modules. For example, a particular mission module may only interact with the environment through the bottom of the cell. This module would have a protective shield on the top that locks into the cell, but the bottom would be open or have a "door" to open when the module is active.

On the exterior of the module are four universal joints: one on each side. On either the front or the rear of the module is a connecting joint that would allow the module to latch onto other cells. The opposite side has a receiving joint to establish connection. It is through these two joints, receiving and connecting, that the cells link up into a train of modular cells. While it has not yet been implemented, future design plans intend to make these connections powered, so that cells can interconnect and disconnect automatically. The other two faces with universal plates are used to support the legs. The leg joints are fixed into place after connection and are not designed to be removed during operation. The drop-in modules lock into place and receive power through at least one of two ports on the walls supporting the power busses.

Control Design

Aside from the power busses, there are also two control busses, or instrumentation lines, to control the walker. These redundant control busses run to the motor controllers in the legs and the control panels located within the module. Control is directly linked to communication, so commands and programmed instructions can easily be downloaded to the walker. Each control unit is capable of completely controlling the cell functions and mobility mechanisms. The module, however, operates independently of the control unit, but may work as an aid and even override the cell control in order to perform its intended function.

This control style is typical of the walker's passive control element. The system operates with several control units, but only one is active at a time. Each cell has a control unit. In a train made up of several of these cells, the units are prioritized so that only one is in control of the system at a time. Inactive control units may be used to run diagnostic checks to make sure the active control element is functioning properly. This ensures that the MILLIPEDE always operates under a fully functional control system.

Communication plays a very important role in the walker design and control system. Not only is each cell control unit outfitted with a transceiver, but the system is also designed to work with a communications satellite array orbiting the planet. These Martian satellites are used to locate the walkers via MGPS (Martian Global Positioning System) on the planet surface and transmit data between Mars and Earth. This way, not only can the information obtained by the robotic walker modules be uploaded to Earth as it is collected, but new commands and algorithms also can be downloaded to the same modules to correct problems mid-mission. Dual antenna arrays allow the cells to communicate with the satellites and each other at different carrier frequencies to prevent interference; high frequencies (cellular levels, approximately 900MHz) are used to communicate with the satellites, while lower frequencies are used to transmit between cells to increase range and reduce obstruction of the signal. This allows much more efficient communication in realistic situations, such as blackouts due to dust storms or obstruction of transmission in subsurface or covered regions.

The second purpose of the satellites is to locate the MILLIPEDE on the Martian surface. This is important for the cooperation of unit cells on tasks covering a large surface area

---

MGPS (Martian Global Positioning System)

The eyes and ears of the mission.
- Global Positioning System
    - The MGPS provides the MILLIPEDE with specific location data for surface and sub-surface mapping.

- The Mars – Earth Link
    - Doubling as communication satellites, the MGPS will allow NASA to relay information with the MILLIPEDE, such as new instructions or data retrieval.

and in applications of surface and sub-surface mapping. Modules intended for use of mapping terrain can apply a geographical location to the image and transmit the data to another computer to process the data. Also, units and trains can use this geographical location system to aid or link up with other "loner" or stray cells. The MGPS can be implemented in various effective ways with this universal system.

Detailed Design

Size and Shape of Unit Body

The body segments of the MILLIPEDE perform multiple functions. First, they support and protect the modules. Second, they connect and support the joints and legs. Finally, they house the slave leg controllers and decentralized power storage. Owing to these factors, much consideration was given to the body constraints.

Each modular cell is the same no matter what plug-in module is used. This allows for easy assembly, specific constraints for design of the module units, and easy manufacturing of the cell components. Second, the area allotted for the modular plug-in units is centered within each unit for better weight distribution. Since the cell not only connects to the legs but must also interface with at least two other units, an obvious and simple design for the modular body is a box. Third, the structure must be light and strong to support the weight of the loaded modules, legs and external forces.

The platform has a square design for simplicity and ease of manufacturing. Since all four sides are equal, one generic part can be replicated for use in all the side panels. To provide adequate volume while limiting size and weight, the unit cell is constrained to be half as tall as it is wide. This provides better balance as the center of gravity is better aligned in the middle of the cell. If the center of gravity were too high, the walker would have a tendency to tip over. Likewise, the body of the MILLIPEDE must be high enough off the ground to clear most obstacles.

The size of each body segment must be sufficient to allow modules of reasonable size to be transported while not so large as to consume excessive power. Considering the cost of transporting equipment to the Martian surface, a disproportionately large body segment would not return the expense of transport. Additionally, a larger body implies larger legs and connecting joints, both with reduced travel speeds and ground clearances. A miniscule walker would require miniature actuators and motors, which would increase the manufacturing cost of the
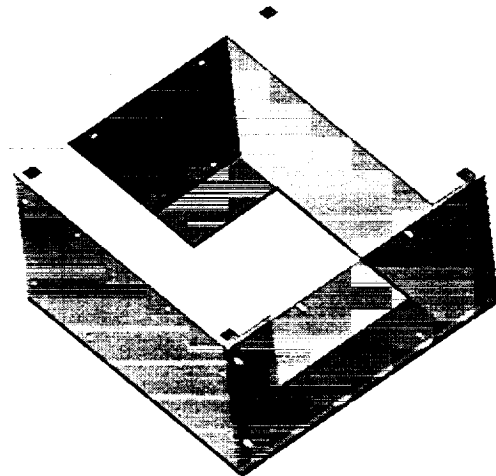

Figure 3: Body Cell of MILLIPEDE

MILLIPEDE. A smaller walker would also not be able to serve as many applications as a larger walker. We finally arrived at external dimensions of 12" wide by 12" long by 6" high. These dimensions best suit both the application and power requirements of the MILLIPEDE. The weight of each body segment plus the component module was approximated using the density of water to fill the volume of the modular cell. This approach yielded a weight of 32 pounds (in earth gravity) for each body segment. All materials for the body segment will be aluminum to maximize strength and manufacturability while minimizing weight and cost.

Other design features include a ¼" thick plate added to the bottom to provide stability and support for the component modules and corner bracing for joining the walls. Each wall has receptacles for leg, joint, or communication connections. Inside the walls are power, communication and control elements housed within the modular cell.

The remaining volume, a rectangular prism of 6" high by 8" wide by 11 ½ " long, is reserved for the component modules. The bottom plate has an access hole in its center to accommodate various component module missions.

Leg Design

The surface of Mars is much like a rocky desert with many perilous obstacles. A vehicle must be able to move over this type of terrain with relative ease in order to successfully navigate the planet's surface. The MILLIPEDE's legs are very versatile and provide the necessary agility to conquer this dangerous terrain: the walker's legs can spread out to keep the unit low and balanced, or it can stand tall to overcome large obstacles in its path. This versatility allows the MILLIPEDE to avoid obstacles by moving over and around them.

Each walker leg is made up of a body-leg adaptor plate, a hip, an upper leg, a knee, a lower leg, and a foot. The body-leg adaptor plate is identical to the body-body plate with the exception of shorter tabs. The hip is mounted on two pins and fits between the two tabs. The upper leg and lower leg are each made up of four members, connecting to the hip, knee, and foot via pin joints. Additionally, each upper leg and lower leg has an actuator attached, while the hip joint houses a servomotor.
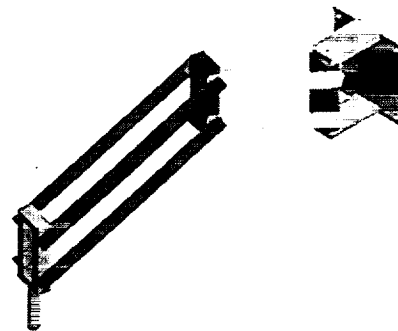
Each walker leg assembly has three degrees of freedom. The hip joint is mounted on two pins and controlled by a servomotor, allowing the leg assembly to rotate forward and backward, level to the ground. The upper leg and lower leg are each controlled by actuators. The motion of the upper leg and lower leg allows the foot to move up, down, towards the body, and away from the body by the combined efforts of the actuators. These three motions alone allow the walker to walk perfectly over a flat surface and avoid numerous obstacles over an imperfect surface.
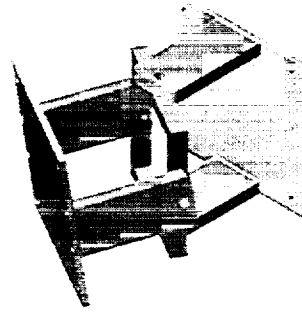
Figure 5: Body-Body Connection Joint

Power Systems

In order to determine the power requirements of the MILLIPEDE some preliminary calculations are necessary. The most important factor determining the required power is the weight of the body and mission modules. The maximum weight of a mission module can be estimated by assuming that the interior volume of the cell is filled with water. The interior volume of one cell is

$$11.5"x11.5"x6" = 793.5 \, in^3 = 0.013 \, m^3$$

The density of water is

$$\rho = 1000 \, kg/m^3$$

So that the mission module mass is

$$\text{Mass: } m_{cell} = V \times \rho_{H_2O} = 13 \text{ kg}$$

The empty mass of each cell (including body, legs and couplings) is 8 kg so that the maximum total cell mass is 21 kg. The weight of a cell is

$$F_{cell} = m_{cell} \times g_{Mars} = 21 \text{ kg} \times 3.69 \text{ m/s}^2 = 77.49 \text{ N}$$

And the weight of a 3-cell segment is

$$F_{segment} = F_{cell} \times 3 = 232.5 \text{ N}$$

Scaling this value by a safety factor of 2 yields a force per segment of

$$F_{segment} = 465 \text{ N}$$
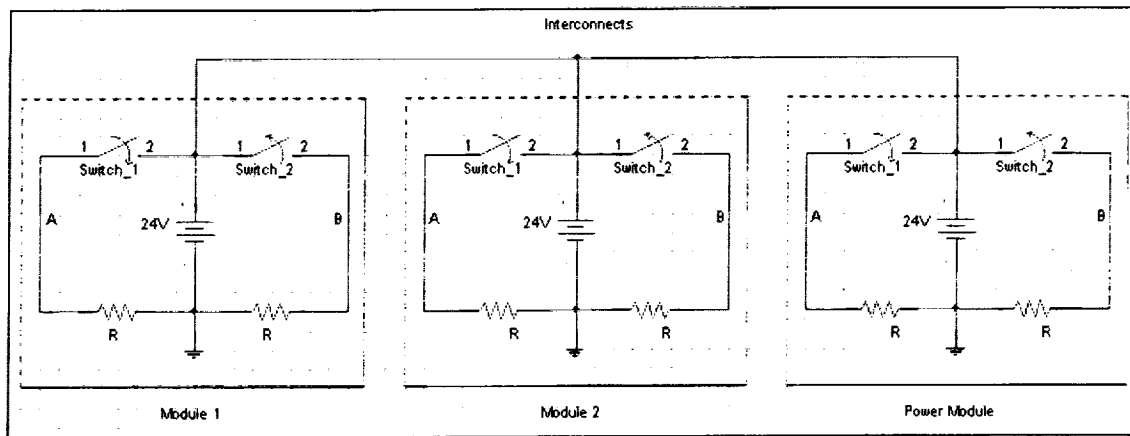
Assuming that the MILLIPEDE travels at 0.1 m/s up a slope of 45°:

$$Power = F_{segment} \times v \times \cos(45°) = 465 \text{ N} \times 0.1 \text{ m/s} \times 0.707$$

$$Power = 32.9 \text{ W}.$$

The MILLIPEDE is designed to operate with a 24V power supply, thus the maximum current draw is 1.37 A or 228 mA per leg for six legs.

Since the MILLIPEDE's mission is long-term, the most ideal source of power is a rechargeable power supply. The existence of natural resources on Mars, what they are, and where they are found is not known at this time. This prohibits the possibility of using Martian resources as a power source for the MILLIPEDE.

While the dust storms on Mars can create wind gusts up to sixty-seven mph, the atmospheric density on the planet is merely sixteen thousandths of that of Earth. Thus, the Martian wind is also not a viable power source.

The only remaining feasible source of power on Mars is solar, although this technology also has drawbacks. The sun is farther from Mars than it is from Earth and thus provides less solar power. Frequent dust storms also limit the amount of power that can be derived from the sun's rays. However, even if dust storms create blackouts for the MILLIPEDE's system, the long-term benefits of solar power are overwhelmingly in favor of the technology. The question is whether solar power on Mars is suitable enough to provide power to the MILLIPEDE. As demonstrated below, solar energy is a sustainable power source for the Martian walker.

Assuming that a standard PV cell used in the following assembly provides 70mW/in^2, an average obtained on Marshall Brain's "How Stuff Works" web site. Each cell produces a set voltage as determined by its internal V/I characteristics. However, current is a

different matter: the amount of current produced by the cell is directly related to the amount of energy absorbed by the panel. Discounting all other conditions, the solar irradiance, or the flux density of Mars is $489.2W/m^2$, while on Earth it is $1367.6W/m^2$. Therefore, the amount of energy hitting the surface of the Martian solar cell is approximately 0.431 times as much as the energy the solar cell would absorb on Earth. Therefore, we can assume that each PV cell on Mars would produce approximately 30.1mW.

Since the systems on the MILLIPEDE operate at 24V, a series of these solar panels must be assembled to provide this voltage. The power collected by the solar panels is then stored in deep-cycling batteries, which are typical in this type of application. Deep-cycling batteries will provide the MILLIPEDE with a long-lasting current supply and can be drained almost completely without harming the battery. Wiring the cells in series will sum the voltages in each solar cell. This 24-volt conglomeration is then referred to as a module. Modules hooked up in parallel will likewise sum the currents produced by each. Using the expected $30mW/in^2$ PV cells, a solar panel of $9ft^2$ will yield approximately 39-Watts. Since the system is expected to draw only 32 W in operation, the excess power generated can be stored in batteries to be used at night or during dust storms.

Figure 6 shows the parallel bus arrangement (A and B) with the circuit breakers represented as switches. Only one breaker is closed at a time during normal operation. Once the charge in the batteries, shown as $24V_{DC}$ supplies on the schematic, drop below a certain level, both breakers would open shutting down the walker and allowing the batteries to charge. These batteries would typically be of a rating of 30-amp-hours or more. At the peak-charging rate, it would take over 18 hours to charge a battery of this rating. Each resistor is representative of the load created by the motors used in the legs and the module's power requirements.

FUTURE RECOMMENDATIONS

There are several sections of the MILLIPEDE and its associated components that could not be implemented within the scope of this one semester project. Control and

communication are based on a conceptual design and require much more practical and thorough design constraints. The MGPS would also require a great deal of research and testing. Control algorithms and implementation are also far beyond the scope of this project and should be handled by highly trained technicians.

As far as the MILLIPEDE is concerned, the largest remaining design problem is that of the interlocking joints between the segments. These joints allow the MILLIPEDE train to segment and reconnect for advantageous arrangements depending on the situation. Should the project continue, implementation of such a device is a necessity.

CONCLUSION

Rovers may be the traditional land vehicles used in previous space missions, but a new age has dawned and with it comes an evolution in technology. While a rover may be more power efficient than the MILLIPEDE, it certainly cannot compete with the agility of a modular walker. Nature has demonstrated that legs are ideal for conquering obstacles like the rocky deserts of Mars. Terrain aside, the MILLIPEDE can move in almost any direction or position, thus allowing it to do more on its own than any rover could possibly hope to accomplish.

As the voyage to reach the Martian frontier continues, a manned mission is just on the horizon. However, before Earth sends new explorers aimed at the Red Planet, all necessary precautions must be taken. The MILLIPEDE is a cost-effective solution to the problem of traversing the surface of Mars. By utilizing this autonomous robotic walker, information can be collected to ensure the safety of the future astronauts on Mars. Its modularity concept also creates a universality and boundless possibility that has not been seen before in any extraterrestrial mission.

REFERENCES

"How many solar cells...?" http://www.howstuffworks.com/question418.htm

Mars Fact Sheet. http://nssdc.gsfc.nasa.gov/planetary/factsheet/marsfact.html

Earth Fact Sheet. http://nssdc.gsfc.nasa.gov/planetary/factsheet/earthfact.html

Sc/cp/1N/54

Advanced Two-System Space Suit

University of California, Berkeley

Team Members:
Camron Gorguinpour
Raven LeClair
Daniel Carval
Matt Estes
Andy Hsieh
Kirsten Howe
Carlos Rodriguez
Mujtaba Saffuden
Sam Saylor
Yung-Ruey Yen

Faculty Advisors:
Prof. Tom Budinger, chair Department of Bioengineering.
Dr. Larry Kuznetz, former NASA scientist.

Abstract

We present the results of our research into the development of an advanced space suit design, based on the concept of separating the head and torso pressurization systems.

Summary

Current Extravehicular Mobility Units (EMU's) must be improved for use in long-duration extravehicular activities (EVA's), as they are at risk of exposing the astronaut to explosive decompression, relatively inefficient in resource consumption, cumbersome, and expensive to maintain due to their complexity. To attack some of these issues, it is the aim of this project to design and develop a two-component space suit—a head bubble and a pressurized body suit—connected to each other through a neck-dam system. The separation of the head from the body will allow the astronaut more time to reach safety in the case of decompression and minimize O_2 loss by allowing for independent pressurization of the body and eliminating loss through the soft joints. Moreover, concurrent research on pressurization methods for the body-- with emphasis on mechanical counter-pressure and the use of dense polyurethane membranes—will pave the way toward a more practical, mobile, and inexpensive unit. For the success of the two-chamber space suit (TCSS) idea, design and functionality of the neck-dam system is vital. As outlined below, the neck-dam system and our ideas for body-suit pressurization show a strong potential for space-flight applicability, thereby, allowing engineers to modify the current EMU to provide maximum resource efficiency, while maximizing safety, reliability, and mobility.

Introduction

Space Suit Background

Technologies for protection from harsh environments, where pressure and temperature extremes are not compatible with human physiology, have had some remarkable milestones over the last sixty years. The beginnings of helmet and pressure suit innovations date from 1934 when Wiley Post with Goodrich Rubber Company developed the first pressurized high-altitude suit, which in its final design, consisted of a can-like aluminum head unit with a front window and rubber waist entry (Mohler 1998). From these early roots, the modern space suits of today evolved.

The current Extravehicular Mobility Unit (EMU) is an improved version of the original developed in 1975 by Hamilton Sundstrand and ILC Dover. The two major subsystems of the EMU are the Portable Life Support Subsystem (PLSS) and the Space Suit Assembly (SSA). The SSA is comprised of a Hard Upper Torso (HUT), Lower Torso Assembly (LTA), boots, gloves, and other integrated components. The EMU provides life support functions, such as oxygen supply, carbon dioxide removal, a pressurized enclosure, temperature control and micrometeoroid protection. The suit and PLSS contain 7 hours of expendables including O_2 for respiration and pressurization, water for cooling via the Liquid Cooling garment (LCG), a battery for electrical systems, and lithium hydroxide for carbon dioxide removal.

The SSA provides full body pressurization and respiration at 4.3 psid using O_2. A Pre-breathe of 40 minutes is required to transition from 10.2 psia habitat or cabin pressure to 4.3 psid (Furr 1987). This period of out-gassing is essential for transitions to a lower

pressure environment and is analogues to the precautions taken in deep sea diving. Inadequate pre-breathing will result in nitrogen bubbles forming in the blood stream; a condition known as the bends that can be fatal. Airflow, supplied by the PLSS, enters the suit at the helmet and flows down to the torso and extremities. Used air containing water vapor and CO_2 is removed at the elbows and feet to be transported back to the PLSS where CO_2 is removed and water vapor is condensed using a sublimation system. The water is then recycled back into the cooling system.

The Liquid Cooling Garment in which water is circulated through a network of fine tubing to remove excess body heat performs thermal regulation. The excess heat is subsequently removed at the sublimator and transferred to the outside environment.

Problem Statement

The use of O_2 in current EMU's to pressurize the whole body presents a number of problems. Even under normal operating conditions, current EMU's lose up to 50 liters of O_2 per eight-hour EVA through the many joints and seams of the suit. This great loss of O_2 limits current EMU endurance and makes it inadequate for long duration missions. A single pressurization system also puts the suit at a high-risk of micrometeoroid puncture. With current EMU's, even a small puncture could result in rapid decompression of the entire suit. This catastrophic situation can easily be fatal, as studies have shown an astronaut has from 9-11 seconds of consciousness in which to save his or herself. (Parker and West 1973)

The Sublimation cooling system is designed for use in a hard vacuum and will fail under terrestrial conditions, such as those found on Mars. Even with only $1/150^{th}$ the pressure of Earth, the delicate balance of the sublimation system will be disrupted and the astronaut will overheat.

Current EMU's have rigid torso and arm sections and soft joints for movable parts. When pressurized, these soft joints become very rigid, limiting mobility, especially in key areas like the hands. The complex designs of current space suits incorporate several control systems that contribute to the weight and complexity of the unit. For example, the liquid cooling layer alone adds 6.5 pounds when dry. These systems have a profound impact not only on resource consumption and cost but on safety and mobility, as well. The more complex the design, the more troubleshooting required, and the more components that have the potential to malfunction or break.

Rationale

The goal of the TCSS development team is to develop a variety of new features that address the problematic areas of current space suit designs. These solutions will be compatible with current EMU's and well suited for integration in the next generation of space suit designs. In contrast to current suit designs that utilize oxygen for full body pressurization, we are developing a two-system suit that separates the respiration and pressure system of the helmet from that of the upper and lower torso. This will be done using an advanced neck dam system. One objective of our project is to limit the amount of oxygen lost by eliminating its use from the neck down. With this in mind, we arrived at the conclusion that a neck dam system can serve as a crucial element for continual expansion of manned space endeavors.

In addition, the neck dam provides added safety while in a hazardous space or terrestrial environment. The neck dam technology, when perfected, can easily be extended to create airtight seals throughout the suit, leading to compartmentalization. A Separation of components allows pressure to be maintained in other parts of the suit, particularly, the 'head region, should one area be compromised. With existing EMU's, a puncture by a micrometeoroid is life threatening. Utilizing a compartmentalized suit, the time of useful consciousness in the event of a puncture is likely to be extended from seconds to minutes or even hours.

Limiting resource consumption is a necessity for long-duration missions. Another key benefit of the neck dam is that, once the head is contained, a variety of options become available for pressurizing the rest of the body. One could use mechanical counter pressure or make use of another readily available gas, such as CO_2, to pressurize the torso and extremities. This would greatly diminish the amount of oxygen consumed and allow a drastic reduction in payload weight, resulting in decrease mission cost. Mechanical pressure affords a wide range of motion. Consisting primarily of a skin-tight layer of material, its simplicity ensures a higher level of reliability and safety. An additional design concept utilizes alternate gases for pressurization of the body. The ability to use alternate gases for pressurization provides the versatility to adapt to many environments.

Breathable polymers are available that can maintain suit pressure while allowing water vapor to exit for recycling or removal. The ability to use evaporative cooling is an option not present in current EMU's and a simplification of the cooling system would significantly reduce weight. Further study is planned to determine whether evaporative cooling will provide adequate thermal regulation. Lower pressures result in increased evaporative water loss and possible dehydration without proper precautions. Further testing is required to adequately understand the requirements of an evaporative cooling system. A method of sweat removal, collection, and recycling is a necessity.

Similar polymers could also be used in a breathing apparatus, which is necessary in a mechanical counter pressure suit due to the high pressure placed on the torso. The breathing apparatus provides direct mechanical counter pressure to the torso and the restraint layer. It also acts as a buffer volume to accommodate the change in chest size during breathing. Integration of the polymer provides a method of removing exhaled water vapor that might accumulate in the apparatus.

The polymer will also serve as an interface within the neck dam, maintaining the gas pressure in the head region, while allowing the moisture expelled while breathing to diffuse to the upper torso where it might then be collected.

Methodology and Results

As mentioned previously, this project focuses on the development of both a neck dam and alternate torso pressurization system. Below are presented the results of research and preliminary testing of these systems, with special emphasis on design concepts and test procedures.

Head Unit

The separation between head and torso is the basis of the new EMU. This separation can be achieved through a neck dam system, which will serve as an interface between the

head bubble and the body of the EMU. It will require careful consideration in development and testing to minimize discomfort and risk. A system of sensors will be used keep the neck dam airtight without restricting blood flow or neck-head mobility (see Figure 1). The new head unit will also contain micro sensors to monitor temperature, oxygen, CO_2, moisture and pressure. The bubble receives ambient gas and humidity control from a backpack.

The functionality of the TCSS relies heavily on the removal of heat and moisture from the head unit and neck apparatus. The cooling requirements of the head and neck in air at sea level are 15.9 and 32.6 Btu/hour, respectively. Insensible water loss rates range between 7 and 11 g/hour for the head and 4 and 5 g/hour for the neck. It has been demonstrated that for each degree of increase in temperature (°F or °C), sensible energy rejection from the body increases by 20 Btu/hour (Parker and West 1973). These factors are part of the design and prototype development.

The Neck Dam System is designed to maintain a regulated pressure against the neck while allowing for comfort and vapor removal. The outer bladder layer maintains proper pressure and the polymer neck seal applies the pressure to the neck while diffusing water vapor. The requirement for a neck pressure bladder separated from the permeable membrane is dependent on the membrane's elastic properties, which have yet to be determined. With an appropriate membrane, the bladder and membrane could be one unit. In this case, pressure and moisture removal would be one system.

The following test procedures will be necessary to determine the viability of the head unit and torso pressurization interface:

1. Neck bladder pressure tolerance window evaluation for personnel comfort and safety. This test will be done with UC Berkeley IRB approval.

2. Evaluation of the seal performance with attached head bubble at ambient 1 atmosphere with differential pressures of –4 psi, +4 psi, +8 psi, and +10 psi while breathing normal air mixture (i.e. 20% oxygen). This test will be conducted with UC Berkeley IRB approval.

3. Integration testing of the complete head unit with various torso pressurization designs. Establishment of the neck unit pressure and moisture/temperature control pack through either ports to the neck unit directly or through the EMU collar plate.

4. Vacuum test after preliminary tests under low atmospheric pressures.

The elements of the design discussed above represent only one of a number of alternative methods for establishing a safe yet comfortable neck seal between the head bubble and lower torso of the EMU. The isolated head unit can be incorporated into current EMU's for improved safety or used with an alternative pressurization system, an example of which is discussed in detail below.
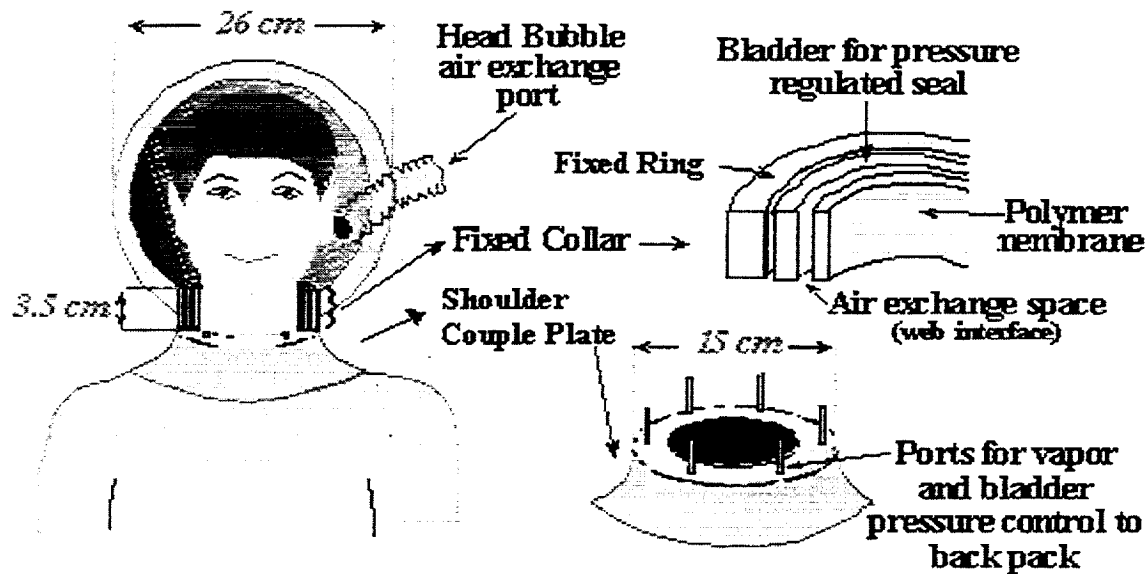
Figure 1. Head Unit Assembly

<u>Mechanical Counter Pressure</u>

During extravehicular activity (EVA), oxygen is normally supplied at 4.3 psi -5.2 psi in a conventional full-pressure suit, with the entire body pressurized with oxygen. An alternate approach is to deliver oxygen to an isolated helmet, while pressure is applied to the torso mechanically. The torso portion is engineered to balance the helmet pressure. A powerful leotard having elastic properties, insignificant gas permeability, and durability can provide many advantages over conventional systems because no hard joints or bearings are needed. Paul Webb (Webb 1968) first published this concept, performed early experiments, and demonstrated a complete elastic mechanical counter pressure (MCP) suit in 1968 as described by Annis and Webb (Annis and Webb 1971).

The original elastic MCP suit developed by Webb (Webb 1968) showed major advantages. It had increased mobility and dexterity, reduced metabolic cost of movement, and had excellent heat dissipation from evaporation of sweat; however, it was never fully developed. The heat dissipation quality of an MCP alone promises significant reductions in the mass and complexity of life support equipment, such as used in the Portable Life Support System designs (PLSS) of current EVA suits that require a cooling garment. Not only does an MCP space activity suit save weight by eliminating stored refrigerant and machinery to dissipate heat, but it is inherently safer because punctures and tears will not cause the catastrophic loss of pressure that is a risk with current EMU's. Human tests showed that there was negligible blood pooling (Annis and Webb 1971).

During the last three years, Honeywell, Inc., in collaboration with Dr. Paul Webb and Clemson Apparel Research, has developed a modern prototype of the original mechanical counter pressure suit (Annis and Webb 1971). The emphasis has been a glove that interfaces with the existing Shuttle EMU lower arm assembly at the wrist disconnect. At

this point in the development program, human testing of this glove prototype has concentrated on the proof of concept. Experiments have been performed in a glove box at a differential pressure of -222 mmHg, which simulates the pressure difference an astronaut would experience during EVA. The duration of the human glovebox tests has typically been up to 120 minutes.

In addition to the glovebox testing at Honeywell, a proof of concept test at low vacuum conditions was performed in the 11-ft chamber at NASA JSC in September 1999 (see Figure 2). The test was performed at pressures as low as 1 Torr for exposure times of up to 60 minutes. Two different test subjects performed identical tests. The results of these tests showed that the MCP technology is adequate to protect a human hand in low vacuum conditions.

In the recent Cooperative Agreement Notice (CAN) issued by NASA, the TCSS Development Team at UC Berkeley designated Honeywell, Inc. as a subcontractor to develop a mock-up MCP suit. The mock-up will interface with the head unit and breathing apparatus (described below) that will be developed by the TCSS Team. This will serve as a proof of concept for both the neck-dam system and the MCP.

Figure 2. Mechanical Counter Pressure Glove with EMU Lower Arm Assembly in Glovebox at –222 mm Hg Differential Pressure (left) and In Vacuum (right)

Breathing Apparatus

The breathing apparatus is a set of conformal chambers located between the comfort layer and the restraint layer. These chambers are made of rubberized materials that inflate at the pressure of the pneumatic system (about 4 psi). Under these conditions the breathing apparatus provides direct mechanical counter pressure to the torso and the restraint layer. It also acts as a buffer volume to accommodate the change in chest size during breathing. Valves are needed to separate the exhaled air from the fresh air.

The objective of this work is to define the Human-Pneumatic interface for a Mechanical Counter Pressure (MCP) space suit.

The MCP Space Suit breathing interface provides the following functions:

1. Pneumatic enclosure to permit breathing in the space environment. This system consists of a helmet and pneumatic seal. The seal must have a minimum leak rate, permit breathing, and not cause discomfort to the crew.

2. Breathing apparatus that permits effortless breathing while the torso is subject to mechanical counter pressure. The apparatus consists of inflated chambers and valves that compensate for the volume displacement of the lungs. It is capable for various levels of exertion and does not cause discomfort to the crew.

3. Passive management of the exhaled humidity so the visor remains clear. The crew will lose orientation and direction if their visor is fogged and they lose visual contact. Gas tight water permeable membranes permit the control of exhaled humidity without the need for air processing equipment.

Breathable Polymer

As previously mentioned, an alternate design concept utilizes breathable polymers to both serve as a pressure garment bladder and as a means to allow sweat to pass through the suit. Several gases can be used with this system, as long as oxygen is provided for respiration. A comfort layer with a polymer coating rests against the skin, while pressurized air flows between the comfort layer and another polymer layer. To maintain shape and integrity, a Pressure Garment Restraint (PGR) layer is used to prevent the polymer from ballooning. Pressurized gas can be obtained from the environment or stagnant air can be used in a closed-loop system. These options allow this suit design operate in a variety of conditions.

Although a variety of polymers exist, we are focusing on a moisture-permeable dense breathable barrier film whose properties would allow us to regulate temperature, pressure, and humidity and provide a biological barrier. Currently, the polyurethanes under testing are Bionate 55D, BioSpan, CarboSil 20 90A, and PurSil 20 80A, all products developed by The Polymer Technology Group, Inc.

The advantage of dense polymer membranes is that they allow the transmission of sweat, in vapor/gas form, via diffusion. This is enabled by the concentration gradient in the material; the side of highest concentration diffuses across the film to establish equilibrium. Sweat vapor/gas arrives on the polymer surface closest to the body, dissolves into the membrane, travels across and then exits the opposite side of the membrane in the form of vapor/gas. The true benefit of this property is that only vapor/gas can transfer. Liquid is unable to pass through the material, regardless of its pressure, viscosity, or surface tension. The rate of transmission for a specific dense breathable barrier film "is directly proportional to the vapor pressure or concentration difference and the film area, and is inversely proportional to the film thickness." (Ward and White, 1991)

Another benefit of the dense breathable barrier film is its relatively high resistance to puncture and tear, which in turn prevents possible leakage. Polyurethanes have a combination of high elongation and high tensile strength, which significantly decreases the possibility of the material cracking or tearing, even under severe conditions. The material is also quite flexible, providing optimum movement and comfort.

All the materials currently under testing are composed of aromatic urethane hard segments and exhibit remarkable mechanical properties. In addition, BioSpan has excellent flex life, hydrolytic stability and elasticity, and the Bionates have good oxidative stability and abrasion resistance.

Polyurethane Testing

We have currently begun testing of various polymers to determine their feasibility in both the body of the suit and the breathing apparatus that would be necessary in a MCP suit.

The material characteristics to be determined are:

1. Water permeability as a function of temperature.

2. O_2 permeability as a function of temperature and pressure.

3. Young's modulus of elasticity.

4. Photochemical behavior (e.g. resistance to ultraviolet light)

5. Aging characteristics of the above attributes.

Test Protocol

The protocol for our experiment can test water and gas permeability, permeability to mineral components of sweat, the ability of the polymers to maintain constant pressure, and durability. Water is poured into the sealed, pressure-retaining flask developed by UC Berkeley undergraduates and staff (see Figure 3). The material is then stretched minimally and secured over the top of the vessel using a clamp. The internal pressure is raised to 5 psig while a heating element maintains constant internal temperature. After the entire system is weighed, the vapor loss is monitored at regular time intervals. After an eight-hour period, the system is weighed again to determine the mass of water that diffused thorough the membrane. Variations of the experiment described above can determine gas retention and water transmission separately as functions of temperature and pressure.

Preliminary Tests and Results

In our preliminary tests, we have measured a sample polymer's permeability to water vapor. The material was stretched over the container with water heated to approximately 40° C. Weight loss was measured approximately once every hour, over 6.5 hours. For comparison, the same experiment was run without anything covering the container and with a non-permeable material covering it. The non-permeable material test was simply to evaluate the efficiency of our test setup. If there were significant weight loss with the non-permeable material, we would conclude that there is some alternate means of vapor loss in the test chamber. By comparing the results for the open chamber to the results of the chamber covered with the polymer, we were able to gauge the polymer's ability to transfer water vapor. If the weight loss with the covering was close to or equal to the weight loss without the material, we could infer that the polymer is efficient in water vapor removal. The results of this preliminary test are given below.
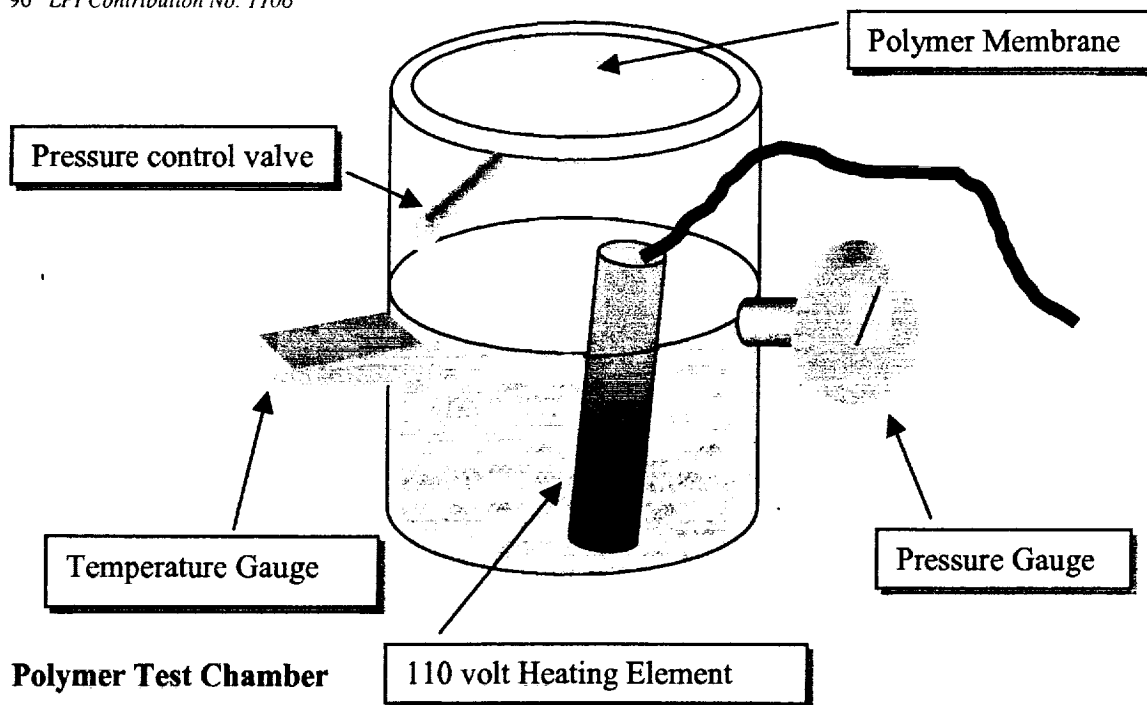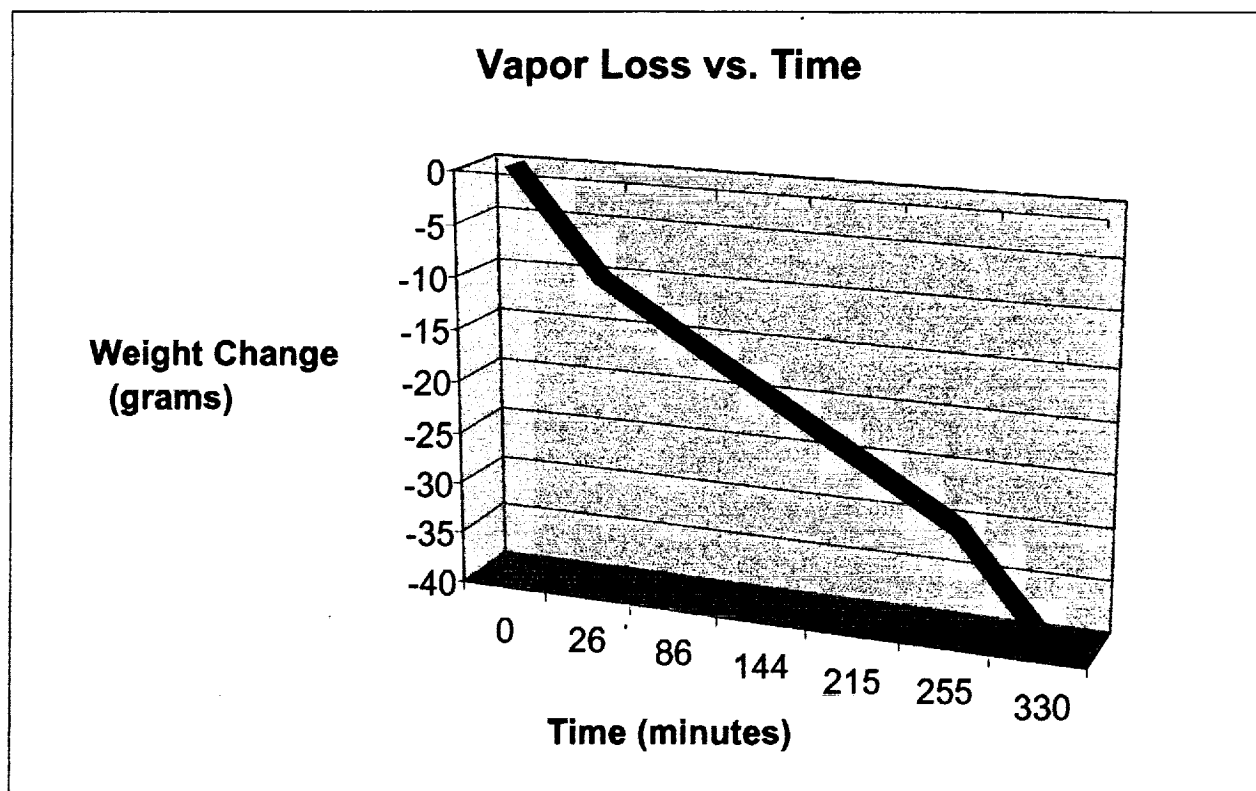
Figure 3. Polymer Test Chamber

Figure 4. Preliminary Test Results

Results

Figure 4 presents the results of the water permeability test conducted with the polymer membrane covering the test chamber. When a non-permeable material (vinyl) was used to cover the chamber, no significant weight loss was recorded over 11 hours. Our data for the open chamber test were tainted by a heating malfunction. The heater has been replaced, and the test will be conducted again. Additional testing was conducted to determine the pressure retention of a polymer sample. However, the sample failed the test when it developed holes under high pressure. This was probably the result of age and mishandling. A new sample was obtained and will be tested.

Further Polymer Testing

Two alternative approaches to polymer testing are as follows:

1. Using two chamber dialysis / diffusion cells, flat membrane permeability is measured.

2. In a second approach, membrane tubes are hydrated and filled with a radioactive labeled solute. They are then placed into a test tube containing solute free solution. The experiment consists of monitoring the radio concentration of the solution in the test tube as a function of time while controlling the temperature at 37 °C. The permeability coefficient could be determined from regression analysis of the radioactivity in the reservoir tube as a function of time as applied previously by Ward in 1993. This experiment assumes permeability of solute is not significantly different for that of water.

These testing procedures, with the preliminary test procedure already developed will provide sufficient data to determine the characteristics of various polymers under various conditions.

Conclusions

By separating pressurization systems between the head and torso, safety, resource consumption, weight, mobility, and complexity can be improved. Furthermore, the separation allows for the development of innovative torso pressurization systems that show definite advantages over the current EMU. The neck-dam system will be tailored for use in the current EMU's, as well. This provides great versatility for varying environments. Alternate torso pressurization systems include, but are not limited to, the mechanical counter pressure suit and the polymer membrane pressurization system described above. Although further testing must be done, the design concepts presented in this paper show promise for space suit applicability.

Future Studies

The TCSS Development Team will continue its research and testing of the above mentioned design concepts, with emphasis on testing. Furthermore, the team has developed collaborations with Stanford University and the Art Center College of Design, in Pasadena, CA. In addition, relationships are being developed with California Institute of Technology and University of California, San Diego. These schools will take on various aspects of an overall suit design in an effort to produce a complete proof of concept suit.

Scientific / Technical References

(1) Annis, J.F. and P. Webb. "Development of a Space Activity Suit." NASA CR-1992, Washington DC: National Aeronautics and Space Administration, 1971.

(2) Furr PA. Probability of oxygen toxicity using an 8 psi space suit. *Aviat Space Environ Med,* A113-20, 1987

(3) Jones RV. Thermoregulation. CSCI E-129, 1999. http://www.deas.harvard.edu/~jones/cscie129/pages/health/thermreg.htm

(4) Hale, F.C., Westland, R.A., and C. Taylor. "Barometric and Vapor Pressure Influences on Insensible Weight Loss." *Journal of Applied Physiology,* 12:20-28, 1958.

(5) Lee, S.M.C.; Bishop, P.A.; Schneider, S.M.; Greenisen, M.C. *Aviation, Space and Envir Med,* 72, 110-114, 2001.

(6) Mohler SR. The world's first practical flight pressure suit. *Aviat Space Environ Med.* 1998 Aug; 69(8):802-5.

(7) Parker, J.F., West V.R., ed. *Bioastronautics Data Book.* 2nd Edition. Scientific and Technical Information Office, National Aeronautics and Space Administration, 1973.

(8) Ward RS, White KA. "Barrier Films That Breathe". *Chemtech.* Nov. 1991: 670.

(9) Webb, P. "The Space Activity Suit: An Elastic Leotard for Extra-Vehicular Activity." *Aerospace Medicine,* 39:367-383, 1968.

(10) Zorpette G. Working knowledge. A spaceship for one. *Sci Am.* Jun;282(6):102-103, 2000

Hyperbaric Chamber Pass-through Mechanism Design

HEDS-UP Document

...orado at Boulder

Team Members:
Jennie Crook
Jason Lechniak
Sheah Pirkle

Faculty Advisor:
Dr. Kim Maute

Hyperbaric Chamber Pass-Through Mechanism Design

Abstract

This project encompassed the design, analysis, fabrication, and testing of a prototype pass-through mechanism to be used on a portable hyperbaric chamber in space. The contents of this report include the scope of the project requirements, how they were met, and improvements for future studies. The main objective of the design was to build a prototype of a mechanism to allow supplies to be passed through the hatch of a hyperbaric chamber and retrieved by the patient, without depressurization. A feasible design, one which could be built while upholding the project budget and schedule, was created using IDEAS CAD software. The design was analyzed and manufactured by the team, then assembled and tested. Following a brief setback in testing, the pass-through mechanism was confirmed to seal effectively and maintain pressure. Strain gages placed in critical stress areas indicated an increase in strain with pressure and a decrease in strain with depressurization; however, no unbearable strain was reached. A total pressure of 56psi was achieved during testing. The pass-through mechanism performed optimally while withstanding the safety margin pressure.

1.0   Introduction

Maintaining a healthy crew on the long trip to Mars will be one of the many challenges faced by those who plan the mission. A solution to many of the medical needs encountered in space is a hyperbaric chamber. A hyperbaric chamber is a pressurized vessel containing excess O_2 that can be used to decrease the recovery time for almost any injury. The project that was completed for the HEDS-UP Forum involved the design, building and testing of a prototype pass-through mechanism that can be attached to the door of a hyperbaric chamber to be used on the International Space Station. The mechanism will permit medical supplies to be passed into the chamber and retrieved by the patient, without depressurization of the chamber. Although the initial design is for use on the international space station, any space application, including a trip to Mars, is feasible for the chamber.

2.0   Approach to the Problem

2.1   Background

A hyperbaric chamber is a pressurized vessel used for medical purposes containing excess O_2. Chambers are normally kept at pressures greater than atmospheric. Hyperbaric Oxygen Therapy (HBO) is a type of medical treatment that is effective for many clinical conditions [3].

2.2   Application

NASA Johnson Space Center is in the process of testing a prototype chamber for use on the International Space Station (see Figure 2.2-1). The chamber may also be used at NASA's Weightless Environment Training Facility (WETF, the water tank containing a mockup of the shuttle's payload bay, where astronauts train in a simulated micro-gravity environment) [4].
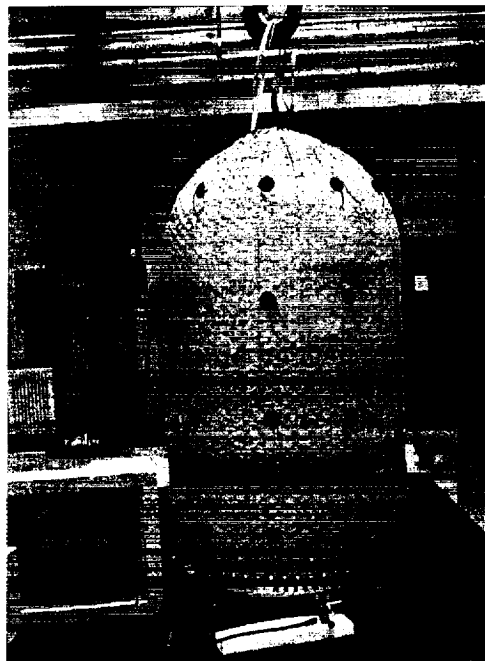
Figure 2.2-1. Hyperbaric Chamber Prototype [1]

2.3   Design Problem

Design a pass-through mechanism to be added to the door of the prototype of the hyperbaric chamber. The mechanism will permit medical supplies to be passed into the chamber and retrieved by the patient, without depressurization of the chamber. Ideally, the mechanism will be removable, attaching to the hatch only when functionally needed. The pass-through module should be approximately coffee-can sized and be able to withstand pressures up to 3.6 atm (safety factor)[1].

2.4   Approach

2.4.1   Design Phase

A number of designs were considered in order to optimize the pass through mechanism for its intended purpose. Each design was evaluated through several criteria to determine the designs' relative functionality when integrated into the system. The optimum design was based on:

1. Ease of integration into the system
2. Most feasible for use in zero-g environment
3. Minimum maintenance requirements
4. Cost and feasibility of construction

Once a design was decided upon, it was analyzed through several avenues:

Material Property Considerations
Static Loading Analysis
Variable Pressure and Contact Force Analysis
Sealing Capability / Analysis
3-D CAD Model (In IDEAS)
Integrated System Analysis
Finite Element Analysis

2.4.2   Building Phase

It is essential to build a prototype in order to determine if the design is functional and operative. The building phase required the necessary parts to be on-hand or built by the engineering students working on the project (in order to stay within the small budget of the project).

2.4.3   Testing Phase

The prototype was tested through several avenues:

Structural Strain Measurements - to confirm finite element analysis
Simulation of usage over a range of pressures
Testing for sealing confirmation

3.0   The Design

Figure 3.0-1 is a schematic of the design chosen by the team, assembled in its entirety.
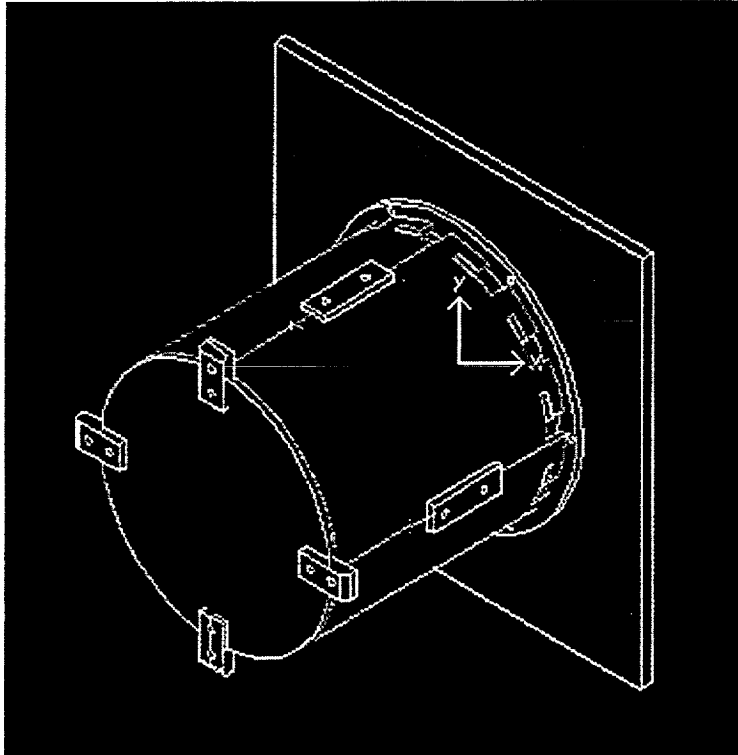
Figure 3.0-1 Assembly Schematic of the Design

The design incorporates a dual-cylinder configuration. The interior cylinder maintains the pressure seal, and the outer cylinder houses the latch attachments, the interior cylinder, and connects to a flange on the chamber door. Because of the complications associated with screw-on devices that require strength in a 0-g environment, the design has a nearly effortless toothed-locking-mechanism (to attach to the hatch itself), instead of a more standard flange design. The exploded view of all parts and the corresponding bill of materials can be found in figure 3.0-2.

1. Latch interfaces
2. Outside End Cap
3. Inner Cylinder
4. Cylinder Spacers
5. Outer Cylinder
6. Latch Mounts
7. Outside Flange
8. Hatch
9. Inside Flange
10. Flange Extension
11. Inside End Cap
12. Window
13. Inside Window Hold

Figure 3.0-2 Exploded view of all fabricated parts

4.0 Results: Theoretical Design Analysis

The analysis performed in this section includes all off-the-shelf part specifications and material properties. Simplifying assumptions were made concerning the homogeneity of the materials and the equal distribution of forces resulting from pressurization (uniform pressure).

4.1 Materials / Parts

There were many factors that were taken into consideration in the process of designing this small pressure chamber. Two of the most important considerations were the availability of materials that were within the budget of the project, and the machinability of parts. The inner and outer cylinders are off-the-shelf Aluminum 6061-T6 stock piping. The inner cylinder was purchased from The Marmon/Keystone Corporation for $80.00. All the sheet metal components, such as the inner and outer flanges and the doors, are made of Aluminum 7075-T6. The outer cylinder and the sheet metal were purchased from Alreco for a total cost of $297. Due to a machining error, an additional slab of Aluminum had do be purchased from Alreco for $87. Material characteristics for both types of Aluminum are shown in table 4.1-1. The material properties were obtained from the MatWeb Materials Property Database website [5].

Table 4.1-1 Material Properties for Machined Aluminum Parts

Material Characteristics	Aluminum 7075-T6	Aluminum 6061-T6
Density (g/cc)	2.81	2.7
Tensile Strength, Ultimate, MPa	570	310
Tensile Strenth, Yield, MPa	505	275
Elongation %; break	11	12
Modulus of Elasticity, Gpa	72	69
Notched Tensile Strength, MPa		324
Ultimate Bearing Strength, MPa		607
Bearing Yield Strength, Mpa		386
Poissons Ratio	0.33	0.33
Fatigue Strength, MPa	160	95
Fracture Toughness, MPa-m(1/2)	29	29
Machinability, %	70	50
Shear modulus, GPa	26.9	26
Shear Strength, MPa	330	205

The attachment parts, such as the nuts, bolts and washers are all made from steel and were purchased from a local hardware store for under $10.00. The specifications for the bolts are given in table 4.1-2 and were obtained from the book *Machine Design: An Integrated Approach [7]*.

Table 4.1-2 SAE Specifications and Strengths for Steel Bolts [7]

SAE Grade Number	Size Range Outside Diameter (kpsi)	Minimum Proof Strength (kpsi)	Minimum Yield Strength (kpsi)	Minimum Tensile Strength (kpsi)	Material
1	0.25-1.5	33	36	60	low or medium Carbon
2	0.25-0.75	55	57	74	low or medium Carbon
2	0.875-1.5	33	36	60	low or medium Carbon
4	0.25-1.5	65	100	115	medium carbon, cold drawn
5	0.25-1.0	85	92	120	medium carbon, Q&T
5	1.125-1.5	74	81	105	medium carbon, Q&T
5.2	0.25-1.0	85	92	120	low-carbon martensite, Q&T
7	0.25-1.5	105	115	133	medium-carbon alloy, Q&T
8	0.25-1.5	120	130	150	medium-carbon alloy, Q&T
8.2	0.25-1.0	120	130	150	low-carbon martensite, Q&T

The Latches are also constructed of stainless steel. The latches were catalog parts purchased from Southco, costing almost $100 for all 4 latches. The latch strength specifications are shown below in table 4.1-3 [9]. The entire latch mechanism is made up of 300 series stainless steel and all parts within the latch are passivated. A picture of the latch is shown in figure 4.1-1 [9].

Table 4.1-3 Latch Specifications

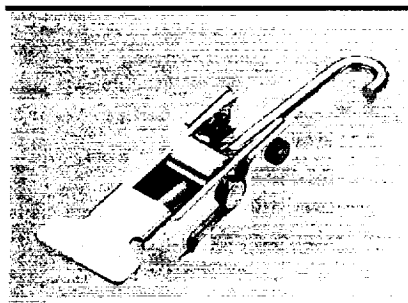| Southco Draw Latches (Latched at center of radius)	
Maximum working load	700 lbs
Average ultimate load	1100 lbs

Figure 4-1-1 Picture of the latch mechanism [9]

4.2 Static Loading Analysis

4.2.1 Pressure Assumptions and Theory

The function of the pass-through mechanism, a small pressure chamber, dictates that it will withstand an internal pressure of 3.6 atmospheres (this value includes a safety margin). The main structural concern is the distributed load resulting from a differential pressure from the 'inside' of the chamber to the 'outside'. The gage pressure, p_g, is a measure of this differential pressure as shown in equation 4.2.1-1.

$$(4.2.1\text{-}1) \qquad p_g = p - p_{atm} = 3.6\text{atm} - 1\text{ atm} = 2.6\text{ atm} = 38.22\text{psi} = .26337\text{MPa}$$

The pressure chamber is built to withstand a total pressure of 3.6atm (52.92psi or .36467MPa). For the analysis of the chamber, the gage pressure will be used instead of total pressure. The chamber, however, will theoretically be able to handle the total pressure inside a vacuum. This is important because the mechanism will be in space, and although it will be kept in a module that is pressurized to atmospheric conditions, an emergency situation may cause that the pressure outside the chamber to approach 0, in the vacuum of space.

4.2.2 Chamber Cap

The exterior cap of the pass-through mechanism is attached to the containment unit by 4 latches (specifications given previously in table 4.1-3). The equivalent force, F, produced by the differential pressure is given in equation 4.2.2-1. This force represents the distributed force acting on the pressurized portion of the cap (assuming uniform pressure along the area). The force calculation utilizes the actual gage pressure exerted on the chamber and the interior diameter of the containment unit, since the pressure will only act on the sealed interior portion of the mechanism, not the entire surface area of the cap.

$$(4.2.2\text{-}1) \qquad F = pA = (38.22\text{psi})\pi(7.25\text{in}/2)^2 = 1577.82 \text{ pounds}$$

The point at which the line of action of the equivalent force intersects the surface, or the center of pressure, is in the center of the circular cap. The free body diagrams in figure 4.2.2-1 reflects the equivalent force, F of the pressure as the large arrow, and the resultant force of the latches as the 4 arrows on the opposing circumference of the cap.

Figure 4.2.2-1 FBD of the Cap or Top

According to the calculation made in Equation 4.2.2-1, each of the four latches has to withstand a quarter of the pressure equivalent force (1577.82 pounds), providing that they are placed symmetrically about the center. The latches have to withstand a minimum of 394.46 pounds in order to satisfy the safety pressure, plus an additional error factor since it is unlikely that will be perfectly symmetrical about the perimeter. The latches chosen met and exceeded this requirement, as can be seen from the specifications given in table 4.1-3.

4.2.3   The Pressure Vessel (Inner Cylinder)

When in use, the pass-through mechanism is essentially a thin-walled pressure vessel that is subject to loading in all directions.   In general, "thin wall" refers to a vessel having an inner-radius-to-wall–thickness ratio of 10 or more (r/t ≥ 10) [7]. In the design of the inner pressure cylinder, the cylinder inner diameter is 7.25 inches and the thickness of the wall is 0.375. Therefore the radius/wall-thickness ratio is approximately 10, so a thin-walled pressure vessel analysis is valid. The inner cylinder is subject to normal stresses in the circumferential, or hoop, direction and in the longitudinal, or axial, direction. Both of these stress components exert tension on the material. Loads are developed by the uniform hoop stress, $\_1$, acting through the vessel wall. Figure 4.2.3-1 illustrates the basic free body diagram of the interior cylinder.
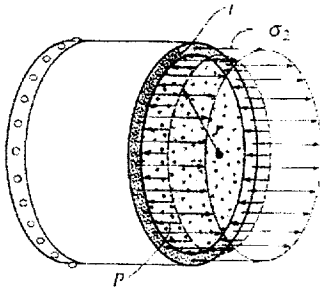
Figure 4.2.3-1 FBD of Interior Cylinder (thin-wall pressure vessel)

Assuming equilibrium in the x direction (the sum of the forces in x are 0), the hoop stress can be calculated by equation 4.2.3-1, where p is the pressure, r is the inner radius and t is the thickness of the cylinder.

(4.2.3-1) $$\sigma_1 = \frac{pr}{t}$$

The maximum hoop stress on the inner cylinder was calculated from the safety pressure of 51.84psi (3.6atm) to be 511.56 psi (3.52516Mpa). If the gage pressure of 2.6 atm is used, the maximum hoop stress is 369.46psi (2.5459Mpa), using the thin-walled pressure vessel assumption. The longitudinal stress, $\_2$, acts uniformly throughout the wall and is calculated from equation 4.2.3-2. The mean radius is assumed to be approximately equal to the inner radius with the requirement that there is equilibrium in the y direction.

(4.2.3-2) $$\sigma_2 = \frac{pr}{2t}$$

The longitudinal stress is half of the hoop stress. Therefore it is approximately 250.56 psi for the inner cylinder, again with a thin walled pressure vessel assumption.

The maximum hoop stress that the pressure exerts on any given section of the interior cylinder was calculated to be 511.56 psi (3.52516Mpa). The material characteristics of the cylinder, or Aluminum

6061-T6, are shown in table 4.1-1. Given a value for fatigue strength of 160Mpa for the cylinder, there is a wide margin between the allowable stress and the stress exerted on the cylinder.

4.2.4 Bolt Calculation for Latch Attachment

The steel latches attach with mounting interfaces to the exterior cylinder in a single-shear connection (lap joint) with two quarter-inch steel bolts. In this analysis, the friction between the members and the mounting interfaces is neglected because it can be assumed that the nuts are not tightened significantly enough to create more than a negligible friction force.

The bolts connecting the latches are subject to shear forces resulting from the pressurization of the mechanism, causing a load to be applied to the cap of the pressure chamber, which propagates through each latch. The free body diagram of the internal uniform shear stress acting on each bolt is shown in figure 4.2.4-1 [7]. Since there are two bolts per latch, each bolt is required to hold a shear stress of 197.23 psi, or half the force on each latch. Equation 4.2.4-1 gives the relationship that the bolts must satisfy in order to effectively stabilize the latches to the outer cylinder given the pressurization of the mechanism.

$$(4.2.4\text{-}1) \qquad \tau_{allow} = \frac{P}{A}$$

Each bolt is a quarter of an inch in diameter, resulting in a area, A, of 0.0490874 inches squared. This requires that each bolt have an allowable shear stress, τ_{allow}, of at least 4.018 kpsi. Therefore each bolt would easily be able to hold the requirement of .19723 kpsi.
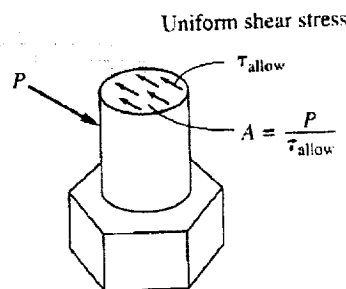
Figure 4.2.4-1 FBD of internal shear on each bolt

4.2.5 Bolt Calculations for Flange Attachment

There are a couple of issues concerning the calculation of the number of bolts and the type of bolts that are needed to attach the interior and exterior flanges together (in compression). First, the threading must be able to withstand the pre-load on each bolt, as well as the load associated with pressurization. In order to avoid breaking contact between the nut, washer and the contact surface (flanges), the pre-load has to be equal to or greater than the load imposed upon each bolt when pressurization occurs. This is important for maintaining an effective seal on the mechanism.

The pre-load on each bolt and the number of bolts depends on the total force applied, the length of each bolt, and the fastener's material, size (cross-sectional area), thread area, and percentage of the minimum proof strength (as given in table 4.1-2). Generally, for statically loaded assemblies, such as the pass-through mechanism, a pre-load that generates bolt stress as high as 90% of the proof strength, Sp, can be used. Assuming that the bolts are suitably sized for the applied loads, these high pre-loads make it very unlikely that the bolts will break during use if they do not break while being tightened. The total length of the bolts, l_{bolt}, is 1.5 inches. The thread length on the bolts is the full 1.5 inches, although only the last .25 inches of threading will be used for attaching to the nut. Each bolt is a _ inch in diameter, d, giving a cross-sectional area, Ab, of 0.0490874 inches squared. Course threaded bolts

are used (20 threads/inch), with a thread tensile stress area, At, of approximately 0.0318 inches squared [7]. Therefore the preload can be as high as 944.46 pounds, using equation 4.2.4-1.

(4.2.5-1)   Preload=Fi=(90%)SpAt

The material, construction, and stiffness of each bolt was taken into account when determining the resultant loads in the bolt and the maximum interior tensile force that each bolt could withstand. It was found that each bolt has to be able to withstand a force of 576.825 pounds. Given the force and the thread area that it acts upon, the actual stress on the bolt may be calculated. This stress was found to be 18,139.15psi for each bolt. The maximum tensile stress allowed in each bolt is approximately 30,717.76 psi. There is a large margin between allowable and actual stress and the safety factor against yielding was calculated to be 1.17196 with a separation point of 7.295 given the loads applied.

4.3   Sealing Capabilities

Elastimetric Viton o-rings were used for sealing the pass-through mechanism. Each sealing interface consisted of an o-ring installed in a gland (cut to specifications). O-ring seals are very dependable and are generally very rugged. Static sealing is needed in the design of the pass through mechanism and o-rings have been proven to seal at high pressures despite slight irregularities in the sealing surfaces, when implemented in a static seal. O-rings are also easily maintained, are compact and lightweight, and no adhesives are needed. Another advantage of o-rings is that if failure does occur, it is usually gradual and detectable, which is an important safety consideration. The metal parts that are integrated with the o-rings were all finished on a lath with a smooth surface in order to potentially increase the sealing capability.

4.4   3-D CAD Model (In IDEAS)

A model of each part to be machined for the hyperbaric pass through mechanism was drawn in IDEAS Master Series 8. An assembly drawing was then completed in order to confirm that all the parts would interface correctly if built to specification. Technical drawings were produced for geometric specifications and tolerances and then each part was fabricated. The final assembly drawing is shown previously in Figure 3.0-1.

4.5   Finite Element Analysis

Finite Element Modeling and Analysis were performed on all loaded parts to confirm their structural integrity and verify that the pass through mechanism would hold under the forces associated with pressurization. The Finite Element Analysis was done in IDEAS under the simulation module. First each part was drawn up as simply as possible. Second, boundary conditions were applied and forces associated with pressurization were included in the simulation. The model was free-meshed and then evaluated for any possible errors. The model was broken down into solid elements with an average size of a _ inch. A solution was run to obtain strain, stress and deflection for each part. The two most critical sections on the structure, the flange teeth/cylinder teeth and the latch mounts, were further analyzed to insure that they would not fail. Illustrated results of the Finite Element Analysis for the critical points can be found within the Appendix.

5.0   Results: Building Phase

During the fabrication process the team members, along with the help of a few experienced machinists, were able to machine all the necessary parts. All machining was completed in campus facilities.

6.0   Results: Testing Phase
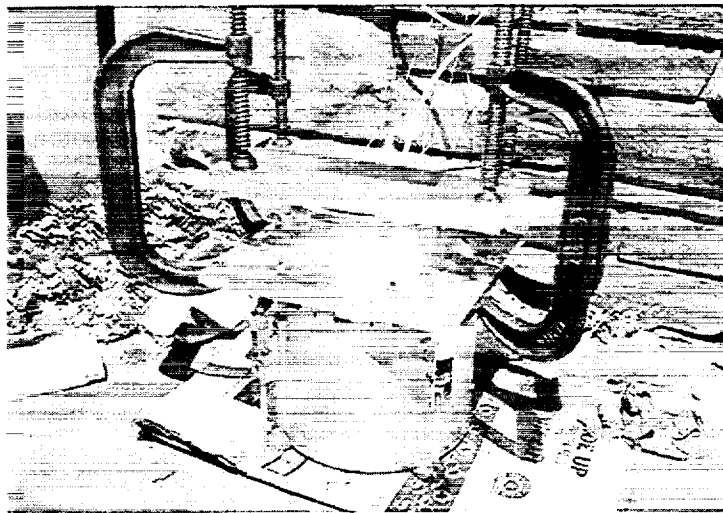
All testing was completed at the Integrated Teaching and Learning Laboratory (ITLL), a facility at the University of Colorado Engineering Center.

The Pass Through Mechanism was assembled with pre-loads on the latches and the flange bolts. The preload is essential for sealing purposes (in order to keep the interfaces tight with no leaks through the o-rings).

The interior door was clamped because the design requires that there would be a pressure match between the interior of the cylinder and interior of the chamber. The chamber itself could not be simulated, so it was not possible to obtain a pressure match.

In order to safely conduct the experiment, the chamber was partially filled with water, leaving some
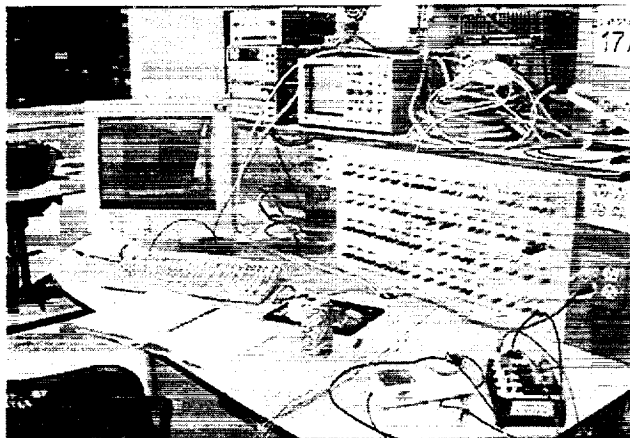
volume for the addition of compressed air. Testing with water is safer than air because it allows high pressures to be obtained without extensive fluid compression. In addition to diminishing safety concerns, it allows for easy leak detection. Air was then pumped into vessel until the system reached and exceeded its design pressure.

Before testing, strain gages were applied at two critical stress areas on the pass

through mechanism. Reference (dummy) gages were also applied to non-stressed points of equivalent material to serve as the fourth resister in each Wheatstone bridge. A Lab-station (shown above) at the ITLL was configured to obtain readouts of the test data.

6.1 Results

The initial phase of testing was to check for leaks at all interfaces of the module. The first time the chamber was filled with water, significant leaks were detected at the weld on the interior flange. Due to time constraints, it was not feasible to reconstruct the weld. Epoxy, rated to 2500 psi, was applied to the inner surface of the weld interface, in an attempt to maintain a proper seal.

Once the epoxy set, the chamber was refilled with water and checked for leaks. No leaks were detected, so the pressurization of the chamber commenced. The chamber attained its maximum pressure, 56 psi, about 30 seconds into the test. This pressure was maintained for approximately 45 seconds, at which point the air compressor was turned off and the chamber was allowed to decompress.

The results obtained from the strain gages indicated that there was micro-strain on the latches and the outer cylinder teeth. The strain on the latch, seen in figure 6.1, increased abruptly during pressurization, reaching a plateau once the desired pressure was attained. The rapid increase in strain is a result of the manner in which the latch hooked onto the exterior door. The single point force on the latch from the top of the chamber was a quarter of the total force on the exterior door, since there were four latches. The slight dip in the trend of the data is likely due to slippage of the bolts that attach the latch to the outer cylinder.

The strain on the aluminum tooth gradually increased with pressure, as shown in figure 6.2. The steady increase is due to a combination of two factors. First, the geometry of the tooth is such that the strain gage had to be mounted in a place where it would only detect an indirect load. Second, the total load is distributed among 12 teeth, so the single tooth where the gage was mounted was only affected by a twelfth of the load.
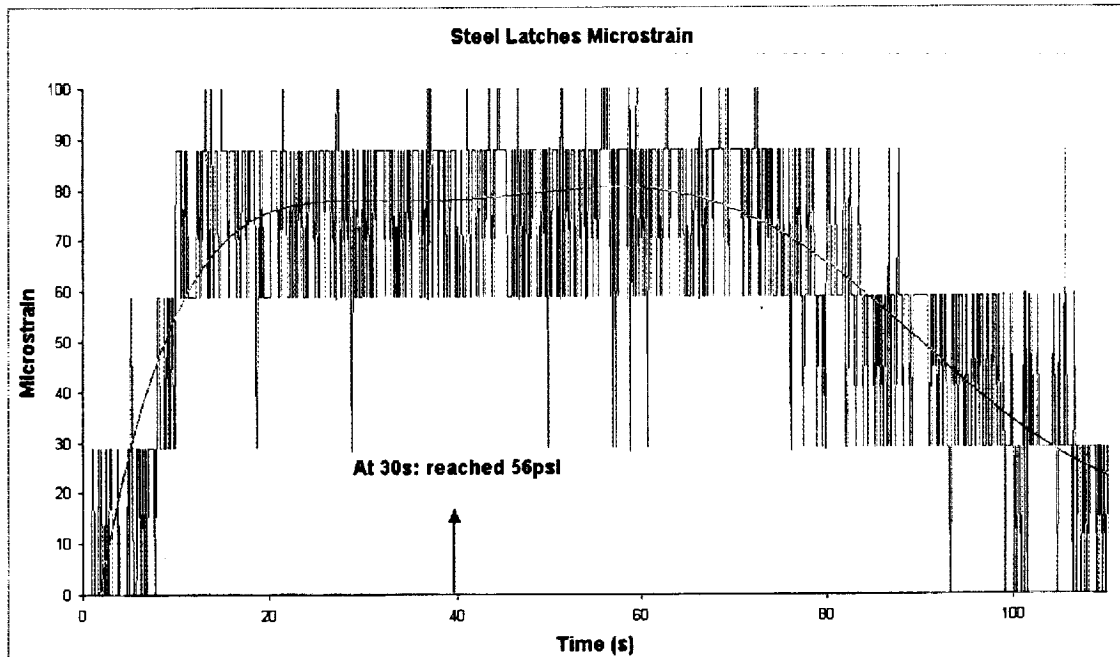
Figure 6.1 Microstrain on the Steel Latch
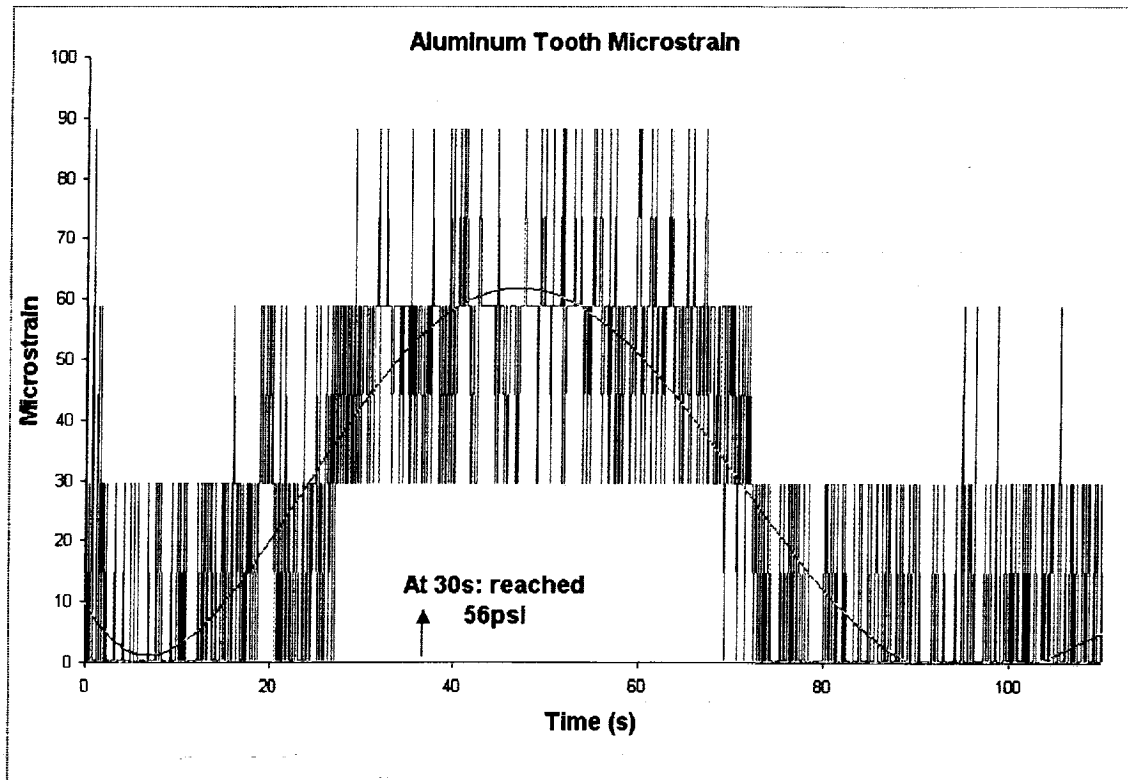
Figure 6.2 Microstrain on the Aluminum Tooth of Exterior Cylinder

7.0   Lessons Learned / Future Studies

7.1   Lessons Learned

- Everything that affects a design cannot possibly be thought of before building a prototype (now we know why sometimes several production models are built before the flight model)

- Ordering parts in small quantities from manufacturers or distributors is often hard, if not impossible

- Allow more time for improvements and changes to the design

- Strain gages are very difficult to correctly and effectively apply

- Money does not go very far on a prototype relying on a limited student project budget

7.2   Improvements to Design

- Do not have an opening on both sides, have only one opening on the side to be attached to the hatch (more coffee-can like instead of latches and a cap), this would allow for less concern with the sealing, leading to a more reliable design

- Obtaining a preload on the latches was physically strenuous (difficult to close)- we didn't think of the implications of the magnitude of preload that was needed

- It was difficult to determine whether the preload was distributed evenly among all four latches

- Use a Metal Inert Gas (MIG) weld instead of a tungsten inert gas (TIG) weld to get better penetration into the crack and maintain better contact with the surfaces ("If you want something done right, do it yourself" – this was the only thing that we didn't do ourselves)

- While positive pressure sealing would have been more difficult, it would be a more reliable design

- If this design were actually implemented for the situation it was built for, the patient would have to deal with o-rings falling out of the mechanism when the interior door was opened: this is a problem that would have to be solved using a integrated sealing surface attached to the inner flange or door

- Sections could be cut out on the exterior cylinder to reduce the weight

- Make a single body (one cylinder) that could both be the sealed containment unit and a locking mechanism

7.3   Unlimited Resource Solutions / Future Studies

7.3.1   Elliptical body and top

Building the body and top in an elliptical formation, as opposed to circular, would allow all seals to be positively sealed with the pressurization of the mechanism. This was not feasible within time constraints and budget constraints, so the design that was built only using off-the-shelf circular, cylindrical piping and aluminum sheets developed and refined on the lathe for the top.

7.3.2   Honeycomb Construction of heavy parts

A relatively simple way to make the mechanism less massive would be to construct the 'tubing' and caps from hollowed-thin cylinder and sheets with honeycomb core for strength and stiffness. This would significantly reduce the weight of the mechanism and is within technological means today. This was not feasible for the initial prototype because of time and budget constraints.

7.3.3   Woven Kevlar Inflatable

With an inflatable structure that can withstand loads associated with pressurization, the mechanism could be significantly less massive and could be easily stowed.

8.0   Conclusions

The senior design project consisted of the design, analysis, manufacturing, and testing of a prototype pass-through mechanism for a space-compliant portable hyperbaric chamber. The development of such a hyperbaric chamber would aid in preserving the health of astronauts in space, especially in long-term applications such as a manned-mission to Mars. The overall design was successful and through the setbacks encountered, many lessons were learned. In the course of assembling and testing the mechanism, an understanding of the importance of building a prototype was realized. Problems such as the o-rings falling out, the latch pre-load issues, and weld failures became evident. A prototype makes apparent previously un-addressed obstacles, allowing for improvements in the design. Concerning the o-ring and the latch difficulties, a second design could incorporate a single door plan where sealing would only be necessary on a single face of the cylinder. Instead of the TIG weld a MIG weld would be recommended. Many problems would be avoided if the parts could be made with mold casting technology. Addition future studies would entail using more advanced lightweight materials and refining the design to be more convenient for astronaut use.

9.0   Acknowledgments

We would like to thank the following people for time they gave in the tasks outlined below:

Jim Ray, Student: Helped machine several parts on the lathe

Lee Thornhill, Student: Gave advise on machining and welding

Al Williams, Student: Helped machine several parts: threading and
                                                       dremmel detail

Chris Muhler, Student: Helped on the Assembly Drawings

Matt Rhode, Aerospace Machine Shop Manager: Assisted in machining several parts as well as giving
                                                       access the Aerospace Machine Shop

Bill Ingino, ITLL Machine Shop Manager: Assisted in machining several parts as well as giving
                                                       access the ITLL Machine Shop

Kurt Filsinger, LASP Facility Manager   Gave advise on o-ring seals

Walt Lund, Aerospace Electronic Shop   Helped provide information and supplies concerning
                                                       electronics

Catherine Flanders & Trudy Shwartz:
ITLL Modulation Integration Engineers   Helped set-up the lab station and electronic for
                                                       testing

10.0   References

[1] Hansen, Chris, 2000. Requirements and Specifications for the Hyperbaric Chamber and Pass through Module. Structures Division, NASA JSC.

[2] http://www.hyperbaric.com   Hyperbaric information

[3] http://www.healthlink.us-inc.com/publiclibrary   Medical Dictionary

[4] http://spaceflight.nasa.gov/shuttle/archives/sts-76/factshts/asseltrn.html   WETF

[5] http://www.matweb.com   Material Database

[6] Vishay Measurements Group, Inc., 1992. Student Manual for Strain Gage Technology. Bulletin 309D, Raleigh, North Carolina., p 17-24.

[7] Norton, Robert L., 2000. Machine Design: An Integrated Approach. Prentice-Hall, New Jersey, p 900-908.

[8] Parker Seals. Parker Seals Handbook 2000

[9] Southco. Southco Handbook 2000. ISO 9001, QS-9000, p 166-167

11.0   Appendix: Critical FEM

RESULTS: 4- B.C. 1,STRAIN ENERGY_4,LOAD SET 1
STRAIN ENERGY - MAG MIN: 1.06E-05 MAX: 7.04E-03
DEFORMATION: 1- B.C. 1,DISPLACEMENT_1,LOAD SET 1
DISPLACEMENT - MAG MIN: 0.00E+00 MAX: 2.87E-03

VALUE OPTION:ACTUAL
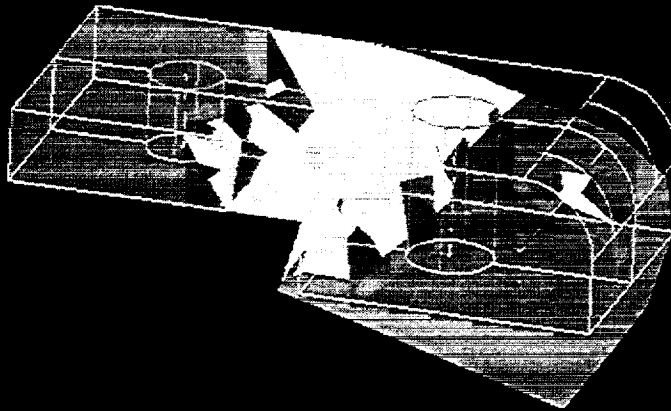
RESULTS: 4- B.C. 1,STRAIN ENERGY_4,LOAD SET 1
STRAIN ENERGY - MAG MIN: 3.43E-08 MAX: 2.04E-03
DEFORMATION: 1- B.C. 1,DISPLACEMENT_1,LOAD SET 1
DISPLACEMENT - MAG MIN: 0.00E+00 MAX: 1.78E-03

VALUE OPTION:ACTUAL
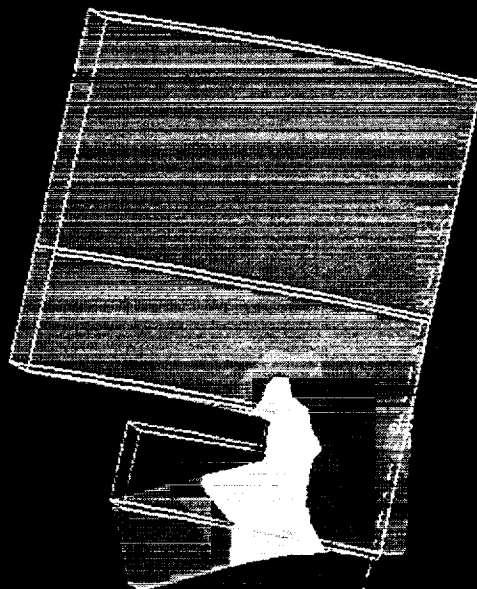
S8/cP/IN/63

Project LaMaR:

Laser-powered Mars Rover

Submitted by University of Colorado at Boulder
Student Group Members:
Emma Dee
Samantha Dimmick
Brian Ickler

Faculty Advisors:
Dr. Lisa Hardaway & Prof. John Sunkel

Corporate Advisors:
Mark Henley & Dr. Seth Potter
The Boeing Company

Presented to:
HEDS-UP Program Committee & Judges
3600 Bay Area Blvd, Houston, TX 77058

Table of Contents

1.0 Abstract

Rover exploration on the Martian and lunar surfaces is limited to areas where direct sunlight can recharge secondary rover batteries. The task of Project LaMaR is to design a laser-power receiving system that can allow the rover to be operated in a shadowed crater or canyon. The design driver is to find a photovoltaic (PV) cell and laser combination that will achieve the greatest power conversion efficiency. In order to minimize the power conversion loss, it is necessary to closely match the laser wavelength and the cell material bandgap.

Power efficiency tests were performed with Silicon (Si), single-junction Gallium Arsenide (GaAs) and dual-junction Gallium Indium Phosphide (GaInP)/GaAs cells. Experimentation was performed using lasers with wavelengths of 632 nm, 720 nm, 830 nm, 1064 nm and 10000 nm. The maximum power conversion efficiency obtained was 68.5% when applying an 830-nm beam to a single-junction GaAs cell. To illustrate the concept for public outreach purposes, a small laser-pointer demonstration model was built.

2.0 Introduction – Design Problem

Advances in robotic technology have had a significant effect on surface exploration and the prospect of human arrival on Mars. Robotic precursors on Mars will allow for enhanced research before human habitation, as well as aid in continual exploration during future missions. According to the Mars Reference Mission [1], the use of robots will play roles in several important areas of human exploration on Mars including, but not limited to, gathering surface information, demonstrating technological advancements, and maintaining a significant portion of surface systems prior to crew arrival.

Powering devices using photovoltaics is a topic of high importance throughout the aerospace industry and significant research has been performed to improve them. However, with current PV technology, there is no practical way to improve mission duration when the rover is not in direct sunlight. Recent discoveries have shown that sources of water may exist on both the Moon and Mars in the form of polar ice. It stands to reason that to reach this ice, an alternative power source needs to be provided to the vehicles to continue to be fully functional in low temperatures and complete darkness. Using laser-photovoltaic power transmission, it should become possible for rovers to explore areas such as craters and deep canyons [8,9]. The focus of Project LaMaR is to present a possible solution to this specific problem and intends on demonstrating that a rover can be operated for extended periods of time in total darkness by harnessing laser-beam energy transmitted from a base station at the crater/canyon rim. The objective is to create a longer life span for both the vehicle and the mission and Project LaMaR will provide a proof-of-concept of this laser-powered rover.

Note that the project does not focus on the technical aspects of the base-station laser, or the method by which the rover and base-station communicate with each other. In the case that obstacles may block the line of sight between the rover and base station, the rover is expected to continue forth only when it is sure that there is sufficient battery power to get back to line of sight again. Further research must investigate the feasibility of building the base-station.

3.0 Approach to the Problem

The proof-of-concept design approach of Project LaMaR can be designated by four areas:
- Background research into PV applications and processes
- Experimentation with different laser and PV cell combinations
- Design for a Martian or lunar application
- Build a demonstration model for outreach and presentation use

3.1 Background Research

The initial project requirements as defined by corporate advisors were as follows:
- Rover operates with 28-volt DC bus and ranging in power from 15 to 50 watts
- Base-station laser specifications: Nd:YAG – 1060 nm and 1000 watt output power
- Expected 50% power loss of laser beam during transmission, therefore the cells will receive 500 watts

From these design specifications, it became evident that traditional solar cell information and resources would not be applicable to the project. Power efficiencies are determined under the full solar spectrum and often the entire area of the cell is covered. In the case of Project LaMaR, monochromatic light is being harnessed and will probably not cover the entire cell area. Therefore, previously generated efficiency curves and data could not be applied. A new set of data must be built to take these never-before-tested factors into account.

Having never taken an undergraduate class to learn the PV process, it was necessary to fulfill the knowledge void by learning what types of solar cells exist and how they work. In doing so, it became evident that Project LaMaR must complete experiments with several types of cells when looking for the optimal design solution.

The sun emits photons across the full spectrum of wavelengths. For this reason multiple-junction cells give the best response for use in the sun because their multiple band gaps cover a wider solar spectrum. Each layer covers a different range of wavelengths. The level of photons that the sun produces at those wavelengths is known when the cells are manufactured. Figure 3.1-1 below shows the spectral response of the 3 layers that make up a triple-junction cell as well as the photon energy of the sun of the spectrum. This graph shows how the range of the three layers help to design a cell where all the layers are producing close to the same power. Understanding this makes it easy to see whey as PV cell technology has improved the industry has stopped making single junction cells and started making advances in double, triple, and even quadruple junction cells.
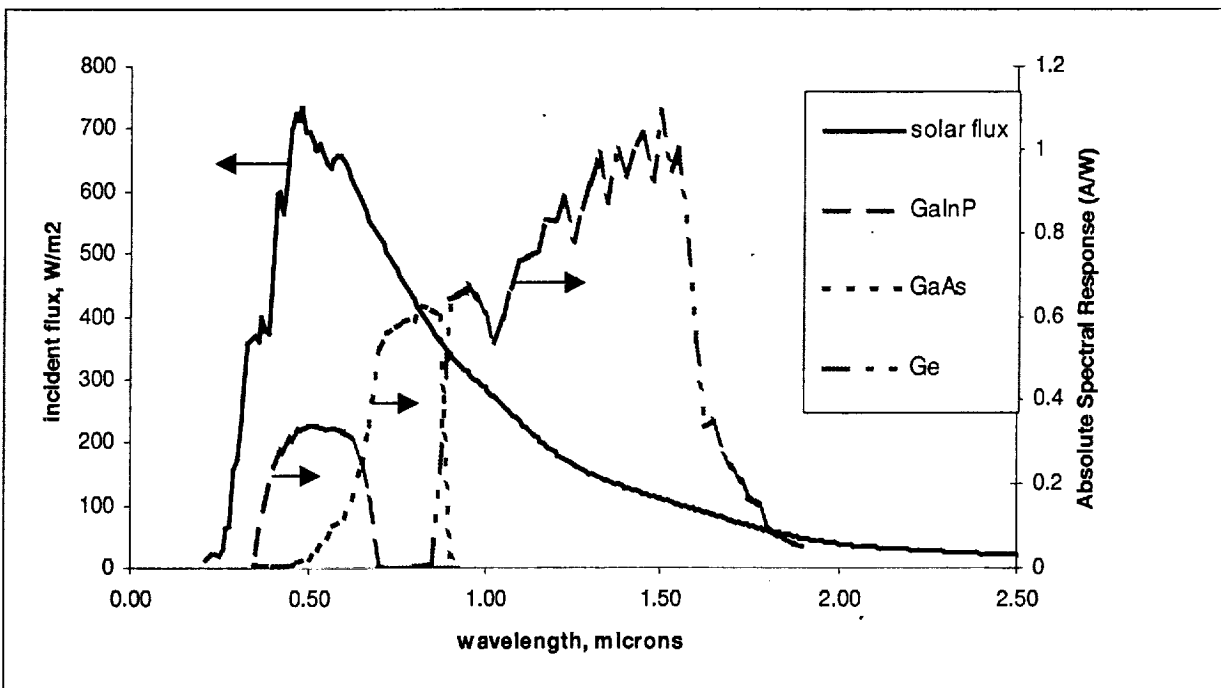
Figure 3.1-1 Solar incident flux and spectral response of three PV materials [7]

3.2 Experimentation

In order to find the best solution (highest power efficiency), experimentation with many types of lasers and selected PV cells was necessary. Commonly used PV cells like Silicon (Si), Gallium Arsenide (GaAs) and Gallium Indium Phosphide (GaInP) cover the broad section of the solar spectrum from below 400 nm to above 1000 nm. Therefore, Project LaMaR decided to test with laser wavelengths falling into this range. Also of concern in the experimentation process is the efficiency performance of single-junction cells versus dual-junction cells.

3.3 Mars Rover Design

Knowing very little about Mars surface conditions and having only one previous Mars rover to refer to (Sojourner, 1997), many assumptions had to be made about the proof-of-concept design. In addition to the previously mentioned 50% laser power loss during beaming, other atmospheric conditions such as dust accumulation on the cells and low operating temperatures must be considered.

The purpose of the Mars design model is to provide an accurate depiction of the laser and PV cell requirements necessary to achieve the goal of highest power efficiency. Project LaMaR intends to create an example for real-world application on Mars based upon the results demonstrated in the experimental phase of the project.

3.4 Demonstration Model

The rationale for having a demonstration model is to achieve a high level of understanding about the project for public observers. This particularly applies to Project LaMaR's outreach at both the University of Colorado Design Expo as well as the presentations given to Boulder-area, high school physics classes. The model is a remote control car mounted with a solar cell, which can be driven when laser beams are applied to the cell.

4.0 Results

Seven different lasers were used for testing, each having different wavelength and power properties. Refer to table 4.0-1 for a complete list of laser specifications.

Table 4.0-1 Summary of laser specifications

Laser #	Wavelength	Power	Type	Location	Technician
1	632 nm	5 mW	HeNe	Handheld	Team LaMaR
2	632 nm	10 mW	HeNe	Portable	Daniel Vigliotti
3	632 nm	30 mW	HeNe	NIST	Tim Quinn
4	720 nm	52 mW	Ti-Sapphire	NREL	Don Selmarten
5	830 nm	48 mW	SDL 800 Diode	NREL	Pat Dippo
6	1064 nm	490 mW	Nd:YAG	NIST	Donna Hurley
7	10,000 nm	5 W	CO_2	NIST	Andrew Slivka

Laser 7 was used only to heat cells for conducting thermal tests. It also served to prove that there is no power generated with a laser at this wavelength. Results from the thermal tests are discussed in section 4.6.

Tests were performed using Silicon, single-junction GaAs and dual-junction GaInP/GaAs cells. The experimental conditions for all tests were held at room temperature and in near complete darkness. Dark readings were taken to ensure that any ambient room lighting was at a minimum. Safety goggles were worn when using the 720 nm, 830 nm, 1060 nm and 10000 nm lasers. Up to five voltage and current readings were taken during all tests to achieve an average value. Each cell was reoriented slightly so that the beam would strike a different area on it when the testing apparatus permitted. The distance between the laser aperture and the cell varied between 10 and 40 cm for the different lasers depending on the equipment setup. The diameter of the beam hitting the cell was typically 1 to 3 mm unless otherwise stated as in section 4.5 where beam expansion and its effect on performance is discussed. Also, the cells were tested with no applied load, and therefore voltage measurements are "open-circuit" and current measurements are considered "short-circuit".

4.1 Dual-Junction Test Results

Four dual-junction solar cells were mounted and had leads soldered for use in the experiment and labeled 'Cell A' through 'Cell D'. Used in the test were lasers 1 through 4 as denoted in table 4.0-1 above. Average voltage and current output were calculated from five separate tests for each cell/laser combination. The maximum power efficiency performance was seen with Cell C; table 4.1-1 displays the data results for Cell C.

Table 4.1-1 Dual-junction test results

Laser Characteristics			Dual-junction Output (Cell C)			
Type	Power (mW)	λ (nm)	Voltage (V)	Current (mA)	Power (mW)	Power Efficiency (%)
HeNe	5	632	1.35	0.52	0.71	14.11
HeNe	10	632	1.40	0.92	1.29	12.86
HeNe	30	632	1.66	3.40	5.64	18.81
Ti-sapphire	52	720	1.11	0.55	0.61	1.16

Although the power efficiency for each of the 632-nm lasers are lower than expected, they are not necessarily abnormal. However, the next concern is trying to explain the extremely poor efficiency at 720 nm. In doing so, it is necessary to analyze what is happening within each individual layer of the dual-junction cell. Figure 4.1-1 displays a view of the layers in a dual-junction GaInP/GaAs cell.
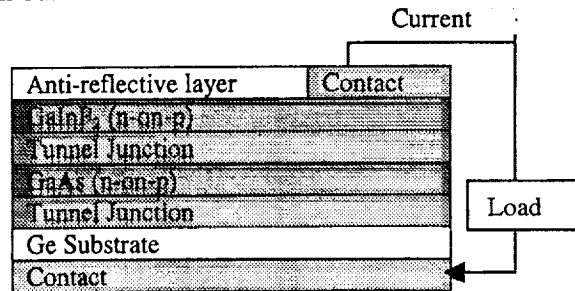
Figure 4.1-1 Diagram of dual-junction cell

The dual-junction cell is a circuit when it is functioning properly. The individual layers act like two batteries linked in series. When light photons strike electrons within the layer, current is generated between the n and p layer of the material. The important characteristic for achieving high power efficiency is to match the current generated within each layer. If a significantly different current is created in each cell, the overall efficiency of the system decreases.

Now that the issue of current matching within dual-junction cells has been discussed, it is possible to visually demonstrate why the power efficiency at 720 nm was so low (1.16%). Looking at the quantum efficiency (QE) (photons/electrons) curves in figure 4.1-2 for GaInP and GaAs, it becomes all too clear why the cell at 720 nm generated such little current.
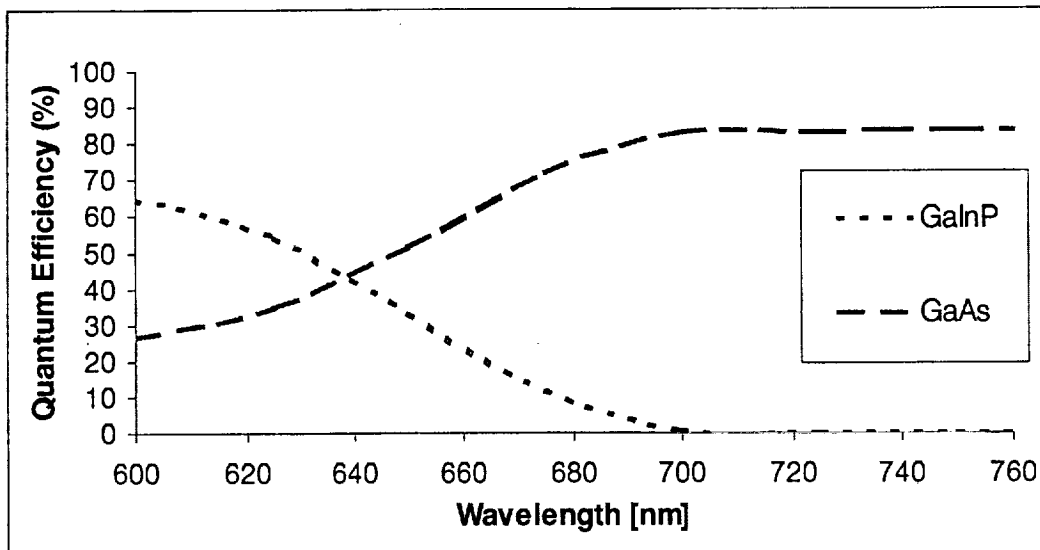
Figure 4.1-2 Quantum efficiency curves for GaInP and GaAs [7]

At 632 nm, it can be seen in the figure that a current response (QE of about 35 to 55%) is generated within each of the individual layers of the cell. However, at 720 nm the GaInP does not respond to the incoming photon and is a transparent layer; the photons go right through the material. Minimal current is generated within the layer and the overall efficiency of the entire cell is decreased significantly. With only one junction generating current, the circuit cannot be completed.

Having witnessed the problem of current matching within a multi-junction cell, the next step is to confirm that single-junction GaAs cells will respond as expected with much higher power efficiency. The next section displays the repeat experiments on the single-junction cells which will allow for a comparison of the two cell types and their power efficiency performance.

4.2 Single-Junction Test Results

Four single-junction GaAs solar cells were also mounted and had leads soldered for use in the experiment ('Cell A' through 'Cell D'). Used in the test were lasers 1 through 6 as denoted in table 4.0-1 above. Average voltage and current output were calculated from five separate tests for each cell/laser combination. The maximum power efficiency performance was seen with Cell B; table 4.2-1 displays the data results for Cell B.

Table 4.2-1 Single-junction GaAs test results

Laser Characteristics			Dual-junction GaInP/GaAs Cell Output (Cell C)			
Type	Power (mW)	λ (nm)	Voltage (V)	Current (mA)	Power (mW)	Power Efficiency (%)
HeNe	10	632	0.65	1.88	1.23	12.30
Ti-sapphire	52	720	0.80	24.88	19.81	38.10
SDL 800 Diode	48	830	0.82	39.92	32.88	68.50
Nd:YAG	490	1064	0	0	0	0

What is important to note is the 68.5% power efficiency achieved with the 830-nm laser. Also note that the relationship between increasing wavelength (632 nm up to 830 nm) and power efficiency is nearly linear. Due to the fact that the bandgap energy of GaAs occurs at a wavelength of 886 nm (1.4 eV) it might be possible to predict that an even higher efficiency will be seen up to the bandgap wavelength. However, Project LaMaR did not want to theorize about this possibility unless the experimentation with a laser wavelength between 830 nm and 886 nm could be performed. The power efficiency at 632 nm (12.3%) is lower than that seen in the dual-junction results (~15 %).

4.3 Silicon Test Results

For a complete analysis, it was necessary to experiment with the most commonly used solar cell – Silicon. They are cheaper, easier to manufacture, and cover a wider range of wavelengths than a single-junction GaAs cell. However, optimum efficiencies for this cell occur at shorter wavelengths, i.e. below 632 nm. Due to the fact that Si operates more efficiently below the red spectrum, it is not a viable choice for a Mars rover application. The dust in Mars' atmosphere alters the spectrum; it is blue deficient. Even though Silicon has lower overall efficiencies, it will be the only cell that responds if a 1064 nm laser must be used. Test results for the one silicon cell are shown in table 4.3-1.

Table 4.3-1 Results of the Si cell tests

Laser Characteristics			Silicon Output			
Type	Power (mW)	λ (nm)	Voltage (V)	Current (mA)	Power (mW)	Power Efficiency (%)
HeNe	10	632	0.38	1.83	0.70	6.95
HeNe	30	632	0.42	6.87	2.88	9.62
Ti-Saphire	81	720	0.46	36.47	16.70	20.62
Nd:YAG	490	1064	0.47	57.1	27.08	5.53

The silicon cell was not available during the time that testing was performed on the 830 nm laser. For the lasers that were tested the maximum power efficiency was seen on the 720 nm laser. If silicon would be used, it would

probably be with a 1064 nm laser, but the efficiency here is only 5.53% this would not serve as viable rover mission selection.

4.4 Using Multiple Laser Beams

The purpose of this section is to explore the effect of beaming more than one laser on a cell. Using Cell B from the single-junction GaAs experiment up to five handheld, 632-nm lasers were added. The results of this experiment are shown in table 4.4-1.

Table 4.4-1 Results of multi-laser test

	Voltage (V)	Current (mA)	Power (mW)	Power Efficiency (%)
Dark Reading	0.01	0.00	0.00	0.0
5mW	0.63	1.13	0.70	14.1
2 x 5mW	0.67	2.33	1.56	15.6
3 x 5mW	0.70	3.51	2.44	16.2
4 x 5mW	0.71	4.59	3.26	16.3
5 x 5mW	0.72	5.75	4.16	16.6

The maximum power efficiency of 16.6% was achieved with all five lasers. The voltage changed very minimally (0.63 V to 0.72 V) as the lasers were added but the current increased from an average of 1.13 to 5.75 mA. The voltage, current and efficiency trends are displayed in figure 4.4-1.
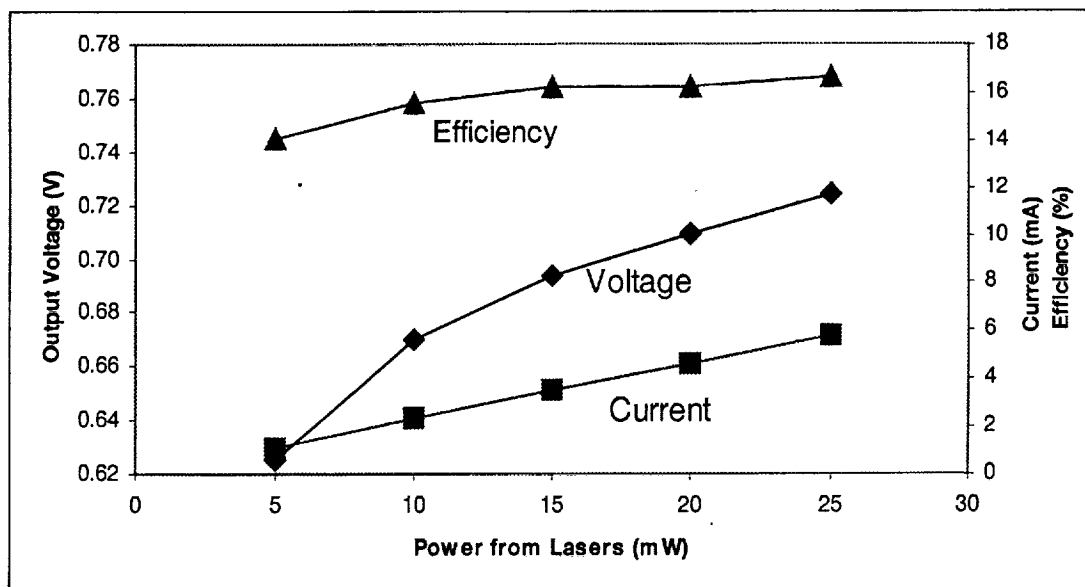
Figure 4.4-1 Effect of multiple lasers on one single-junction GaAs cell

The results of this experiment redefined one of the original Mars rover design requirements. Instead of using one 1000-watt laser, it would be more beneficial to use additional lasers at lower power output. The power efficiency of two 5-watt lasers from table 4.4-1 is 15.6%, whereas the efficiency of one 10-watt laser in table 4.2-1 is only 12.3%. Section 5.1 discusses the real-world application of multiple laser beams for the laser-powered Mars rover.

4.5 Effects of Beam Expansion

Lasers 3 and 6 were collimated, and lasers 4 and 5 had adjustable beam diameters. The effect of beam expansion was analyzed using the latter two. The beam diameter of the 720-nm laser went from 1mm to 1cm and that of the 830-nm laser increased from a 5 mm circle to an oval about 2.5 cm x 0.75 cm. In both cases the power efficiency decreased when the beam was expanded (see figure 4.5-1) on single-junction GaAs cells.

Power Efficiency of Expanded vs. Point Laser Beam -- 720 and 830 nm
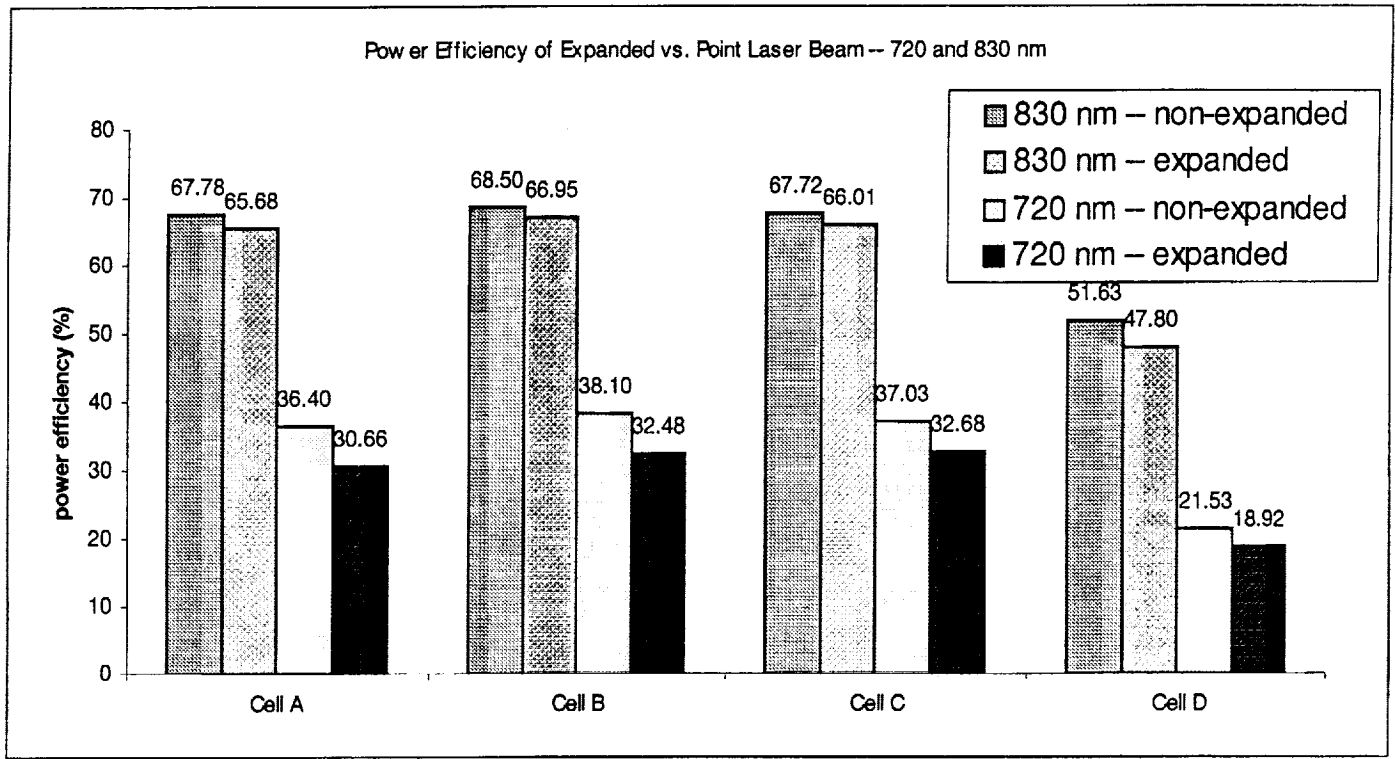
Figure 4.5-1 Effect of beam expansion on power efficiency

The fact that the power density decreases as the beam expands, less current is generated in return. The efficiency decreases more quickly at the 720-nm wavelength because it is farther away from the bandgap of GaAs than the 830-nm wavelength. This is also relative to the size of the cell and power of the beam.

4.6 Thermal Testing

In order to investigate the effects of thermal changes as a cell heats up, tests were performed with a 5-W laser (# 7, table 4.0-1). With a wavelength of 10μm, the cell appears transparent to the laser beam, and therefore the cell heats without current generation. A thermocouple was positioned on the backside of a single-junction GaAs and Si cell. Figure 4.6-1 shows the relationship between voltage and temperature. The source of the voltage being generated is due to a small desk lamp that facilitated data taking.

The GaAs seems to be affected more significantly by the temperature change. This indicates that it will operate more efficiently when used in a colder environment. The Si cell is not affected as much by the change in temperature from the high intensity beam. From these tests trend lines were created which were compared with the thermal coefficient data obtained from Spectrolab data sheets (see table 4.6-1). The Spectrolab test simulates the solar spectrum of AMO conditions, or 135.3 mW/cm^2 (1 sun). The intensity of the laser used for thermal testing in figure 4.6-1 was 20,000 mW/cm^2 (~148 suns).

Table 4.6-1 Thermal coefficients of GaAs and Si cells

Cell Type	Spectrolab	Team LaMaR
Silicon	-2.2 mV/°C	-3.89 mV/°C
Single-Junction GaAs	-1.9 mV/°C	-0.94 mV/°C
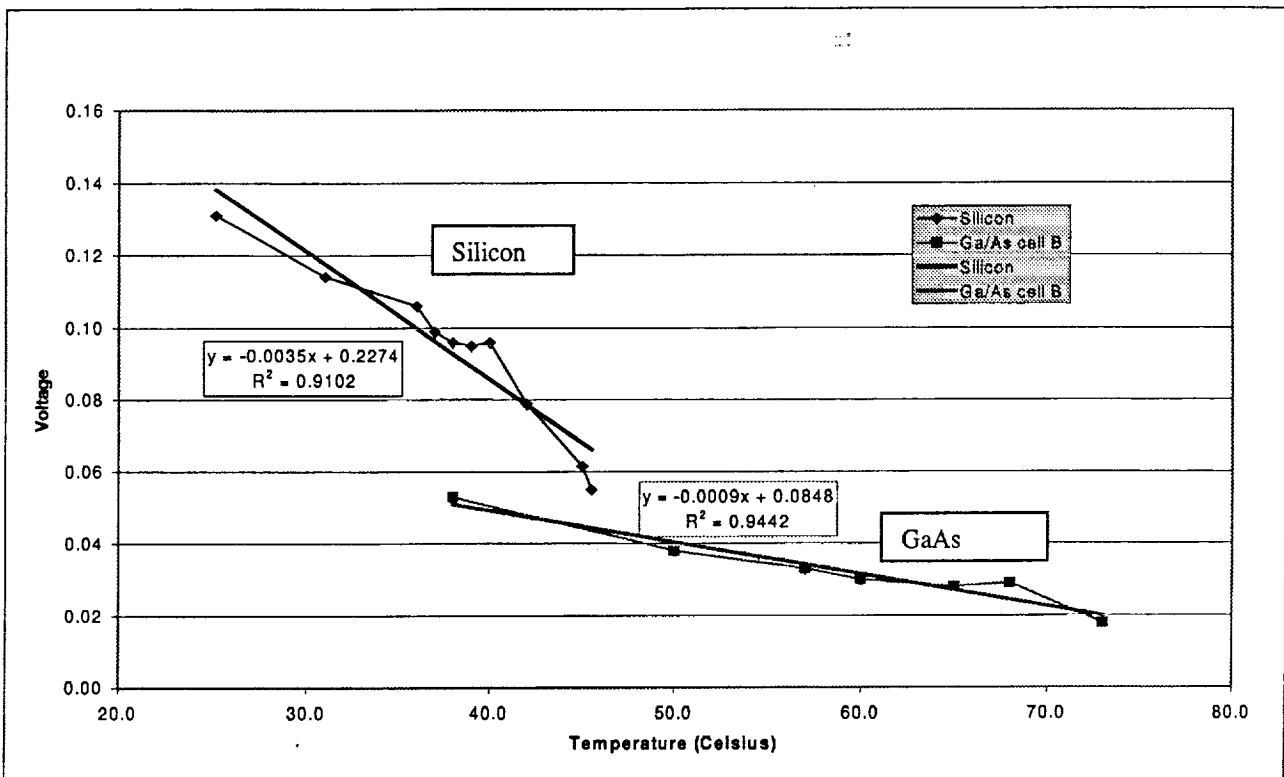
Figure 4.6-1 Thermal effects on single-junction GaAs and Si cells

The discrepancies in table 4.6-1 between experimental results and Spectrolab values can be attributed to several factors. First, the Spectrolab test illuminates the entire cell whereas the laser beam only covers a spot about 5 mm in diameter. Also, the thermocouple was placed on the back of the cell as close to the area where the beam was hitting. Therefore the temperature reading was not uniform across the cell, but local to that spot. The thermal coefficients obtained using the 5-W laser are only localized results, but are useful in determining how a single laser will affect the thermal properties of the cells.

5.0 Conclusions

Although the optimal results were achieved using single-junction GaAs cells, the testing on dual-junction cells turned out to be very useful. It provided a clearer understanding of how multi-junction cells function when subjected to monochromatic light, and it clarified the issue of current matching.

5.1 Mars/Moon Application Conclusions

Based on the results obtained from testing with dual-junction and single-junction cells, the overall proof-of-concept Mars/Moon rover was designed. To do so, atmospheric effects as well as surface conditions were taken into consideration.

The design assumptions are as follows; (1) the maximum efficiency can to be achieved by closely matching the laser wavelength and cell bandgap, (2) the laser power output should be enough to produce the needed requirements for the rover, (3) excess heat generation should be avoided, and (4) the surface and atmospheric conditions must be estimated. The significant atmospheric problem on Mars is the dust. In a typical 30-day mission, dust will deposit on 6.6% of a horizontal array [6]. One goal of this project is to increase the mission life to 1 year or more. This would mean that over 50% of a horizontal array would be covered in dust. Therefore, a vertically mounted array would be beneficial in reducing this negative effect. As a best estimate, it is assumed that the laser beam power will be reduced by 50% during transmission to the rover. Dust factors can be eliminated for a moon application.

Temperature is also an important factor in the performance of the cells. The minimum predicted temperature on Mars is -112°C. Fortunately, based on our thermal studies, single-junction GaAs cells have enhanced performance at lower temperatures.

From the data collected, the application assumptions were devised. A minimum of 68% power efficiency is expected when using single-junction GaAs cells and an 830-nm laser. This forms the basis for determining the power of the lasers and the cells area. Multiple lasers with small diameters have shown to interact better with cells than one laser with an expanded beam. Multiple lasers also offer a degree of redundancy, enhancing system level reliability in the event that one of the lasers might not perform as expected. Low-power lasers are also less costly than a single, high-power laser. One benefit of using lasers instead of sunlight is that the angle at which the beam hits the solar array does not produces significant losses in power. They are small enough to be considered negligible. Based upon the power requirements of Sojourner (max 16.5 W at noon), it is predicted that 30 W would be desired for a larger rover with increased functionality.

The final step of the design was to determine the type of cell, power and wavelength of the laser, and the array size. The cell selected was a single-junction GaAs cell. This was based on the efficiency, ease of manufacturing, atmosphere constraints, and experimental performance. To generate 30 W for the rover, and considering a 68% power efficiency conversion, a total of 45 W must be striking the photovoltaic cell. However, taking the 50% transmission loss into account results in a total of 90 W to be beamed from the base station. Since multiple lasers were desired, 4 lasers of 22.5 W per laser were selected to achieve the 90 W. The laser must be designed for the arriving beam diameter of 10 cm (when the rover is 10 km from the base station), and therefore a total cell array of 400 cm^2 has been selected to capture all four beams. Each beam creates about one sun of illumination, and therefore ensures that the cells are not heated to any abnormal degree. With this design, all of the requirements and objectives have been met. Figure 5.1-1 shows a schematic of this design concept.
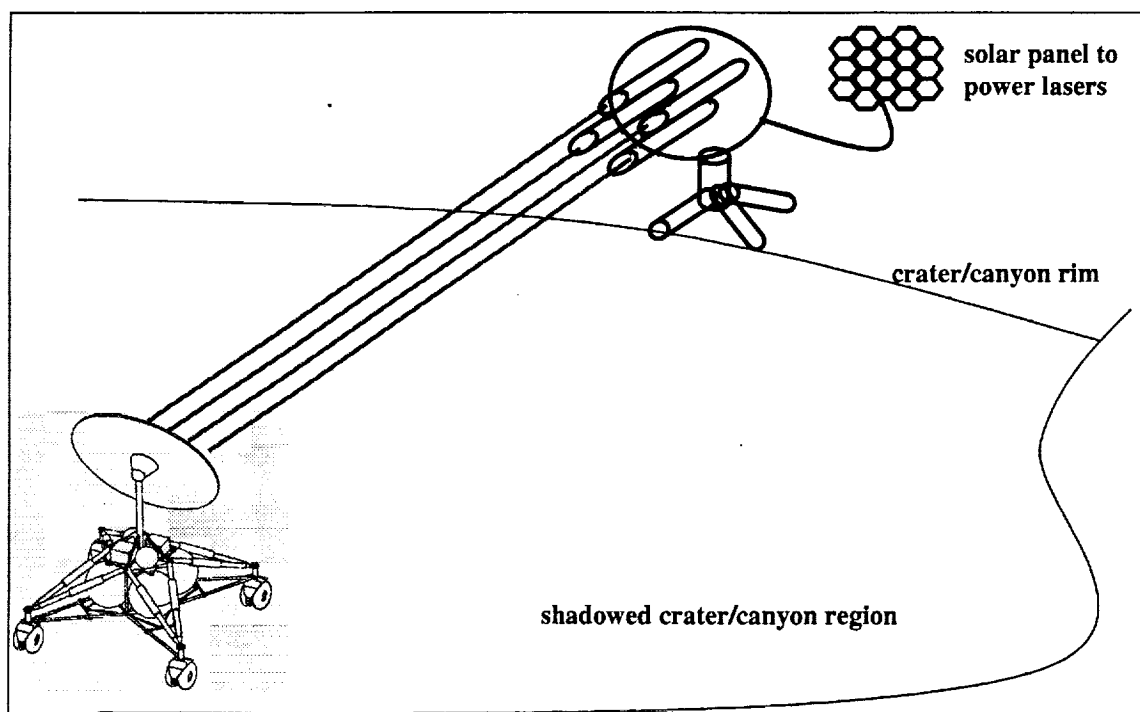
Figure 5.1-1 Schematic of design concept

This design incorporates a base station equipped with the four lasers and a rover that can move up to a distance of 10 km away from the base and operate is the darkest crater or canyon (farther distances would be possible, with reduced power levels). The rover will not be much larger than the Sojourner rover, but can be equipped with digging tools and other collection and analysis mechanisms. The rover will also be equipped with a secondary source of battery power for use when the rover does not have line of sight with the base station. The solar array will be mounted as shown in Figure 5.1-1. It will be mounted in such a way to minimize dust collection and will be able

to rotate for maintaining line of sight with the base. A gimble attachment allows for angle deflection and minimizing dust deposits.

5.2 Demo Conclusions

For both our outreach efforts and the HEDS-UP Forum we wanted to physically demonstrate the capabilities of the system with a toy, such as a remote control car. Lasers for the demonstration were selected based on safety, portability, cost, and availability. The design driver for selecting a toy car was to minimizing the required power to run it. Conveniently this also minimized the safety concerns as well as the portability concerns for the presentation. It was decided that the best laser for our demo would be not be just one laser, but multiple handheld lasers. They were small, did not cause permanent damage to the eye, inexpensive, and already demonstrated positive results when combined on one cell. The lasers for the demo were 632nm wavelength, so the best cells to use were the Dual-Junction cells with an efficiency of 14%.

A small remote control car that normally operates on two AA batteries was the first selection. This car was tested to determine the exact voltage and current requirements. Even though the combined voltage of the batteries was 3.0 V it was shown that the car could run on low batteries down to approximately 2.5 V. An ammeter was used to determine that the car run will run on anywhere from 190 to 210mA of current. Obviously this was well out of the range for an application with the 5mW lasers. A different demonstration was needed. Searches for a toy that ran on only one AAA battery proved useless. It was determined that we the demonstration effectiveness can be achieved by simply moving the car, as opposed to directly powering it with the laser beam power. A circuit board was designed to replace the existing circuitry in the car.
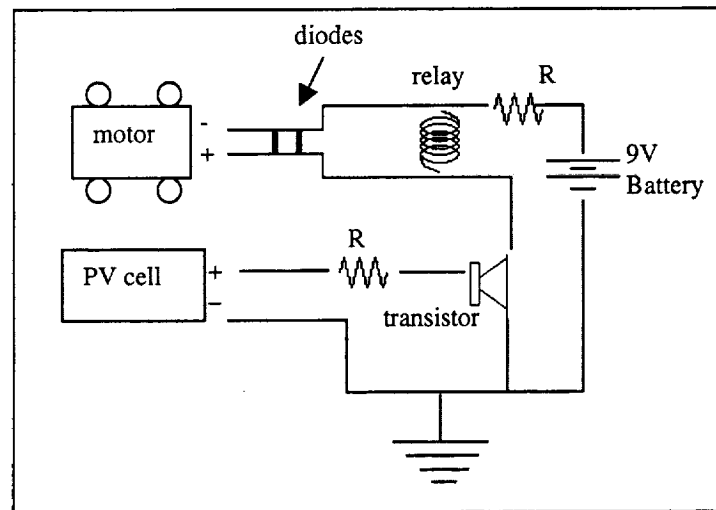
Figure 4.3-2 Demo circuit

The circuit uses the power from the solar cells to close the switch in the transistor. When the transistor is closed the power from the 9V battery operates the circuit, and the relay closes the circuit to the car. Two diodes were used to help prevent the relay from welding permanently. Resistance was added to control the power flow in the circuit. After the circuit was working it was noticed that the ambient florescent room lighting was enough to power the transistor. To increase the amount of power required from the cells a second resister was added. This allowed for a clearly defined demonstration. When the lasers are on the cells the transistor is closed and the motor runs, but it does not when just the room lights hit the cells. Depending on the ambient lights in the room where the demo is being displayed, the cells may require more lasers, or the resistance may need to be increased to ensure that the cells are not activated without lasers.

6.0 Future Studies & Lessons Learned

Possible additional testing for this system would use a tunable laser that is adjustable to both wavelength and power. This would allow for studies into the best possible wavelength for each type of cell. Of interest are the efficiencies generated between the wavelengths of 831 nm and 890 nm. Above 890 nm, a significant decrease in power efficiency would be expected in the single-junction GaAs cell. The efficiencies that we have witnessed in these tests could be increased by perhaps another 10 to 20%.

Based on the QE and Spectral Response curves for the three materials, it looks like the obvious choice cell material would be Germanium. If a laser could be designed to match the exact desired wavelength in Germanium's band gap, it should have an excellent efficiency. Single junction Germanium cells have never been manufactured because, when the solar spectrum in analyzed, there are relatively few photons emitted in Germanium's range. This vehicle will not be dependent on the sun's photon emittance, however, considering the total system requirements for the vehicle, this may not be the best choice. Figure 6.0-1 below shows that there may be other issues to consider

Light IV curves of GaInP, GaAs, and Ge subcells, and a
production Triple Junction solar cell.
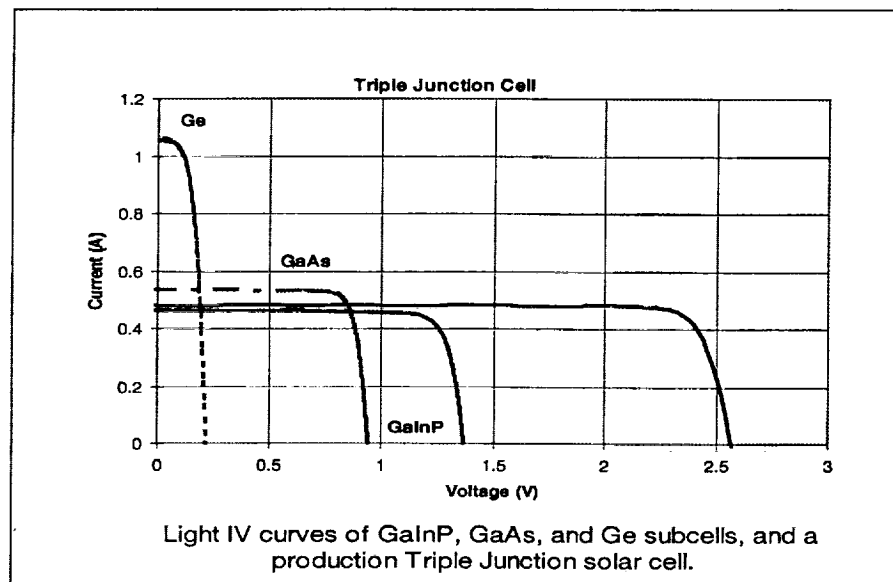
Figure 6.0-1 Quality of power produced [7]

It is well known that that power is the product of voltage and current. The power generated by each junction of cell type is not always made up of the same proportion of voltage and current. The figure clearly shows that Germanium converts most of the power into current while the other two materials create more voltage than current. It is common practice in building circuits to use voltage dividers when the voltage is too high. To do the reverse and turn the current into voltage is usually much harder. For this reason, even though the overall efficiency for Germanium may be higher, it might make more engineering sense to select GaInP or GaAs for the application.

7.0 Project LaMaR Outreach

In late April of every year, the University of Colorado Engineering Council (UCEC) sponsors a design expo as part of its Engineering-Days celebrations. Undergraduate design teams are given the opportunity to present their project and be judged by industry leaders and faculty. Members of the local press, community and industry representatives were invited to see the 73 groups that presented. Projects are grouped into similar disciplines and experience levels. Some of the more popular categories are the Assisted Technology group, Rube Goldberg Machines, and interactive children learning stations. Project LaMaR received the award for Best Aerospace Project.
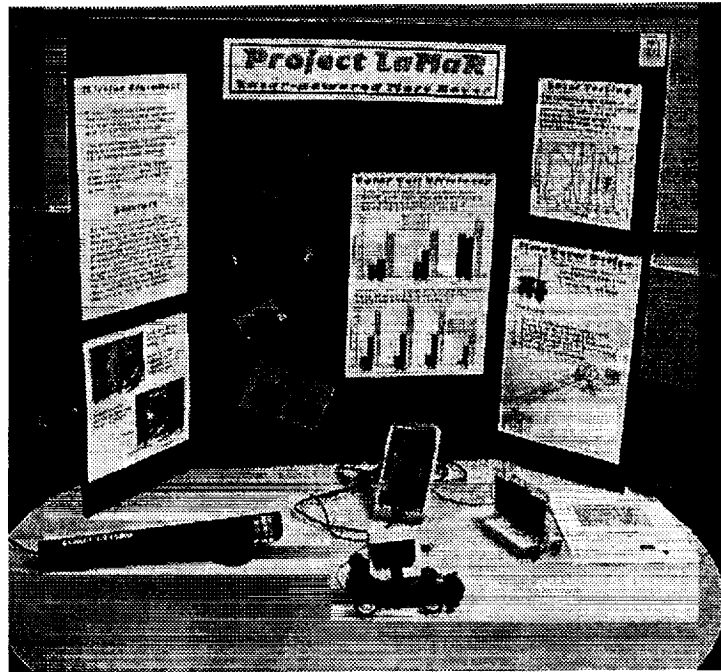
Figure 7.0-1 Display at University of Colorado Design Expo

Whereas the design expo brought people to CU, Project LaMaR extended its outreach into the community by visiting a Boulder-area high school. Presenting to a senior-level physics class at Fairview High School, the demonstration appealed to scientific, college-bound students. This generated interest in the engineering profession in addition to showing the public what projects aerospace students are involved in at the University of Colorado. The short presentation was well received by the students and was followed with a question and answer session. As was predicted, the demonstration model proved to be the most useful aspect of the presentation, generating interest in all of the students. In addition, the students were given an opportunity to ask questions about college life in general.

Project LaMaR will also be presented at the International Space Development Conference being held May 24-28, 2001 in Albuquerque, NM. This is the National Space Society's (NSS) annual conference and is being co-sponsored by AIAA. See the following site for more information: http://www.isdc2001.org/.

8.0 Acknowledgements

9.0 References

1. Hoffman, S. J. and D. L. Kaplan 1997. Human Exploration of Mars: The Reference Mission of the NASA Mars Exploration Study Team. (URL: http://exploration.jsc.nasa.gov/marsref/contents.html)
2. Landis, G., M. Stavnes, S. Oleson and J. Bozek 1992. Space Transfer With Ground-Based Laser/Electric Propulsion. *AIAA-92-2313.*
3. Landis, G. 1993. Photovoltaic Receivers for Laser Beamed Power in Space. *Journal of Propulsion and Power*, Vol. 9 No. 1, 105-112.
4. Landis, G. 1992. Laser Beamed Power: Satellite Demonstration Applications. *IAF-92-0600.*
5. Landis, G. 1998. Solar Cell Selection for Mars. *Proceedings of the 2nd World Conference on Photovoltaic Energy Conversion*, Vol. III, 3695-3698.
   (URL: http://powerweb.lerc.nasa.gov/pvsee/publications/wcpec2/cells4mars.html)
6. Landis, G. 1998. Mars Dust Removal Technology. *AIAA Journal of Propulsion and Power*, Vol. 14 No. 1, 126-128.
7. courtesy of Jennifer Granada at Spectrolab
8. Enright, J. and Carroll, K. A., Laser power beaming for Lunar Polar Exploration, SPS '97 Conference, Montreal Canada, 1997
9. Potter, S., Willenberg, H., Henley, M., and Kent, S. Science Mission Opportunities Using Space Solar Power Technology. IAF-99-r.3.07, 50th International Astronautical Congress, 1999, The Netherlands

$S9/CP/IN/66$

A Basic Utility Rover for Research Operations

University of Maryland
College Park, MD

Student Editors:
    Corinne Ségalas, Rhiannon Peasco, David Hart, Paul Frontera

Student Authors:
    Jean-Pierre Chaumon, Michael Flanigan, Paul Frontera, David Hart, Jamie Lennon, Erica Lieb,
    Rhiannon Peasco, Yannick Penneçot, Nicolas Perriault, Juan Raymond-Santamaria, Corinne
    Ségalas, Gregory Shoup, Melissa Turner

Faculty Advisor:
    Dr. David Akin
    Associate Professor and Director, Space Systems Laboratory

Abstract

Technology is advancing such that, in the not-too-distant future, Mars will be opened to human exploration. A robotic field assistant would improve an astronaut's ability to conduct surface exploration. This paper describes the Basic Utility Rover for Research Operations (BURRO), a 625 kg rover to provide such aid. The rover was designed to meet specified Given requirements while operating in the known conditions of the Martian environment. The system is able to: (1) drive over a 0.5 m obstacle; (2) carry a 200 kg astronaut, robot arms weighing 150 kg, and 100 kg of mission-specific payload; (3) carry a second astronaut in case of emergency; (4) maintain a 5 km/h speed through the duration of an eight hour traverse; (5) sustain a 10 km/h sprint for one hour; (6) be directly driven by an on-board astronaut, teleoperated, or operated in semi-autonomous or fully autonomous modes; (7) traverse up or down a 30° slope or perpendicular to a 20° slope; and (8) park parallel to a 45° slope or perpendicular to a 30° slope.

Introduction

In the next few decades, NASA and its partners will most certainly land humans on Mars for an extended exploratory mission. As the Apollo Lunar Roving Vehicle showed, it is helpful to have a transportation vehicle to assist astronauts in scientific exploration [1]. A robotic field assistant could carry instruments and samples, perform dexterous tasks with its robotic arms, and even transport the astronauts themselves, minimizing fatigue. In addition, a rover could autonomously take samples at previously identified sites while the astronaut continued to explore, enhancing the productivity of the extravehicular activity (EVA). Furthermore, the rover can accurately photograph and catalog the sample site, increasing the accuracy of the information being harvested. Different levels of autonomy and remote command allow the rover to explore areas uncharted or unsafe for humans. Our goal was to design a vehicle that could accompany astronauts to Mars and help them as much as possible. BURRO is shown in Figure 1.

Figure 1: BURRO

Design Approach

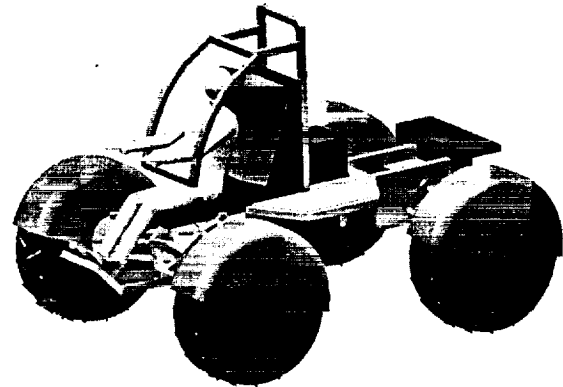### Given Requirements

The design for BURRO meets the following requirements:

- Carry one 200 kg astronaut, plus 100 kg of mission specific payload and two dexterous robotic arms weighing a total of 150 kg
- Accommodate a second EVA crewperson in case of emergency
- Be driven at 5 km/h for 8 hours
- Be driven at 10 km/h for 1 hour
- Climb and descend a 30° slope and drive across a 20° slope

- Remain statically stable while parallel to a 45° slope or perpendicular to a 30° slope
- Drive over a 0.5 m obstacle
- Be driven directly by an on-board astronaut, teleoperated, or operated in semi-autonomous or fully autonomous modes.

Derived Requirements

The specifications outlined above led to the development of further assumptions:

- All missions are performed by a pair of rover/astronaut teams
- All samples must fit inside the allotted science trays
- The base provides maintenance and storage facilities for the rover
- The batteries are rechargeable by the base power supply
- Both astronauts can successfully return to base in the case of one rover or one astronaut becoming incapacitated.

Martian Environment

Known characteristics of the Martian environment also drove our design, and are presented here [2]:

- Highly abrasive dust requires all moving parts to be sealed
- Temperatures ranging from -80°C to 0°C require systems to be thermally insulated
- Extremely low pressure requires astronaut life support systems
- Nighttime carbon dioxide frost requires electronics to be sealed and heated
- The terrain ranges from hard rock to drift material
- The gravitational field strength of Mars is 3/8 that of Earth.

Mass Budget

The total mass of a fully-loaded system is just under 1000kg (Table 1).

Table 1: Mass budget for BURRO

ELEMENT	MASS
Science Payload and Tools	30.2 kg
Wheels + Drivetrain (each)	45.0 kg
Frame (including suspension)	155.0 kg
Seat	24.0 kg
Robotic Arms	150.0 kg
Power and Thermal Control	140.4 kg
Scientific Payload (fully loaded)	100.0 kg
Astronaut + PLSS	200.0 kg
Total	979.6 kg

Design Scenarios

The design requirements and derived assumptions led to the development of a nominal mission and an emergency scenario.

Reference Mission

The reference mission describes nominal astronaut-rover operations. An 8-hour mission consisting of one-hour legs, each composed of forty minutes of travel followed by twenty minutes of scientific data collection. Three of these legs are up a 30° inclination, three are down the same slope, and two are across flat ground.

Emergency Scenario

The emergency mission is contrived to highlight the Given requirements, and is thus a worst-case scenario. This mission is proceeding normally, with the rover traveling for 4 hours at 5 km/h without science stops. At 20 km out, it turns around and starts back at the same speed. Having completed two more hours of travel, an emergency arises that requires a sprint back to base at 10 km/h.

Structure

Three things drove the structural design of BURRO. First, the rover had to fulfill all Given requirements. Second, the design should maximize functionality. Finally, the rover should be reliable and durable since spare parts will not be readily available. Vehicle layout focused on situating tools and instruments within the workspace of a space-suited astronaut. The astronaut can easily board the rover and ride in comfort. In addition, the astronaut's seat is located at the front of the vehicle to provide maximum forward visibility. The deck space is all within arm's length and provides substantial storage volume and work area. The robotic arms are attached to the rear of the vehicle to provide a large work envelope.

A square footprint was selected to provide vehicle stability in rough terrain. All large rover systems are located low in the body to enhance this stability. A 2.0 m length was selected to provide adequate clearance between the wheels and ensure sufficient structural volume for rover systems and payload. The main body section is tapered to allow for a 45° steering arc for each wheel. This feature, in conjunction with four wheel steering, adds the ability to turn in place, avoiding an obstacle directly in front of the rover. The main body section is 2 m in length and 1.6 m wide at mid-body, but tapers to 1.1 m between the wheels to the fore and aft.

Structural material selection was made in keeping with three priorities. First, the rover must be able to withstand a worst-case impact (0.5 m obstacle at 10 km/h) and maintain structural integrity. Second, the frame must be able to withstand continuous bending and vibrational loadings while in motion. Finally, the rover must be relatively light and easy to transport. Hollow 5 cm 7075 Aluminum was selected for its properties of high strength to weight ratio, adequate fatigue life, availability, and ease of manufacturing. Encasing the aluminum frame will be paneled shell built of a composite material.

Suspension

The objective of the suspension is to maintain continuous contact between the wheels and the ground. This will provide efficient power transfer from the drive system and a stable ride. A trade study was conducted between the six-wheel Rocker-Bogey style of suspension and a four-wheel independent suspension system. Although the former has been used on recent Martian rovers, it is not readily adaptable to our larger, faster-moving vehicle. Although the Rocker-Bogey system has proven its ability to clear obstacles in excess of twice the diameter of the wheel, this capability has only been proven in quasi-static conditions. In contrast, a properly designed four-wheel independent suspension demonstrates good dynamic stability. In addition, the six wheels of the Rocker-Bogey suspension system add mass and complexity to the drive and control systems. As a result, a four-wheel independent suspension is implemented. Since the center of gravity has been located low on the vehicle, we are able to use a 1.1 m wheel diameter to clear the specified 0.5 m obstacle at design speed, as BURRO is shown doing in Figure 2.

The suspension damping system is tunable to provide an optimal ride in all terrain and loading conditions. This is accomplished through utilization of multiple sensors by the control system to determine the required damping coefficient and accordingly adjust the damping with a magneto-rheological fluid [3]. The suspension has 50 cm of total vertical deflection.

Wheels

As discussed above, the wheels have a 1.1 m diameter. The wheel width of 0.35 m was selected to accommodate the motor and geartrain internally while limiting wheel sinkage.
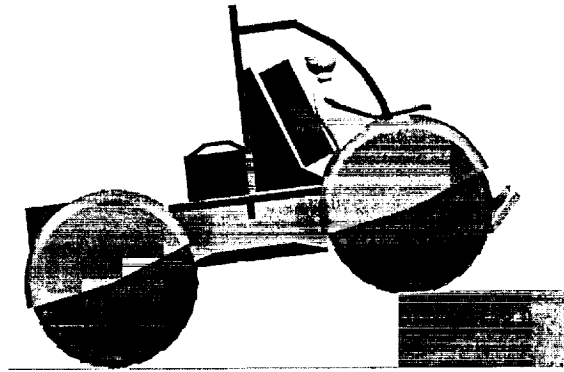
Figure 2: Rover navigating 0.5 m obstacle

The design incorporates moderate compliance to achieve a number of performance goals. Compliance in the wheels aids traction and handling on hard surfaces and adds a small amount of additional suspension. The criteria for material selection were an extended fatigue life and a high strength to weight ratio. Woven IM7 carbon fiber was chosen for its small fiber diameter and high-density wrap, which mitigates the common failure modes of composite structures, namely delamination and matrix cracking. This material is resistant to the extreme temperature changes present in the Martial environment. The wheel tread is wrapped with Aramid fiber to increase traction and protect the wheels from puncture.

The basic shape of the wheel is a toroid, as can be seen in Figure 3, supported by an internal structure that is tapered to allow a 45° turning angle on the wheels.
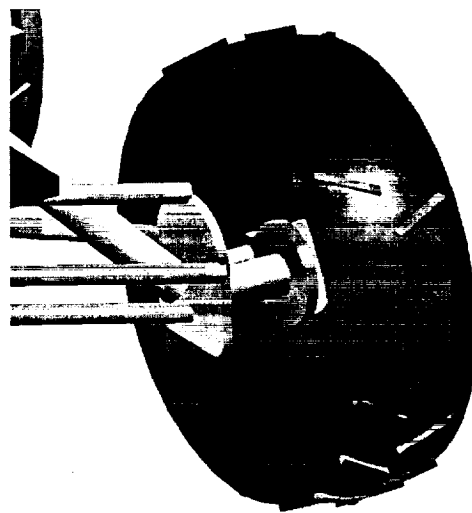
Figure 3: Wheel and suspension detail

Steering

BURRO employs full Ackermann steering to reduce dragging of the inside wheel, which helps maintain traction in turns. Full Ackermann steering is accbmplished through independent actuation of each wheel. To minimize the torque required for steering, the kingpin axis is located at the center of the wheel. A linear actuator secured to the suspension drives a 30 cm steering arm to provide the necessary torque. This can be seen in Figure 4.
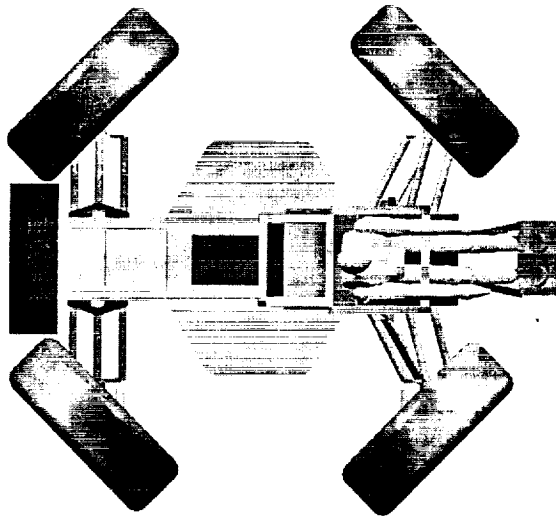
Figure 4: Four-wheel independent suspension

Brakes

We will use a regenerative braking system as our main source of stopping. The motors are run in reverse, which has the effect of recharging the batteries. We will also utilize an auxiliary parking brake, similar in design to that on a car, when the rover is stopped on a slope or in case of emergency. Braking software will calculate the force required to stop the motors based on the relationship between the current speed of the motor and the weight load on the rover.

Drivetrain Specification

The operating environment and the specifics of wheel geometry and loading drive the motor and drivetrain selection. For the purposes of this analysis, the operating environment is described by soil properties and terrain inclination. The general geometry of the wheel as outlined above will be used in this analysis. Finally, the wheel loading is influenced by the weight of the rover and varies as weight is transferred between wheels due to suspension action.

The soil on Mars varies from rock to a drift material similar to fine sand. The only broad category of soil unlikely to be encountered by the rover is mud. Thus strong parallels exist between soil types to be encountered on Mars and soil types that can be found on Earth. There are no inherent differences in the soil types between Earth and Mars that would preclude the application of standard soil description techniques to the Martian environment. In fact, many of the experimentally developed relationships used to describe wheel and soil interactions are most successful in predicting performance in dry soil types.

Empirical testing conducted by Bekker found the relationship for rolling resistance shown in equation (1).

$$R = \frac{0.87}{(b \times k)^{\frac{1}{2}}} \times \frac{W^{\frac{3}{2}}}{D^{\frac{3}{4}}}, \qquad (1)$$

where R is the rolling resistance in pounds-force, b is the wheel width in inches, k is the soil cohesion coefficient in pounds per square inch, W is the wheel loading in pounds-force, and D is the wheel diameter in inches [4].

Fortunately, the Viking probes performed the necessary tests to determine soil coefficients for the Martian environment. The soil types sampled by the Viking probes are divided into three basic types: drift, blocky, and rock. As expected, operation in drift produces the highest rolling resistance, since the soil cohesion is minimal.

The remaining variable for the rolling resistance equation is the wheel loading. Because the rover does always operate on level ground, the wheel loading is not limited to one quarter of the rover weight. In extreme obstacle clearance situations, a single wheel could support the majority of the vehicle weight. The worst-case scenario occurs when the rover attempts to navigate a large obstacle in loose soil. Combinations of wheel loading conditions and soil types were examined to produce a range of force requirements at different operating points.

One final characteristic of any terrain is inclination. A design requirement for the rover is the ability to traverse a 30° slope. Simple geometry dictates that, in the absence of rolling resistance, the wheels must be capable of producing a combined force equal to half the weight of the rover to fulfill this requirement. The total force required is the sum of the force required to lift the vehicle against the force of gravity and the force required to overcome rolling resistance.

Before specifying a drivetrain, the forces imparted by the wheels must be converted to torques. The required torque is the force required multiplied by the radius of the wheel. There are some insights to be gained from this simple relationship. The rolling resistance equation indicates that the required force application is reduced as the diameter is increased. Unfortunately, the torque required increases linearly with the radius of the wheel. The linear increase in the torque requirement outpaces the benefits seen due to the reduced rolling resistance. Since the force required for slope climbing is independent of soil conditions, the torque requirement will further increase in proportion to wheel diameter. The increase in required torque is offset by a reduced speed requirement for the wheel. However, since electric motors are inherently high speed, low torque devices, the reduced speed requirement is not a beneficial tradeoff [4].

It is important to carefully analyze the applicability of empirical formulas before drawing general conclusions. Taking Bekker's equation as a complete model of rolling resistance would lead to wheel designs with extremely small diameters and extremely wide treads. This would minimize both the rolling resistance and the required torque. However, Bekker's equation is only applicable in relatively low sinkage situations. Bekker characterized another effect, known as bulldozing resistance, which becomes dominant when the wheel sinks to a significant percentage of the diameter of the wheel. So, while the large wheel diameter is primarily dictated by the requirement to clear 0.5 m obstacles, even if that requirement were relaxed, the optimal wheel diameter would be determined by both the standard rolling resistance and the bulldozing resistance [4].

Motor and Drivetrain Specification

A brushless direct current motor coupled to a planetary geartrain represents the final design decision for the independent actuation of the wheels. This decision was reached after careful consideration of the attributes of both elements.

The brushless motor removes the need for physical commutation of the windings through brushes. Instead, the windings are incorporated into the stator and the motor is commutated electronically. Brushes

traditionally represent a likely failure mode for the motor. In addition to simply wearing out, the erosion of the brushes can cause conductive dust to foul other components of the motor. The brushless motor removes this failure mode and provides the extra benefit of easier thermal control. Since the windings are in the stator, the heat generated by the electrical losses can be removed through heat sinks connected directly to the stator. In contrast, the heat generated in the windings of the rotor can only be removed through radiation directly from the windings and conduction through the bearings and brushes.

Gearing is required in the design to reduce the size and weight of the motor. As stated above, motors are inherently high speed, low torque devices. Gearing converts the motor mechanical power to a lower speed at a higher torque. A larger gear reduction results in a smaller motor size. However, large gear ratios are difficult to accommodate in the limited space of the wheel. The planetary gear design is capable of fairly large gear reduction within a small package. The harmonic gear design represents another option that obtains similar gear reduction for even less weight and volume. Unfortunately, harmonic gears require tighter tolerances and generally wear out faster than planetary gears. The robustness of the planetary gear design makes it an attractive option for the rover drivetrain.

A motor and a planetary gear were sized for the rover drivetrain based on the required torque and speed from the cases examined above. The final design incorporates a commercial off-the-shelf motor and a two stage planetary gear based on manufacturer specifications. The specific design of the planetary gear is not dictated here but requirements include output torque (500 Nm), input speed (3500 rpm), efficiency (85%), and gear reduction (36:1). Since an actual motor is specified for the design, it is possible to show the performance envelope of the rover based on the torque curve of the motor. The curve in Figure 5 represents the maximum continuous torque output of the motor as a function of the motor angular velocity. Also represented on the plot are a number of important operating points for the rover. These include both the design requirements as well as interesting values such as the top speed on a hard surface and the maximum slope that can be traversed in drift.
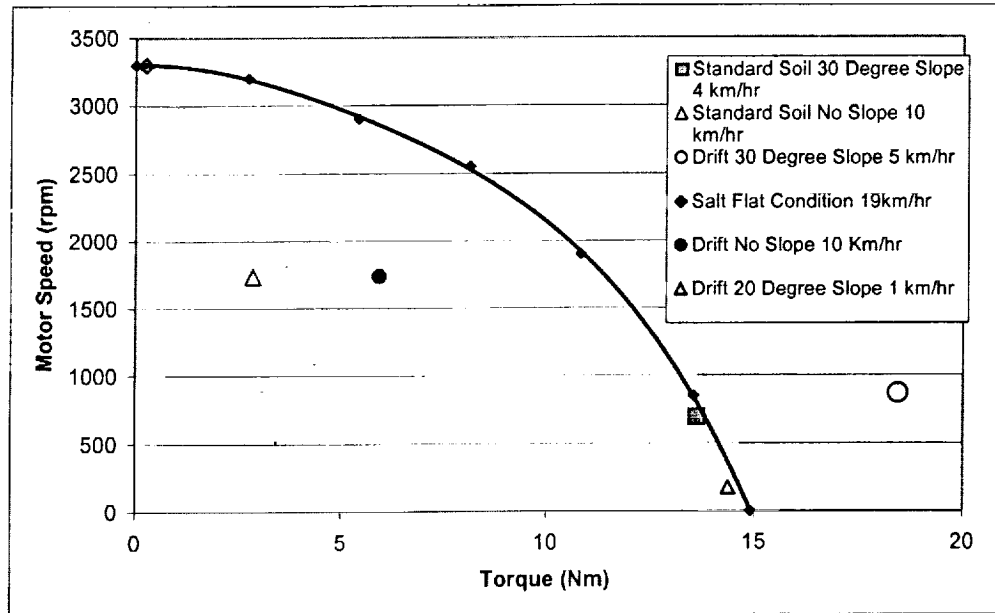
Figure 5: Motor operating curve

Figure 5 shows that the rover can easily handle flat ground situations. In fact, over flat terrain, the rover exceeds the speed requirement of 10 km/h. However, when the rover encounters a slope, the performance margin quickly erodes. The torque requirements rise dramatically due to both the requirements to lift a significant percentage of the rover weight as well as the effect of the suspension as weight is transferred to the rear wheels. This analysis indicates that the rover is barely capable of traversing a 30° slope on the blocky Martian soil but is limited to crawling up a 20° slope in drift. The limits shown in Figure 5 indicate that the drivetrain would benefit from a higher gear reduction, which would reduce the maximum speed while increasing the maximum torque capability of the system. However, planetary gear reductions in excess of 36:1 may require a special design.

Batteries and Electronics

Space-rated, lithium-ion batteries from Eagle-Pitcher were chosen to power BURRO as an example of commercially available battery technology. The battery dimensions are 16.99 cm length by 9.22 cm width by 21.92 cm height. Each battery weighs 8.89 kg and is capable of providing 170 Watt hours per kilogram of energy [5]. Several scenarios were examined to determine the required battery mass, with results given in Table 2;

1. Worst-Case: An 8-hour traverse at 4 km/h through standard soil; the first half of the trip is down a 30° slope, and the second half is back up the slope to base.

2. Given Speed: Maintain a speed of 5 km/h for a full 8-hour traverse across flat, drift-covered terrain.

3. Given Sprint: Maintain a speed of 10 km/h for a 1-hour sprint across flat, drift-covered terrain.

4. Reference Mission: The 8-hour mission previously described, in which the uphill traverses climb a 30° slope at 4 km/h through standard soil, the downhill traversals descend a 30° slope at 6 km/h through standard soil, and the flat legs are 5 km/h through terrain covered by drift material.

5. Emergency Scenario: This is the worst-case scenario outlined earlier in this paper.

Table 2: Energy Consumption for Different Scenarios

Scenario	Energy (overcome resistance due to soil compression) [4]	Energy (overcome effects of gravity)	Energy (power the electronics)	Total Energy (after 30% loss due to mechanical transmission)	Total Battery Mass Necessary	Total Number of Batteries Necessary
Worst-Case	1.14E+07 J	3.72E+07 J	1.44E+07 J	9.00E+07 J	147 kg	17
Given Speed	1.14E+07 J	0 J	1.44E+07 J	3.69E+07 J	60 kg	7
Given Sprint	3.56E+06 J	0 J	1.80E+06 J	7.66E+06 J	13 kg	2
Reference Mission	9.50E+06 J	1.49E+07 J	1.44E+07 J	5.54E+07 J	91 kg	11
Emergency Scenario	2.55E+07 J	0 J	1.26E+07 J	5.44E+07 J	89 kg	10

The worst-case scenario would suggest that this rover requires approximately 150 kg of batteries. However, this scenario is highly improbable. A more likely yet still conservative scenario is the reference mission, as all the uphill traverses involve a worst-case 30° slope and all flat travel is through drift material. After including a 30% safety margin to the total battery mass necessary, we find that loading the rover with fifteen batteries, for a total weight of 135 kg, will provide enough battery power for all likely missions. Figure 6 gives a graphical representation of the energy drained from the batteries over the duration of the reference mission.

The batteries are only operable between -5°C and 30°C. This motivated the design of a warm battery box (WBB), similar to the one aboard Sojourner, to keep the batteries warm in the extreme Martian temperatures [5]. This 71 cm long, 67 cm wide, and 52 cm high box will enclose the fifteen batteries

arranged in a five-by-three-by-one array. The heat from actively-controlled, resistive heating strips will be contained by 10 cm of Silica Aerogel plus carbon black insulation. The heating strips can be turned off during the day when the ambient temperature is relatively warm, allowing heat stored inside to dissipate slowly.

The electronic components also need to be in a sealed box to protect them from the harsh Martian environment. It is assumed that the electronics will have an operating temperature range of -40°C and 40°C, similar to that of Sojourner. In order to keep the electronics warm despite the extreme Martian temperatures, a 20 cm by 30 cm by 40 cm warm electronics box has been proposed, which will be insulated with 5 cm of the same Silica Aerogel as the WBB and also contain actively-controlled resistive heating units [6].
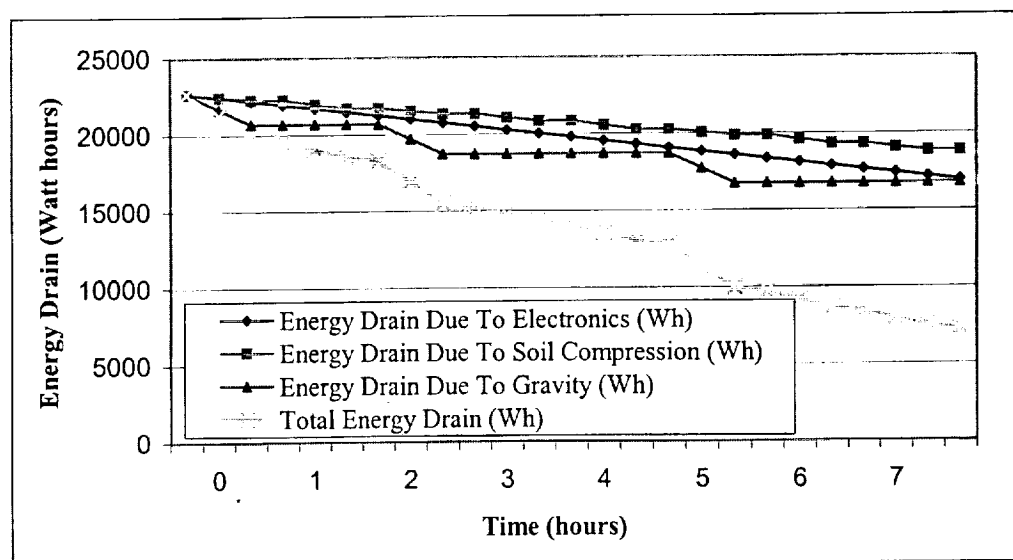

Figure 6: Energy drain from batteries through reference mission

Vehicle Control

The controls input system provides the astronaut with a comfortable and reliable way to control the rover and associated systems. The governing concept for the control input systems is a "Drive-by-Wire" design. This concept is utilized to allow flexibility in the design, thereby supporting multiple methods of rover control. This will provide enhanced reliability and usability. Astronaut controlled rover missions can be separated into three command environments: spacesuit-based control, manual operations from the rover, and teleoperations from base.

Voice Command System

The astronaut will utilize spacesuit-based control when the rover is acting as a field assistant. In this mode, the astronaut is assumed to be primarily involved in surveying the surface for geological purposes. The astronaut will be mobile and involved in tasks that require the use of both hands as he surveys different areas. Voice activation technology will be utilized. The majority of control inputs to the rover will consist of pre-defined tasks such as moving to the next marked area or conducting sampling and field documentation operations. An automated pilot feature would also be appropriate in this scenario to minimize required control input.

Voice activation systems are non-intrusive control input systems. This prevents interruption of tasks that require the use of the hands or visual attention. This input technology is very suitable for the astronaut who requires assistance from the rover while he is mobile on the field performing geological research. The system will efficiently recognize and execute voice commands spoken by the astronaut. A voice identification system is more appropriate than voice verification system, since there exists no concern for strict verification of the user's identity to control access. Voice verification would also introduce problems of false rejection of commands because it did not match the specific range for parameters such as pitch and frequency of speech stored in the user's profile. Voice identification systems only attempt to identify the spoken command and provide a best match to stored command profiles [7].

Voice activation systems may be either text-dependent or text-independent. Text-independent systems will recognize unexpected words and then use complicated algorithms to determine their meaning. These systems require significantly more training time and have lower word recognition rates than text-dependent systems. Since unexpected commands are unlikely, it is more robust to implement text-dependent command profiles. These are lists of commands that the rover is programmed to recognize and the user trained to use. In addition to text-dependency, voice activation systems can be designed with whole-word models, where a match must be made for the entire word, or sub-word models, where the system can recognize part of the word and interpret the remainder of the command. In this design, whole-word models are used to minimize false interpretation [8]. Errors can be further reduced by selecting command parameters with minimal similarities and by creating robust command profiles through system and user training [9]. The system requires a microphone for input and will utilize the one located inside the helmet for audio communication. This is the preferred location as several studies have shown that close-talking microphones are optimal for speech recognition. A second microphone will be used for noise cancellation that will reduce error due to noise interference. The expected word recognition rate for this system is 99% based on current technology [10].

The astronaut will address commands to be executed either by the rover computer or at a portable computer integrated in the Primary Life Support System (PLSS). Commands addressed to the rover include all steering commands, lights, cameras, robotic arms and rover computer system. Commands addressed to the spacesuit portable computer include control of display information, PLSS status, rover assignment, etc. The command structure will be "Receiving Computer + Operation + Directive-1 + Directive-2."

Examples to Rover
"Rover-1...Easy...Right...270"
or
"Rover-1...Stop"

Examples to Spacesuit-Based Computer
"Computer...Display...Nav"
or
"Computer...Helmet...Light...Off"

Manual Command System

At times, the astronaut may also desire fine control of the rover. Redundancy in case of problems with the voice control system is also desirable. This can be achieved manually from onboard the rover or from base. In these situations, the astronaut can dedicate the use of his hands to controlling the rover. Hence, the integration of a manual hand controller or control pad, both very well developed and reliable control input technologies.

The spacesuit control pad serves as a backup to voice control when the astronaut is away from the rover. The arm pad also permits fine control of the rover and robotic arms when the astronaut is dismounted, as extensive fine control is tedious via voice input. The layout of the input buttons and switches will be designed to meet General Design Requirements Document (GDRD) specifications. The arm pad provides controls operation of:

- Lights and Cameras (On/Off/Positioning)
- Robotic arms (On/Off/Positioning)
- Stop all rover motion (Safety)
- Helmet-mounted display and arm liquid crystal display (LCD) configurations
- Communications/"SOS" message

A hand controller is located on the right armrest of the rover. It is similar in design to that used to control the lunar rover, utilizing a four-direction input device shown in Figure 7. The astronaut will push the hand controller forward to accelerate; pull the hand-controller towards his body to brake; or rotate hand controller left or right to turn in those directions. The center position is an idle mode. Using a switch on the rover control panel, the astronaut will select either the forward or reverse direction. The hand controller is the primary control input while the astronaut is onboard the rover. It provides quick response to steering commands and is thus preferable for navigating around obstacles. For long traverses an autopilot function will be used to minimize required astronaut intervention.
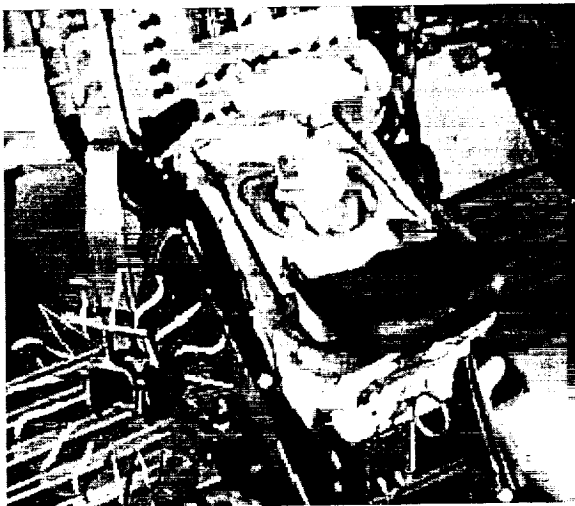
Figure 7: Hand controller [11]

A control panel is located on the left armrest of the rover to compliment the hand controller. The control panel acts as a backup to voice commanding and provides speed regulation and emergency stop

functions. The rover control panel layout will also be designed to meet GDRD requirements. The functions available from the control panel include the same operations as are available from the arm pad, plus a display of speed regulation and rover direction.

Rover Display System

The rover display system tries to complement an astronaut conducting surface exploration. In this role, the astronaut will benefit substantially from having a large quantity of information available while both on and off the rover. However, the information must not obstruct the view of the environment. With these requirements in mind, a display system incorporated into the helmet of the astronaut's space suit has been selected as the most suitable solution for the primary display. An LCD integrated within the spacesuit arm will back up the above display system.

The best design for the helmet mounted display would have a high resolution system visible in a wide range of lighting conditions that has a data rate capable of supporting video broadcast. A traditional projection style of display is selected to meet the rover display requirements. Military rotorcraft pilots currently use these systems to display information during flight. These designs could be adapted to meet the requirements of a surface exploration mission. The helmet-mounted display will consist of a miniaturized projection device mounted in the spacesuit helmet that will display information on a transparent screen mounted inside the spacesuit helmet. This internal screen design is selected to improve resolution of the display through optimal material selection with regards to optical properties and strength requirements. In addition, the display system will utilize the PLSS computer to control image display and communication with the rover's systems. Voice commands allow the astronaut to select which information is displayed. If the voice command system malfunctions, the control pad in the arm of the spacesuit will allow the astronaut to make these selections manually.

The rover periodically broadcasts its status and navigation information to the astronaut's space suit. This information allows control of the rover via the voice activated command system or the spacesuit arm integrated control pad. Voice activated commands are displayed to permit verification of the command by the astronaut prior to execution. Navigation information and rover status will enhance astronaut situational awareness while conducting dismounted

field operations. In addition, PLSS status can be monitored via the helmet-mounted display.

The astronaut is able to view images obtained by cameras mounted on the rover. This includes both telescopic and microscopic images obtained in support of the scientific mission. This feature enhances the astronaut's ability to conduct geological exploration. The astronaut also would have access to other information, including checklists, procedures and reference information that would enhance the performance of field exploration.

The spacesuit arm will contain an integrated LCD device that is able to display alphanumeric information. This device will serve as a backup to the helmet-mounted display during periods when the astronaut is not aboard the rover. While the astronaut is riding the rover, a rover mounted LCD will serve the same function. This technology is very rugged and requires minimal electrical power. While these displays do not have the same functionality as the helmet-mounted display, the mission can still be performed in the event of a malfunction.

Navigation and Obstacle Avoidance

The rover must be capable of two navigational modes. The first mode is "human in the loop," which includes the astronaut riding on the rover, the rover following the astronaut, and either local or remote teleoperation. The second is an autonomous mode, in which the rover will drive itself to a location (probably previously marked by an astronaut as being of interest), perform some work there, and then return to base. These two modes call for different navigational approaches.

When a human is controlling the rover, either directly or by setting a path for it to follow, he is already performing the primary navigation for the vehicle. There is no strong need for computationally complex systems to duplicate the astronaut's excellent obstacle avoidance, navigation, and path planning abilities. There is, however, the chance that the astronaut may overestimate the rover's abilities and try to drive it in dangerous ways. For instance, the astronaut may attempt to drive up an incline that would capsize the rover. To avoid damage, simple reactive sensors like tilt switches and bump sensors can be used to alert the astronaut that there is a problem. Several sets of such small, compact sensors can be used to specify risky or "yellow" rover configurations and dangerous or "red" configurations. In a "yellow" situation, the rover

could function safely, nearing its stability limits. A "red" situation represents reaching these limits, within a specified safety margin. When a sensor goes to "red," the rover will stop and alert the astronaut, who must carefully remove the rover from that situation.

When the rover is operating autonomously, it may need to travel more slowly. It will need to process its stereo video data of the area to determine obstacles, which is computationally expensive. Stereovision can be used to determine the height and range of obstacles in the area. Once the obstacles are identified, artificial potential field techniques can be used to avoid them. Artificial potential field techniques identify obstacles and assign "potential fields" which "repel" the mobile robot. The closer the robot gets to the field, the stronger the "repulsive force" becomes. This pushes the robot away from dangers and towards a safer path. The autonomous path planner will use this information to determine the path. It will interface with the other rover systems as if it were a human user. Its actuation commands will be packaged like those sent by the astronaut. This way, any predicted user, human or not, can use the same software to actuate the rover's controls.

Passive Astronaut Following

The astronaut may wish to explore a worksite on foot, but keep the rover nearby to hold tools and accept samples. In this case, it is desirable to have the rover semi-autonomously follow the astronaut. The astronaut is constrained to pick a path the rover can follow in this case. A passive color vision-based astronaut tracking system is selected since it utilizes the cameras mounted onboard the rover for the autonomous mode. Moreover, there are no transceivers that could fail. Although color-based systems are sensitive to changes in lighting conditions, this can be mitigated to some extent by the methods used to train the tracking software. Current research intends to quantify how robust the tracking system is to differences in lighting.

In the proposed system, the astronaut will wear a colored target. The vision software can be trained to recognize this color and extract "blobs" of it from a frame of video. This "blob tracking" is a much faster process than other vision techniques such as object recognition. The size and orientation of the color blob translates to the range, heading, and orientation of the astronaut. If the target is a circle, for instance, a nearby, front-facing astronaut is identified by a

large colored circle. The area of the circle corresponds to the distance from the rover to the astronaut. If the astronaut is further away and turned slightly, the target is smaller and more elliptical [12]. The rover can, in this manner, track the astronaut and record his path relative to the rover. This can be stored in some short-term memory, allowing the rover to follow the astronaut's footsteps

Communications

The communications subsystem is intended to provide reliable communications between the astronaut, the rover, and the base during planetary explorations. Two different communication links are required to transmit video, voice, and data in these missions. The first would accommodate local communications, which is defined as astronaut-to-astronaut, astronaut to rover, and astronaut to base when astronaut is less then 10 km away from the base. For this link, the driving requirements are the bandwidth and data rate, rather than the distance between receiver and transmitter. The second is for distant communications when the rover is more than 10 km away from base, or in the case of an obstacle higher than the 3 m high antenna on the rover. Video, voice, and data will be compressed in the same data stream to enhance efficiency and minimize electromagnetic interference [13].

Communication Links

Astronaut to Astronaut
Primarily, this link will allow voice interactions between the astronauts during the conduct of EVA. Astronauts will be able to communicate with each other without being in the vicinity of a rover. It will function over short distances. This link will be supported by transceiver and antenna contained within the astronaut's spacesuit.

Astronaut to Rover
This link supports video, voice, and data exchange between the astronaut and the rover over short distances. The astronaut will send voice commands to control rover operations and functions. Mission video is transmitted to the rover from the spacesuit helmet-mounted camera. In addition, the astronaut's physiological information will be transmitted to the rover. The rover status and navigation information is transmitted to the astronaut to enable rover control when the astronaut is dismounted. Video from rover-mounted cameras is also sent to the astronaut to support geological exploration.

Astronauts to Base
This link utilizes either the local or distant communication antennas depending upon distance from base. If far from base, the rover functions as a relay station between the astronaut and base by utilizing the distant antenna to retransmit astronaut communication. In addition, the rover will intercept voice communications between the astronauts for retransmission to the base, if desired.

Rover to Base
This link allows for transmission of video and data from the rover to the base in support of teleoperations, autonomous missions, and EVAs. The local or distant antennas will be utilized depending upon distance from base. Rover and astronaut status is periodically transmitted to base during the EVA to allow for monitoring while minimizing power consumption. Furthermore, all information can be transmitted continuously depending upon the mission profile.

Antenna
As mentioned above, the rover will have one antenna for local communications and a second for distant communications. The data rate of 8 megabits per second and the bandwidth of 12 megahertz are a compromise between the amount of data we want to transfer (video, voice, and data) and the power required to transmit it with an omni-directional antenna [14]. The main advantage of this type of antenna is that it does not need to continuously track the astronaut for communication, but it requires greater power, as it is a low-gain antenna. Quadrature phase shift keying modulation is used to minimize bandwidth, and thus power requirements [14, 15, 16]. For distant communications, a parabolic antenna was chosen to minimize the power requirements for transmission over long distances. When line of sight is compromised, this antenna overcomes the problem by rotating the dish to communicate with a satellite assumed to be orbiting about the planet.

Human Interfaces

The main objective of the human interface aspect of the rover design is to establish astronaut access to the rover for data collection and seating, and to improve the comfort for the astronaut while riding onboard. In the design, minimization of fatigue, the need for special training, and simplicity of design, use and maintenance were also emphasized. The study focused on a 25th to 75th percentile American male in a spacesuit.

Vehicle Access

The astronaut has access to the vehicle in four locations. Ingress to and egress from the vehicle is at the front of the rover, as the wheels restrict the area directly to the right or left of the seat. Access to tools and workspace is at mid-body, between the wheels, where an 80 cm envelope allows ample room for an astronaut wearing a spacesuit. The robotic arms and sample tray, which can carry up to 100 kg of samples, are located at the back of the vehicle. The astronaut should have minimal contact with the robotic arms, but can access the arms and vehicle from the rear if necessary.

In the case that one rover breaks, the astronaut riding that rover would stand in the workspace area located in the mid-body section of first rover and hold onto the overhead structure. If the astronaut were to be incapacitated, he/she would be put in his/her own rover, which would follow the functional rover back to base.

Storage Workspace

The storage bins located between the wheels provide space for the astronaut to store manually collected samples as well as access the data collection computer and microscope. The upper surfaces of the bins provide a workspace for cataloging samples and an interim location for samples and tools while working. The work envelope for the suited astronaut allows him to reach to the center of the vehicle, where the portable toolbox is located, making the entire workspace accessible.

Seat Design

The astronaut is seated at the front of the rover such that the footplate is forward of the main rover body, but aft of the front tires. This position provides the best visibility as well as providing a counterweight at the front of the vehicle for the weight of the robotic arm system at the rear. The seat structure conforms to the spacesuit and PLSS to provide lateral stability.

The relative positions and angles of the seat, footplate, and back were chosen based on the experimental findings of a Johnson Space Center test [17]. Four different suits were tested for comfort and ingress/egress mobility into a rover seat mock-up. Adjustments were made in the seat height, the distance between the footplate and the front of the seat, the angle of the seat back, and the relative position of the t-handle controller. Tests were conducted in 1-g and in Martian gravity simulation aboard the KC-135 aircraft. The results of this study demonstrate that there is a preferred range of seat settings that corresponds to all suits. This study also

revealed two key elements of the astronaut's sense of security and comfort, solid contact at the footplate and height. The distance between the footplate and the front of the seat must be short enough that the astronaut can provide a stabilizing force at his feet, yet large enough for ample space to stand in front of the seat. The resulting preferred range is 36 to 46 cm. The BURRO is designed with a 36 cm distance. In regards to seat height, lower seat heights from 32 to 47 cm were more conducive to easy ingress and egress as well as providing a feeling of greater security. The BURRO seat height is 35 cm from the deck of the footplate.

Good visibility is dependent on a third variable, seat back angle. Test results demonstrated a range in preferred angles from 60° to 110° measured from the horizontal. BURRO is shown to have an 80° seat back, but is adjustable within the stated range. Due to the seat height and orientation of the footplate relative to the seat, a pivot is incorporated such that the footplate may be rotated downward to provide a step. Once on the step, the astronaut backs up and is aided into the seat by rotating the footplate back up to the riding position.

Restraint System

The astronaut restraint system is designed for both safety and comfort. A pivoting shoulder harness is incorporated instead of a traditional lap belt. Apollo astronauts were dissatisfied with the lack of lateral restraint provided from the lap belt, as a shoulder harness will help to limit lateral slip. In addition, the lap portion of the restraint may be used to incorporate control interfaces and vehicle status displays. Pivot joints must be protected from dust to avoid degradation of the mechanisms.

Science Payload and Tools

The science payload is comprised of geological sampling tool, which are shown in Figure 8, cameras, and the robotic arms. The geological tools include:

- Wrench
- Rock hammer
- Scoop
- Magnifying Glass
- Power Drill
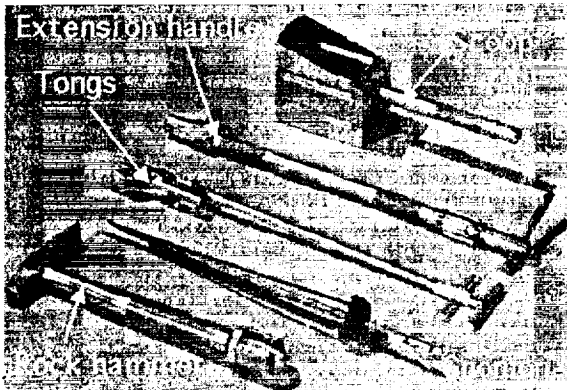- Robotic End-Effectors (scoop, gripper)
- Flag markers

Figure 8: Hand tools available to the astronauts [18]

The tools selected are easy to use and require little training or workload. They are located on shelves directly behind the astronaut's seat and in the portable toolbox. This toolbox can be removed from the deck of the rover so that the astronaut can conduct science activities away from the rover and return samples easily using a dedicated sample bag.

The rover also carries flags to mark sites of scientific interest or danger to the astronaut. The flags have a green background that contrasts with the Martian soil and have a shape code to indicate whether samples have to be collected (circle in the lower right), pictures taken (triangle in the upper left), both, or just warning of a hazardous area (large X), as shown in Figure 9.
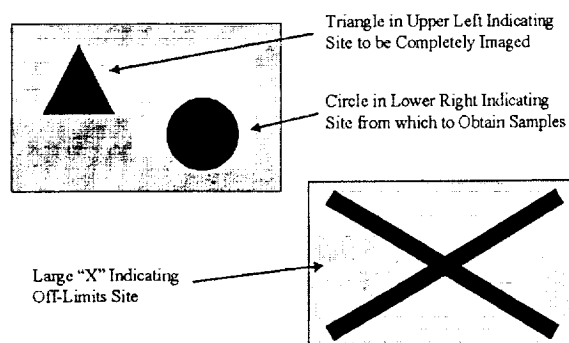
Figure 9: Flags marking sites

Surveying of the landscape is done with the panospheric camera, providing global knowledge of the Martian environment and vehicle position with respect to the surrounding area. However, during rover teleoperation, the operator utilizes the pan/tilt stereo camera to provide a close-up view of the terrain through which he is navigating.

Detailed science imaging is conducted using the infrared camera with 3 to 5 micrometer wavelengths, providing information on thermal activity. This camera also provides a wider spectrum of observations, enhancing the inspection of the landscape [19]. The telescoping zoom lens has better resolution than the stereo camera and provides detailed images of samples and the surrounding area before they are collected. The entire vision system is mounted on the overhead structure, which can be seen in the picture of BURRO in Figure 1.

The astronaut uses the microscope to examine rocks and soil that have been sampled manually. The zoom magnification capability is greater than that of a hand lens and provides a stable base upon which to observe objects and take measurements. Images are transmitted through a video link to the data collection computer and are projected on the computer screen. The data collection computer accepts video inputs from the microscope, telescoping zoom, infrared camera, and the robotic arm-mounted camera. The data collection computer and microscope are stored in the bins located at the rover mid-body, between the fore and aft wheels.

Conclusions

As detailed in this paper, BURRO will greatly enhance the efficiency of astronaut exploration and experimentation on Mars. Utilization of the rover mitigates astronaut fatigue since it carries scientific instruments and samples and performs dexterous tasks with its robotic arms, freeing the astronaut to walk longer and explore further. By employing a number of imaging tools, the rover allows more exact knowledge of in situ samples and mapping of the Martian terrain. BURRO increases the area about which astronauts can safely roam by providing an amplification of the communications relay between the explorer and base and ensuring the transport of an incapacitated astronaut. When NASA plans its first manned exploration of Mars, BURRO would significantly increase the knowledge gained from the experience.

Future Work

A number of design elements remain to be addressed. These include a preliminary cost analysis, detailed reliability analysis, and component level design. A preliminary reliability analysis was conducted using a fault tree method. This revealed that the rover/astronaut pair concept of operations is fundamentally sound with regards to minimizing risk.

However, a detailed reliability analysis should be conducted upon completion of the component level design.

The next logical step in the design process should include the construction of a test vehicle for research operations on Earth. The rover subsystems outlined in this paper could then be implemented and analyzed. This rover testbed would validate the design concept and provide an experimental basis for future enhancements.

Acknowledgements

This work was completed as part of a graduate-level design course in the spring of 2001 taught by Dr. David Akin, Associate Professor of Aerospace Engineering and Institute for Systems Research, and Director of the Space Systems Laboratory. Members of the design team include: Yannick Penneçot and Melissa Turner, Systems Integration; Jamie Lennon, Rhiannon Peasco, and Juan Raymond-Santamaria, Electrical Systems; Jean-Pierre Chamoun, Paul Frontera, Erica Lieb, and Corinne Ségalas, Human Interfaces; and Michael Flanigan, David Hart, Nicolas Perriault, and Gregory Shoup, Structures and Mechanisms.

We would like to thank Rob Ambrose and Chris Culbert from NASA/Johnson Space Center for their invaluable input to this project.

We would also like to thank Glen Henshaw and Gardell Gefke for their comments, edits, and commiseration.

Acronyms and Symbols

°	degrees
BURRO	Basic Utility Rover for Research Operations
C	Celsius
cm	centimeter
EVA	extravehicular activity
GDRD	general design requirements document
J	joule
kg	kilogram
km	kilometer
km/h	kilometer per hour
LCD	liquid crystal display
m	meter
mm	millimeters
N	Newton
NASA	National Aeronautics and Space Administration
Nm	Newton meter

PLSS	primary life support system
rpm	rotations per minute
WBB	warm battery box
Wh	Watt hour

References

[1] Wade, Marc. Apollo LRV, April 27, 2001. <http://www.friends-partners.org/mwade/craft/apololrv.htm>.

[2] Carr, Michael H. "Mars". The New Solar System, Fourth Edition. Ed. J. Kelly Beatty, Carolyn Collins Petersen, and Andrew Chaikin. Cambridge: Sky Publishing Corporation, 1999.

[3] Rheonetic Magnetic Fluids and Systems – Products: Magneto-Rheological Fluids. Lord Corporation. April 30, 2001. <http://www.mrfluid.com/fluid_begin.htm>.

[4] Bekker, M. G. Introduction to Terrain-Vehicle Systems. Ann Arbor: The University of Michigan Press, 1969.

[5] Lithium-Ion. Eagle-Pitcher Technologies, LLC. March 22, 2001. <http://www.tech.epcorp.com/pwrsubsys/li-ion.htm>.

[6] Questions and Answers for Mars Team Online: Thermal Control System. Mars Team Online. April 12, 2001. <http://quest.arc.nasa.gov/mars/ask/about-rover/Keeping_Rover_Warm.txt>.

[7] Schmandt, Christopher. Voice Communications With Computers. New York: Van Nostrand Reinhold, 1994.

[8] DeMori, Renato. Spoken Dialogues With Computers. San Diego: Academic Press, 1998.

[9] Klevens, R. and R. Rodman. Voice Recognition. Norwood: Artech House, Inc., 1997.

[10] Beugelsdijk, T. and P. Phelan. Controlling Robots With Spoken Commands. Los Alamos National Laboratory, 1997.

[11] NASM – Apollo to the Moon. National Air and Space Museum. April 12, 2001 <http://www.nasm.edu/galleries/attm/atmimages/99-15216-9.f.jpg>.

[12] Lennon, Jamie and Ella Atkins. "Color-Based Vision Tracking for an Astronaut EVA Assist

Vehicle." To appear in Proceedings of the International Conference of Environmental Engineers, Orlando, July, 2001.

[13] Berkelman, Peter. *Design of a Day/Night Lunar Rover.* Pittsburgh: Carnegie Mellon University, 1995.

[14] Freeman, Roger L. Telecommunication System Engineering: Third Edition. New York: John Wiley & Sons, Inc., 1989.

[15] Gibson, Jerry D. Principles of Digital and Analog Communications: Second Edition. New York: Macmillan Publishing Company, 1993.

[16] Dunlop, J. and D. G. Smith. Telecommunications Engineering. Workingham: Van Nostrand Reinhold (UK) Co., Ltd., 1984.

[17] Ross, Amy. *Lunar Rover Vehicle Mock-up Advanced Space Suit Ingress/Egress Test.* JSC 39922, CTSD-ADV-409, May 2, 2000.

[18] Alton, Judith H. Apollo Geology Tool Catalog. April 12, 2001. <http://www.hq.nasa.gov/office/pao/History/alsj/tools/judy26.jpg>.

[19] *Design of an Astronaut Assistant Rover for Martian Exploration.* Ed. Glen Henshaw and Debbie Theobald. SSL document 98-009, December 1998.

$\int_{\mathcal{J}} o / c^{p} / r \mathcal{N} / \mathcal{18}$

Clarke Station:
An Artificial Gravity Space Station at the Earth-Moon L1 Point

University of Maryland, College Park
Department of Aerospace Engineering Undergraduate Program

Matthew Ashmore, Daniel Barkmeyer, Laurie Daddino, Sarah Delorme, Dominic DePasquale, Joshua Ellithorpe, Jessica Garzon, Jacob Haddon, Emmie Helms, Raquel Jarabek, Jeffrey Jensen, Steve Keyton, Aurora Labador, Joshua Lyons, Bruce Macomber Jr., Aaron Nguyen, Larry O'Dell, Brian Ross, Cristin Sawin, Matthew Scully, Eric Simon, Kevin Stefanik, Daniel Sutermeister, Bruce Wang

Advisors: Dr. David Akin, Dr. Mary Bowden

Abstract

In order to perform deep space life sciences and artificial gravity research, a 315 metric ton space station has been designed for the L1 libration point between the Earth and the Moon. The station provides research facilities for a total of eight crew in two habitats connected to their center of rotation by 68 m trusses. A third mass is offset for stability. Solar arrays and docking facilities are contained on the axis perpendicular to rotation. A total of 320 m^2 of floor space at gravity levels from microgravity to 1.2g's are available for research and experimentation. Specific research capabilities include radiation measurement and testing, human physiological adaptation measurement, and deep space manned mission simulation.

Introduction

Space is a harsh and unforgiving environment. In addition to basic life support requirements, radiation exposure, cardiovascular deconditioning, muscle atrophy, and skeletal demineralization represent major hazards associated with human travel and habitation in deep space. All of these hazards require special attention and prevention for a successful mission to Mars or a long duration return to the Moon. Greater knowledge of human physical response to the deep space environment and reduced gravity is required to develop safe prevention methods.

An artificial gravity space station would provide a facility for exploring these issues. The primary purpose of the station will be to explore the ability for humans to live and work in artificial gravity in deep space across a wide range of gravity levels up to 1.2g. In preparation for a future mission to Mars, the station will also simulate a full-length Mars mission. The simulation will acquire valuable data about the body's adaptation to Mars gravity, and will allow astronauts to test technologies at Mars gravity. Artificial gravity also provides opportunities for life sciences and advanced technology research with application to Earth based needs.

Positioning this station at the Earth-Moon L1 point provides an ideal location for study of the deep space environment. A human presence at the L1 point, over 300,000 km from Earth, will require the closed loop life support systems and increased radiation protection common to any deep space mission. An artificial gravity station at the L1 point could also serve as a transportation node for Mars missions, providing storage, supply, and crew recuperation in artificial gravity.

In 1961, Arthur C. Clarke predicted the establishment of a space station at L1 in his book "A Fall of Moondust." Clarke's "2001: A Space Odyssey" portrayed yet another incredible station with artificial gravity. In tribute to Arthur Clarke's vision and inspiration, the University of Maryland L1 habitat is named Clarke Station.

Challenges

Artificial Gravity

In 1966, astronauts Conrad and Gordon achieved a low level of artificial gravity when they tethered together the Gemini capsule to the Agena target vehicle and rotated slowly for 2 ½ orbits around the Earth. While artificial gravity production through rotation has been demonstrated on a small scale, knowledge of the ability for humans to live and work in a large scale rotating artificial gravity environment is limited. Research conducted in centrifuges on Earth has concluded that humans can adapt and live for extended periods to rotation rates as high as 8.5 RPM. To ensure that astronauts can live and work comfortably, Clarke Station will have a maximum rotation rate of 4.0 RPM. Changes in gravity level are accomplished through control of the rotation rate. Since the station generates a maximum gravity level of 1.2g, or 12m/s^2, and has a maximum rotation rate of 4 RPM, the radius of the

station is 68.4 m. The station must also be capable of accepting a docking vehicle while it is spun up in order to dock to the station without disturbing the science missions and to reduce propellant expenses.

Floor Space

Clarke Station will support 8 crewmembers during normal operations and has the capability of supporting 16 crewmembers for short durations during crew transfers. The crew must have enough space to live and work effectively for long durations. Because Clark Station has gravity, floor space area requirements, not volume, must be considered. For long duration space flight, the minimum floor space per crewmember is 40 m^2. The open floor space requirement is 8 m^2 per crewmember. This requirement results in a station with a total floor space of 320 m^2.

Radiation Exposure

Space radiation consists mainly of high energy-charge particles such as protons and heavy ions. At the L1 point, shown in Figure 1, beyond the protection of the Van Allen Belts, radiation from Galactic Cosmic Radiation and Solar Particle Events threaten the health of Clarke Station inhabitants. Galactic Cosmic Radiation (GCR), originates from outside the solar system, and consists mainly of hydrogen. GCR is indirectly related to the 11-year cycle of the Sun, where its maximum is at the solar minimum. During a solar minimum, an unshielded dosage is about 60 rem/year, and a factor of 2.5 lower at solar maximum. Solar flares are explosions on the Sun that generate Solar Particle Events (SPEs), and shoot them into outer space. SPE's occur once or twice a solar cycle. One of the largest solar flares occurred in 1972, producing a dose of 350 rem for several hours.

According to NASA requirements, maximum radiation dosage for Blood Forming Organs is 50 rem/year. Since solar flares can occur throughout the solar cycle, the worst-case scenario is a large solar flare occurring during solar minimum, when GCR is largest. This scenario requires shielding against GCR along with sufficient shielding for a solar flare.
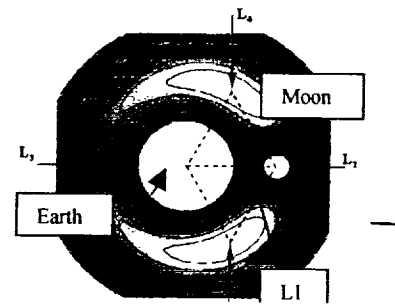
Figure 1. Libration points for the Earth-Moon system shown with contours representing gravitational and centripetal forces.
Adapted From: [Dr. Soho. 2001. "SOHO FAQ: Astronomy."*sohowww.nascom.nasa.gov/explore/faq/a stronomy.html*]

Mission

Bone and Muscle Research

In microgravity, a significant number of bone forming cells die, and healthy bone cells produce fewer minerals. Muscle size decreases dramatically and there is a reduced capacity for muscles to burn fat for energy. Clarke Station science will determine the rate, location, and magnitude of bone and muscle loss as affected by gravity level. Changes in muscular performance as related to gravity level will be documented. Equilibrium bone/muscle levels, and the extent of bone loss reversal due to increases in gravity level will be determined. Exploring the relation between bone loss and decreasing muscle strength at other than Earth's gravity will aid in developing protocols for long duration space missions. Physical measurements and performance measurements, Dual Energy X-ray Absiorptiometry (DEXA) and ultrasound scanning will provide accurate measurements of bone structure and density.

Human Physiology Research

In addition to causing changes in bone and muscle strength, microgravity is known to cause drastic changes in the lungs and heart. Central venous blood pressure decreases, baroreflexes are impaired, and heart rate increases. There is a shift in body fluid toward the head, blood volume decreases, and red blood cell count decreases. Experiments in the cardiovascular field will help understand cardiac and circulatory hemodynamics, biochemical changes, baroreflexes, and dysrhythmias at different gravity levels. Reduced gravity environment adaptation and circadian rhythms will be analyzed and related to performance. Immunology research will focus on the ability for astronauts to respond to and recall antigens at different gravity levels. Neurotransmitter and overall neurosensory changes in response to a change in gravity remains incomplete. Experiments designed in the field of neuroscience will aim to understand space motion sickness, how sensory motor skills are affected, and rotating environment effects on the neurovestibular system.

Radiation Science

Radiation science experiments will provide accurate radiation monitoring and measurements to assess and reduce health risks of the crew as well as chart the radiation environment of deep space. Dosimetric Mapping will provide a quantitative description of the radiation field inside and outside Clarke Station. Active dosimeters will measure localization of charged particles and the energy spectrum of radiation, and the crew will wear passive dosimeters to measure absorbed dose. Outside the station, the Phantom Torso, a torso and head constructed from a muscle-tissue plastic equivalent with over 350 passive dosimeters embedded in it, will be used to measure organ level radiation doses. The Bonner Ball Neutron Detector (BBND) uses six detector spheres filled with He_3 to determine neutron radiation effects. Results from these experiments will provide more accurate and reliable radiation prediction models for future missions.

Mars Simulation Science

Mars simulation missions will allow for valuable experimentation and learning in preparation for a future mission to Mars. Physiological changes resulting from long-term exposure to Mars gravity will be documented. Communication time delays that would occur on a Mars mission, of 21 minutes maximum length, will be simulated. Astronauts will utilize the Range, an open area of approximately 10 m^2, for Mars suit mobility testing, structure building, and interaction with autonomous robots. To prove the ability to grow plants for consumption at Mars gravity, as necessitated in the Mars Reference Mission, three plant growth modules totaling 3 m^2 of growth area will be on Clarke Station. These plants will also be analyzed on the cellular level in the biology lab. Completion of the full-length Mars simulation in 2012 will allow time to integrate the lessons learned from the simulation into a Mars mission design for the opportune window of 2016-2018 when travel durations will be as short as 130 days.

Advanced Technology – Future Research

After the full-length Mars simulation, Clarke Station will transition to a life sciences and advanced technologies station. Biotechnology, Microbiology, Materials Engineering, Reproduction and Development, Lunar research, Electrical Engineering, and Exobiology research will further help scientistics understand the human response to the space environment, the composition of the solar system, and lead to important medical and technological discoveries that have benefits on Earth.

Gravity Level Timeline

Table 1 shows the station gravity levels for the first six years beginning with initial station operation in January 2007. Crew rotations occur once a year for the first three years. Gravity level step increases are conducted the first year to study adaptation and living abilities of astronauts at various gravity levels. The second year is a short-term Mars mission simulation. This short-term simulation assumes the astronauts will have a ½g artificial gravity transfer vehicle. The third year is devoted to another short-term Mars mission simulation. Mars transfer in this simulation is in microgravity. A comparative study of the second and third years will give scientists valuable insight into the transportation needs for a Mars mission. Following the short-term Mars mission simulations is a full-length Mars mission simulation. The gravity level for the first 5 and last 4 months of the full-length Mars simulation will be decided based on information gathered over the initial three years and Mars mission plans in 2010. The durations for the full-length Mars simulation match the durations of the long stay fast transit mission outlined in the Mars Reference Mission. Completion of the full-length Mars simulation in 2012 will allow time to integrate the lessons learned from the simulation into a Mars mission design for the opportune window of 2016-2018 when travel durations will be as short as 130 days. The station gravity levels following the full-length Mars will be selected based on experience gained from the critical six-year period and to accommodate research needs.

Table 1. Gravity Level Timeline

Year	Gravity Level	Duration (months)
Year 1 (2007)	Lunar (.17g)	2
	Mars (.38g)	2
	½ Earth	2
	¾ Earth	2
	Earth	2
	Maximum	2
	Crew Change	
Year 2 (2008)	½ Earth	3
	Mars (.38g)	6
	½ Earth	3
	Crew Change	
Year 3 (2009)	Microgravity	3
	Mars (.38g)	6
	Microgravity	3
	Crew Change	
January 2010	TBD	5
–	Mars (.38g)	21
July 2012	TBD	4
	Crew Change	
July 2012	TBD	TBD

Systems Design

General Configuration

The crew and equipment for conducting these experiments is distributed into two manned habitats at equal distances from their center of rotation. To allow docking while spinning, a non-spinning truss was placed on the axis through the center of rotation, perpendicular to the plane of rotation (Fig. 2). The station fixed coordinate system used to describe the location of station components uses the spin axis as the z axis. The z truss serves two purposes: to eliminate the relative rotational motion of the rotating section from the docking procedure and to serve as a sun-tracking axis to accommodate solar array pointing with minimal support structure mass. Thus, the z truss will rotate at a rate of approximately 1°/day with respect to an inertial frame. Stiff trusses were chosen in order to adequately transmit torques required during station keeping and docking.

In order to maintain a stable spin situation, the rotating section of the station must have its center of gravity at the center of rotation and the station must be spinning about its minor or major principal axis. Modeling the station as a gyrostat, a dual-spin system with an axis-symmetric z truss, showed that having two collinear masses (habitats, labs, or other mass) spinning about the z truss is unstable because the spin axis would then be the intermediate principal axis. Therefore, three spinning masses were required to maintain spin stability.

Using expended transfer vehicle boosters for the third mass minimizes the expense of delivering additional mass to L1 while providing for station stability. Based on the assembly and delivery schedule, 5 expended boosters with 3 tons of inert mass each will arrive at Clarke Station. Because this mass totals only 15 tons compared to the 42-ton habitats, the habitat trusses must be at an angle of 160° from one another, and the boosters at an equal distance of 68.4 m from the center of rotation. By making use of this excess mass, only about 1½ tons of extra truss will be needed to connect the boosters to the rotational center.

The Z-truss

The z truss is actually two separate free-spinning trusses, the +z truss and the –z truss, which are attached to each side of the rotating section perpendicular to the plane of rotation. The –z truss rotates with the habitats the entire way to the docking system and is sun-tracking from the docking collar to the –z end of the station. The attachment points will have rotational interfaces as described below. Although only the +z truss contains the solar arrays, both sections will track the sun to maintain alignment of the reaction control thrusters, which are housed at the ends of the z trusses.

The angular momentum of the rotating section will be on the order of 10^8 kg-m²/s. The reaction control thrusters are placed 30 m from the rotating plane on the + and - z trusses in order to produce a sufficient torque to adjust this angular momentum. The transfer vehicle docking system was placed 25 m away from the rotational section to reduce plume impingement on the structures from the transfer vehicle thrusters.

Depending on whether one, two, or no transfer vehicles are docked to the station, the center of mass and moment of inertia will change. The moment of inertia for the station was calculated using the coordinate system shown in Table 2, which depicts the center of mass and moment of inertia as a function of the number of docked transfer vehicles.

Figure 2. Station Overall Configuration

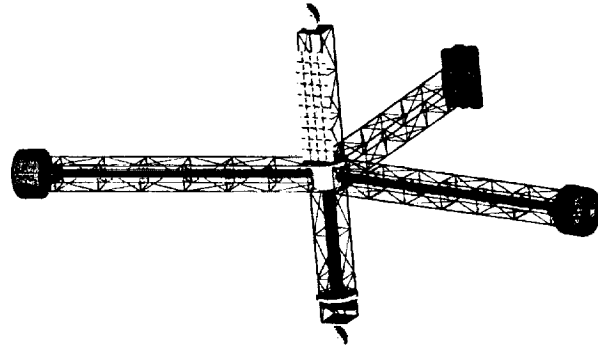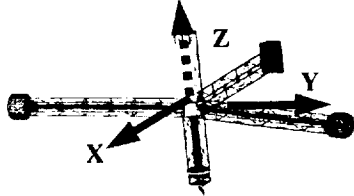**Table 2. Station Center of Mass and Moment of Inertia**

Center of Mass (m) as a function of Transfer Vehicles Docked	Moment if Inertia	
No x-fer vehicle docked: (0, 0, -4.6)	$I_x = 3.9 \times 10^8$	
1 x-fer vehicle docked: (0, <<1, -9.2)	$I_y = 0.84 \times 10^8$	
2 x-fer vehicles docked: (0, 0, -13.8)	$I_z = 4.6 \times 10^8$	

Habitat Modules

An inflatable structure was chosen for the habitats because of its low weight, small packaging volume, strength in terms of pressure, ability to withstand impact of micrometeoroid debris and better radiation shielding as compared to conventional modules. The inflatable habitat is mounted longitudinally to the truss and has the inflated dimensions of 5.4 m radius, 7.6 m length, and 0.3 m wall thickness. The habitat interior consists of two floors with 2.5 m ceilings and 1m storage space located above the upper ceiling and below the lower floor. The floors are connected by a 3.5 m diameter core. The habitats were designed to accommodate crewmembers from the 5th percentile Japanese female to the 95th percentile American male.

The habitat's internal pressure creates both longitudinal and transverse pressurization loads on the habitat wall. In addition to the longitudinal pressure loads, the habitat also sees longitudinal loads due to centripetal acceleration. The habitat shell consists of multiple layers of woven Kevlar that are responsible for the module shape, loads, and protection from micrometeoroid debris. The micrometeoroid protection is made up of alternating layers of woven Kevlar and polyethylene foam. Inside those layers are bladders made up of viton to hold water for radiation shielding. The innermost layer is Nomex cloth protecting the viton bladders from scuffs and scratches. This design has a safety factor of 3 and a margin of safety of 1% for transverse stress and 2.7% for longitudinal stress. The total mass of the module is 42,000 kg, which consists of 15,000 kg empty mass, 23,000 kg radiation shielding mass, and 4,000 kg of equipment.
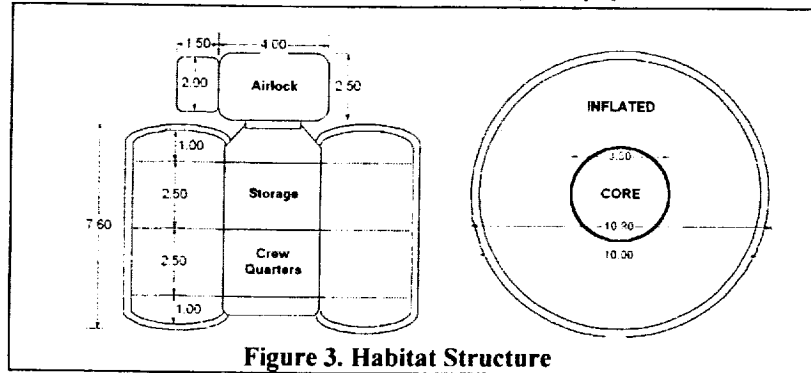
Figure 3. Habitat Structure
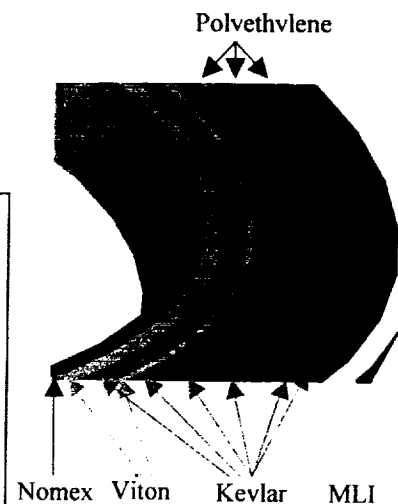
Figure 4. Habitat Layers

Truss Structure

The truss is the main structural backbone of Clarke Station. It is separated into three Rotating Truss (RT) spokes and two Z-Truss (ZT) elements (positive and negative). The truss provides a pass-through for the transfer tunnel and hard mounts for attached payloads. The RT passes around the hub module by means of a spoke interconnect structure, thereby decoupling the hub from reacting station bending and axial loads.

Both the RT and the ZT are 6m box trusses having four tubular main spars of outer diameter 250 mm and cross-members of 130 mm diameter. The main spars are two concentric tubes of a 1.5mm thick composite laminate. The laminate is Toray M55J/Fiberite 934-3 carbon/cyanate ester in a $[90/\pm30/\pm15/0]_s$ symmetric fiber orientation. The tightly woven plies offer superior micrometeoroid impact resistance and superior corrosion resistance. Furthermore, the laminate possesses ultra-high dimensional stability under thermal cycling.

The truss is weakest in its resistance to buckling. Bending in the RT due to angular rate adjustment thrusting loads truss members in compression and causes lowest M.S. on buckling. The truss design was driven both by resistance to buckling and resistance to natural frequency excitation in bending of the RT spokes. Longitudinal and Bending Natural Frequencies were calculated for both the RT and ZT spokes and are tabulated in Table 3. For the operational load environment, margins of safety are presented in Table 4 below.

Table 3. RT and ZT Bending Natural Frequencies

Natural Frequencies	RT Spoke, Habitat at End	RT Spoke, Offset Mass at End	+Z-Truss	-Z-Truss, 2 Transfer Vehicles Docked
Longitudinal, Hz	4.5	7.5	46.8	5.9
Bending, Hz	0.37	0.63	10.5	1.3

Table 4. Truss Margins of Safety

Description of Limiting Load Case	Applied Stress	Failure Mode	Margin
Axial Loads			
Axial Stress in Rotating Truss Habitat Spoke at .42 rad/s (MPa)	63	Tension	10.6
Axial Stress in Rotating Truss Offset Mass Spoke at .42 rad/s (MPa)	19	Tension	38.4
Bending Loads			
Bending in Rotating Truss Spoke due to 1 Hour Spin-up from 0 to .42 rad/s (MPa)	1.8	Euler Buckling	0.2
Bending in -Z-Truss due to Worst-Case Docking Impact (MPa)	2.2	Euler Buckling	0.0
Bending in -Z-Truss due to Attitude Control Thrusting (kPa)	4.6	Euler Buckling	483
Bending in +Z-Truss due to Attitude Control Thrusting (kPa)	4.9	Euler Buckling	451
Shear Loads			
Shear in Rotating Truss due to 1 Hour Spin-up from 0 to .42 rad/s (kPa)	87	Shear	994
Shear in Rotating Truss and Z-Truss due to Worst-Case Normal Plume Impingement (kPa)	13	Shear	6630
Shear in -Z-Truss and +Z-Truss due to Attitude Control Thrusting (kPa)	0.49	Shear	176000
Shear in -Z-Truss due to Worst-Case Docking Impact (kPa)	240	Shear	358
Shear in -Z-Truss and +Z-Truss due to Worst-Case Mass Eccentricity at .42 rad/s (kPa)	420	Shear	204
Shear in +Z-Truss due to Solar Pressure (Pa)	0.12	Shear	690000

Transfer Tunnel

The transfer tunnel provides crew passage between the habitats and docking areas. It consists of four major parts: an inflatable tunnel, consisting of eight layers of material that are similar to the layers of the habitat module but without water filled bladders for radiation shielding; aluminum stiffening rings; Kevlar stringers attaching the tunnels to the trusses; and aluminum lockout doors located at every 10 m of the tunnel to maintain pressurization of the tunnel in the event of a breach in one section of the tunnel wall (Fig. 5).

Transfer through the tunnel will be by use of ladders or a winch mechanism. Two 10 m ladders will be placed along either side of the tunnel wall in each 10m section of the tunnel. The winch is a 12 VDC planetary gear winch for carrying loads and crewmembers up and down the tunnel.

The major loads on the transfer tunnel, given in Table 5, are the force of the lockout doors on the walls from centripetal acceleration, the pressure loading on the tunnel walls, the stress on a closed lockout door due to pressurization, the stress in the Kevlar stringers due to torsion in the truss, and the maximum stress on the aluminum stiffening rings. .

Table 5. Transfer Tunnel Margins of Safety

Load Considered	Applied Stress (MPa)	M.S.
Force of Lockout doors on walls from centripetal acceleration	54.0	21.23
Transfer Tube Pressure Load, Hoop stress walls @ 101 kPa	108	10.13
Stress on Lockout door from pressurization @ 101 kPa	31.9	6.91
Maximum Forces on Kevlar Stringers	63.4	0.39
Maximum Forces on Stiffening Rings	121	1.09
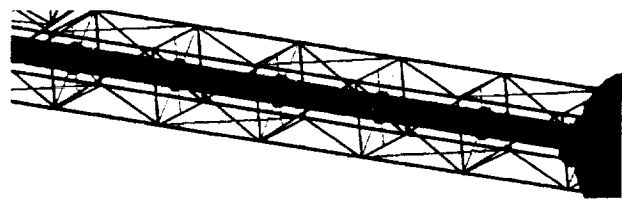
Figure 5. Transfer Tunnel

Rotational Interface

Rotational interfaces are located on the positive and negative despun trusses to allow these sections to rotate independently of the rotating section. The –z interface has three modes of transmission: electrical, consisting of both power and data; biological, or life support and human passage; and structural resistance to moments created by spinning up and down the rotational section, thrusting for attitude and station keeping, and docking the transfer vehicle. The +z interface will need to handle only power, data, and structural loading. The –z interface is also the

junction between the –z tunnel and Airlock-Docking System (ADS), which will be separated by an airlock that can be opened during transfer times. Therefore, the ADS will have a separate atmosphere control that will also be used for EVA pre-breathe.

Main loading on the rotational interfaces stems from either impact with the transfer vehicle or from thruster firing. Forces from docking are about 2250 N on a 1 m moment arm on the –z truss, and the thrusters fire at about 500 N on a 30 m moment arm on the +z truss. Thus, the greatest loading on the rotational interfaces comes from the thrusters on the +z section. Using this information, the thickness of each bearing collar and its flanges must be at least 0.045 m of aluminum. Stainless steel shims are used inside on contact surfaces to minimize the coefficient of friction.

Each rotational joint will also have a bearing assembly to overcome friction losses on the rotating interface and a vacuum seal to separate the internal atmosphere and the outside vacuum of space. To maintain constant relative angular velocity, the interfaces will also contain two redundant constant-spin motors.

Hub

The station hub serves as a storage center as well as a pass-through from the two spokes and the –z truss (Fig. 6). The hub shell is designed to handle only pressurization loads. To handle a maximum internal pressure of 101 kPa, the total thickness of inflatable material is 0.024 m. Since the hub and the transfer tunnel share similar functions and loading environments, their inflatable weaves are identical. Accounting for attachment points, the hub final dimensions are 7.0 m in diameter and 5.5 m high with an interior volume of 210 m³.
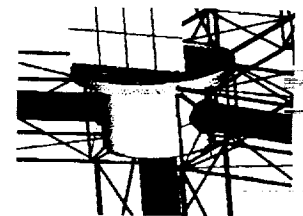
Figure 6. Hub

Airlocks

The station is designed to handle 2 person EVA's on a daily basis. Most EVA's would be for upkeep and repair of the station. In order to facilitate ease of mobility and safety about the trusses, an airlock is placed next to each habitat and one by the docking collar. The airlocks on the rotating section needed to accommodate two astronauts and their EMU's, so the dimensions of the chambers are 4 m diameter and 2.5 m high. An access tunnel allows the astronauts to pass through the truss to exit the station. The dimensions for this tunnel are 2.0 m in diameter and 1.5 m long. Because the loads on this structure are due mainly to pressure, an airlock skin thickness of 0.002 m results from the equation for hoop stress. A 0.001 m offset micro-meteriod shield is placed on the airlocks to increase crew safety. Kevlar stringers to the truss support any bending stress due to centripetal acceleration (Fig. 7). Both of these airlocks will have pressure doors to the habitat and to the transfer tunnel. These doors will be nominally open.
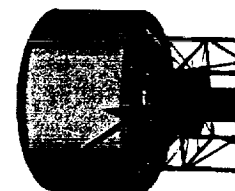
Figure 7. Airlock

The –z airlock (ADS) is designed in the same fashion as the airlocks on the rotating section. However, as a component of this assembly, two docking collars are required at this point, one for the escape vehicle docked at all times, and one for the transfer vehicle (Fig. 8). Loading on this structure came mainly from impulse impact loading during docking. However, due to the truss requirement that impact velocity be at a maximum of 0.033 m/sec, the stresses applied on this assembly are very low.

Figure 8. Docking

Subsystems

Guidance and Control

- Station-keeping -

Clarke Station is required to orbit about the collinear libration point, L1, between the Earth and the Moon in the Earth-Moon system. The distance between the Earth and L1 is approximately 326,400 km and the distance between the Moon and L1 is about 58,000 km.

Lissajous orbits are the natural motion of a satellite around a collinear libration point (Fig. 9). Hoffman described a large lissajous orbit with diameters of 18,000 km in the x-direction, 50,000 km in the y-direction, and 50,000 km in the z-direction, using a coordinate system where the line from the earth to the moon is the primary direction and the earth-moon orbit plane is the primary plane. In this orbit, the Earth and the Moon can block the

Sun from the station, causing an eclipse. Eclipses of the Sun by the Earth will occur a maximum of 4 times per year and each will last a maximum of 160 minutes. Eclipses of the Sun by the Moon will occur a maximum of 3 times per year and each will last a maximum of 50 minutes. The minimum amount of time in between eclipses is 14 days.

This lissajous orbit was found to require station-keeping of 36 m/sec/yr and was chosen because of decreased station-keeping compared to a halo orbit. In general, all of the disturbances that require station keeping are quite small, but add up over time, making thruster maneuvers necessary. The largest disturbance is due to the Sun's gravity and it applies a constant force of 0.0058 N. Other disturbances from the Earth, the Moon, and solar radiation pressure are even smaller than the force from the Sun's gravity. Station-

Figure 9. Lissajous orbit of Clarke Station.
From: [Hoffman, David. *Station-keeping at the Collinear Equilibrium Points of the Earth-Moon System.* 1993. NASA JSC-26189.]

keeping will require a total of 50 m/sec/yr change in velocity including a 30% margin in maneuvers. Corrections should be performed about nine times per year, at about 4 m/s of ΔV per correction to provide the baseline 36m/sec/year. For 15 minute burns, the total force required is 1400N. Two thrusters at each end of the z-truss fire during station keeping, requiring each thruster to produce approximately 350 N of force.

When the total mass of the system is considered (mass of propellant, tanks, and structure), storable bipropellents are the best option, with a total mass of 3600 kg. Clarke Station will use MMH/N_2O_4 thrusters for station keeping and the propellant tanks for this system will be located on both the negative and positive z-axis, one fuel and one oxidizer tank on each.

In order to provide the station with its position, daily ephemeris will be generated on Earth by the Flight Dynamics team and uplinked to the station. This is the most efficient way of updating position onboard. The ephemeris is an instantaneous snapshot of the orbit at a given time, and will contain three – axis position and velocity, calculated on the ground using current orbital models.

- Attitude determination and control -

The most prominent external torques are from gravity, solar pressure radiation, aerodynamic forces, and magnetic field forces. In our case the gravity force (1.1×10^{-7} N-m), magnetic field force (2.3×10^{-17} N-m) and aerodynamic force are negligible. At L1, the solar pressure results in a constant torque of approximately .028 N-m, which effectively pushes the station around the y-axis since the difference distance between the center of gravity of the entire station and the center of solar pressure is offset from the geometric center of the station.

With the station's angular momentum in the positive z direction, the solar pressure torque rotates the station approximately 11 degrees per month if the spinning section is rotating to produce artificial gravity of 1×10^{-4} m/s^2 and 0.03 degrees per month of the spinning section is rotating at 4RPM to produce maximum gravity of 1.2g.

The attitude sensors chosen for the station include one CT – 632 Star Tracker, one Precision Sun Tracking Sensor, and six coarse sun sensors. The star tracker will be the primary attitude sensor, placed on one of the pods on the rotating section facing away from the sun towards deep space. This particular tracker can track up to five stars at one time in its large field of view (FOV), 18° x 18°. It contains an onboard star catalog, which allows the sensor to provide a quaternion instead of raw sensor measurements. This prevents the need for extra flight software coding to process raw data.

The Precision Sun Tracking Sensor, also manufactured by Ball Aerospace, provides accurate information regarding any deviation from the sunline. This sensor will be located along the +Z truss, an inertial portion of the station, in order for the FOV to always face the Sun. The sun sensor has a 110° FOV, and outputs fully processed, ready-to-use 16-bit sun position angles to the onboard software.

The station's attitude control subsystem will also use ADCOLE Coarse Sun Sensors, one on each side of the rotating pods, for a total of six. As the station rotates, two of the coarse sun sensors will always detect the Sun in their FOV. This output will determine the rate of the rotating section by calculating the time it takes for one sensor to view the sun twice.

To obtain a more accurate rate of motion of the station for any station keeping or changing activities, Space Inertial Reference Unit (SIRU) Dual String Gyros, manufactured by Litton, were selected. The SIRU contains two sets of three-axis Inertial Reference Units with radiation hard internal components. The gyros will sense the rate of
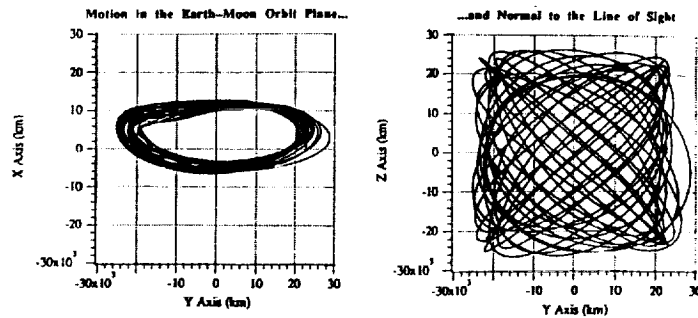
the spacecraft in all three axes, providing a measurement of the station's velocity (rate of change) and acceleration (rate of change over time). The box will be located along the +Z axis truss

All of the sensors will be designed to output data at 10 Hz over a single MIL-STD-1553 bus or multiple buses as needed (TBD). The software will take in data from all of the sensors, but will have the flexibility to choose how often it samples the 10 Hz output.

Hot gas thrusters have been chosen as the method for counteracting these disturbances. Attitude will be maintained to within 1°, with thrusters firing 30 seconds in duration. For a 3 year mission with varying degrees of gravity, the station will need to reorient approximately 650 times with a 4.7N thrust, producing a total propellant mass of 300kg. This includes a 100% margin to take into account internal disturbances and emergency circumstances. There will be a total of 56 thrusters, 8 on each spoke of the rotating section for control about the z-axis, and 16 on each end of the z-truss sections, two at the center of each straight section and 2 at each corner 90 degrees apart from each other for control about the x, y, and z axes (Fig. 10). The thrusters on the rotating sections, which also have habitat modules, are offset at least 2 m from the truss in order to avoid plume impingement on the habitats themselves.
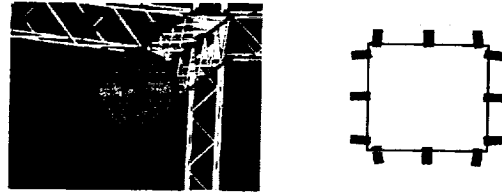
Figure 10: Left: Thrusters on spinning section. Right: Thruster placement on positive and negative z-truss sections.

- Spin-up/Spin-down -

In order to achieve full spin up or spin down of the station in one hour, 855 N must be applied at the 62.1 m point on each rotating spoke. Two thrusters fire on each spoke so each thruster must produce 428 N of force. Using MMH/ N_2O_4, the thrusters, propellants and tanks for a full spin-up or spin-down will have a mass of 2900 kg. The propellant storage tanks for this system will reside on the rotating spokes, one fuel and one oxidizer tank on each.

Computer System

A computer system in Clarke Station is necessary for monitoring and housekeeping. Connections used throughout the station will include ethernet, 1553 buses, RS-422, and RS-232 cables. The centralized computer system will store all information collected throughout the station. Laptops for each crew member will be available to connect to the main computer system anywhere on the station. The duties of the centralized computer system include data processing and housekeeping, sensing and processing of station structure and astronauts, attitude and orbit control functions, thermal control, power management, and communications. Station-ground communications include interface and telemetry, station monitoring, and station fault detection/recovery.

Communications

Clarke Station will have 4 channels of high definition television (HDTV) for both uplink and downlink. The 1.485 Gbits/s uncompressed HDTV can be compressed to 8 Mbits/s. Typical data rates will be on the order of 2 Kbits/s for command and 80 Kbits/s for status and telemetry. Modulation will be Differential Phase Shift Keying because it utilizes the frequency spectrum and because it is not susceptible to phase disturbances. The frequency band used will be the Ku band to allow for enough bandwidth for the data rate. Two parabolic center-feed transmitter antennas of 0.8m diameter, located at either end of the z truss, will communicate with the Deep Space Network with continuous link availability. Table 6 gives the link budget for uplink and downlink.

Table 6. Link Budget for Station Communications

Communication	Frequency	Power Flux Density	Effective Isotropic Radiated Power	Link Margin
Uplink	14.50 GHz	2E-10 W/m²	3E+8 W	18 dB
Downlink	12.75 GHz	9E-14 W/m²	1E+5 W	20 dB

Power and Thermal

- Power generation -

The systems on Clarke Station will require, with a 30% margin, about 62 kW of constant electrical power. This power will be provided by sun tracking solar arrays mounted on the inertial axis of the station. The solar arrays, which use gallium arsenide (GaAs) solar cell technology at an efficiency of 25%, are sized at 220 m² area and 1600

kg mass. Corrections to within 15-degree sun-normal conditions will be made for the arrays by a rack and pinion system incorporated into the mounting structure of the arrays. These measures provide for an average of 70 kW of power to the power conditioning and storage system.

- Fuel Cells -

Fuel Cells will be used to store power for use during the periods of darkness. Although regenerative fuel cells require reactants they are still much more efficient in mass than batteries or most other storable power sources. The fuel cell chosen for Clarke station is the hydrogen-oxygen fuel cell (referred to as "alkaline" because of the KOH electrolyte). The alkaline fuel cell has a specific power of approximately 275 kW/kg. It also has a low hydrogen and oxygen reactant mass, and a useful byproduct of water. All of the water will be held in the power circuit to use electrolysis to create more reactants for the fuel cell. The alkaline fuel cells have a 15 minute start-up time and a lifetime of approximately 2400 hours before refurbishment. A gas storage system was chosen over a cryogenic system for the fuel cells because of the small night cycle and low operating time. The total mass for the fuel cells and storage system is approximately five tons.

- Thermal System -

All of the computer systems as well as the astronauts produce heat. All 70 kW of input power becomes heat, and 70 watts per astronaut of heat must be dissipated to maintain an ideal living environment of 18-24 degrees Celsius. Another source of heat is the sun. Although the sun emits a large amount of energy, because of the large amount of radiation shielding and structural thickness there is a very small amount of heat transfer through the skin of the station. The radio antennas mounted on the exterior of the station, along with any storage tanks, will be coated with a white epoxy (high emittance, low absorbptance) to keep these devices within their operating temperature range.

All electronics will be mounted to cold plates with heat pipes connected to them. The electronics thermal control loop will operate at 10-20 degrees Celsius. A second thermal control loop operating between 0-6 degrees Celsius will cool the air inside the habitat modules. All excess internal heat will be removed through heat exchanges to exterior radiator panels.

The power required by the thermal control system is approximately 1 kW, mostly to pump the fluid through the various cooling components. The working fluid for the heat pipes is water, while the working fluid for the radiator is anhydrous ammonia. With water as the working fluid for the radiator panels, the necessary area to radiate the internal thermal energy of approximately 71 kW is 5 m^2 for each habitat module. Small heaters will be dispersed throughout the habitat and transfer tubes to ensure the temperature does not fall below the required 18 degree Celsius minimum. There will also be thermisters distributed throughout the station to monitor and control the temperature.

Life Support

- Radiation Shielding -

Hydrogen based materials are the most effective shielding materials, since these materials produce less heavy ions, which add to the radiation, when hit with high energy particles. Liquid hydrogen is the most effective shielding material, however it must be kept at temperatures near absolute zero (20 K) to remain in liquid state. Lithium hydride is also an effective material, however it is extremely difficult to handle. This material is extremely reactive to any water, even moisture in the air, and can spontaneously ignite due to rubbing or grinding. Water, however, is much easier to use and can be easily contained.

The crew quarters have heavier shielding so this smaller area can be used as a bunker to protect the astronauts against a solar flare, since these events produce a large amount of radiation in a short period of time. In addition, the astronauts will spend a minimum of 8 hours a day inside their quarters, and therefore will also have a much thicker shield against GCR radiation for this time, further reducing the shield thickness needed for the skin. Also, if an astronaut is exposed to more than their limit of radiation in a given period of time, that astronaut could remain in the crew quarters for a "quarantine" period, in order to have a thicker shield for an extended period of time.

The shielding needed to achieve the exposure limits was calculated from data received from the Johnson Space Center Spaceflight Radiation Health Program. The outer walls of the habitats contain 27 cm of polyethylene foam with a density of 36 kg/m^3, which is equivalent to a 1 cm thickness of water in terms of density. Polyethylene has roughly the same radiation protection qualities as water, and combined with a 4 cm thick water shield for the skin and a 16 cm thick shield for the crew quarters would reduce the radiation exposure in a worst-case scenario of a

large solar flare at solar minimum to 50 rem/year. These thickness values give weights of 35100 kg for skin shield mass and 11500 kg for crew quarters shield mass. The total shielding mass for Clarke Station will then be 46600 kg.

- Air -

A given astronaut will consume up to .85 kg of oxygen (O_2) per day, and generates about 1 kg per day of waste carbon dioxide (CO_2). O_2 can be stored in a gaseous or liquid form, generated from decomposition of oxygen-containing compounds, or reycled from water (H_2O). CO_2 can be removed with either disposable or regenerable filters, or can be converted into H_2O and waste carbon. For converting CO_2 into H_2O, the systems considered were the Bosch, Sabatier, and Advanced Carbon-formation Reactor System (ACRS). For releasing O_2 from H2O, Solid Polymer Water Electrolysis (SPWE) system was the best system. It was found that the combination of a Sabatier reactor and an SPWE had a lower overall mass than a system in which O_2 was stored onboard and wasted. For CO_2 collection, two and four bed molecular sieves (2BMS/4BMS), Solid Amine Water Desorption (SAWD), and Electrochemical Depolarization Concentration (EDC) were considered; SAWD was found to be the best. For emergency O_2 generation equipment, the optimal oxygen-releasing compound was found to be lithium perchlorate candles (LiClO4). O_2 lost to leakage and inefficiencies in the Sabatier/SPWE processes will be scavenged from fuel tanks. For emergency CO_2 removal, the optimal system is lithium hydroxide (LiOH). Both O_2 generation and CO_2 removal can be accomplished using plants, but the necessary mass of this alternative is prohibitively high.

Nitrogen (N_2) is an important non-reactive component of the air. Nitrogen lost to leakage must be replenished from a tank. Stored liquid nitrogen was compared to stored hydrazine, which decomposes into nitrogen. As hydrazine is a storable liquid, it was found to be the more efficient way of storing nitrogen.

- Water -

Humans in space generate about 1.2 kg per day of urine, 1.4 kg per day of water from sweat and breathing, and about 27 kg per day of waste water used for hygienic purposes (cleaning, bathing, etc.). For recovering urine, the systems considered were Vapor Compression Distillation (VCD), Vapor Phase Catalytic Ammonia Removal (VAPCAR), Thermoelectric Integrated Membrane Evaporation System (TIMES), and an Air Evaporation System (AES). For recovering water used for hygienic purposes, the systems considered were Reverse Osmosis (RO), Multifiltration Unibed (MF), and Electrodialysis. The only mechanical system considered for collecting humidity (from sweat and breathing) was that used on the MIR space station. In addition, for each of these three water losses, simply replenishing the lost water from a tank was also considered. The optimal solution was found to be to recycle all water using the VAPCAR, Electrodialysis, and MIR systems. However, a significant amount of water is lost mainly due to inefficiency in the Electrodialysis system, so about 2000 kg of stored water will have to be provided each year to replenish that loss. For removing human solid waste, the Supercritical Water Oxidation (SCWO) method was the only method available.

- Mass and power -

A 10% margin was included in all life support system masses, heat loads, volumes, and power requirements. The total mass of all systems in each habitable module is 1700 kg, which occupies 5.5 m^3. The floor space required to house these systems is 3.1 m^2. The total power required for life support systems for the entire station is 7.7 kW. The total heat generated by these systems, for the entire station, is 1 kW. The Sabatier reactor produces 12 kW of heat and for this reason is located outside the habitat modules. Masses external to the station are the Sabatier reactor, which weighs 730 kg, and LiOH and LiClO4 at 40 kg per day of emergeny O_2 generation/CO_2 removal.

- Extravehicular Activity -

For routine maintenance and attending to science experiments, Clarke Station supports daily 2-person Extravehicular Activities (EVAs) or spacewalks. EVAs may also be necessary in emergency situations. Airlocks are located atop each habitat module and at the docking collar. Each airlock has ample room for two suited crew members and their gear. Clarke Station will be equipped with 6 Extravehicular Mobility Units, two in each habitat airlock and two in the main airlock at the docking collar. Each EMU has a mass of approximately 127 kg. The EMU suits have interchangeable components, which allow for use by numerous crewmembers. Prior to every EVA, crewmembers are required to pre-breathe pure oxygen at ambient station pressure for 45 minutes. Because of the spin of Clarke Station, an extensive tether system will be used to ensure crew safety during EVAs.

- Food -

Food supplies aboard Clarke Station will be ambient instead of refrigerated to reduce mass and power required. In addition, ambient food has a longer shelf life than refrigerated food. For a one-year supply for eight crew, plus a week supply for sixteen crew during transfer and a 10% emergency margin, the required consumable mass is 5600 kg. The total volume needed for food and beverage is approximately 18 m^3.

- Safety Systems -

Several safety measures are built into the station design in the event of a structural emergency that may be caused by micrometeoroid impact. These safety measures include lockdown hatches in the transfer tunnels, tunnels that are passable even when decompressed, and strategically placed personal rescue enclosures. To ensure crew survivability, EVA access is available from every habitable section of the station. In a 'worst-case' scenario, sixteen crew could be trapped in a damaged module during a crew transfer period. To safeguard against this scenario, four pressurized spacesuits, 12 rescue enclosures, and a personal life support system for each individual are required in each habitat as well as at the hub and in the docking section.

In addition to structural safeguards, a Cautions and Warning System, Fire Safety System, Health Monitoring System, and a Medical Facility will be integrated throughout Clarke Station. The Caution and Warning System, similar to the one installed on the International Space Station, will allow the crew look up caution and warning messages and their required actions. In addition, The Caution and Warning System will consist of visual and audio cues that will alert the crew when any system has exceeded or strayed from its operational limits. Fire detection and suppression equipment, such as smoke detectors, alarm and warning lights, fire extinguishers, and breathing apparatus will be strategically placed in each habitat, the tunnels, and hub. Usage of nonflammable materials, such as fireproof bags to place worn clothing in, will further reduce fire risk.

Health monitoring equipment will insure crew livelihood and gather useful scientific data. Biomedical sensors will gather physiological data for telemetry, while Impedance Pneumographs will continuously record heart beat (EKG) and respiration rate. Individual dosimeters will measure the amount of absorbed radiation over a given period, while Telemedicine Instrumentation Packs (TIP), will be use to conduct telemedical examinations. Clarke Station will have a medical unit for each habitat containing a Monitor/Diagnosis System, a Medical Care System, and a Countermeasures and Medical Data Management System.

Habitat Interiors

Figures 11-15 show the interior of the habitat modules. Blue labels are crew systems related equipment while green labels are science related equipment. Habitat 1 focuses more on science that will be conducted across multiple gravity levels, physiology, bone and muscle research, and radiation detection. Habitat 2 is focused more on Mars simulation single gravity level science. There are a total of 4 International Standard Payload Racks (ISPR) in the habitats to allow for science expansion and commercial scientific use.
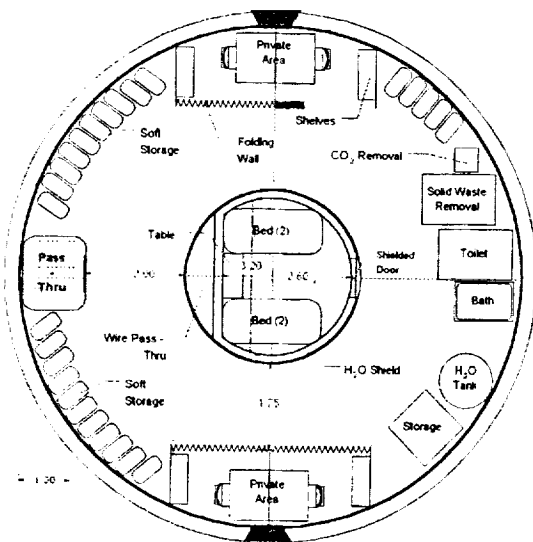
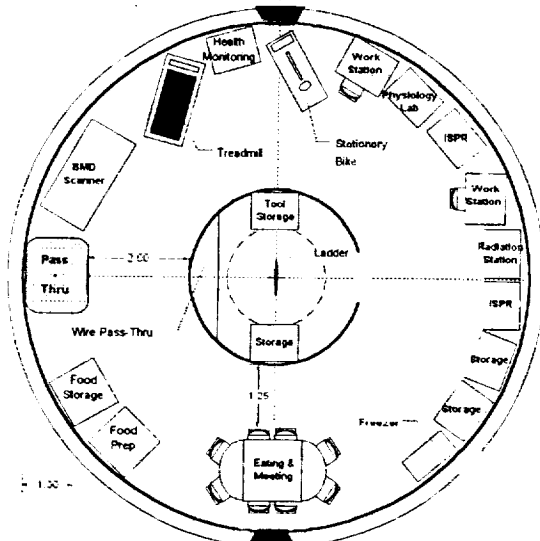**Figure 11. Habitat 1 Bottom Floor**

Figure 12. Habitat 1 Top Floor
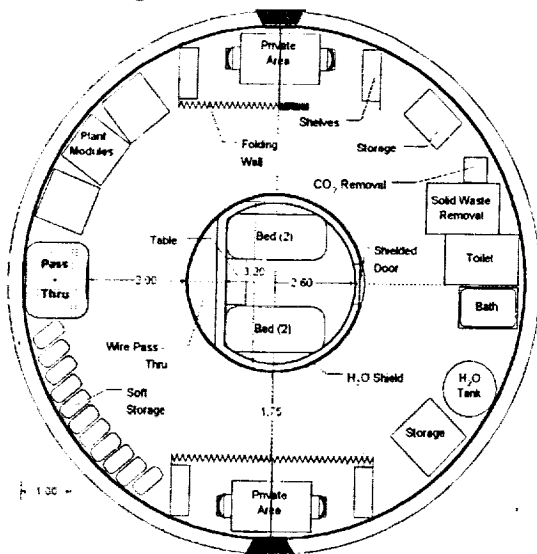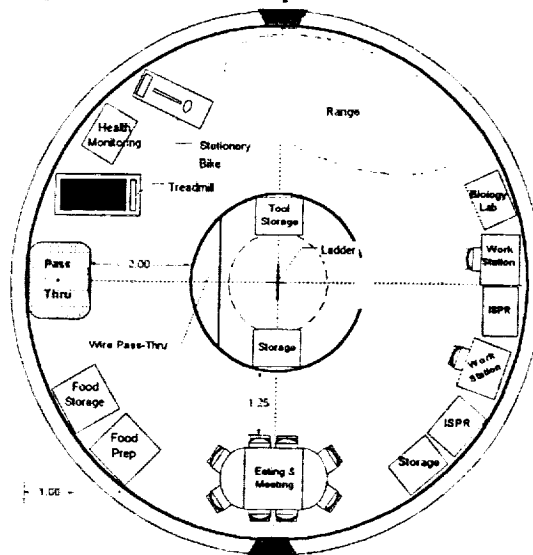
Figure 13. Habitat 1 Bottom Floor

Figure 14. Habitat 1 Top Floor

Assembly/Delivery

- Vehicles-

The delivery and return of station hardware and personnel includes four distinct missions, the delivery of station hardware, the delivery of station supplies, the delivery and return of crew for rotations, and the return of crew in an emergency. From the orbit of the International Space Station (ISS) a delta V of 3.1 km/s is required to insert into a trajectory towards the moon. A second delta V of 0.7 km/s is required at the L1 point to insert into a Lissajous orbit around L1. The return trip requires the same deltaV unless aerobraking is used. A multi-pass aerobraking trajectory was designed for a bent bi-conic vehicle to save 3.1 km/s of deltaV on the return trip.

The delivery of station hardware is the largest of these missions, in terms of mass required, at 315 tons. Because the station hardware delivery does not require a round trip, expendable chemical boosters based on the currently flying Delta IV upper stage were selected for this mission. Each booster has a fully loaded mass of approximately 24 tons with an inert mass ratio of 0.12. One such booster can deliver 11 tons to the station, and staging two boosters enables the delivery of 26 tons. The expended booster weighs 3 tons.

A 24 ton manned transfer vehicle was designed to carry crew to and from Clarke Station. This crew transfer vehicle (CTV) is delivered to Clarke Station using two of the hardware delivery boosters. It is capable of returning independently using MMH/N2O4 propellents to de-orbit from the L1 point, and using the multi-pass aerobraking to return to an LEO orbit for rendezvous with ISS or the Space Shuttle. Because the propellants are storable, this vehicle can also be used as an emergency return vehicle. One CTV must be at the station for to provide a mission abort capability whenever the station is manned.

- Launch and Assembly -

The first hardware launches will be of the station truss, power supply and docking modules. Crew #1 will fly to ISS and construct the lower z truss, consisting of the docking module and the hub. The entire truss structure for the station, pre-assembled at ISS will then be launched to L1. Crew #2 will travel to L1 on the first crew transfer vehicle to do further truss assembly and inflate components. Then, #2 will return to ISS for construction of the habitat modules. Crew #3 will go to L1, install the habs and become Clarke Station's first inhabitants. There they will receive and install equipment packages. Crew #4 will arrive on the second crew transfer vehicle, marking the first crew transfer. Crew #5, arriving in July of 2006 will conduct final preparations of the station and station wide troubleshooting.

In addition to hardware, launches will be made for boosters. These cryogenic rockets will take hardware to L1. For a 20 ton payload, two boosters are needed, for a 40 ton, three are needed. The two crew transfer vehicles will also be launched. These two vehicles will transfer not only the construction crew, but handle future crew rotation.

Cost Analysis

Top-level cost estimations were made for this project using Johnson Space Center's web based cost calculators. The cost estimate for development and production was primarily based on mass, and was calculated for the station using a total mass of 315 metric tons. The crew transfer vehicle also has a cost estimate based on a dry mass of 18 metric tons. Boosters for transfer to L1, while relatively light and simple systems, also need to be developed and produced. All estimates were calculated using a cost fraction of 0.5 and a peakedness of 1. The costs for developing the station were spread over six years (2001-2006), and the costs for the crew transfer vehicle and the boosters were spread over four years (2001-2004).

The calculated production and development costs do not include launch costs. The need to use US launch vehicles scheduled to be in use in 2005 led to examinations of the Atlas V-500 series, the Delta IV Heavy, and the Space Shuttle. A comparison of the three vehicles showed that launching everything on Atlas V's would be the most cost-effective approach. Unfortunately, because of time constraints and the need to transport crew, both of the more expensive vehicles were found to be necessary. This schedule calls for 28 Atlas V, 21 Delta IV, and 6 Shuttle launches over two years for a total cost of 7.9 billion dollars as seen in Table 7.

From calculated cost estimates for development and production a yearly estimate for mission operations and data analysis was obtained for each system, and a cost estimate for the first five years of operation was also calculated. The total program costs for development and production, plus the first five years of operation of Clarke Station are 50.7 billion dollars in 2001-year dollars. Performing a cost discounting analysis with a 10% discount rate showed that to start the program now and fund through the first five years 37.1 billion dollars should go in the bank today.

Table 7: Cost Summary

Development Costs	2001 $M	Cost Discounting
Station development cost	23200	18400
T. Vehicle development cost	7600	6600
Booster development cost	2700	2300
Launch costs	7900	5100
Total development costs	41400	32400
Operational Costs through 2011		
MODA station costs (5yrs)	4000	1900
MODA t. vehicle costs (7yrs)	2300	1200
Booster production cost (5yrs)	500	400
Operational launch costs (5yrs)	2500	1200
Total operational costs (5yrs)	9300	4700
Total program costs: develop-5yrs	50700	37100

Mass Budget

The mass budget for Clarke Station was formulated by combining subsystem masses. The total mass at the time of final configuration design was calculated to be 220 metric tons. That mass plus a 30% margin was set as the mass budget (315 metric tons) for all calculations. Since then, subsystem designs have been refined and in many areas the current mass is less than the budgeted mass. The current total mass gives a 44% margin to the original mass budget. Figure 15 shows a comparison between the budget and the current usage. Masses that are over 5000 kg are individually represented; all others are folded into a miscellaneous category.

Figure 15: Mass Summary
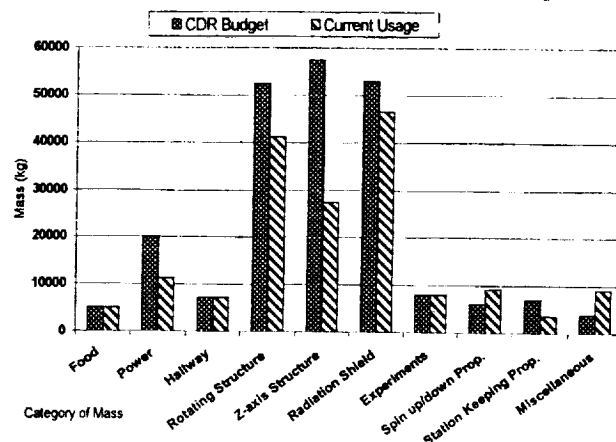
Conclusion

An artificial gravity space station at the L1 point is a feasible project that can return valuable scientific results about the ability of humans to live and work in deep space. Such knowledge would be a valuable contribution to efforts to develop manned missions to Mars and long duration lunar missions. The current design balances the need to maintain a rotating structure to provide artificial gravity with the complexities of maintaining and protecting life in deep space while minimizing the costs of developing and delivering the station.

Outreach

A design project as exciting as an artificial gravity space station draws attention from aerospace professionals and nonprofessionals alike. To foster relations with the community, the University of Maryland community and guests were invited to attend formal Preliminary and Critical Design Reviews. Attendees at the design reviews included professionals from NASA, University of Maryland faculty, graduate students, undergraduates, and family members of the design team. During project development, relationships were fostered with engineers at NASA Goddard Space Flight Center, Swales Aerospace, and the MIT Man Vehicle Laboratory. The fourth member of the presentation team to the Lunar and Planetary Institute received funding for his trip from NASA Goddard. The development and design of Clarke Station is documented on an interactive website, www.clarkestation.com, with the hope and potential of reaching a global audience.

References

1) Hoffman, D. 1993. *Station-keeping at the Collinear Equilibrium Points of the Earth-Moon System.* U.S. Government: NASA JSC-26189.
2) "SOHO FAQ: Astronomy." Available: *sohowww.nascom.nasa.gov/explore/faq/astronomy.html* (March 12, 2001)
3) Swingby (software). 1998. U.S. Government: NASA Goddard Space Flight Center.
4) Szebehely, V. G. *Theory of Orbits: The Restricted Problem of Three Bodies.* Academic Press: New York. © 1967.
5) Wertz, J. R. and W. J. Larson. *Space Mission Analysis and Design (3rd Edition).* Kluwer Academic Publishers: California. 1999.
6) Ball Aerospace. Attitude Sensors/Star Trackers. Available: http://www.ball.com/aerospace/sensors.html (April 30,2001).
7) Litton. Guidance Sensors. Available: http://www.littongcs.com/products/2guidance/space/overview.html (April 25, 2001).
8) Wilson, J.W., Miller, J., Konradi, A., Cucinotta, F.A. *Shielding Strategies for Human Space Exploration.* NASA Conference Publication 3360. December
9) Tribble, Alan C. *The Space Environment: Implications for Spacecraft Design.* Princeton University Press. Princeton, NJ. 1995.
10) *Spaceflight Radiation Health Program at JSC.* Available: http://srag-nt.jsc.nasa.gov/docs/TM104782/techmemo.htm (March 3, 2001).
11) NASA Johnson Space Center. Advanced Missions Cost Model Available: http://www.jsc.nasa.gov/bu2/AMCM.html (April 20, 2001).
12) NASA Johnson Space Center. Mission Operations Cost Model. Available: http://www.jsc.nasa.gov/bu2/MOCM.html (April 18, 2001).
13) NASA Johnson Space Center. Cost Spreading Calculator. Available: http://www.jsc.nasa.gov/bu2/beta.html (April 20,2001).
14) NASA Johnson Space Center. GDP Deflator Inflation Calculator. Available: http://www.jsc.nasa.gov/bu2/inflateGDP.html (April 20, 2001)
15) Isakowitz, S., et al. *International Reference Guide to Space Launch Systems, Third Edition.* AIAA. Reston, VA. 1999.
16) Freeland, R. E., Bilyeu, G. D., Veal, G. R. and Mikulas, M. M. *Inflatable Deployable Space Structures Technology Summary.* International Astronautical Federation. 1998.
17) GD-ED-2205. *Design and Manufacturing Guideline for Aerospace Composites.* Marshall Space Flight Center.
18) Hibbeler, R. C. *Engineering Mechanics: Dynamics.* Fifth ed. New York. Macmillan Publishing Company, Inc. 1989
19) MIL-HDBK-17-2E. *Composite Materials Handbook: Volume 2. Polymer Matrix Composites Materials Properties.* December 1998.
20) NASA-STD-5001. *Structural Design and Test Factors of Safety for Spaceflight Hardware.* Marshall Space Flight Center. June 1996.
21) Earl, J.E., "Artificial Gravity Space Station Physiological Effects and Design Criteria," NASA CR-114982, April. 1971.
22) Lemke, L.G., "An Artificial Gravity Research Facility for Life Sciences," 18th Intersociety Conference on Enviromental Systems, SAE 881029. San Francisco, CA, July 11-13, 1988.
23) NASA Office of Space Science and Applications, "Life Sciences Space Station Planning Document: A Reference Payload for the Life Sciences Research Facility," NASA TM-89188, 1988.
24) Eckert, Peter, Spacecraft Life Support and Biospherics. 1996 Kluwer
25) Melton, Robert G., ed. "Space Station Radiation Dosimetry and Health Risk Assessment", p41-47. Space Station Technology. Society of Automotive Engineeers, Inc. Warrandale, PA, 1996.
26) Napolitano, L.G., ed. ""Medical Results of the Skylab Program", p171-179. Space Stations: Present and Future. Pergamon Press: New York, 1976.
28) Nelson, H.F. Thermal Design of Aeroassisted Orbital Transfer Vehicles. New York: AIAA. 1985.
29) Regan, Frank J. Re-Entry Vehicle Dynamics. New York: AIAA. 1984.
30) Wie, Bong. Space Vehicle Dynamics and Control. Virginia: AIAA. 1998.

Designing a Closed Ecological System to Support Animal Populations for Greater than Thirty Days: Palm Sized Ecosystems

University of Washington, Seattle, WA

Authors: Kristen Durance and Andrew Bryant

Research Team: Andrew Bryant, Jessica Benthuysen, Patrick Cheung, Kristen Durance, Hans-Karl Isern, Gavan Kaizawa-Miyata, Jonathan Lowry, Flora Nisanova, and Justin Phillips.

Faculty Advisor: Dr. Frieda Taub, University of Washington, School of Aquatic and Fishery Sciences.

Abstract

The study of closed ecological systems (CES) has wide implications for study of ecological interactions both on earth and in space. Our design problem was to create closed ecological systems that were able to support animal grazer populations for greater than thirty days. CES were developed for freshwater and marine systems, in 75 mL Tissue culture flasks. Systems were studied under various influences, such as different light levels, and after the introduction nutrients into the systems. Results from saltwater systems observed under varying light levels suggest that six hours of light per day was adequate and longer light periods were not beneficial. Results from the nutrient introduction experiment indicate that nitrogen was a limiting factor in the health and survival of Daphnia in freshwater CES, but phosphorus was not.

Design problem

To design closed ecological systems that sustain themselves for thirty days or greater.

Introduction

Systems that have no or very little mass exchange with their surroundings are considered to be "closed" to the environment. The planet earth can be described as such—a biosphere in which very little is exchanged to space. Life is sustained by the cycling of carbon, nitrogen, oxygen and other elements throughout the planet in a way that is self-sustaining. In other words, the life on this planet has interacted in ways that continue this cycling of nutrients. This process is one of the many intriguing aspects of our planet's ecology. Organisms have evolved to not only consume each other but are able to recycle the waste products of each other as well. Plants, by photosynthesis use light energy to convert CO_2 and H_2O into organic material:

$$6CO_2 + 12\ H_2O + \text{light energy} \rightarrow C_6H_{12}O_6 + 6O_2 + 6H_2O$$
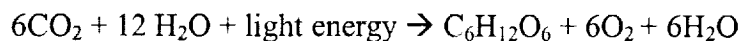
The opposite reaction is respiration:

$$C_6H_{12}O_6 + 6O_2 + 6H_2O \rightarrow 6CO_2 + 12\ H_2O + \text{light energy}$$
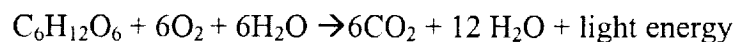
The CO_2 is a waste product of respiration of organisms including grazers that in turn use the byproduct of photosynthesis, oxygen, to survive. These grazers are eaten by higher-level predators which contribute to the cycle with their waste products. This cycle is continuous and vital to aerobic organism survival. Species interactions can also be seen in the cycling of nitrogen throughout the planet. While this cycle is more complex, with many chemical transformations, the basic concept is the same: plants (primary producers) need nitrogen in the form of nitrate or ammonia. nitrogen is the fourth most abundant element on the planet but very little is in a form usable by plants. This makes nitrogen one of the most limiting factors in plant growth. nitrogen is fixed into nitrate by a number of ways including plant/microbe symbiosis, prokaryotes and lightening. Grazers and predators secrete waste in the form of urea, which contains ammonia, and this can be transformed into nitrate by soil bacteria. All of the steps involved require an intimate coordination with other organisms.

Studying ecology on a planetary level has many drawbacks. The scale of our planet allows for a wide variety of climatic and ecological effects with very little idea of what is driving them. There is also a long lag period before many effects are seen at the planet-wide level. This is clearly seen in the development of our atmosphere. The oxygen content of our atmosphere did not develop the day after cyanobacteria started producing oxygen as a waste product. It has taken millions of years and many organism permutations to get to the atmosphere content we have today. The atmosphere most likely went through many cycles of aerobic and anaerobic conditions to reach the state it is in. This lag time would make it hard to see the effects of a chemical that has become off balance within the Earth's environment. Planetary size also effects how smaller ecosystems within the larger biosphere react to stresses. The condition of the planet may not affect every community or ecosystem the same way due to distinct differences in species diversity. This makes it hard to determine what effect a stress may have on more than one ecosystem. Many organisms travel through large tracts of the planet, such as whales and birds, while other organisms, especially plants, are non-motile. It would be very impractical to just release a stress onto the planet and "see" what happens. Further complicating the picture is the conditions that organisms face at the local level. These conditions are often dynamic and not optimal. This makes producing things like computer models difficult because one must account for all the changes an ecosystem may experience and optimal conditions are very seldom seen in nature.

With all of these limitations on ecological study, how can we even hope to discover all the secrets of the planet? One way the scientists have developed is laboratory ecosystems. These are often small-scale models of systems seen in nature that can be as complex or simple as needed. These systems can be used to study species interactions and such but since most of them are open to and rely on inputs from scientists, effects may be based on many factors . One way to eliminate this problem is to develop systems that are "closed" to the surrounding environment. These systems

would receive light energy from outside but would recycle everything needed for species survival without any inputs from the outside [Beyers and Odum 1993]. This is essentially what happens on Earth. We receive light energy from the sun and release energy in the form of heat into space, but we must recycle everything else from within the boundaries of our atmosphere. With closed ecological systems (CES) research, scientists can make the system as complex or as simple as needed in order to study as few or as many aspects of the ecosystem as desired [Odum 1989]. These systems are easier to monitor and reduce the problems that large-scale systems have as described above. Using CES to study patterns and effects of elements within an ecosystem allows one to not only observe specific interactions, but replicate and reproduce experiments and results [Taub 1980].

Experimental Background

Closed ecological systems have been over looked as research tools for some time. Research began in the field in the early 1960's and has evolved from small glass bottles to the Biosphere II project and the Closed Ecological Life Support System (CELSS) project funded by NASA [Straight et. al. 1994]. The two latter projects were extremely costly, which may be one reason that research is not pursued in this area. The data that have been gathered from these experiments, however, are extremely useful and continue to be used to develop new methods of researching CES. One application of this data is thought to be sustaining organisms in space for long periods of time. By developing a system that is self-regenerating, astronauts would be able to spend longer periods of time in space while utilizing a more efficient source of oxygen. This research is also important on a species level. By looking at invertebrates, for example, in a small CES, information can be gathered on tolerance to differing levels of nutrients, light or oxygen, all of which help to describe the limits of the species. By knowing when a specific species may be killed by a pollutant, one may be able to extrapolate the health of an ecosystem based on the condition of these species. Data gathered from CES research could be utilized in many different ways, from understanding what upsets balances in lakes to create algal blooms to allowing long-term space flight an option to combat bacterial blooms that may disturb oxygen and other balances vital to the survival of the vehicle occupants. At a seminar for closed ecological systems in 1982, it was found that CES "promise to become a significant resource for the resolution of global ecology problems which have thus far been experimentally inaccessible..." [NASA 1982] due to the reasons stated previously. For our closed ecological systems, we looked at what environmental factors affect the ability of a system to sustain itself for greater than 30 days. Using both freshwater and marine systems, we explored how differing both day length and levels of nitrogen and phosphorus affect algal and invertebrate populations.

Methods

All of our CES were constructed using 75mL tissue culture flasks. These are inexpensive, sealable containers typically used to culture tissue cells. The benefit of

using these containers versus glass culture tubes or other types of containers is they have an optically flat surface. This allows easier observation of the grazers as well as the opportunity to place the entire flask on a dissecting or inverted microscope to observe algal cells. Each flask, both marine and freshwater, was filled with water, media and , algae and allowed to sit open for 5 days. This allowed for gas exchange to take place and for any unexpected organics to oxidize. The invertebrates were then added and the flasks were placed in their perspective incubators.

Freshwater Systems:

Freshwater closed ecological systems for various studies followed the same initial set-up and composition: Kent water and T82-LoSi (an algal medium) [Appendix I] served as the liquid environment and initial source of nutrients for the algae. Three types of algae—*Ankistrodesmus, Scenedesmus,* and *Chlamydomonas*—were introduced, along with 6 *Daphnia magna,* a freshwater invertebrate. They were added in the following composition:

45 mL Kent water

15 mL T82-LoSi

0.8 mL *Ankistrodesmus*

0.8 mL *Scenedesmus*

0.8 mL *Chlamydomonas*

Systems were allowed to sit open to the atmosphere for five days and on day five 6 *Daphnia magna,* generally 3 adults and 3 juveniles, were added and the systems were sealed.

Two studies were performed with freshwater closed ecological systems:

Light Exposure Length Experiment:

The first study looked at the effect of different light exposures on the health of closed systems. Systems were placed under varying light cycles—0, 6, 12, and 18 hours of light—while kept at constant temperature and (except for the 0-hour set) constant light transmittance. Each set was observed for algae content, *Daphnia* (adult and juveniles), number of carapaces or carcasses present, and the overall state of the system.

Nitrogen and phosphorus Introduction Experiment:

In the second study, we asked whether the viability of closed ecological systems was limited by the uptake of nutrients in the form of *Daphnia* carapaces, carcasses or in other forms. It is thought that nutrients, especially nitrogen, are removed from the systems by being held in these durable forms. Slightly open systems, into which nutrients were added, were used to gain an understanding of the limitations on entirely closed ones.

Nutrients were introduced into the systems by means of syringes; a second syringe was used to relieve the increased pressure by taking up an amount of atmosphere from the flask equal to the nutrients added. While technically not *closed* systems, we were able to limit the openness to a single variable. The first nutrient introduced was a Nitrate (NO_3) solution to test whether nitrogen is taken out of the systems and becomes a limiting factor. To examine the possibility of phosphorus becoming a limiting factor after nitrogen is introduced, an NO_3/PO_4 solution was injected into the second set. The third set of flasks was injected with Kent water, acting as the control.

Nutrients (and the control) were injected two weeks after the systems were sealed. The amount of NO_3 added was equal to the amount originally introduced in the system with the T82-LoSi, effectively doubling the amount available to algae and *Daphnia*. Introduction of the NO_3/PO_4 solution doubled both the NO_3 and the PO_4 available in the system. Control sets were injected with equal amounts, but of Kent water, which contains no nitrates or phosphates.

Marine Systems:

Marine closed ecological systems employed many of the same techniques as freshwater. Three different species of algae were employed: *Nanochloropsis, Isochrysis* and *Tetraselmus*. The salt water used was obtained at the Seattle Aquarium, Seattle, Washington. It was pumped from Puget Sound through a sand filter process to eliminate contaminants. It was not autoclaved so bacteria and other microorganisms were allowed to become part of the system. The elements of each flask were added as follows:

45mL of filtered salt water

15mL of f/2 media [Appendix I]

0.8mL of *Nanochloropsis*

0.8mL of *Isochrysis*

0.8mL of *Tetraselmus*

Each system was allowed to sit for 5 days, after which four *Tigriopus californicus* were added to 24 of the flasks and sealed. We then sealed 24 more flasks that did not receive any invertebrates. Six flasks of each treatment were then placed in four light treatments. Three incubators were set up at a temperature of 20°C each with a different light treatment: 18 hours light, 12 hours light, 6 hours light and 0 hours light based on a 24 hour day. These treatments are generally expressed as 18L:6D or 18 hours light to 6 hours dark and so forth. The 0L:24D flasks were wrapped in tin foil and placed in a dark box within the 6L:18D incubator in order to minimize any light leaks.

Daphnia and *Tigriopus* (juveniles and adults) were counted and observed using the naked eye as well as the aid of a dissecting microscope. Trials were done to observe animal populations using a video camera, but this method is still being perfected. Algal growth was determined using a Plant Stress Meter (PSM), which measures the in vivo fluorescence of the algae. This method was successful until the algae began to fall out of

suspension and clump together. At this point the PSM was unable to get a reading. In the experiments performed, algal growth continued throughout the duration of the experiment. Naked eye observations were also conducted on the overall health of the systems.

Results

Freshwater Systems:

Results of the light exposure length experiment indicate that balances are achieved between the plant and animal populations in the 12- and 18-hour light-cycle sets. Populations of *Daphnia* remained fairly stable over the 2-week time period. In the 0-hour light cycle set, *Daphnia* persisted for longer than expected. While adults died off quickly, juveniles lived beyond the point when any visible algae could be detected. The 6-hour set also showed a drop-off in adults, but a rise in juveniles.

Introduction of nitrogen into the system, in comparison to the control sets of Kent water, showed a relatively higher population of *Daphnia* (both adult and juvenile) and, over the first 4 weeks, a higher PSM level—indicating more algae. Systems into which nitrogen and phosphorus were added showed similarly high levels of *Daphnia* and algae, but in two systems the *Daphnia* died off completely (Fig. 3). Overall, *Daphnia* in the nitrogen and nitrogen/phosphorus sets were more populous, produced more young, and appeared healthier (their guts were dark, indicating high food consumption, while *Daphnia* in the Kent sets appeared quite pale after the first three weeks, as visible algae diminished). Only the nitrogen and nitrogen/phosphorus sets showed, after 74 days, an average population of *Daphnia* about that number originally introduced.

Fig. 1 – Daphnia Populations for Kent Water
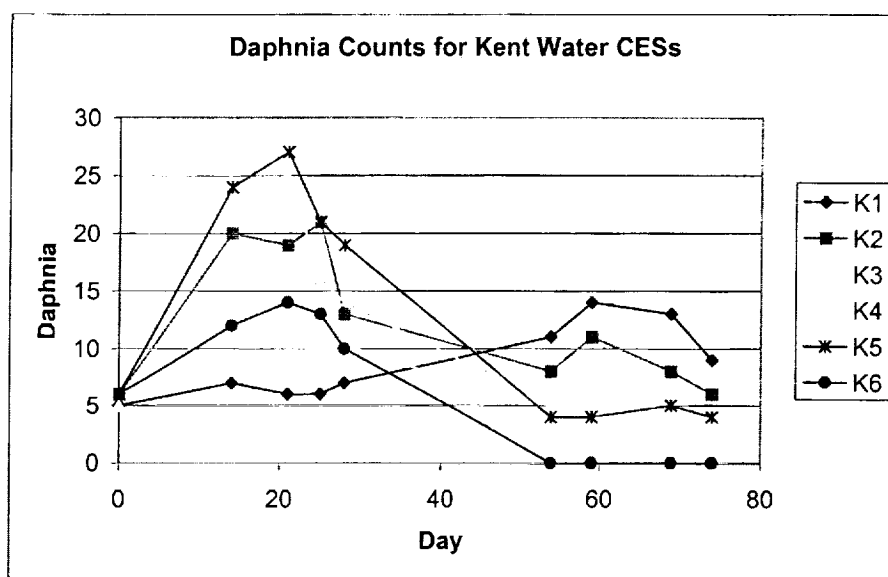
Fig. 2 – Daphnia Populations for Nitrogen Added

Daphnia Counts for Nitrogen CESs
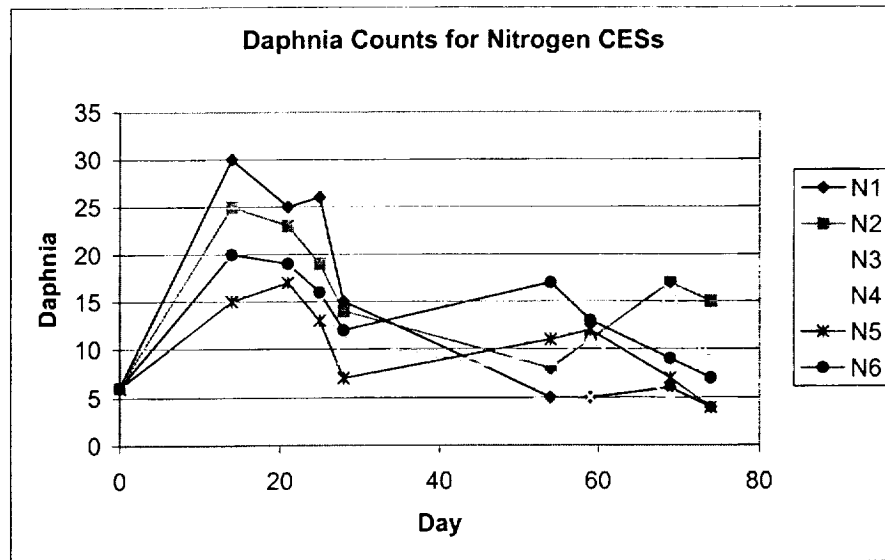
Fig. 3 – Daphnia Populations for Nitrogen and Phosphorus added

Daphnia Counts for Nitrogen/Phosphorus CESs

Fig. 4 – Daphnia Populations Averages

Average of Daphnia Counts for All Three Sets

Marine Systems:

Effects on *T. californicus:*

In the flasks containing both algae and grazers, the results show that *T. californicus* has a considerable range of survival. At the end of week three, all replicates showed egg hatching at least once, with many replicates still containing egg-bearing females. This suggests that to this point the day length had very little direct effect on the *T. californicus*. The replicates in the 0L:24D and 6L:18D had eggs hatch earlier than the replicates in 12L:12D and 18L:6D. The number of *T. californicus* did increase in all replicates until the end of week three, at which point the 0L:24D began to expire. The other three light treatments showed a slight decrease and leveling off at the same time.

Fig. 5 – *Tigriopus* populations at zero hours light.

0L:24D

Fig. 6 – *Tigriopus* populations at six hours light.
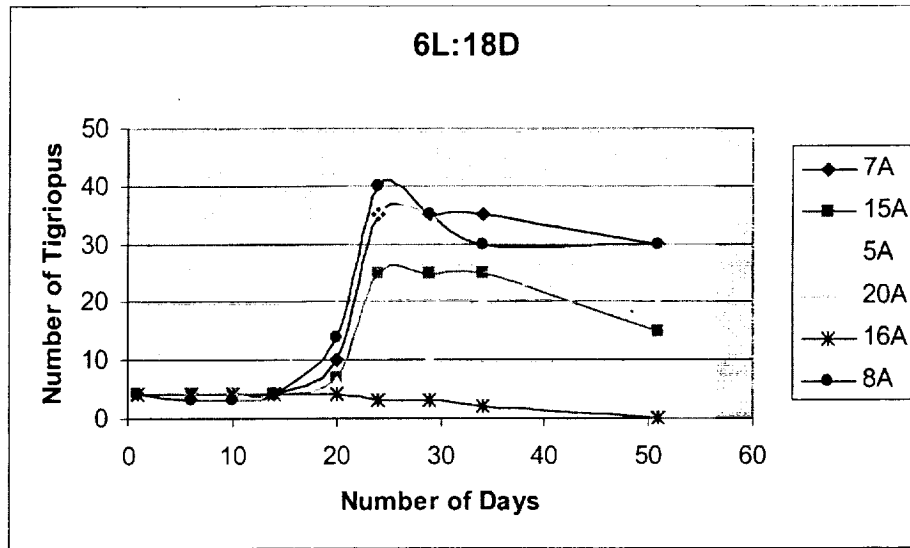
Fig. 7 – *Tigriopus* populations at twelve hours light.
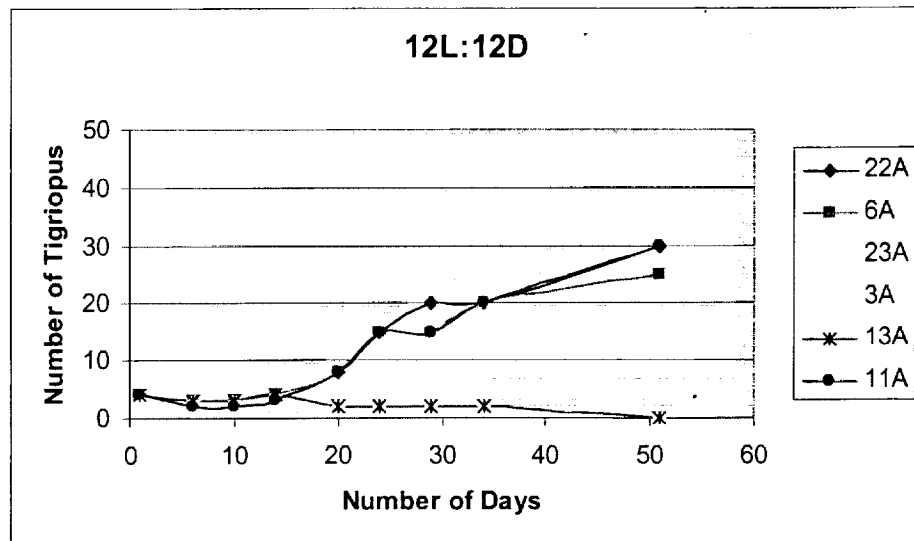
Fig. 8 -- *Tigriopus* populations at eighteen hours light.

18:L6D
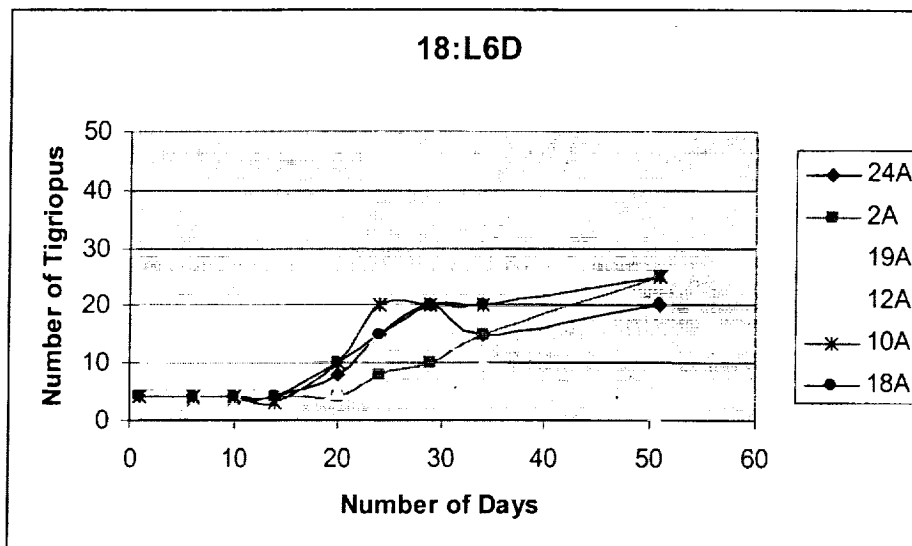
Effects on Algae:

The algae in the 6L:18D without grazers shows a much higher amount of growth than the other three light treatments. The overall difference between the algal growth in the flasks without animals and those with animals is expected. The flasks without animals (Flasks numbered with a 'W') showed a fairly consistent growth. The 0L:24D did begin to see a decrease in algal cells around day 11 and visual observations did not show an increase in clumping, which could account for the decrease in PSM readings. This would mean that the algal cells were dying off from the lack of light. The flasks that contained animals showed a sharp decrease in PSM readings but visual observations showed an increase in cell clumping at the bottom of the flasks.

Fig. 9 – Chlorophyll concentrations over time in CES with and without *Tigriopus*.

Chlorophyll Concentration over Time
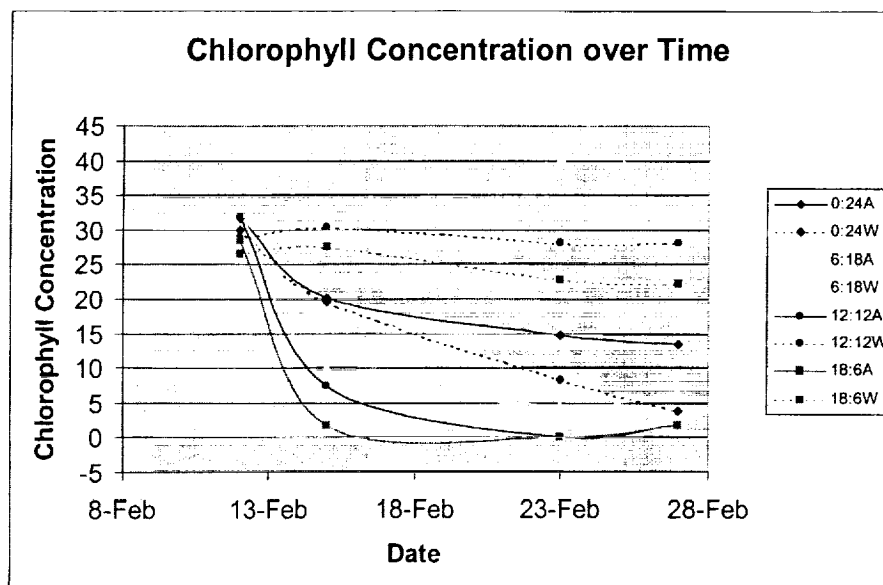
Conclusions

All replicates indicated survival past the thirty day mark. The *Daphnia* did not hatch an F2 generation but this has been seen with past research in *Daphnia* studies [do we have a reference for this somewhere?]. In the marine systems, *Tigriopus* did hatch eggs past the F2 generation and were still producing eggs at the end of the experiment.

Freshwater Systems:

Data from the experiment introducing nitrogen and phosphorus into the otherwise closed system suggest that nitrogen is a limiting factor in closed ecological systems because the health of algae was significantly higher in systems where NO_3 was introduced, and average the *Daphnia* population was slightly higher (Fig. 4). There were no indications that phosphorus was a limiting factor, and in fact systems with nitrogen and phosphorus performed, on average, worse than those with only nitrogen.

Marine Systems:

When there are no grazers present, algal abundance was much greater than those systems where the algae is being grazed upon. In grazed systems, the algae tend to clump together, which may be a defense mechanism against predation. The amount of light needed to sustain an invertebrate population past 30 days seems to be quite variable. The 0L:24D systems did show a much quicker growth increase than those in the 12- and 18-hour light treatments. There seemed to be very little immediate advantage to increasing the day length over six hours. This may have been due to the intensity of the light which was measured at 32 $\mu E\ m^{-2}\ s^{-1}$. Longer day lengths may increase the amount of time needed to hatch out eggs as all the flasks reached about the same animal density, just at different times. It took the 0L:24D treatments approximately 24 days to start showing any decline in *Tigriopus*. Once these systems began to decline, they did so very rapidly.

Overall Results and Implications for the Future:

Our small, closed ecological systems are a great stepping stone for further research in the field. Future investigations include creating larger systems with slightly more complexity and varying trophic levels. What we have learned from these simple systems will help us to know what the starting point is for larger systems and what limitations these organisms have in any system. We are also working on more efficient ways to record the growth of animal populations using a video camera. Documenting animal populations on video will not only allow us to get a more accurate count of animals present but will also allow us to do visual analysis of swimming patterns and other behaviors of both *T. californicus* and *Daphnia magna*. We would also like to develop ways to determine the exact O_2 and CO_2 amounts within the systems so that we can get actual amounts and not relative amounts based on the health of the invertebrates. This will also allow us to get a better picture of what they can tolerate. The data gathered in these experiments as well as those done by pervious groups will allow us to pursue the goal of creating more complex systems with the ability to sustain large organisms for many years.

References

Addey and Loveland, 1998. <u>Dynamic Aquaria</u>. Academic Press.

Byers, R. J. and H. T. Odum. 1993. <u>Ecological Microcosms</u>. Springer-Verlag.

Monk, C. R. 1941. Marine Harpacticoid Copepods from California. Trans Am Microscopic Soc. Vol. 60, 75-99.

NASA 1982. Workshop on Closed System Ecology. Jet Propulsion Laboratory. 82-64. July 15th, 1982.

Straight, C. L., Bubenheim, D. L., Bates, M. E. and Flynn, M. T. 1994. The CELSS Antarctic Project: An Advanced Life Support Testbed at the Amundsen – Scott South Pole Station, Antarctica. *Life Support and Biosphere Science.* Vol. 1, 52-60.

Taub, Frieda B. and Michael E. Crow. 1980. *Synthesizing Aquatic Microcosms.* Microcosms in Ecological Research. Symposium in Augusta Georgia, November 8-10th, 1978.

Appendix I – Media contents

Freshwater Algal Media (T82)   **(Taub, 1993)**

Compound	Element	
NaNO₃	N	7.0 mg/L
MgSO₄ • 7H₂O	Mg	2.43 mg/L
KH₂PO₄	P	1.23 mg/L
NaOH	Na	2.27 mg/L
CaCl₂ • 2H₂O	Ca	40.0 mg/L
NaCl	Na	34.5 mg/L
Al₂(SO₄)₃ • 18H₂O	Al	0.26 mg/L
Na₂SiO₃ • 9H₂O	Na	36.8 mg/L
	Si	22.4 mg/L
FeSO₄ • 7H₂O	Fe	.00625 mg/L
EDTA	EDTA	0.4145 mg/L
H₃BO₃	B	0.008 mg/L
ZnSO₄ • 7H₂O	Zn	0.0015 mg/L
MnCl₂ • 4H₂O	Mn	0.0135 mg/L
Na₂MoO₄ • 5H₂O	Mo	0.0024 mg/L
CuSO₄ • 5H₂O	Cu	0.00032 mg/L
Co(NO₃)₂ • 6H₂O	Co	0.00015 mg/L

Table 2
Salt water Algal Medium (f/2)   **(McLachlin, 1973)**

NaNO₃	0.075 g/L
NaH₂PO₄ • H₂O	0.005 g/L
CuSO₄ • 5H₂O	0.25 ml/L
ZnSO₄ • 7H₂O	0.25 ml/L
CoCl₂ • 6H₂O	0.25 ml/L
MnCl₂ • 4H₂O	0.25 ml/L
Na₂MoO₄ • 2H₂O	0.25 ml/L
O3 Stock A	0.76 ml/L
f/2 vitamins	0.5 ml/L
TRIS	5.0 ml/L

Table 3
Kent Water   **(Kent Marine, Marietta, GA)**
A combination of carbonates, sulfates and chlorides of sodium, magnesium, calcium and potassium with all necessary minor and trace metals necessary for cichlid fish. Contains no phosphates, nitrates or organics.

$5/2/cp/in/20$

Incorporation of the Mini-Magnetospheric Plasma Propulsion System (M2P2) in a Manned Mission to Mars

Department of Aeronautics and Astronautics
University of Washington, Box 352400
Seattle, WA 98195-2400

Department of Geophysics
University of Washington, Box 351650
Seattle, WA 98195-1650

Contributors:
Hillary Cummings,[†] Mike Ross,[*] Daren Welsh,[*] Paul Choe,[*] Derek Inaba,[*] Chris Kachel,[*]
Katherine Ready,[*] Elspeth Suthers,[†] Ben Warrick,[†] Luke Winstrom,[†] Allen Yoo[*]

Faculty Advisors:
Adam Bruckner,[*] Robert Winglee[†]

ABSTRACT

This paper presents two variations of a manned mission to Mars incorporating the Mini-Magnetospheric Plasma Propulsion (M2P2) System, under development at the University of Washington by Professor Robert Winglee, as a less expensive, flexible alternative to the traditional nuclear propulsion systems proposed in the NASA Mars Reference Mission. The M2P2 produces a magnetic plasma bubble that interacts with the ambient solar wind to produce an energy-efficient, high specific impulse thrust. Two scenarios are presented to show the versatility of the M2P2 propulsion system. The first consists of a standard mission similar to the NASA Mars Reference Mission, in which cargo is sent to the Martian surface prior to the piloted mission. The second scenario is a non-traditional mission, in which a single, piloted mission is sent to Mars with multiple landers. These landers would be able to explore multiple sites on the surface of Mars. Multiple orbit trajectories with varying total and Martian surface stay times have been calculated to show the time flexibility of this advanced propulsion system versus the limited launch windows dictated by traditional propulsion systems. The minimum round trip time is shown to be 1.7 years, with potentially 50% less departure mass from low Earth orbit than required by the Mars Reference Mission.

[†] Department of Geophysics
[*] Department of Aeronautics and Astronautics

Nomenclature

F – Thrust
g – Local gravitational acceleration
M – Mass
P_r, P_ϕ - Radial and tangential components of thrust
r – Radius from central gravitational body
θ – Flight path angle
ϕ – True anomaly
ΔV – Change in velocity
DIPS – Dynamic Radioisotope Power System
ECLSS – Environmental Control and Life Support System
EDV – Earth Descent Vehicle
ETV – Earth Transfer Vehicle

GEO – Geosynchronous Earth Orbit
ISRU – In-Situ Resource Utilization
ISS – International Space Station
LEO – Low Earth Orbit
M2P2 – Mini-Magnetospheric Plasma Propulsion
MAV – Mars Ascent Vehicle
MDV – Mars Descent Vehicle
MMH – Monomethyl Hydrazine
MTV – Mars Transfer Vehicle
THCS – Temperature and Humidity Control System
WAVAR – Water Vapor Adsorption Reactor
WM – Waste Management
WRM – Water Recovery, Management

1. INTRODUCTION

A mission to Mars is often thought of as the next step in human exploration of space. An integral part of making a mission to Mars possible is developing a feasible propulsion system. The traditional nuclear propulsion methods suggested by "The Reference Mission of the NASA Mars Exploration Study Team" [1] has the disadvantages of being restricted to short launch windows, causing long mission duration and high costs. With the implementation of an advanced propulsion system such as the Mini-Magnetospheric Plasma Propulsion (M2P2) System, the mission would enjoy the benefits of flexible launch capabilities, reduced mission durations, and lower costs. Two different scenarios for the M2P2 Mission to Mars are presented here. Both demonstrate the low mass requirements and the adaptability of the M2P2 System. The first scenario demonstrates how a Mars Reference-type mission would look using the M2P2. The second scenario shows how the M2P2 can be adapted to an unconventional, "one-trip" mission.

1.1.The Mini-Magnetospheric Plasma Propulsion (M2P2) Device

The Mini-Magnetospheric Plasma Propulsion (M2P2) device is a system, developed by Professor Robert Winglee at the University of Washington [2], which uses energy from the solar wind to provide enhanced propulsion for the spacecraft. The M2P2 uses a solenoid (Figure 1) to create a magnetic field into which plasma is injected, resulting in an inflated "magnetic bubble" tens of kilometers in diameter. In much the same manner as the Earth's magnetosphere, this bubble intercepts and deflects the solar wind, which has a velocity between 350 and 800 km/s, although it can occasionally travel as fast as 1000 km/s. Unlike the Earth, however, the momentum acquired by the M2P2 from the solar wind is sufficient to raise or lower the orbit of the spacecraft. This acquired momentum results in a radial force on the spacecraft. In a multiple M2P2 ship configuration, varying the pointing of the magnetic field of the M2P2 devices can generate a tangential force component, up to an angle of 15° [2] off the radial direction from the sun.
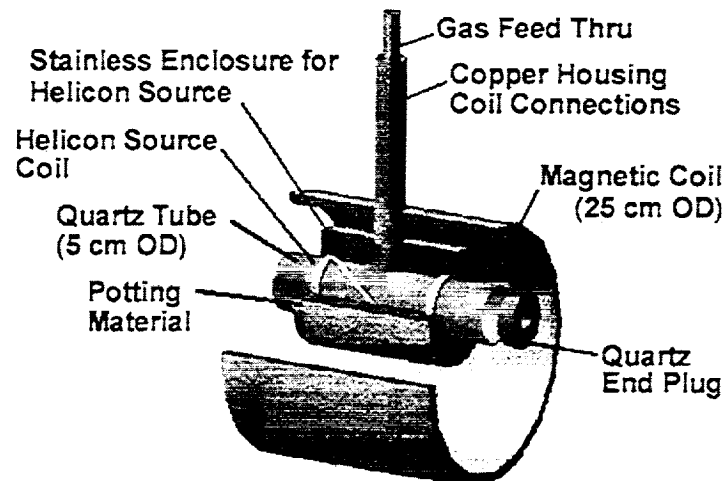
Fig. 1: The components of the M2P2 lab prototype [2].

1.2. Benefits of the M2P2

The M2P2 was chosen as an advanced propulsion system for this mission because it offers several considerable advantages over chemical or nuclear propulsion: the M2P2 provides a constant force, while at the same time using very little fuel compared to the amount that would be needed with conventional rockets. Thus, by using a M2P2, a crew arrives at Mars more quickly than if they were simply launched from Earth and coasted along a Mars intercept trajectory, and more efficiently than if they were to use chemical rockets. Using the M2P2 to provide thrust also allows the mission to leave Earth at a lower velocity, conserving fuel for both manned and unmanned spacecraft. In addition, the magnetic bubble created protects the crew from a substantial amount of particle radiation.

The M2P2 has an advantage over solar sails in that it is both smaller and lighter. The M2P2 requires only a solenoid and plasma injection system, which have a combined mass of less than 70 kg. Also, as the M2P2 travels away from the sun, the magnetic bubble self-adjusts to the fluctuations in the solar wind so that the total force transmitted to the ship remains constant. This feature is not available with solar sails, as the force transmitted to a ship with a solar sail falls off at the same rate as the photon flux, i.e., inversely as the square of the distance from the sun [2].

2. APPLICATIONS TO A MISSION TO MARS

Another benefit of using M2P2 systems is that of having more frequent launch windows. With traditional chemical or nuclear propulsion the launch windows for Mars arrive approximately once every two years [1]. This creates a strict time schedule on any multi-phased mission to Mars. Our research shows that when using a M2P2 system, launch windows occur several times a year. This allows for a greater flexibility in the pre-placement of supplies for future manned missions. The frequent launch windows also allow for the ability to choose between many different surface stay and total mission durations. We have calculated some examples of these different mission times, and some feasible ones are given in Table 1.

Reducing the ΔV's required during an interplanetary mission is an ongoing challenge. We propose that it is possible, due to the low thrust nature of the M2P2 device to effectively tailor the approach to a target planet so as to result in a lower required ΔV in a planet's sphere of influence. The ΔV for several different missions, a Hohmann Transfer, the Mars Reference Mission [1], and a M2P2 mission, which will be discussed below, are shown in Table 2. The ΔV required for the

Table 1: M2P2 mission times

	Days			Years
Departure	Surface	Return	Total	
223.4	448	180.2	851.6	2.33
249.4	363	203.8	816.2	2.24
268.9	290	207.4	766.3	2.10
287.2	204	228.3	719.6	1.97
305.5	108	256.3	629.2	1.72
324.5	1	324.5	616.2	1.69

M2P2 device to leave Earth from LEO is around 3.25 km/s. As the craft approaches Mars the M2P2 system can be used to tailor the approach to achieve a ΔV of less than 2.5 km/s, and leaving Mars a chemical ΔV of 2 km/s results in acceptable Earth return trajectories. These are compared to the other missions in Table 2. Because of the low thrust nature of the M2P2 , it has to be operated in a different fashion to chemical propulsion systems. First, it must be left on for long periods of time in order to produce any significant change in the trajectory of the spacecraft. Second, the orbits attainable are vastly increased, and we have found that varying the amount of time the M2P2 is turned on can drastically change the mission travel and surface stay times.

By comparing the M2P2 system to a typical mission to Mars using nuclear propulsion we have found that a M2P2 mission requires less mass and is more flexible overall, because of the variety of trip durations and launch windows available. We are no longer constrained by long surface stays; thus we can be creative when designing missions to Mars using the M2P2 system. We have decided to present two variations on a mission to Mars using an M2P2 system (See Sections 2.1 and 2.2). The first mission, Scenario I, is similar to the Mars Reference Mission in that it is a "typical" mission, in which the time at Mars is spent on the surface. The second mission (Scenario II) is different from the Mars Reference Mission in that it takes advantage of the short required stay. It leaves a manned ship in orbit around the planet and sends a crew to the surface in a small lander for four weeks, returns them to the ship and sends another lander down for another 4 weeks. Because the surface stay is shorter, less maintenance is required and therefore fewer man-hours are needed for equipment upkeep. We have chosen to present each mission with only a crew of 4 for comparison's sake, as opposed to the Mars Reference Mission, which has a crew of 6 [1]. Table 3 compares the total masses of the Mars Reference Mission, which uses nuclear propulsion [1], and the M2P2 missions. The M2P2 missions require less mass than the Mars Reference Mission, mostly due to lower chemical propellant mass requirements. As can be seen from Table 3, using M2P2 systems can result in a significant mass savings over conventional approaches. Scenario I is able to reduce by over 100,000 kg the amount that needs to be lifted to LEO. Scenario II is able to reduce, by over 50%, the mass needed in LEO to complete the Mars Reference Mission [1].

Table 2: Mission ΔV comparison

Mission	Chemical ΔV (km/s)			
	Leaving Earth	Arriving Mars	Leaving Mars	Total
Hohmann Transfer	3.6	2.26	2.26	8.12
Mars Reference	5	0	4	9
M2P2	3.2	2.5	2	7.7

Table 3: LEO departure mass comparison

	Mars Reference Mission (Crew of 6) (kg)	M2P2 Scenario I (Crew of 4) (kg)	M2P2 Scenario II (Crew 4) (kg)
Cargo I	134,473	90,300	N/A
Cargo II	147,472	120,750	N/A
MTV	137,406	101,310	173,440
Total	419,351	312,360	173,340

2.1 Scenario I

Scenario I is presented to show how The Reference Mission [1] would be modified if the advanced M2P2 propulsion system were used. Scenario I is similar to The Reference Mission in that multiple launches are made from Earth, in an attempt to reduce the mass of the manned spacecraft, and to take the first step in establishing a permanent human base on the surface of Mars. Two cargo vehicles and a manned spacecraft are sent from Low Earth Orbit (LEO), as shown in Figure 2. The first cargo vehicle carries a nuclear reactor, one large rover, food and water for the surface stay, science equipment, an *In Situ* Propellant Production Plant with storage tanks, and a dry Mars Ascent Vehicle (MAV) [3]. The second cargo vehicle takes a surface habitat to the surface of Mars. These cargo missions will be powered by solar panels and utilize the M2P2 system. Once at Mars, the transfer vehicle aerobrakes in the Martian atmosphere and aerocaptures, then uses rockets and parachutes to land on the surface [3]. Once the transfer vehicle has landed safely on the surface, the rover carries the nuclear reactor to a site far from the landing site. At the landing site the *In Situ* Propellant Production Plant is set up and begins making rocket propellants, methane and oxygen [3]. The third vehicle leaves Earth after the first two have reached the Martian surface. This third vehicle consists of the piloted Mars Transfer Vehicle (MTV), which also acts as the Earth Transfer Vehicle (ETV), and the fuel needed to escape Earth Orbit and capture at Mars. The MTV contains a Mars Descent Vehicle (MDV), an Earth Descent Vehicle (EDV), a rover, living quarters, food and water for four astronauts while *en route* to Mars and for the return to Earth. The solar panels are deployed in Geosynchronous Earth Orbit (GEO).

Finally, the crew of four is brought to the MTV on a carrier such as the Space Shuttle Endeavor [4]. The MTV utilizes M2P2 propulsion on the way to Mars. At Mars, the MTV uses aerobraking combined with a small chemical burn to capture in Mars orbit. Once in Mars orbit the astronauts will leave the MTV/ETV using the MDV. The landing site will be within walking distance of the *In Situ* Propellant Production Plant, Habitat, and MAV. In the event that the landing site is missed, the astronauts will have spacesuits and an unpressurized rover that can travel up to 150 km. Food and water for the surface stay will already be at the habitat. Power for the surface stay is provided by the nuclear reactor. The astronauts spend the entire duration of their stay on the surface of Mars.

Due to the extended surface stay and the pre-located cargo missions of Scenario I, a significant reduction in mission mass is attained by using *In Situ* Resource Utilization (ISRU). To produce water for both the astronauts and for the production of return propellant a Water Vapor Adsorption Reactor (WAVAR) [7] was decided upon. This device is capable of extracting the natural water vapor out of the Martian atmosphere, which contains 0.03% water by volume. This water will then be used by the crewmembers for life support needs and also by a Sabatier process [1,3,8] to produce propellant for the return trip. The water from the WAVAR process is decomposed into hydrogen and oxygen through electrolysis. The oxygen is then liquefied and saved in a tank for later use. The hydrogen is combined with carbon dioxide from the Martian atmosphere to produce methane and water using the Sabatier process [1,2,8]. The methane is stored in cryogenic tanks to be used in the Mars ascent and Mars escape burns, while the water is again decomposed through electrolysis and sent back through the process. These two processes allow the fuel and water needed on the surface and for the return trip to be produced at Mars and removes the need to include the return propellant and some of the required water in

CARGO I
Nuclear Reactor for Surface
Unpressurized Rover
Surface Habitat
Food and Water for 100 Days
Science Equipment
Mars Ascent Vehicle
In Situ Propellant Production

MTV
Living Quarters
Mars Descent Vehicle
Unpressurized Rover
Earth Descent Vehicle
M2P2 Systems
Solar Panels
Food and Water for 440 Days
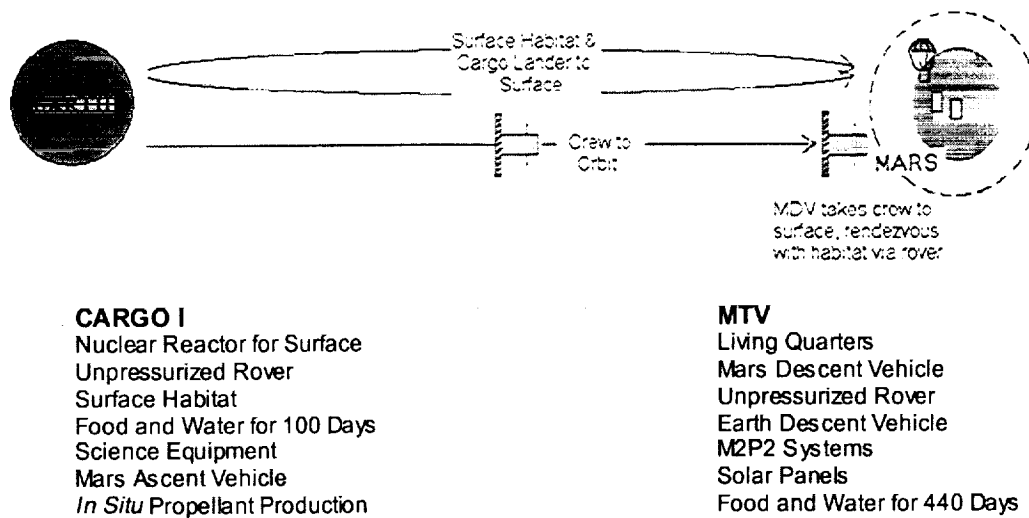
CARGO II
Surface Habitat

Fig. 2: Scenario I.

the initial launch from Earth. Further research and development of ISRU processes is needed, and these processes must be demonstrated before a full-scale human Mars exploration program can be launched. Current plans call for methane/oxygen propellant ISRU strategies to be implemented on an unmanned Mars sample return mission in about a decade.

The Mars Ascent Vehicle delivered on the cargo mission provides the crew a way to leave the Martian surface and dock with the transfer vehicle. The dry mass of the ascent vehicle module is approximately 3,300 kg [8]. The MAV fueled with the *In Situ* Propellant returns the astronauts to the ETV [3]. The MAV will carry back enough fuel for the MTV/ETV to escape Mars orbit and will itself run on *In Situ* Propellant. The ETV uses *In Situ* Propellant to escape Mars Orbit. Once back inside Earth's sphere of influence the astronauts are ejected from the ETV in the EDV and make for an Apollo type re-entry or a docking maneuver with the International Space Station. Table 4 gives an itemized breakdown of the mission components and their masses for this scenario and compares it to Scenario II.

2.2 Scenario II

The main goal of Scenario II is to show the M2P2 system can be applied to a non-traditional mission. With Scenario II we will show that with the short Martian stays allowed by the M2P2 system we can eliminate the need to rendezvous with supplies on the Martian surface and can greatly reduce overall mass. Scenario II sends only one vehicle, the MTV/ETV, to Mars (See Figure 3.). Unlike "The Reference Mission" [1], this scenario does not send any cargo to the surface of Mars before the piloted mission arrives. Instead of attempting to establish a permanent Martian base, this scenario focuses on a single comprehensive mission. For the purpose of this study it was decided to send two small two-person landers with all the supplies needed to the surface for four weeks each. One of the advantages to having a mission of this type is eliminating the need to rendezvous with supplies on the Martian surface. This allows a more comprehensive study of the planet by enabling visiting the surface at more than one location (using multiple landers), and reducing pollution of the planet by eliminating the need for a nuclear power source and permanent habitat on the surface. While two of the crew are on the
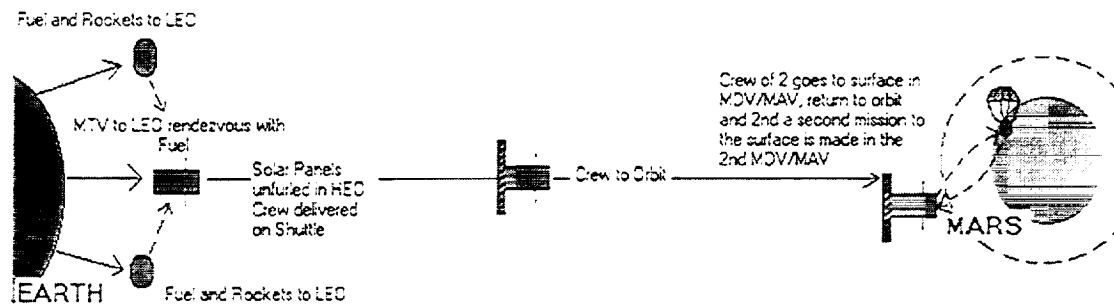
Fig. 3: Scenario II.

surface the other two crewmembers remain in orbit processing data and maintaining the MTV/ETV.

The MTV for Scenario II is assembled in LEO. It carries science equipment, living space, food and water for four astronauts for the entire duration of the trip, inflatable habitats for the surface of Mars, two small MDV/MAV, and an EDV. In Scenario II most of the man-hours at Mars will be in orbit around the planet. After the MTV is in a stable orbit, two of the crew will descend to the Martian surface in a small MDV/MAV. Propellant for the ascent will be carried down to the surface. The MDV/MAV is equipped with an inflatable habitat, batteries, and enough consumables for four weeks. The astronauts will not have a rover on the surface. All science equipment will also be brought from the MTV to the surface. The MDV, which also acts as a MAV, will be used to return to the MTV in orbit. The other two astronauts will make a second trip to the surface in a similar manner as the first. This eliminates the need to rendezvous with a habitat and power source on the surface of Mars, and allows the astronauts to visit two different sites on the Martian surface. Though this trip has the benefit of redundancy with two MDV/MAVs, it does not allow for the possibility of using *in situ* propellant. This varies greatly from the Reference Mission [1], which places the entire crew on the surface for the full duration of the stay at Mars. The return to Earth is done in a similar fashion as Scenario I, except that no *in situ* propellant is used. Again, Table 4 gives an itemized breakdown of the mission components and their masses for this scenario and compares it to Scenario I.

2.3. Transfer Vehicle

The Transfer Vehicle (See Figure 4) consists of several independent sections, which are connected together. Each of these sections contains complete systems for the vehicle. This modular design allows each separate system to be built and carefully tested on Earth before it is lofted into space. Once in space, the components can be assembled into the Transfer Vehicle, and astronauts can be sent up to begin Earth escape procedures. From the exterior, the Transfer Vehicle is a long cylinder with sections of solar panels at one end and an array of long booms in the middle. There are four solar panels, arranged so that they form a plus sign. These panels will constantly face towards the sun, and the rest of the ship extends from the middle of the solar array away from it. Because of this arrangement, there is no possibility of shadows on the panels, which could result in various power difficulties. During the initial stages of escape, the panels are folded and stored within the body of the Transfer Vehicle.

Attached to the center of the solar array is the power control center. This is designed to regulate and control the flow of power to all of the ships component sections. It also contains batteries and other redundant back-up systems. Proceeding away from the sun, the living quarters are attached to the power systems. These are designed for a zero gravity environment, and are thus very space-efficient. The living quarters are shaped as a cylinder, and attached to the outside wall of the cylinder are four storage containers. These contain the necessities for a voyage of such duration. There are also maneuvering thrusters positioned along the circular boundaries of the cylinder. Attached to the other end of the living quarters is the M2P2 machinery. There are 6 booms that radiate from the central axis of the ship, and each of these

Table 4. Mass budgets of Scenarios I and II

Scenario		I Mass (kg)	II Mass (kg)
Cargo			
	Nuclear Reactor [1]	3,960	-
	Unpressurized Rover [1]	500	-
	Food and Water [3,	1,490	-
	Science Equipment [1]	1,700	-
	Aerobrake [8]	2,000	-
	M2P2 Systems	1,300	-
	Power Systems	2,450	-
	Mars Ascent Vehicle [8]	2,400	-
	In Situ Prop. Production [2]	9,000	-
	Structure	5,500	-
	Propellant	60,000	-
Total		90,300	N/A
Habitat			
	Surface Habitat [8]	32,000	-
	M2P2 Systems	1,300	
	Power Systems	2,450	-
	Aerobrake [8]	2,000	
	Structure	4,000	
	Propellant	79,000	
Total		120,750	N/A
MTV			
	EDV(s) [8]	3,000	3,000
	Power Systems	4,260	4,260
	M2P2 Systems	1,600	1,600
	Food & Water	8,350	9,830
	EC/LSS [10,11]	3,400	3,400
	Communication [3]	350	350
	MDV(/MAVs) [3,8]	3,000	6,000
	Fuel for MDV(/MAVs)	1,000	4,000
	Unpressurized Rover [1]	550	-
	Science Equipment [3]	-	900
	Batteries [3]	1,000	2,900
	Inflatable Habitats [10]	-	900
	Ship Structure	5,200	5,200
	Aerobrake	2,500	2,500
	Propellant	67,100	128,500
	Total	101,310	173,340
TOTAL		312,360	173,340

houses two (2) M2P2's. Like the solar panels, these are folded when leaving earth. In addition to the M2P2's, these booms house the communications dishes of the M2P2 project, allowing a clear path to Earth.

The other side of the M2P2 system is attached to a cylindrical section of the Transfer Vehicle which functions differently depending on which permutation of the Mars Mission is employed. It holds a Mars Lander system, which is propelled from the craft and transports the crew from orbit to Mars. This is not used during the Transfer stage of the mission, and so is activated at Mars. The end of the lander section is attached to the main engine, which is used for orbital capture and escape. Most of the space is for a large fuel tank, containing hydrazine. The section of the ship oriented farthest from the sun holds the main rocket engines used for capture and escape, and the propellant tank. This is used to leave both Earth and Mars, as well as slow the Transfer Vehicle at Mars.
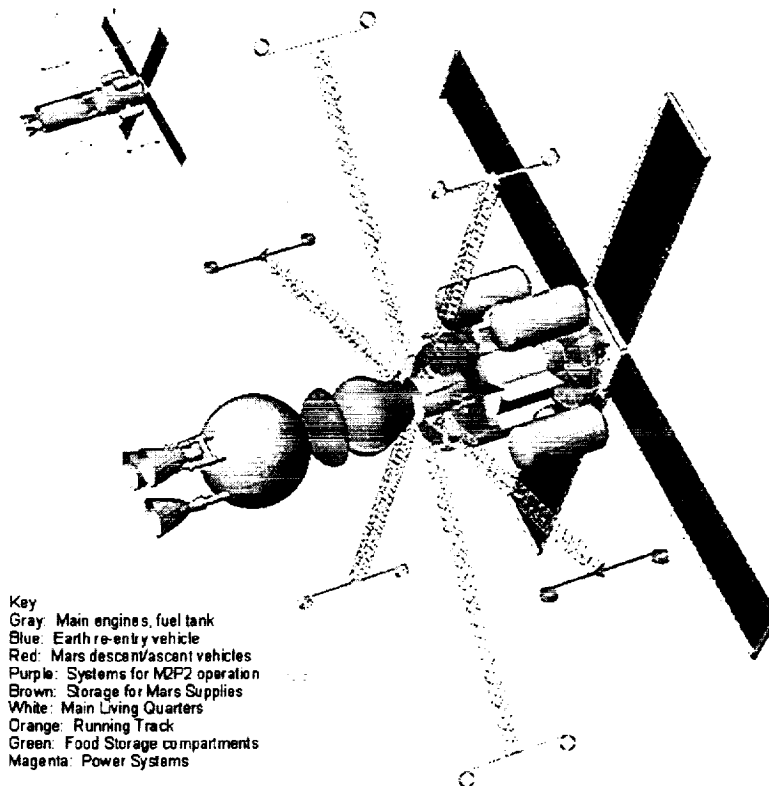
Key
Gray: Main engines, fuel tank
Blue: Earth re-entry vehicle
Red: Mars descent/ascent vehicles
Purple: Systems for M2P2 operation
Brown: Storage for Mars Supplies
White: Main Living Quarters
Orange: Running Track
Green: Food Storage compartments
Magenta: Power Systems

Fig. 4 The transfer vehicle.

3. PROPULSION SYSTEM

3.1. Requirements for the M2P2 system

In both scenarios the ship has twelve M2P2's; adjusting the amount of power going into each device can vary the resulting force. By combining the twelve M2P2's a specific force of 1 N per 200 kg is produced at Earth and a specific force of 1 N per 100 kg is produced at Mars. This specific force results in the required force of 280 N near Earth to complete Scenario II in 1.8 years. Each individual unit will have to produce 24 N and this falls within the current capabilities of the M2P2 device. In order to generate 24 N each device requires 3 kW of electrical power, which results in a total of 36 kW required by the twelve M2P2's near Earth and 18 kW near Mars (this allows for the size of the solar panels to remain constant over the mission duration), these values were determined to be acceptable power requirements based on what could be attained using the latest generation of solar panels (see Section 4). Using twelve M2P2's also allows for a small level of redundancy, if one or two units should fail, power can be rerouted to the remaining M2P2's in order to maintain the required 280 N. Each device, including the surrounding electronics, has a mass of 66 kg, for a total mass of 400 kg. The M2P2's are held twenty meters away from the ship so that the high plasma densities at the devices do not interfere with the ship or the astronauts. The M2P2's are supported on Stacking Triangular Articulated Compact Beams (STACBEAM) that have the ability to retract when needed [3]. The beams have a combined mass of 600 kg [3].

The M2P2 is capable of using a variety of propellants. Virtually any easily ionizable gas can be used [2]. Suitable propellants include H_2, He, N_2, Ar, CH_4, NH_3, and CO_2. While hydrogen and helium make excellent ionizable propellants, they are not stored easily for long periods of

time. In order to have a reasonable storage density, hydrogen and helium would have to be stored in liquid form. This would require cryogenics, which involves a large mass and power cost.

We have chosen to use hydrazine (N_2H_4) as propellant, because it can be ionized and has a long history of use onboard many robotic and man-rated space missions. Although hydrazine is more massive, on a molecular scale, it can be easily ionized into its light element constituents and can be easily stored in liquid form using current propulsion tank technology. Hydrazine will also be used for the attitude control thrusters. This redundancy will result in a more efficient propellant storage system.

Each M2P2 device requires 0.25 kg of hydrazine per day. For our ship's twelve M2P2 devices, a total of 3 kg of hydrazine per day will be required. This propellant requirement is a result of plasma leakage from the edges of the M2P2 bubble. This leakage is caused by energy from the incident solar wind heating the ions within the mini-magnetosphere; these heated ions (with their large gyro-radius) can become demagnetized near the boundary of the magnetosphere and lost from the system.

3.2. M2P2 Missions

In order to generate several different M2P2 missions quickly, a computer program was written. This program was written in Matlab and was used for all mission calculations. The input variables for this program were the number of days the M2P2 operates. It was quickly discovered that the best way to utilize the M2P2 is to allow the spacecraft to travel beyond Mars orbit and then rendezvous with the planet as the spacecraft was falling back toward the sun. This allows for a faster realignment of the planets so that the return mission can leave Mars, resulting in shorter total mission times and also for a reduced ΔV required at Mars. When the M2P2 is first on as it is leaving Earth, the shortest mission and lowest ΔV's result when the tangential force is vectored opposite the direction of motion. As the craft approaches Mars the M2P2 is again turned on with the tangential force vectored in the direction of motion. This second use of the M2P2 allows for a reduction in the radial velocity of the spacecraft, due to the mostly radial force, as it reaches Mars and an increase in the tangential velocity to better match that of Mars.

To calculate the path of the spacecraft as a function of time the equations of motion of Stuhlinger for low thrust missions [5] were used (See Figure 5). The force of the propulsion system is F, and the angle the force is vectored off the radial direction is θ. The local gravitational force is g and φ is the true anomaly. These equations were solved together using Matlab. From the solution the position and velocity of the spacecraft as a function of time was determined.

For the return trip, it was found that if the M2P2 is turned on as the craft is leaving Mars with the tangential force vectored opposite the spacecraft's momentum, the true anomaly that the return trip traveled though is greatly reduced. This allows for mission times of about 2 years without having to use large chemical burns. Before the spacecraft leaves Mars orbit, the M2P2 is turned on, which over the course of several days places the ERV in a highly elliptical orbit about Mars, thereby decreasing the chemical burn requirements. As the spacecraft nears Earth, the M2P2 is used in order to slow the radial velocity of the craft as it falls in toward the Sun and to reduce the tangential velocity, for a smaller chemical burn requirement at Earth. An example of

$$F \cos(\theta) = M(\ddot{r} - r\dot{\phi}^2 + g)$$

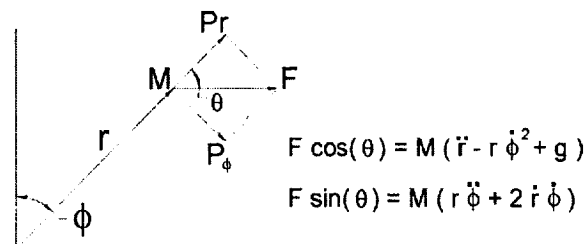$$F \sin(\theta) = M(r\ddot{\phi} + 2\dot{r}\dot{\phi})$$

Fig. 5 Polar coordinate system used in trajectory analysis [5].

one of these missions is shown in Figure 6.

The main benefit of using M2P2 devices is the ability to launch human missions to Mars which last less than two years. This particular mission results in a total mission duration of 670 days. The trip outbound lasts 249 days, followed by a surface stay on Mars of 130 days, and a 290-day return trip. As can be seen in Figure 6 the mission travels beyond the orbit of Mars before actually entering orbit around Mars. This is done to allow for both a reduction in the ΔV required to enter into orbit around Mars and to allow for the correct positioning of the planets to result in a shorter mission time. After the spacecraft leaves Mars on its way back to Earth, the M2P2 is again turned on in order to reduce the tangential velocity of the craft. This reduction decreases the true anomaly the mission travels though on the return voyage, allowing for a total duration of under two years. The times for this trip are compared to the Mars Reference Mission [1] and a Hohmann Transfer [6] in Table 5. These missions also demonstrate the wide adaptability of the M2P2 device to a variety of missions.

The cargo missions were also designed using M2P2 systems to capitalize on the availability of additional launch windows not available to chemical or nuclear propelled missions. The ability to use the M2P2's to reduce the ΔV's required (thereby reducing the amount of propellant that needs to be carried), and the fast transit times, are another benefit of using the M2P2 systems on the cargo missions. Using a M2P2 system it is possible for the cargo to arrive on Mars 135 days after leaving Earth, however a longer transit time may be more desirable due to launch window spacing. This time is equivalent to chemical or nuclear propellants, but can be done with a lower amount of propellant, thereby saving mass.

Table 5: Scenarios I & II compared to Mars Reference Mission

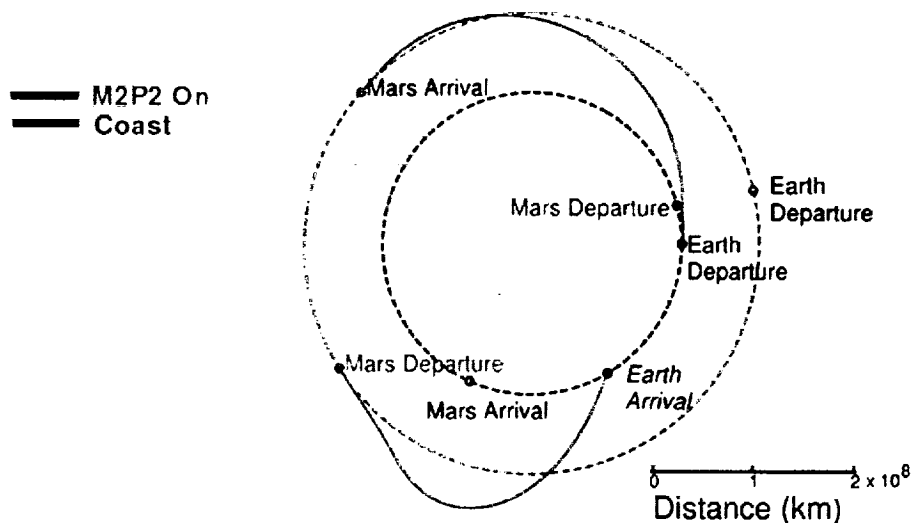| Mission	Days				Years
	Departure	Surface	Return	Total	
Hohmann Transfer	259	454	259	972	2.66
Mars Reference	150	619	110	879	2.41
Scenario 1	250	131	291	672	1.84
Scenario 2	230	60	365	655	1.79

Fig. 6: M2P2 trajectories to Mars.

4. POWER SYSTEM

4.1 MTV Vehicle Power

The MTV uses solar panels as its primary power source. Solar panels are safe for the crew, have been used in space for years with minimal problems, and the power requirements are low enough that the size and mass of the panels does not become prohibitively heavy. The power requirements for the MTV are listed in Table 6. The solar panels are deployed just after passing through the Van Allen radiation belt.

The panels use triple-junction gallium arsenide cells and have cell efficiencies of 26.8%[7]. The solar flux at Mars aphelion is 490 W/m^2 [3]. There the cells generate an electrical output of 131 W/m^2. The solar panels are divided into four sections, each 6 m x 18 m, for a total area of 432 m^2, and generate 57 kW of power at Mars. The specific mass of the panels is 2.09kg/m^2 [2], thus their total mass is 900 kg. While in Mars orbit the M2P2's are no longer used. Thus, the power generated is more than sufficient to power all ship systems, and charge the batteries used in Scenario I and Scenario II. The power system mass is shown in Table 7.

At the distance the M2P2's are separated, the plasma densities near the solar panels are comparable to those in the ionosphere. Plasma densities in the ionosphere have been shown to have no significant effect on satellites in low Earth orbits, and thus should not present a problem to this mission.

Batteries will be used as a power storage point used only as backup in emergencies related to the solar panels. In Scenario II, batteries will also be used for the Mars surface mission. Since the time on the surface for Scenario II will only be a few days, batteries are the most efficient source of power.

4.2. Martian Surface Power Supply

For Scenario I, the power requirement for the surface of Mars is estimated to be 100kW. This includes power for environmental control and life support systems, In Situ Propellant Production and experiments. Similar to the Mars Reference Mission [1] a nuclear reactor will be used for power on Mars. A nuclear reactor was chosen because of the very low solar flux on the Martian surface. The 490 W/m^2 solar flux during transit is modeled for the worst possible case, which occurs at the aphelion of Mars' orbit. The solar flux on the surface of Mars depends on the latitude and the solar declination, which is an angle dependent on the orbit and seasons of Mars. The average solar flux at 35° north on the surface of Mars (using its mean distance from the sun) is 160 W/m^2 [3,8]. Dust storms also play an important role in the modeling of the solar flux on Mars. Dust storms on the average decrease the solar flux by 50% [3]. Based on this, the average solar flux used for sizing the solar arrays on Mars is 80 W/m^2. To produce 100 kW power on the surface would require over 6,000 m^2 of solar panels, which is not a feasible option.

One of the cargo missions sent before the astronauts has a power module. The SP-100 nuclear reactor uses controlled fission of uranium 235 to convert 2.2 MW of reaction power to 100 kW electrical power [8]. Despite the 4% thermal to electric efficiency of the SP-100, this unit still provides a higher energy density (about 40 kg/kW) compared to solar panels. This unit is also capable of high peak-power mode (500 kW) for short durations. A battery of nickel-hydrogen cells will supplement the SP-100 during peak power loads. Table 8 below shows the mass breakdown for the power unit.

Table 6. MTV power requirements

System	Requirements
M2P2	36 kW
Life support	9 kW
Communications	9 kW
Heating	3 kW
Total	57 kW

Table 7. MTV power system mass

	Mass (kg)
Solar Panels	900
Support Structure	3040
Equipment	320
Total	4260

Table 8. Nuclear reactor

Reactor	640 kg
Radiation Shield	860 kg
Heat Transport	445 kg
Reactor instrumentation and control	210 kg
Power conversion	315 kg
Heat rejection	835 kg
Power conditioning, control, and distribution	370 kg
Mechanical and structural elements	285 kg
Total	3,960 kg

The SP-100 unit has an approximate mass of 4,000 kg and when stowed is about 6 meters long and 4 meters in diameter. This power plant is capable of providing continuous power for a minimum of seven years. With minor modifications, the SP-100 can last 15 years at full power [8].

5. ENVIRONMENTAL CONTROL & LIFE SUPPORT SYSTEMS

For this particular mission, current technologies used on the International Space Station (ISS) [12] and the Space Shuttle [4] can be utilized. The Environmental Control and Life Support System (ECLSS) consists of a semi-closed system in which air and water are regenerated and regulated with the use of Air Revitalization, Temperature and Humidity Control System (THCS), and Water Recovery, Management (WRM), and Waste Management (WM) [10,11]. For the mass calculations of each component done by studies of the Advanced Life Support [10], a volume of 50 cubic meters has been allotted to each person. It is assumed that equipment is of the same mass, regardless of the number of crewmembers. Table 9 shows the mass break down for the ELCSS. Comparatively, the Mars Reference Mission [1] is bringing 4661 kg for life support.

Table 9. Environmental Control & Life Support Systems

System	Mass (kg)
Air Revitalization	448
Temperature & Humidity Control	148
Water Recovery & Waste Management	734
Total	1330

5.1 Consumables

The majority of the consumables transported are food and water for the four-member astronaut team. These consumables are housed in disposable modules that are discarded when the module is emptied [3]. From studies in Advanced Life Support [10], the total amount of food and water per day for four humans is 14.84 kg per day. Table 10 shows the mass breakdown of the consumables for a four-member crew. For 671 days, we have calculated the total mass of food and water to be 9,420 kg assuming a 90% water recycling efficiency. This mass plus 410 kg extra is on the MTV in Scenario II for emergencies. This extra food and water will be stored in the MDV/MAV if for some reason the crew must stay on the surface longer than the allotted time. Comparatively, the Mars Reference Mission [1] allots 12058 kg for a 6-member crew. The Ares Explore [3] mission allots 7810 kg for its 4 crewmembers. For Scenario I, the consumables used

Table 10: Consumables for a four-member crew

	Mass per day (kg)	Total for Scenario I (kg)	Total for Scenario II (kg)
Dry Food	2.4	1610	1296
Water	11.64	7810	6286
Oxygen	1.17	840	683
Nitrogen	2	1300	1300

on the return trip to Earth can be sent to Mars on a cargo mission, saving in mass costs to Mars. The astronauts spend 130 days on the surface of Mars, and therefore the food and water for the surface stay can be sent to Mars. A 1% leakage rate is assumed for the Nitrogen and Oxygen, and an 80% recycling efficiency is assumed for the Oxygen. An initial 50kg of Oxygen and 200kg of Nitrogen is also included.

Furthermore standard Atmospheric Revitalization, Control and Supply, Temperature Control, and water waste management will be standard procedures. Humans generate 1.0 kg of CO_2 and consume 0.84 kg of O_2. per day [3]. Therefore, CO2 will need to be eliminated from the habitat and oxygen will need to be produced. WAVAR will produce oxygen [9]. Zeolite sieves will remove CO_2 [9]. The atmosphere within the habitat must be pressurized to 10 psi for the stay on the surface [3,8]. The inside temperature must be maintained at 18-27°C, with humidity at 25-70%[8]. Excess heat must be ventilated to prevent overheating, and will also serve to mix the habitat's atmosphere [8]. Ultrafiltration will be used to filter gray water (laundry, dishwasher, and showering) and wastewater [10,11].

6. COMMUNICATIONS SYSTEM

Communications between the Mars Mission and Earth are facilitated by a fairly standard radio system. In order to penetrate the plasma surrounding the spacecraft, this radio system need only operate in the range of gigahertz frequencies. A design similar to those radios used to penetrate the ionosphere can be employed here. Since the ship ferrying astronauts to Mars will remain in orbit during the surface stay/s, the radio connection to earth may continue through these systems during the crew's Mars exploration. There will, of course, be time periods when the ship will be out of touch with NASA. The longest (approximately 5 weeks) of these periods will occur when the Sun obstructs the communications from Mars to Earth; others occur when Mars is between the spacecraft and earth. During this time, the data gathered by the mission team will reside on the ship computers, and once communication can be resumed with Earth, the information will be transmitted.

Conclusions

The results from this study show that using the M2P2 system on a manned mission to Mars results in increased mission flexibility and a significant mass savings over conventional nuclear or chemical based missions. Use of the M2P2 system in the trajectories shown above significantly reduces the ΔV required to capture at Mars, resulting in a large savings in chemical propellant over conventional missions. The M2P2 can save over 50% of the LEO departure mass required for the Mars Reference mission. Assuming a cost to LEO of $22,000 per kilogram, this saves over $5.4 billion. Another demonstrated benefit of the M2P2 is a reduction of the total mission time to less than 2 years. This shorter mission time decreases the risk from the potential failure of critical sensitive instrumentation and life support systems that will be exposed to harsh environments over very long periods. Also, use of the M2P2 results in a more flexible mission schedule. Several launch windows occur each year and a variety of transit and surface stay times may be chosen to meet mission needs. This is a vast improvement over the once every twenty-six month launch windows of conventional or nuclear propelled missions.

The first M2P2 mission scenario presented, is similar to a conventional approach with an extended surface stay. This mission takes advantage of the M2P2 to reduce the overall mission time of the Mars Reference Mission from 879 days to 670 days. In addition, using the M2P2 over

the nuclear propulsion methods used in the Mars Reference Mission results in a large reduction in the amount of mass that needs to be lifted into low Earth orbit. This savings in mass comes almost entirely from the chemical propellants not needed when using the M2P2 devices. The second mission scenario takes an unconventional approach. Instead of the astronauts landing on one site for the duration of the stay at Mars, this approach allows for the exploration of two landing sites by performing two separate landings of shorter duration. The reduction in surface requirements in this mission results in the lowest mass requirements of the three compared missions, a savings of over 50% of the LEO departure mass of the Mars Reference Mission.

REFERENCES

1. Drake, B., "Reference Mission Version 3.0, Addendum to the Human Exploration of Mars: The Reference Mission of the NASA Mars Exploration Study Team," June 1998. http://spaceflight.nasa.gov/mars/reference/hem/hem2.html.

2. Winglee, R., et al. "Mini-Magnetospheric Plasma Propulsion: Tapping the energy of the solar wind for spacecraft propulsion," *Journal of Geophysical Research*, Vol. 105. 2000, pp. 21067-21077.

3. Grover M.R., Odell, E.H., Smith-Brito, S.L., Warwick, R.W., Bruckner, A.P., "Ares Explore: A Study of Human Mars Exploration Alternatives Using In Situ Propellant Production and Current Technology" Proceedings, Case for Mars VI, Boulder, CO, July 17-20, 1996, in press; also http://www.aa.washington.edu/research/ISRU/ARES/ares.htm.

4. Space Shuttle Endeavor (OV-105), http://science.ksc.nasa.gov/shuttle/resources/orbiters/endeavour.html.

5. Stuhlinger, E., *Ion Propulsion for Space Flight*, New York: McGraw-Hill, 1964, pp. 118-119.

6. Wiesel, W.E., *Spaceflight Dynamics*, 2nd ed, Boston: McGraw-Hill, 1997.

7. http://www.spectrolab.com/prd/prd.htm.

8. Lusignan, B., Reeves, E., Collin, L., Binford, T., Merrihew, S., Fuller, R., "The Stanford US-USSR Mars Exploration Initiative", Report No. E235, Department of Electrical Engineering, Stanford University, Stanford, CA, July 1992.

9. Adan-Plaza, S., Carpenter, K., Elias, L., Grover, R., Hilstad, M., Hoffman, C., Schneider, M., Bruckner, A.P., "Extraction of Atmospheric Water on Mars for the Mars Reference Mission," Proceedings, Mars Exploration Forum, Lunar and Planetary Institute, Houston, TX, May 5-7, 1998, pp. 171-194.

10. Advanced Life Support Research and Technology Metric-Initial Draft, http://peer1.idi.usra.edu/peer_review/prog/als.htm

11. Environmental Control and Life Support System, NSTS 1988 News Reference Manual, http://science.ksc.nasa.gov/shuttle/technology/sts-newsref/sts_eclss.html, August 2000.

12. International Space Station, Press Book Information: Station Systems, http://www.boeing.com/defense-space/space/spacestation/systems/eclss.html, The Boeing Co., 2001.

Omit to End

LIST OF FORUM PARTICIPANTS

David L. Akin
University of Maryland

Eric P. Blumenstein
Colorado School of Mines

Forest Bommarito
Colorado School of Mines

Angelo M. Bonavita
Embry Riddle Aeronautical University

David W. Bowen
Rowan University

Andrew J. Bryant
University of Washington

Levent B. Cakcak
Pennsylvania State University

Joan M. Chapman
University of California, Berkeley

Victoria C Christini
Pennsylvania State University

Toni L. Cisar
Colorado School of Mines

John Connolley
NASA Johnson Space Center

Eric W. Constans
Rowan University

Dexter C. Cooke
Pennsylvania State University

Mark D. Cotler
Rowan University

Jennie K. Crook
University of Colorado, Boulder

Hillary Cummings
University of Washington

James D. DePasquale
University of Maryland

Emma L. Dee
University of Colorado

Samantha R. Dimmick
University of Colorado

Michael Duke
Lunar and Planetary Institute

Kristen M. Durance
University of Washington

Matthew R. Ellsworth
Colorado School of Mines

Matthew D. Estes
University of California, Berkeley

Michael L Flanigan
University of Maryland

Joseph P. Fledderman
Pennsylvania State University

Paul J. Frontera
University of Maryland

Jeffrey E. Gallagher
Embry Riddle Aeronautical University

David C. Gan
University of California, Berkeley

Jessica M. Garzon
University of Maryland

Joshua S. Geiple
Pennsylvania State University

Camron S. Gorguinpour
University of California, Berkeley

Alexander M. Hamling
Pennsylvania State University

Alan Harnish
University of California, Berkeley

Kip Hodges
Massachusetts Institute of Technology

Deborah J. Hutchings
University of California, Berkeley

Brian P. Ickler
University of Colorado

Alex Ignatiev
University of Houston

Michael W. Jacobs
Pennsylvania State University

Kathleen Johnson
Lunar and Planetary Institute

Timothy S. Koken
Georgia Institute of Technology

Lawrence Kuznetz
University of California, Berkeley

Raven LeClair
University of California, Berkeley

Jason A. Lechniak
University of Colorado, Boulder

Steven S. Lee
Georgia Institute of Technology

Anthony Maida
Embry Riddle Aeronautical University

Joseph R. Masiero
Pennsylvania State University

Kurt K. Maute
University of Colorado, Boulder

Barbara J. McKinney
Colorado School of Mines

Jeffrey J. Miller
Georgia Institute of Technology

Michael R. Morrell
Georgia Institute of Technology

Joshua Neubert
Massachusetts Institute of Technology

John R. Olds
Georgia Institute of Technology

Lewis L. Peach
USRA Headquarters

Igor Pesenson
University of California, Berkeley

Sheah N. Pirnack
University of Colorado, Boulder

Michael B. Pritts
Pennsylvania State University

Mahmut Reyhanoglu
Embry Riddle Aeronautical University

David J. Richie
Georgia Institute of Technology

Joel D. Richter
Pennsylvania State University

Reuben R. Rohrschneider
Georgia Institute of Technology

Michael Ross
University of Washington

Sara E. Roxby
University of California, Berkeley

Bryan Ruddy
Massachusetts Institute of Technology

Jeanette D. Schreilber
Pennsylvania State University

Vernon C. Schwanger
Rowan University

Corinne C. Segalas,
University of Maryland

Gregory J. Shoup
University of Maryland

Eric J. Simon
University of Maryland

Christopher A. Skow
Embry Riddle Aeronautical University

Kevin F. Sloan
Pennsylvania State University

Lisa C. Smith
Massachusetts Institute of Technology

Paul Spudis
Lunar and Planetary Institute

Eric J. Staton
Georgia Institute of Technology

Mark Stayton
University of Wyoming

Kevin L. Stefank
University of Maryland

John W. Sunkel
University of Colorado

Jamie M. Szmodis
Pennsylvania State University

David R. Thomas
Embry Riddle Aeronautical University

Jonathan R. Trump
Pennsylvania State University

Scott B. Watson
Rowan University

Daren Welsh
University of Washington

Jordan R. Wiens
Colorado School of Mines

Robert Winglee
University of Washington

Yung-Ruey Y. Yen
University of California, Berkeley

Laura E. Yingling
Pennsylvania State University